

Plasma Membrane Organization and Endocytosis of CD36 in
Human Microvascular Endothelial Cells

by

John Maringa Githaka

A thesis submitted in partial fulfillment of the requirements for the degree of

Doctor of Philosophy

Department of Biochemistry
University of Alberta

© John Maringa Githaka, 2016

Abstract

The plasma membrane is a dynamic lipid bilayer that surrounds the cell, embedded with different plasma membrane proteins, aiding communication between the inside and outside of the cells. Its functions are achieved through an intricate organization of lipid-lipid, lipid-protein and protein-protein interactions in this environment. An emerging organizational feature of plasma membrane-associated receptor proteins is nanoclustering, although the mechanisms leading to this nanoclustering and its functional consequences for signaling remain largely unknown. We sought to investigate the plasma membrane organization of the clustering-responsive receptor CD36 and its endocytosis in endothelial cells (ECs).

During tumorigenesis, thrombospondin-1 (TSP-1), an endogenous extracellular matrix anti-angiogenic factor, is down-regulated. TSP-1 inhibits angiogenesis through binding to its receptor, CD36, and subsequent activation of Fyn, a Src family kinase (SFK), leading to ECs apoptosis. The binding of a monoclonal mouse anti-CD36 immunoglobulin M (IgM) to CD36, mimicking a multivalent ligand, similarly induces ECs apoptosis while divalent monoclonal mouse anti-CD36 immunoglobulin G (IgG) does not, suggesting that CD36 clustering is important in the initiation of TSP-1-CD36-Fyn signaling. Following signal transduction, the ligand-receptor is internalized within the cells. The characterization of the organization of CD36 into multimeric complexes upon TSP-1 binding, the factors that regulate it and the endocytic pathway through which CD36 internalizes TSP-1 in ECs are investigated here.

To assess the spatial organization of CD36 and its effector, Fyn, upon TSP-1 stimulation, we used biochemical and both conventional and super-resolution imaging techniques, combined

with quantitative image analysis. We found that a substantial fraction of unligated CD36 at rest exists in clusters that are enriched with Fyn at all times. Upon TSP-1 stimulation, CD36 clustering is enhanced with the optimal clustering occurring at 10 minutes, forming larger, more compact clusters, leading to Fyn activation. The spatio-temporal organization of pre-existing CD36 clusters as well as Fyn is highly dependent on actin and lipid rafts. Disruption of actin or lipid rafts abrogated TSP-1's ability to enhance CD36 clusters, resulting in inhibition of Fyn activation. Our analysis deciphered a correlation between CD36 cluster size and actin, suggesting growth of the clusters along actin which enables Fyn activation.

Following 10 minutes of TSP-1 stimulation, CD36-TSP-1 internalization occurs. To explore the endocytic mechanism involved and its kinetics, we resorted to antibody labelling and acid washes to follow the internalized receptors. CD36 endocytosis was through the clathrin-independent carrier, GPI-enriched early endosomal compartments pathway (CLIC/GEEC pathway). This internalization was through polymorphous tubules and was dependent on dynamin, actin, cholesterol and Cdc42.

These observations demonstrate a role for nanoclustering in priming receptors for signaling by retaining their downstream effectors in close proximity, ready to signal upon ligand binding and consequent cluster reorganization. The internalization of CD36 through the CLIC/GEEC pathway also opens a new paradigm of cell type specific receptor internalization, as other endocytic mechanisms in different cell types have been characterized for CD36 endocytosis. These observations will also allow future investigation of the role of TSP-1-CD36 endosomes on the TSP-1-CD36-Fyn signaling pathway in ECs. The new insights unraveled in

this study will play a key role in providing clues to design effective and better-targeted TSP-1 based anti-angiogenic compounds.

Preface

The experiments and results presented in this thesis are entirely an original, independent work by the author, John Maringa Githaka, unless otherwise stated. Having completed three lab rotations from September 2009 to December 2009 in Biochemistry Department, University of Alberta, I decided to join Dr. Nicolas Touret lab for my MSc program in January 2010 and later transferred for the PhD program in August 2011. Given my passion for mathematics and physics in life sciences, I got attracted to the fluorescence imaging approaches in his lab.

Touret lab focuses on molecular events at the plasma membrane level and we are part of the Membrane Protein Disease Research Group (MPDRG), University of Alberta. During my first year in the lab, we got into a collaboration with the biophysicist Dr. Khuloud Jaqaman, who at the time was a Systems Biology instructor, Harvard Medical School, a collaboration that led to the findings I present in this thesis. Our project focuses on the organization of the receptor CD36 at the plasma membrane of endothelial cells (ECs), with respect to its interaction with its ligand, thrombospondin-1 (TSP-1). Nicolas and Khuloud have worked together on the organization and dynamics of CD36 at the plasma membrane of macrophages. They had observed a cytoskeletal control of this receptor's diffusion promoting its chances of clustering and signaling function. Their findings led us to investigate if similar mechanism was conserved in CD36 role as an anti-angiogenic receptor in ECs through TSP-1 binding.

The goals of this work is to understand the dynamic changes of CD36 upon TSP-1 ligation, which could play a big role in providing clues to design effective and better-targeted TSP-1 based anti-angiogenic compounds. The contribution of the plasma membrane environment and the endocytic mechanism through which CD36 is internalized is also

investigated. We employed biochemical approaches as well as conventional and advanced imaging techniques combined with quantitative analysis to address our goals. *Chapter 1* introduces the plasma membrane environment, the receptor CD36 and the signaling cascade upon TSP-1 binding. *Chapter 2* details all the materials and methods employed in this thesis. *Chapter 3* reports data that gives us insights into CD36 organization on the ECs plasma membrane, its association with its downstream effector kinase Fyn, and TSP-1's effect on this organization upon binding. *Chapter 4* describes the role actin and lipid rafts play in priming CD36-Fyn organization and association and how this facilitate the TSP-1-CD36-Fyn pathway. *Chapter 5* highlights the possible endocytic pathway, through which CD36 is internalized in ECs. *Chapter 6* summarizes the results from our data, giving perspective to the initiation of TSP-1-CD36-Fyn pathway and future directions.

Dedication

To my wife Sarah, my son, Jonathan and my parents, Duncan and Rosemary, I hope this thesis will help you understand how I got addicted to caffeine ☺. I love you all!

Acknowledgements

Firstly, I would like to express my sincere gratitude to my supervisor Dr. Nicolas Touret for his relentless support of my PhD research. His guidance helped me in all the time of research and writing of this thesis. He has been very supportive in my quest to learn more in the bioimaging world and provided me with opportunities to network and advance my skills. I wish to also extend my gratitude to our collaborator Dr. Khuloud Jaqaman, currently an assistant professor, Department of Biophysics, UT Southwestern Medical Center, and her graduate student, Anthony Vega. The biweekly Skype meetings between us helped build on ideas and develop novel ways to interpret data as well as steering the project in the right direction.

My sincere thanks also goes to my committee members, who are also part of my PhD examining committee, Dr. Carlos Fernandez-Patron and Dr. Ing Swie Goping. They have been very supportive and insightful in overseeing my progress in my project. I could not have wished for a better committee. Special thanks to my external examiner Dr. Ivan Robert Nabi and internal examiner Dr. Maria Febbraio, who despite their busy schedules, have agreed to be part of this defense. They are both experts in areas my project touches on, and I am very grateful for their constructive feedback.

During my research, I have met and made networks with many people who made life easier in this journey. I thank my former lab mates, Andrew and Dr. Amira and current lab mates, Sandra and Swai for all the stimulating discussions and fun we have had in Touret lab. Thank you Aruna, Mohamed and all the graduate students I came to know, for making me laugh even during rough times. Thank you Dr. Barbara Niemeyer and Dr. Markus Hoth and your

awesome research group for hosting me in Germany and teaching me new skills in imaging and electrophysiology.

I wish to thank all the funding agencies; Canadian Institutes of Health Research, Canada Foundation for Innovation, Natural Sciences and Engineering Research Council (NSERC Discovery Research grant), Alberta Innovates Health Solutions Research and International Research Training Group in Membrane Biology from the NSERC-CREATE, whose monetary support made this research possible.

Last but not least, I thank my number one priority, my family, for being so supportive in my research. Special thanks to my lovely wife Sarah, who has selflessly sacrificed so much of her career to see me finish graduate school, I will forever be grateful. Thanks to my son Jonathan, who always manages to put a smile on my face even when I am at my lowest point. To my dad, Duncan and mum, Rosemary, thank you so much for working so hard to put me through school, I hope I make you proud. Thank you to my brother Francis and sister Mercy for all your encouraging words and support, I hope my journey will encourage you in your career paths.

Table of Contents

Abstract.....	ii
Preface.....	v
Dedication.....	vii
Acknowledgements.....	viii
List of Figures.....	xvi
List of Abbreviations.....	xix
Chapter 1 – Introduction.....	1
1.1 Plasma membrane environment.....	2
1.1.1 A brief history of plasma membrane.....	2
1.1.2 Plasma membrane organization.....	5
1.1.2.1 Plasma membrane lipid bilayer.....	6
1.1.2.2 Plasma membrane proteins.....	8
1.1.2.3 Architecture of the Plasma Membrane.....	9
1.1.2.4 Cortical cytoskeleton apposed to the plasma membrane.....	16
1.2 CD36.....	18
1.2.1 CD36 identification and expression.....	18
1.2.2 CD36 ligands and cellular responses.....	21
1.2.2.1 CD36 ligands.....	21
1.2.2.2 CD36 in diseases and immunity.....	22
1.2.2.3 CD36 in metabolism and animal behavior.....	26
1.2.2.4 CD36 in anti-angiogenesis.....	27

1.2.3 CD36 mediated anti-angiogenesis in endothelial cells	28
1.2.3.1 Angiogenesis and tumorigenesis	28
1.2.3.2 Thrombospondin-1	30
1.2.3.3 Fyn.....	33
1.2.3.4 TSP-1-CD36-Fyn pathway in anti-angiogenesis.....	35
1.2.3.5 Clinical Trials of TSP-1 mimetics.....	39
1.2.3.6 Elucidating TSP-1-CD36 signaling in ECs.....	40
1.3 Rationale, hypothesis and objectives.....	41
References	43
Chapter 2 - Materials and methods.....	66
2.1 Cell culture, molecular cloning and stable expression of CD36	67
2.1.1 Cell culture.....	67
2.1.2 DNA plasmids and stable expression of the constructs.....	67
2.2 Western Blotting	68
2.3 Drug Treatment	69
2.4 Chemical Crosslinking	69
2.5 CD36 Knockdown	70
2.6 Immunofluorescence.....	70
2.6.1 TSP-1 labelling	70
2.6.2 Fab fragment generation and labeling.....	71
2.6.3 Immunostaining	71

2.7 Immunofluorescence Imaging.....	72
2.7.1 Confocal Imaging.....	72
2.7.2 TIRFM Imaging.....	73
2.7.3 PALM Imaging.....	73
2.7.4 FRAP Imaging.....	74
2.7.5 FRET Imaging.....	74
2.8 Immunofluorescence Image Analysis.....	74
2.8.1 Miscellaneous image analysis.....	75
2.8.2 FRAP image analysis.....	75
2.8.3 PALM image analysis.....	76
2.8.4 Spatial pattern analysis.....	76
2.8.5 Puncta-continuum colocalization analysis.....	78
2.8.6 Cell mask segmentation.....	80
2.9 Endocytosis-Exocytosis Assay.....	80
2.10 Triton X-100 extraction.....	81
2.11 Cholesterol assay.....	82
2.12 Flow cytometry.....	82
2.13 Graphing and statistical analysis.....	83
References.....	85
Chapter 3 - Insights into CD36-Fyn reorganization upon TSP-1 binding.....	87
3.1 Introduction.....	88

3.2 Results	89
3.2.1 Expression of CD36 in HMEC-1	89
3.2.2 TSP-1 binding in ECs depend heavily on CD36	91
3.2.3 TSP-1 activates caspase 3 in ECs	93
3.2.4 Fyn activation in ECs is CD36 and multivalency dependent	96
3.2.5 CD36 is clustered at steady state; TSP-1 induces further clustering	106
3.2.5.1 TSP-1 induces more clustering of CD36.....	106
3.2.5.2 Spatial Pattern Analysis optimization	109
3.2.5.3 TSP-1 induces compaction of CD36 clusters.....	114
3.2.5.4 Compaction of CD36 clusters is multivalency dependent	123
3.2.6 CD36 clusters are enriched with Fyn at all times	124
3.3 Discussion.....	130
References	133
Chapter 4 - Actin and lipid nanodomains control TSP-1-CD36-Fyn pathway	137
4.1 Introduction.....	138
4.2 Results	139
4.2.1 The membrane-targeting domain of Fyn is sufficient for its recruitment to CD36 clusters	139
4.2.2 CD36-Fyn association is primarily along the actin cytoskeleton	142
4.2.3 CD36-Fyn associate in lipid nanodomains along the actin cytoskeleton	145
4.2.4 CD36 partitioning into rafts is actin dependent	151

4.2.5 Actin cytoskeleton and lipid nanodomains control CD36-Fyn spatial organization	153
4.2.6 TSP-1-CD36-Fyn signaling depends on the actin cytoskeleton and lipid nanodomains...	155
4.2.7 Actin cytoskeleton and lipid nanodomains controls TSP-1 binding to CD36.....	159
4.2.8 CD36 cluster enhancement by TSP-1 depends on the actin cytoskeleton and lipid nanodomains	161
4.2.9 Actin cytoskeleton and lipid nanodomains control CD36 mobility necessary for TSP-1- CD36-Fyn pathway.....	164
4.3 Discussion.....	169
References	175
Chapter 5 - Endocytosis of CD36 in endothelial cells.....	179
5.1 Introduction.....	180
5.2 Results	181
5.2.1 CD36 is endocytosed through CLIC/GEEC pathway, with or without TSP-1	181
5.2.2 CD36 is endocytosed through polymorphous tubules	187
5.2.3: CD36 endocytosis is dynamin dependent.....	190
5.2.4 CD36 endocytosis is dependent on actin, cholesterol and Cdc42	193
5.3 Discussion.....	196
References	198
Chapter 6 - General discussion and conclusions.....	202
6.1 Discussion.....	203
6.2 Conclusions and future work.....	208

References 214

List of Figures

Figure 1-1: Plasma membrane environment.....	5
Figure 1-2: Types of membrane proteins.....	9
Figure 1-3: Schematic of CD36.....	20
Figure 1-4: Angiogenic balance.....	29
Figure 1-5: Schematic linear representation of TSP-1 structure.....	32
Figure 1-6: Schematic representation of Fyn structure.....	35
Figure 1-7: Schematic of TSP-1-CD36-Fyn anti-angiogenic pathway initiation.....	38
Figure 2-1: Representative boxplot features.....	84
Figure 3-1: CD36 expression in HMVECs, HMEC-1 and HMEC-1 stable cell lines.....	90
Figure 3-2: TSP-1 binding in ECs depends on CD36.....	92
Figure 3-3: FRET Caspase 3 biosensor use in monitoring caspase 3 activation.....	95
Figure 3-4: CD36 expression in HMEC-1 recapitulates TSP-1-CD36-Fyn signaling.....	97
Figure 3-5: Fyn activation is CD36 and multivalency dependent.....	100
Figure 3-6: P-Y420 activation increases with CD36 enrichment upon multivalent ligand binding.....	103
Figure 3-7: P-Y420 activation by CD36 multivalent ligands is specific for Fyn.....	105
Figure 3-8: TSP-1 induces more clustering of CD36 in ECs.....	107
Figure 3-9: TSP-1-CD36 complex is at the plasma membrane at 10 minutes time point.....	108

Figure 3-10: Cluster radius R and H-function rMax correlation	111
Figure 3-11: Cluster properties extraction validation using simulations	113
Figure 3-12: SRI of CD36 in HMEC-PAmCherryCD36.....	117
Figure 3-13: TSP-1 effect on CD36 endocytosis-exocytosis axis at 10 minutes time point.	119
Figure 3-14: CD36 is clustered at steady state; TSP-1 induces further clustering	122
Figure 3-15: CD36 clusters compaction is multivalency dependent	124
Figure 3-16: CD36 clusters are enriched with Fyn at all times	127
Figure 3-17: CD45 helps in activation of Fyn in TSP-1-CD36-Fyn pathway.....	129
Figure 4-1: The membrane-targeting domain of Fyn is sufficient for its recruitment to CD36 clusters	141
Figure 4-2: SRI of Fyn-PA-GFP showing its variable anisotropic spatial distribution.....	143
Figure 4-3: CD36-Fyn association is primarily along the actin cytoskeleton	144
Figure 4-4: CD36-Fyn association is independent of actin and lipid nanodomains.....	147
Figure 4-5: CD36 partitions in lipid nanodomains along the actin cytoskeleton	150
Figure 4-6: GPI anchor, a raft marker, partitions along actin.....	150
Figure 4-7: CD36 partitioning into rafts is actin dependent	152
Figure 4-8: Actin cytoskeleton and lipid nanodomains control CD36-Fyn spatial organization	154
Figure 4-9: CD36-Fyn signaling is along the actin cytoskeleton	156
Figure 4-10: CD36-Fyn signaling depends on the actin cytoskeleton and membrane integrity.	158
Figure 4-11: Actin cytoskeleton and lipid nanodomains control TSP-1 binding to CD36.....	160

Figure 4-12: CD36 cluster enhancement by TSP-1 depends on the actin cytoskeleton and lipid nanodomains	163
Figure 4-13: CD36 diffuses and forms clusters along actin	166
Figure 4-14: Actin cytoskeleton and lipid nanodomains control CD36 mobility.....	169
Figure 4-15: PI(4,5)P2 is reduced while PI(3,4,5)P3 is increased in CD36 spots.....	173
Figure 5-1: CD36 is endocytosed through CLIC/GEEC pathway.....	184
Figure 5-2: CD36 endocytosis kinetics.....	186
Figure 5-3: Polymorphous tubules formed during CD36 endocytosis	188
Figure 5-4: CD36 colocalizes with reported tubular structure compartments cargoes.....	189
Figure 5-5: CD36 endocytosis is dynamin dependent	192
Figure 5-6: CD36 endocytosis is actin and cholesterol dependent.....	194
Figure 5-7: CD36 endocytosis is Cdc42 dependent.....	195
Figure 6-1: Proposed model for TSP-1-CD36-Fyn signaling initiation and CD36 endocytic mechanism	210

List of Abbreviations

AF	AlexaFluor
CAA	Cerebral amyloid angiopathy
CD	Cluster of differentiation
Cdc42	Cell division cycle 42
CLESH	CD36, LIMP2, EMP, SRB-1 Homology
CLIC	Clathrin-independent carrier
CtxB	Cholera toxin subunit B
DAPI	4',6-diamidino-2-phenylindole
DIC	Differential interference contrast
DRM	Detergent-resistant membranes
DTSSP	3,3'-dithiobis(sulfosuccinimidyl propionate)
ECM	Extracellular matrix
ECs	Endothelial cells
EGF	Epidermal growth factor
Fab	Fragment antigen-binding
Fc	Fragment crystallizable
FGF	Fibroblast growth factor
FRAP	Fluorescence recovery after photobleaching
FRET	Förster resonance energy transfer
GEEC	GPI-anchored-proteins enriched early endosomal compartment
GFP	Green fluorescent protein
GPI	Glycosylphosphatidylinositol

GPIIIb	Glycoprotein IIIb
GPIV	Glycoprotein IV
GT	Ground truth
HMEC-1	Human dermal microvascular endothelial cell line
HMVECs	Human microvascular endothelial cell line
JNK	c-Jun N-terminal kinases
kDa	Kilodalton
Lat B	Latrunculin B
LCFA	Long chain fatty acids
LIMP-2	Lysosome membrane protein 2
LPA	Lysophosphatidic acid
MHC	Major histocompatibility complex
M β CD	Methyl beta cyclodextrin
NFATc2	Nuclear factor of activated T-cells, cytoplasmic 2
NHS	N-hydroxysuccinimide
nm	Nanometer
nM	Nanomolar
p130Cas	p130 Crk-associated substrate
p38MAPK	p38 Mitogen-activated protein kinases
PALM	PhotoActivated localization microscopy
PCC	Pearson's correlation coefficient
PFA	Para-formaldehyde
PfEMP1	<i>Plasmodium falciparum</i> Erythrocyte Membrane Protein-1

PS	Phosphatidylserine
PTP	Protein tyrosine phosphatase
ROI	Region of interest
SD	Standard deviation
SDS PAGE	Sodium dodecyl sulfate polyacrylamide gel electrophoresis
SEM	Standard error of the mean
SFKs	Src family kinases
Spt-PALM	Single particle tracking PALM
SR-B1	Scavenger receptor class B type I
SRI	SuperResolution imaging
STS	Staurosporine
TEM	Tetraspanin enriched microdomains
Tf	Transferrin
TfrR	Transferrin receptor
TIRFM	Total internal reflection fluorescence microscopy
TSP-1	Thrombospondin-1
VEGF	Vascular endothelial growth factor
Wt	Wild type
β A	β -Amyloid
β ME	β -mercaptoethanol
μ g	Microgram
μ m	Micrometer

Chapter 1 – Introduction

1.1 Plasma membrane environment

1.1.1 A brief history of plasma membrane

Since the emergence of cell theory by Robert Hooke with the help of 17th century microscopes (Hooke 1665), there has been tremendous progress in cell biology research. Despite major advances in discovering properties of the cells, it took nearly three hundred years to accurately predict the structure that separates the inside and outside of the cell, the plasma membrane (Robertson 1959, Edidin 2003). The plasma membrane is a dynamic lipid bilayer that surrounds the cell, interspersed with different plasma membrane proteins, aiding communication between the inside and outside of the cells as well as molecule transport across the membrane (Grecco, Schmick & Bastiaens 2011, Lodish et al. 2000). The lipids in this structure are amphipathic, exposing their hydrophilic head group to the polar cell cytoplasm and extracellular space fluid, while shielding their more hydrophobic tails resulting in an outer and inner leaflet (Tanford 1978).

By mid 1800s, it was generally accepted that the interior of cells were made up of amorphous liquid state substance, commonly referred to as cytoblastema then (Schwann 1847). However, observations such as infusorias (minute aquatic creatures termed so in 1800s (Kent 1881)) pseudopodia formation which wouldn't exist if cells were entirely liquid, led to the postulation of a solid membrane film surrounding individual cells (Meltzer 1906). Work pioneered by Quincke and Overton pointed to this cell film behaving like a “fatty oil” (Edidin 2003) and hence, it was believed cholesterol and phospholipids were its main components (Lombard 2014). This work paved way for concentrated efforts to elucidate the lipid nature of the cell membrane. With the help of 'Langmuir's trough' (Langmuir 1917), Gorter and Grendel

Chapter 1– Introduction

measured the surface area occupied by monolayer lipids extracted from known number of erythrocytes from different mammalian species (Gorter, Grendel 1925). They found the ratio of this surface area to the surface of the total erythrocytes used to be around 2:1, suggesting the plasma membrane was a bilayer (Gorter, Grendel 1925). However, Dervichian and Macheboeuf performed similar experiments and found a 1:1 ratio, predicting a monolayer plasma membrane (Dervichian, Macheboeuf 1938). With the advancement in electron microscope and staining methods, the controversy of whether the plasma membrane was mono or bi-layer was resolved with Robertson's work providing the first visualization of the plasma membrane as a lipid bilayer (Robertson 1959, Robertson 1960).

During most of the 20th century, the plasma membrane was viewed simply as a static passive barrier. A major step in our understanding of this membrane was the postulation of the then famous Singer-Nicolson fluid mosaic model which envisioned a homogeneous random distribution of lipids with proteins embedded in the plasma membrane (Singer, Nicolson 1972). This model still viewed the lipid bilayer as a passive fluid solvent, with the integral membrane proteins contributing to the main functionality of the membrane. While Singer and Nicolson admitted that "...our understanding of the molecular organization of membranes is still rudimentary...", barely a decade passed before experimental findings suggested inaccuracies in the envisioned random distribution of proteins and lipids in the membrane. Observations such as "clusters of lipids" arising from thermal effects on the membrane suggested otherwise (Lee et al. 1974, Wunderlich et al. 1975). Indeed, work done over the last 40 years shows that there is in fact an intricate organization of lipid-lipid, lipid-protein and protein-protein interactions at the plasma membrane environment (Simons, Gerl 2010). This results in functional signaling platforms at the plasma membrane environment such as the 'elusive' lipid rafts (plasma

Chapter 1– Introduction

membrane domains enriched with sphingolipids and cholesterol) (Lingwood, Simons 2010, Munro 2003), tetraspanin enriched microdomains (TEM, membrane domains formed by tetraspanin proteins web) (Yanez-Mo et al. 2009), caveolae domains (flask-shaped invaginations of caveolin-rich membrane domains) (Lisanti et al. 1994), glycosphingolipid-enriched microdomains (Yoshizaki et al. 2008), galectin lattices (Garner, Baum 2008, Nabi, Shankar & Dennis 2015) and flotillin-enriched membrane microdomains (Cremona et al. 2011). Besides the membrane microdomains, there's increasing evidence of the cytoskeleton apposed to the plasma membrane (referred to hereafter as cortical cytoskeleton) and its associated proteins being key regulators of this plasmalemmal organization (Jaqaman, Grinstein 2012, Raghupathy et al. 2015). Their influence ranges from regulating plasma membrane proteins and lipids diffusion and segregation (Edidin, Zuniga & Sheetz 1994, Andrews et al. 2008, Treanor et al. 2010, Jaqaman et al. 2011), as well as their clustering (Lillemeier et al. 2006, Jaqaman et al. 2011, Goswami et al. 2008, Chen et al. 2009).

The complexity of the plasma membrane organization and function has drawn attention of both biologist and physicist in an attempt to unravel its mysteries. As recently noted by (Grecco, Schmick & Bastiaens 2011), advancement in technology and vast amount of research has been dedicated to understanding the structure composition and organization of this membrane since the fluid mosaic model. However, our understanding of this intricate yet well-organized structure "...can still be considered "rudimentary" in light of the complexity of its dynamics that have become apparent since then" (Grecco, Schmick & Bastiaens 2011). More research on the organization at the plasma membrane level is needed to fully understand how molecule transport as well as communication across and within the plasma membrane occurs.

1.1.2 Plasma membrane organization

Most animal's plasma membrane is composed of approximately 50% lipids and 50% proteins, which coordinate in contributing to most of the plasma membrane functions (Dowhan, Bogdanov & Mileykovskaya 2008). As aforementioned, mounting evidence point to a complex yet organized plasma membrane lipid bilayer, not only primed to facilitate membrane protein functions but also directly influencing or regulating their activity and interactions (see Figure 1-1). To dissect cell functions in this environment, we must understand the dynamic organization exhibited by this membrane structure and the behavior exhibited by the membrane lipids and proteins, ranging from their diffusion, anchoring, clustering and interactions of lipid-lipid, protein-lipid and protein-protein complexes. To achieve this, we must focus on elucidating the basic principles underlying their organization and how this supports cellular functions.

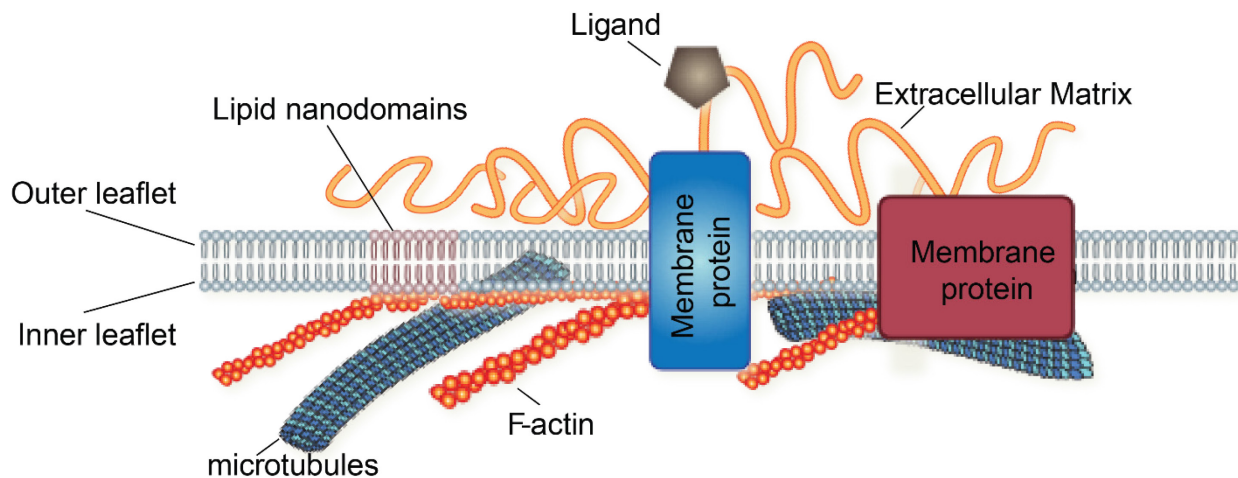


Figure 1-1: Plasma membrane environment

Schematic representation of the plasma membrane environment (adapted from Nicolas Touret's schematics) depicting plasma membrane proteins embedded in the lipid bilayer (composed of inner and outer leaflet). The lipid composition of the

Chapter 1– Introduction

bilayer is not homogeneous and lipid nanodomains have been observed, and thought to provide signaling platforms. The extracellular matrix and apposed cortical cytoskeleton (Filamentous actin (F-actin) and microtubules) have been hypothesized to play a role in organizing the plasma membrane components, aiding communication within and across the membrane.

1.1.2.1 Plasma membrane lipid bilayer

Lipids form the basic structure of the plasma membrane, the lipid bilayer. These lipids are amphipathic in nature and are composed of hydrophobic tails and hydrophilic head groups (Tanford 1978). The hydrophobic tails self-associate to minimize their contact with polar fluid in an entropy driven organization, while the polar head groups are exposed to the aqueous cell environment. This results in a stable energetically favorable closed compartment lipid bilayer, separating the inside and outside of the cell (Dowhan, Bogdanov & Mileykovskaya 2008).

Eukaryotic plasma membranes lipids can be classified into 3 main categories; glycerophospholipids, sphingolipids and sterols, with cholesterol being the only sterol in mammalian cells membranes (Simons, Sampaio 2011). Glycerophospholipids can vary from the composition of the head group, to the length and extent of saturation in the fatty acids chains (the lipid tails) (Hishikawa et al. 2014). Most variation is observed in sphingolipids whose head group composition can take over 500 different forms of the carbohydrate moiety of glycosphingolipids, besides the tendency to have different ceramide backbones (Futerman, Hannun 2004). In addition, the amount of energy and steps required to synthesize sterols in eukaryotes is enormous (Ye, DeBose-Boyd 2011, Mouritsen, Zuckermann 2004), involving about thirty enzymes which control sterol concentration. The diversity in these lipids results in

Chapter 1– Introduction

hundreds of lipids species in the eukaryotic membranes (van Meer, Voelker & Feigenson 2008). This is thought to help prevent membrane leakage by matching ‘holes’ in lipid-protein interface of membrane proteins, given the diversity that comes with the membrane proteins transmembrane domains (Simons, Sampaio 2011).

Besides forming a physical barrier and housing the membrane proteins, the lipid bilayer lipids also plays an active role in most of the cell signaling pathways (Fernandis, Wenk 2007) and energy storage (Jensen 2002). For instance, storage of lipids in adipose tissue provides an excellent long term energy source for the body (Scherer 2006). The phospholipids, phosphoinositides, utilize their different phosphorylation states to act as molecular signatures in regulating endocytic pathways (Clague, Urbe & de Lartigue 2009). The hydrolysis of plasma membrane phosphatidylinositol 4,5-bisphosphate (PI(4,5)P₂) by phospholipase C (PLC) generates secondary messengers inositol 1,4,5-trisphosphate (IP₃) and diacylglycerol (DAG), which are used in signal transduction and lipid signaling (Berridge 1984). The polar IP₃ diffuses into the cytoplasm and binds IP₃ receptors on endoplasmic reticulum (ER), causing Ca²⁺ release into the cytosol from ER (Thatcher 2010). The binding of Ca²⁺ and the earlier generated DAG to protein kinase C (PKC) activates it (Kadamur, Ross 2013), a kinase that has been implicated in different signaling pathways (Marengo et al. 2011).

All these observations seem to be well coordinated, implying a synchronized effort by the cell to organize the lipids and proteins in specific manners to either activate, inhibit or propagate specific signaling pathways. Studying specific pathways occurrences on the plasma membrane will be key in delineating the specific molecular organization involved, and the contribution of this environment in that pathway.

Chapter 1– Introduction

1.1.2.2 Plasma membrane proteins

The plasma membrane lipid bilayer houses proteins, termed plasma membrane proteins, which aid in communication laterally within the membrane and across the membrane between the cell and its environment (Rucevic, Hixson & Josic 2011). They constitute approximately 30% of the proteins encoded by a cell (Krogh et al. 2001). Their functions are critical as highlighted by the wide range of cell dysfunctions and diseases associated with membrane protein(s) alteration(s) (Ng, Poulsen & Deber 2012). Understanding how these proteins orchestrate their functions within the plasma membrane will unlock doors to identification of new biomarkers and therapeutic targets (Rucevic, Hixson & Josic 2011).

There are four different types of membrane associated proteins; GPI-anchored (glycophosphatidylinositol), transmembrane proteins (includes type I, type II and multi-pass proteins), lipid-anchored and peripheral membrane proteins (Figure 1-2) (von Heijne 2006). An emerging feature of these proteins has been their compartmentalization in the membrane, governed by lipid-lipid, lipid-protein and protein-protein interactions (Garcia-Parajo et al. 2014). The widely accepted hypothesis that accounts for this organization is the formation of membrane domains, which can form either through segregation of specific types of lipid (Lingwood, Simons 2010) or domains supported by proteins such as caveolin-1, flotillin and tetraspanins (Lisanti et al. 1994, Otto, Nichols 2011, Yanez-Mo et al. 2009). This is thought to help in increasing regulation efficiency of signalling pathways within the membrane (Garcia-Parajo et al. 2014).

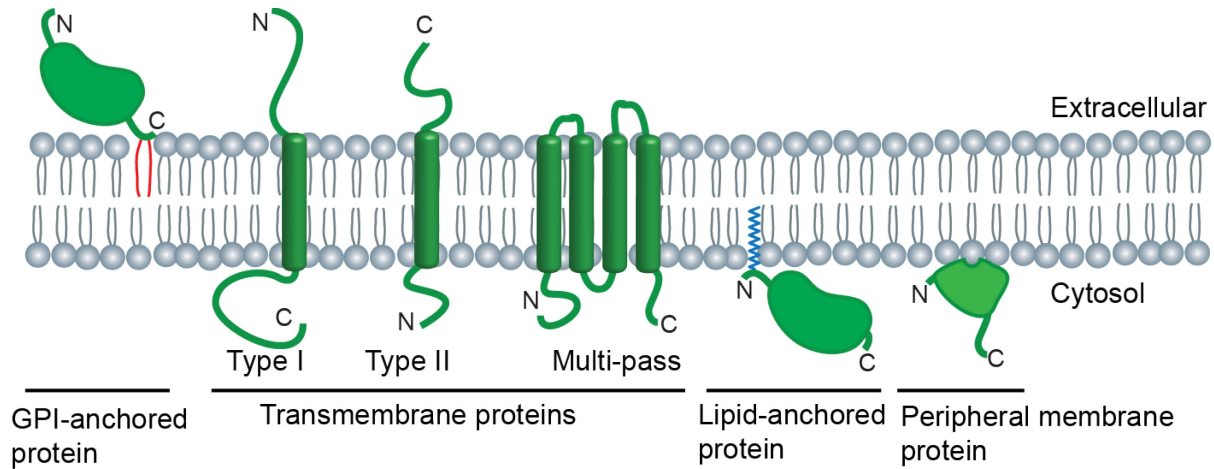


Figure 1-2: Types of membrane proteins

Classes of associated membrane proteins, with their amine- and carboxyl-termini depicted as N and C respectively. GPI-anchored proteins are extracellular and are linked at their carboxyl-terminus by a GPI-anchor in the outer leaflet. Type I and type II have single transmembrane domain with either the N-terminus in the extracellular or intracellular space respectively. Multi-pass transmembrane proteins traverse the bilayer more than one time. Lipid-anchored proteins are attached to the inner leaflet of the membrane by lipid(s). Peripheral membrane proteins attach to the inner leaflet, often temporarily, through interaction either with transmembrane proteins or via specific lipid binding domains that directly interact with the peripheral regions of the inner leaflet.

1.1.2.3 Architecture of the Plasma Membrane

The plasma membrane is divided in numerous mesoscale domains, in which specific molecules are enriched (Garcia-Parajo et al. 2014). To date, the full extent of these domains heterogeneities is still unknown, and represent an intense field of investigation. However, some of the domains have been described, a quick review of these domains and their functions will be presented below.

Chapter 1– Introduction

- *Tetraspanin enriched microdomains*

Tetraspanins is a large group of membrane proteins with four transmembrane domains, sharing conserved secondary and tertiary structure but low sequence homology (Yanez-Mo et al. 2009). Their ability to self-associate as well as interact with other receptors at the plasma membrane enables them to form proteins web like compartments termed tetraspanin enriched microdomains (TEM) (Yanez-Mo, Mittelbrunn & Sanchez-Madrid 2001, Yanez-Mo et al. 2009). In humans, 32 members have been identified (Yanez-Mo et al. 2009), a diversity that brings heterogeneity in these domains sizes. For instance, TEM in urinary tract epithelium apical membrane form 16 nm protein complexes (Min et al. 2006) while in other cell types, their area size ranges between 200 nm² to 400 nm² (Barreiro et al. 2008, Nydegger et al. 2006, Espenel et al. 2008).

Tetraspanins interact with different membrane receptors (over 55 different receptors (Yanez-Mo et al. 2009)) resulting in their implication in cell adhesion, membrane fusion, intercellular communication as well as intracellular signaling (Hemler 2003, Liu et al. 2007, Berditchevski 2001, Levy, Shoham 2005, Yanez-Mo, Mittelbrunn & Sanchez-Madrid 2001, Yanez-Mo et al. 2009). For example, TEMs have been implicated in trapping major histocompatibility complex I and II (MHC-I and II) signaling molecules at the immune synapse hence regulating antigen presentation (Kropshofer et al. 2002, Unternaehrer et al. 2007). Tetraspanins could also be potentially used as novel cancer therapeutic targets, as there is increasing evidence pointing to a role of these proteins in promoting multiple cancer stages and tumor vascularization (Hemler 2014).

Chapter 1– Introduction

- *Lipid rafts*

Lipid supported membrane domains remain the most intriguing and controversial concept in membrane organization. They were first hypothesized to explain lipid sorting in epithelial cells (Simons, van Meer 1988) and later postulated as sphingolipid-cholesterol enriched microdomains (Simons, Ikonen 1997). They are thought to have tight lipid packing due to enrichment with long saturated sphingolipids hydrocarbon chains, with cholesterol acting as a glue by filling in to compensate hydrophobic mismatch (Raghupathy et al. 2015, Munro 2003). Brown and Rose were first to describe lipid rafts as ‘detergent-insoluble microdomain’ as they found sphingolipids and GPI-anchored proteins were present in the insoluble detergent resistant membranes (DRM) upon non-ionic triton X-100 detergent solubilization at 4°C (Brown, Rose 1992, Cerneus et al. 1993). This, together with the finding that cholesterol was involved in this detergent insolubility (Schroeder, London & Brown 1994), became the defining method for lipid rafts residents as proteins and lipids partitioning in DRM (Simons, Ikonen 1997, Brown 2006, Lingwood, Simons 2007). This biochemical approach to defining lipid rafts has been marred with controversy as questions arise whether the observed lipid phase separation really pre-exists on the surface of living cells or it is just an artifact of the detergent solubilization itself (Munro 2003).

Characterization of these lipid imposed corals remains elusive, due their proposed transient nature and small size (from 10th to hundreds of nm) (Simons, Gerl 2010). Recent advancement in technology has expounded on our understanding of these lipid nanodomains. They are nanoscale dynamic sphingolipid-cholesterol enriched lipid nanodomains which can coalesce to form larger domains (Simons, Gerl 2010). Their clustering, stability and functions is

Chapter 1– Introduction

governed by lipid-lipid, lipid-protein and protein-protein interactions with the membrane and its environment (Lingwood, Simons 2010, Simons, Gerl 2010). They have been implicated in membrane trafficking, signaling and viral infection (Simons, Gerl 2010). It's worth noting that there is raft heterogeneity, owing to the type of sphingolipids and proteins present in individual rafts (Pike 2004, Mishra, Joshi 2007, Lingwood et al. 2009). However, this heterogeneity has drawn skepticism and lipid nanodomain existence remains controversial (Hancock 2006). Currently, lipid rafts are among the top five mysteries of the cell (Travis 2011, Leslie 2011). More work is needed to better define rafts heterogeneity, their dynamics and functions.

- *Flotillin domains*

Flotillin are ubiquitous membrane associated proteins and comprise flotillin 1 and flotillin 2 (Otto, Nichols 2011). Their tendency to self-associate into distinct nanodomains, just like tetraspanins, facilitates compartmentalization (Frick et al. 2007, Solis et al. 2007, Otto, Nichols 2011). Flotillin-1 and 2 co-assembly is necessary to form these flotillin domains, with the two colocalizing in small plasma membrane puncta (Frick et al. 2007, Babuke et al. 2009). Just like lipid rafts, flotillin also partitions into DRMs, but the necessity for flotillin 1 and 2 to form these domains, makes them distinct domains (Otto, Nichols 2011, Babuke, Tikkanen 2007). Their lack of any interaction or signaling motifs combined with less information on the proteins flotillins interact with, has made the understanding of these domains functions a challenge (Otto, Nichols 2011). However, there are some reports suggesting the involvement of these domains in making signaling platforms as well as endocytic domains (Otto, Nichols 2011).

Flotillin domains have been implicated in providing signaling platforms. For example, the polarization of flotillins into one side of the T cells, forms a flotillin 'cap', the site at which

Chapter 1– Introduction

the immunological synapse forms (Rajendran et al. 2003). These domains localize a Src family kinase, Lck, and co-stimulating these T cells with anti-CD28 and anti-CD3 antibodies recruits linker for activation of T cells (LAT) to these domains for signaling (Slaughter et al. 2003). Flotillin domains have also been shown to mediate clathrin-independent endocytosis (Hansen, Nichols 2009). For instance, flotillin domains mediate internalization of two neurotransmitter transporters, SLC6A3 (solute carrier family 6, member 3) and SLC1A2 (solute carrier family 1, member 2), i.e. dopamine and glutamate transporters respectively (Cremona et al. 2011, Otto, Nichols 2011). While the mechanistic details of this flotillin-mediated endocytosis remains unclear (Otto, Nichols 2011), Src family kinase, Fyn, has been shown to phosphorylate flotillin 1 tyrosine 160 and flotillin 2 tyrosine 163, and mutating these tyrosines to phenylalanine abrogates flotillin domain mediated endocytosis (Riento et al. 2009). More research is needed to better define flotillin domains functions and regulation.

- *Caveolae domains*

Caveolae domains are 60 nm to 80 nm wide pits on the plasma membrane, commonly described as flask shaped due to their constricted necks, although their shape has been described as craters or open cups in cryofixation (Schlormann et al. 2010, Richter et al. 2008, Parton, del Pozo 2013). Membrane associated caveolin proteins (Caveolin 1 and 3) drive the formation and functions of caveolae, with the help of cytoplasmic proteins called cavins (Parton, del Pozo 2013). Similarly to flotillin domains, caveolae also partition into DRM, but the necessity for caveolin and cavins proteins to form these domains, makes them distinct domains (Lingwood, Simons 2007).

Chapter 1– Introduction

Besides their role in the vastly studied caveolae mediated endocytosis (Lajoie, Nabi 2010) as well as protective role in mechanosensing, where caveolae pits flatten upon plasma membrane stretching (Sinha et al. 2011, Lee, Schmid-Schonbein 1995, Dulhunty, Franzini-Armstrong 1975, Kozera, White & Calaghan 2009), caveolae domains also play a role in plasma membrane organization and signaling (Parton, del Pozo 2013). Caveolae have been shown to provide signaling platforms by spatially segregating signaling components. For example, in the plasma membrane, caveolae maintains store-operated channel TRPC1 (Transient receptor potential channel 1), at the junctions between plasma membrane and ER (Pani et al. 2009, Parton, del Pozo 2013). Caveolin 1 enables TRPC1 clustering as well as regulating TRPC1 interaction with ER protein STIM1 during store-operated calcium entry (SOCE) (Pani et al. 2009). Evidence points towards caveolin 1 driven plasma membrane domains being critical in enabling this localized calcium signaling (Sharma et al. 2010, Isshiki et al. 1998, Yamamoto et al. 2011). Caveolae dysfunction has been linked to various diseases and further investigations to decipher these domains functions and regulation will shed new light and offer possible therapeutic targets (Parton, del Pozo 2013).

- *Galectin lattices*

Galectins, a family of multivalent lectins (i.e. glycan-binding proteins), have been shown to organize plasma membrane into domains commonly referred to as galectin lattices (Garner, Baum 2008, Nabi, Shankar & Dennis 2015). The mammalian family consists of 15 members, galectin-1 to 15, sharing a common single or dual CRD (carbohydrate recognition domain) motif (Nabi, Shankar & Dennis 2015). Once secreted from the cells, galectins can bind plasma membrane glycans such as N- and O-glycans on glycoproteins (Nabi, Shankar & Dennis 2015).

Chapter 1– Introduction

Galectins have been implicated in regulating glycoproteins and glycolipids segregation, mobility and internalization at the plasma membrane (Garner, Baum 2008, Nabi, Shankar & Dennis 2015). For example, in the intestinal cell microvillar membranes, galectin-4 has been shown to organize plasma membrane glycoproteins such as aminopeptidase N and alkaline phosphatase into glycan-dependent galectin lattice, stabilizing their partitioning into lipid raft domains (Braccia et al. 2003). Recently, galectin-3, a galectin that can oligomerize into pentamers, has been shown to drive formation of the endocytic structures, clathrin-independent carriers (CLICs) (Lakshminarayan et al. 2014). In this case, the binding of monomeric galectin-3 to glycosylated cargo proteins compartmentalizes these proteins at the plasma membrane, causing galectin-3 oligomerization and subsequent glycosphingolipids recruitment. This in turn results in plasma membrane bending and CLICs endocytic pit formation to internalize the cargo proteins (Lakshminarayan et al. 2014). There is still more to be elucidated in the world of galectin lattices as we try to understand this additional level of plasma membrane glycoprotein and glycolipids organization.

- *Other plasma membrane domains*

There has been reports of other plasma membrane microdomains, which have either been categorized into one of the aforementioned domains or have not been fully described. For instance, microdomains of GPI-anchored proteins (Friedrichson, Kurzchalia 1998), which are found in DRM, are generally considered lipid raft domains (Simons, Gerl 2010). Formation of other plasma membrane microdomains has been demonstrated through ionic protein-lipid interactions, independent of cholesterol or lipid phases (van den Bogaart et al. 2011).

Chapter 1– Introduction

1.1.2.4 Cortical cytoskeleton apposed to the plasma membrane

The cell cytoskeleton is a dynamic three-dimensional structure made up of actin filaments, microtubules and intermediate filaments (Fletcher, Mullins 2010). In the classic description of its role, it maintains cell shape and internal organization, while providing mechanical support that is key for cell functions like movement and division (Fletcher, Mullins 2010). Over the last 20 years, mounting evidence has emerged, suggesting cytoskeleton involvement in organizing the crowded plasma membrane environment (Jaqaman, Grinstein 2012). This has been accredited to the portion of the cytoskeleton that is found just beneath the plasma membrane, termed cortical cytoskeleton. (Jaqaman, Grinstein 2012).

The first evidence for role of the cortical cytoskeleton in controlling membrane organization comes mainly from the group of Dr. A. Kusumi, which proposed an explanation for the decreased diffusion of outer leaflet lipids by the ‘fence and pickets’ model (discussed below) (Kusumi et al. 2005, Kusumi, Sako 1996, Feder et al. 1996). Indeed, some of the aforementioned membrane domains have also been shown to be controlled by the cortical cytoskeletal mesh. There are two possible mechanisms through which the cortical cytoskeleton organizes and regulates the plasma membrane environment, either independently or interdependently.

One, as put forward by the ‘fence and pickets’ model, the cortical cytoskeleton can aid formation of barriers that affect distribution and diffusion of proteins and lipids not even associated with this mesh (Kusumi et al. 2005). Lipids showed reduced diffusivity, up to a factor of 5–100 in cells plasma membrane, compared to their counterparts in artificial bilayers (Fujiwara et al. 2002). The reduced mobility was shown to be due to plasma membrane’s cortical cytoskeleton compartmentalization, a finding that helped coin the ‘fence and pickets’ model

Chapter 1– Introduction

(Kusumi et al. 2005, Fujiwara et al. 2002). This model hypothesizes the cortical cytoskeleton mesh forming the ‘fences’ with the transmembrane proteins anchored to it, directly or indirectly, forming the ‘pickets’. This results in compartments with the ‘pickets’ standing in the way of protein and lipid diffusion, with occasional, hop diffusion from one compartment to another (Kusumi et al. 2005, Fujiwara et al. 2002). It is worth noting that hop diffusion can also result from transmembrane protein cytoplasmic tails bumping into the mesh, and occasionally ‘hopping’ over the mesh barrier (Suzuki et al. 2005, Fujiwara et al. 2002).

Two, membrane proteins can be attached to this mesh directly or indirectly through adaptor molecules. This affects their mobility around the membrane, as well as their stability and functional relevance, depending on how strongly and how long they are associated with the cytoskeleton. For instance, TEMs are connected to the cortical actin, and direct binding has been shown between tetraspanins and actin linkers ezrin–radixin–moesin (ERM), possibly regulating signaling in TEM web (Sala-Valdes et al. 2006). Cortical actin has also been implicated in GPI-anchored protein nanodomain formation and regulation (Goswami et al. 2008, Gowrishankar et al. 2012, Raghupathy et al. 2015). Recent data suggests that the trans-bilayer coupling of long saturated acyl-chain lipids on the outer leaflet with long acyl-chain-containing phosphatidylserine (PS) in the inner leaflet, together with cholesterol filling in the hydrophobic mismatches, drives GPI-anchored protein nanocluster formation in an actin dependent manner (Raghupathy et al. 2015, Goswami et al. 2008). In line with these observations, cortical actin filaments have been implicated as the main driving force for lipid raft domain formation (Dinic, Ashrafzadeh & Parmryd 2013).

Chapter 1– Introduction

It is becoming increasingly clear that cortical cytoskeleton plays a critical role not only in regulating membrane dynamics and organization but also in controlling transmembrane signaling. The latter phenomenon is at the center of my PhD work which focuses on how plasma membrane organization affects CD36 signaling. CD36 is a transmembrane protein that has been shown to be controlled by the cell cortical cytoskeleton at the plasma membrane of macrophages (Jaqaman et al. 2011). A subpopulation of this receptor diffuses along the cortical cytoskeleton troughs, a phenomenon that increases its chances of colliding and clustering together. This was hypothesized to prime this receptor for ligand binding and signaling (Jaqaman et al. 2011). CD36 is a multi-ligand receptor regulating different pathways in different cell types (Ge, Elghetany 2005). The following section introduces CD36 and its many biological functions.

1.2 CD36

1.2.1 CD36 identification and expression

CD36 is an integral membrane protein belonging to the scavenger receptor family which includes structurally unrelated receptors grouped based on their ability to bind modified forms of lipoproteins (Moore, Freeman 2006, Pluddemann, Neyen & Gordon 2007). It falls in the class B scavenger receptor subfamily, which also includes LIMP-2 (Lysosomal integral membrane protein 2) and SR-B1 (Scavenger receptor class B type 1) (Pluddemann, Neyen & Gordon 2007). It was first identified as glycoprotein IV (GPIV) or Glycoprotein IIIb (GPIIIb, according to the nomenclature of (Clemetson et al. 1977)), the fourth major platelet membrane glycoprotein (Okumura, Jamieson 1976, Tsuji, Osawa 1986). GPIV was later found to be identical to the leukocyte differentiation antigen designated CD36 (Shaw 1987).

Chapter 1– Introduction

CD36 has two transmembrane domains, a large extracellular loop and two intracellular short N- and C- terminal tails (Figure 1-3) (Kralisz 2001). The extracellular loop contains three disulfide bonds arranged in a 1-3 (C243-C311), 2-6 (C271-C333) and 4-5 (C313-C322) pattern (Rasmussen et al. 1998). There are ten putative glycosylation sites on the external loop, nine of which have been shown to be *N*-linked glycosylated (Hoosdally et al. 2009). CD36's molecular weight of unglycosylated form is only 53-kDa, with different glycosylation states shifting this weight to 78–94 kDa on SDS-PAGE (Hoosdally et al. 2009, Daviet et al. 1997). There are four intracellular cysteine residues, two on each N- and C- terminal tails, which are all palmitoylated (Tao et al., 1996) and necessary for its proper targeting to the plasma membrane (Thorne et al. 2010). Phosphorylation of its threonine 92 residue regulates its ligand binding (Asch et al. 1993, Chu, Silverstein 2012).

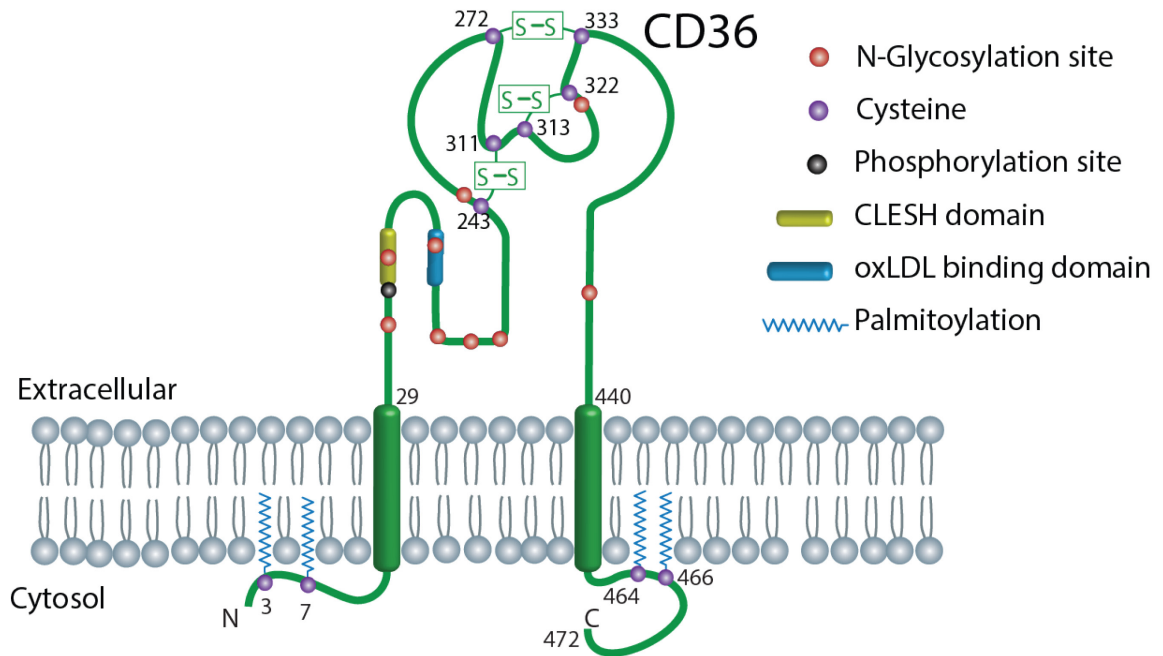


Figure 1-3: Schematic of CD36

CD36 is a two transmembrane domain protein, with two short cytosolic domains at the N- and C-termini that are dually palmitoylated on intracellular cysteine residues. It has a large extracellular domain that is heavily glycosylated and contains six cysteine sites all involved in intramolecular disulfide bonds formation. It has a phosphorylation site on threonine 92. Its two major ligand binding domains, CD36, LIMP-2, Emp, SRB-1 Homology (CLESH) domain (CLESH domain) and oxLDL (oxidized Low Density Lipoprotein) binding domain, are highlighted in yellow and blue respectively.

CD36 is expressed mainly in platelets (Tandon et al. 1989), adipocytes (Harmon, Abumrad 1993), hepatocytes (Miquilena-Colina et al. 2011), macrophages (Fadok et al. 1998), dendritic cells (Albert et al. 1998), microglia (Coraci et al. 2002), retinal pigment epithelium

Chapter 1– Introduction

(Ryeom et al. 1996), intestinal epithelial cells (Goncalves et al. 2014), taste bud cells (Simons et al. 2011) and microvascular endothelial cells (Dawson et al. 1997). Over the years, it has been shown to bind a wide array of different ligands, triggering different signaling pathways depending on ligand and cell type (Silverstein, Febbraio 2009, Ge, Elghetany 2005). It has attracted a lot of attention as its intracellular tails are very short and lack any canonical signaling motif, yet it is involved in many cellular pathways.

Currently, the structure of CD36 has not been experimentally solved. However, the elucidation of X-ray crystal structure of the extracellular portion of LIMP-2, a close homolog of CD36, has allowed homology modeling using this 3D structure as a template (Neculai et al. 2013, Tarhda, Ibrahimi 2015). The model structure reveals an interconnected cavity traversing the whole CD36 extracellular domain, possibly representing the tunnel through which CD36's ligands, such as LCFAs (long chain fatty acids), passes on to get to the plasma membrane and subsequent penetration into the cell cytoplasm. Being a multiligand receptor, to fully understand the initial ligand binding steps and conformation changes involved if any, different molecular docking tests need to be done. Indeed a recent docking and simulation study between model CD36 structure and LCFAs showed a flexible docking of the ligand, as it pass through the tunnel to get to the plasma membrane and penetrate into the cell cytoplasm (Tarhda, Ibrahimi 2015). A review of the known CD36 ligands and their resulting cellular responses will be next discussed.

1.2.2 CD36 ligands and cellular responses

1.2.2.1 CD36 ligands

CD36 has emerged as a multi-ligand receptor mediating different signaling pathways that invoke different cellular responses depending on the type of ligand and cell type. This has led to

Chapter 1– Introduction

its implication in several pathophysiological conditions involving immunity, metabolism, angiogenesis and animal behavior (Silverstein, Febbraio 2009, Febbraio, Hajjar & Silverstein 2001). CD36 ligands include oxidized low density lipoprotein (oxLDL) (Endemann et al. 1993, Nicholson et al. 1995), oxidized phospholipids (Podrez et al. 2002), thrombospondin (Asch et al. 1987), LCFAs (Baillie, Coburn & Abumrad 1996), anionic phospholipids (Ryeom et al. 1996), *Plasmodium falciparum* Erythrocyte Membrane Protein-1 (PfEMP1) (Oquendo et al. 1989), collagen (Tandon, Kralisz & Jamieson 1989), native lipoproteins (Calvo et al. 1998) and β -amyloid (Coraci et al. 2002). The cellular responses and pathological states elicited by the binding of these ligands to CD36 are discussed below.

1.2.2.2 CD36 in diseases and immunity

CD36 has been implicated in various diseases and immune responses. Below is its ligands, their involvement in diseases and immunity and emerging roles of CD36 as a potential prognostic marker of pathological states.

- *Phosphatidylserine*

Clearance of apoptotic cells is essential in maintaining tissue homeostasis and normal development (Poon et al. 2014). During apoptosis, phosphatidylserine (PS) exposure from inner to outer leaflet of the apoptotic cells plasma membrane is a classic “eat me” feature, triggering their efferocytosis by phagocytic immune cells (Marino, Kroemer 2013, Segawa, Nagata 2015). CD36 in macrophages and dendritic cells has been proposed to mediate this PS recognition on apoptotic cells (Fadok et al. 1998, Albert et al. 1998). Although unmodified PS is generally considered as the “eat me” signal, oxidized PS (oxPS) has also been implicated (Kagan et al.

Chapter 1– Introduction

2002). Recent findings suggest macrophage CD36 interaction with oxPS is essential in apoptotic cells efferocytosis as clearing of apoptotic cells in CD36 knockout mice wounds was significantly impaired compared to wildtype (Greenberg et al. 2006). Its role in efferocytosis seems to be evolutionary conserved. In *Drosophila* macrophages, CD36-related receptor, croquemort, has been shown to be required in the clearing of apoptotic cells, although the ligand it recognizes in this process is yet to be identified (Franc et al. 1996, Franc et al. 1999). CD36 has been shown to bind unmodified PS (Rigotti, Acton & Krieger 1995, Ryeom et al. 1996), and oxPS (Greenberg et al. 2006). More research is needed to better define if CD36 mediated efferocytosis is exclusively through PS or oxPS or both.

Cytokine induced macrophage fusion to form multinucleated giant cells is characteristic of granulomatous infections, though the significance of this is unknown (Anderson 2000, Helming, Gordon 2007). CD36 binding to PS has also been implicated in formation of these multinucleated giant cells. Transient exposure of PS in non-apoptotic macrophages has been reported (Callahan, Williamson & Schlegel 2000), and shown to be necessary in the macrophage fusion (Helming, Winter & Gordon 2009). CD36 has been suggested to mediate recognition of this PS during the cytokine-induced macrophage fusion (Helming, Winter & Gordon 2009).

- *oxLDL*

Atherosclerosis, a disease characterized by plaque builds up of fibrous elements and lipids accumulation in arteries, has been accredited to be the leading cause of heart disease and stroke (Lusis 2000). A key feature in atherosclerosis pathogenesis is the uptake of oxLDL in macrophages via CD36, to form cholesterol-engorged macrophages termed foam cells in arteries, enhancing plaque buildup (Febbraio et al. 2000, Rahaman et al. 2006). De-lipidated oxLDL lacks

Chapter 1– Introduction

the capacity to bind CD36, suggesting that oxLDL binding to this receptor is mediated by oxidized lipids (Silverstein et al. 2010, Podrez et al. 2002). Indeed, oxLDL has recently been shown to bind CD36 in a fatty acid dependent mechanism (Jay et al. 2015). oxLDL binding to CD36 has been shown to activate the transcription factor, PPAR- γ (peroxisome proliferator activated receptor-gamma), increasing CD36 expression in macrophages, which would in turn increase foam cells turn over (Tontonoz et al. 1998, Feng et al. 2000) . The molecule curcumin was recently shown to inhibit oxLDL induced CD36 expression in macrophages, abrogating foam cell formation (Min et al. 2013). Similarly, the molecule icariin downregulated CD36 expression, resulting in inhibition of foam cell formation (Yang et al. 2015). These observations suggests inhibition of CD36 expression or inhibiting CD36-oxLDL interaction could serve as a target in abrogating foam cells formation, and possibly delaying any atherosclerotic onset.

- *PfEMP1*

For over a hundred years, malaria parasite infected erythrocytes have been known to be sticky in blood capillaries (Marchiafava, Bignami 1894, Berendt, Ferguson & Newbold 1990), a characteristic that has dire consequences especially in cerebral and placental malaria (Clark 1915, Storm, Craig 2014). The malaria parasite *Plasmodium falciparum* infected erythrocytes (IEs) adheres to the microvascular endothelial cells through expression of antigens belonging to a family of proteins termed *Plasmodium falciparum* Erythrocyte Membrane Protein-1 (PfEMP1) (Howard et al. 1988, Baruch et al. 1995, Smith et al. 1995, Su et al. 1995). To achieve this adherence, PfEMP1 binds to CD36 on ECs (Baruch et al. 1996). The importance of CD36 binding PfEMP1 is controversial as some see it as a means for IEs to evade host splenic clearance, which benefits the parasite (Rowe et al. 2009, Serghides et al. 2003), while others

Chapter 1– Introduction

argue that this traps the IEs making it easier for immune cells to detect, and phagocytose the infected RBCs, ironically using CD36 on the immune cell as a scavenger receptor (McGilvray et al. 2000, Serghides et al. 2003). Recent evidences suggest that expression of PfEMP1 specific for CD36 binding on IEs is characteristic of *Plasmodium falciparum* from uncomplicated, less severe malaria (Cabrera, Neculai & Kain 2014, Ochola et al. 2011, Hviid, Jensen 2015). There is need for further studies on the precise functions of CD36 in malaria infection and progression in order to fully harness the potential of CD36 being a target for malaria treatment (Cabrera, Neculai & Kain 2014).

- *β-amyloid*

There is a correlation between alterations in cerebral blood vessels and Alzheimer's disease (AD) resulting from brain dysfunction (Iadecola 2010, Holtzman, Morris & Goate 2011). Deposition of β -amyloid (β A) in cerebral blood vessels, which causes cerebral amyloid angiopathy (CAA), is mediated by CD36 in microglia cells (Park et al. 2013). Indeed microglia CD36 has been implicated in initiating inflammatory responses by binding β A fibril deposits in senile plaque, a key feature in AD pathology (Coraci et al. 2002). CD36 also causes β A deposition in cerebral blood vessels independent of AD (Ricciarelli et al. 2004) with the resultant CAA often giving rise to brain hemorrhage, cognitive impairment and silent ischemic infarcts (Kimberly et al. 2009, Gorelick et al. 2011). From these findings, inhibition of β A binding to CD36 would serve as a therapeutic target against β A accumulation, hence CAA and AD prevention.

- *Potential pathological state marker*

Recently, a soluble circulating form of CD36 has been reported in human plasma (Handberg et al. 2006) and shown to be associated with circulating microparticles (Alkhatatbeh et al. 2011). This form of CD36 has been found to be elevated in plasma in pathological states like steatosis (Garcia-Monzon et al. 2014), liver injury (Himoto et al. 2013, Fernandez-Real et al. 2009), plaque instability, atherosclerosis, monocyte activation and inflammation (Handberg et al. 2008), obesity, insulin resistance (Fernandez-Real et al. 2009) and diabetic nephropathy (Shiju et al. 2015). Increased mRNA levels of CD36 in peripheral blood mononuclear cells has been proposed to be a marker for diagnosis of atherosclerosis (Yazgan et al. 2014). Soluble CD36 role in these pathological states remains unclear, but its elevation in the plasma can be utilized as a plausible prognostic marker.

1.2.2.3 CD36 in metabolism and animal behavior

CD36 has long been known to bind long chain fatty acids (LCFAs) (Baillie, Coburn & Abumrad 1996) and the implications of this has become apparent in metabolism and animal behavior (Silverstein, Febbraio 2009). For instance, in the gastro-colic and crypt-to-villus axes of the proximal small intestine epithelial cells, CD36 has been shown to facilitate uptake of dietary LCFAs and cholesterol which are important for energy, storage, and other cellular processes (Drover et al. 2008, Nassir et al. 2007, van Bennekum et al. 2005). In the human intestinal epithelium, CD36 has been implicated in the uptake of dietary vitamin K1 (Goncalves et al. 2014), a fat-soluble vitamin commonly regarded as “haemostasis vitamin”, essential for blood clotting and bone calcification (Willems et al. 2014). Of note, while it is generally agreed CD36 facilitates uptake of these fatty acid molecules, the mechanism of uptake is controversial,

Chapter 1– Introduction

as Pownall and Moore recently put it, “the Diffusionists versus the Translocatists” (Pownall, Moore 2014). More investigation is needed to decipher whether CD36 helps fix the fatty acids into the plasma membrane, hence facilitating their diffusion into the cytoplasm or CD36 acts as a transporter, transporting fatty acids across the plasma membrane into the cytoplasm.

There is also evidence that lingual CD36 on taste bud epithelial cells acts as a taste receptor for dietary fatty acids (Laugerette et al. 2005). Most dietary fat is present as triglycerides, which lingual lipase hydrolyzes to free fatty acids (Abumrad 2005). The binding of these free fatty acids to CD36 has been shown to increase host palatability for fatty food (Khan, Besnard 2009). Interestingly, sensory neuron membrane protein (SNMP), the CD36 homolog found in most insect antennae neural cells has been shown to be key in detecting fatty acid based pheromones, which determines the sexual and social behavior of the insects (Nichols, Vogt 2008, Forstner et al. 2008). These observations suggest CD36 role is beyond facilitating uptake of fatty acid like molecules, but rather, it can also invoke signaling cues in response to the bound molecule.

1.2.2.4 CD36 in anti-angiogenesis

CD36 binding to thrombospondin-1 (TSP-1) in nascent microvascular ECs leads to anti-angiogenic effects through inhibiting their migration and triggering their apoptosis (Dawson et al. 1997, Jimenez et al. 2000). This pathway was the focus of my thesis research. In the section below (1.2.3 CD36 mediated anti-angiogenesis in endothelial cells), I will introduce the pathway and the biological question at the center of my study.

1.2.3 CD36 mediated anti-angiogenesis in endothelial cells

1.2.3.1 Angiogenesis and tumorigenesis

One of the key hallmarks of cancer is angiogenesis, the formation of new blood vessels from pre-existing ones (Hanahan, Weinberg 2011). Initial tumor formation is governed by genetic and epigenetic changes that transform cells. A key step to enhance primary tumor and metastatic tumor proliferation and survival is the induction of angiogenesis (Bergers, Benjamin 2003). This provides cancerous cells with nutrients, oxygen and means for waste disposal. In adults, vasculature is normally quiescent and is tightly regulated by pro- and anti-angiogenic factors. Tumor cells offset this balance by down-regulating anti-angiogenic factors and up-regulating pro-angiogenic ones (Bergers, Benjamin 2003) (Figure 1-4). Up-regulation of pro-angiogenic factors like vascular endothelial growth factor (VEGF), which binds to its cognate receptor VEGF receptor 2 (VEGFR2), favors tumor growth, tumor metastasis and tumor recurrence by promoting angiogenesis (Hoeben et al. 2004). This is achieved by the increased proliferation and migration of nascent ECs, which line the lumen of the blood vessels, to form new blood vessels from pre-existing ones.

Since the hypothesis of tumor growth relying on angiogenesis by Dr. Folkman in 1971 (Folkman 1971), research in tumor angiogenesis has led to clinical trials and approval of various angiogenic inhibitors as cancer therapeutics (Loges, Roncal & Carmeliet 2009). Most of these inhibitors target the VEGF pathway. Unfortunately, clinical trial results have not been promising hence a need to develop novel targets and better angiogenesis inhibitors to improve and prolong the total efficacy (Loges, Roncal & Carmeliet 2009). A major endogenous anti-angiogenic protein down regulated during tumorigenesis is thrombospondin 1 (TSP-1) (Figure 1-4), a CD36

Chapter 1– Introduction

ligand (Good et al. 1990, Asch et al. 1987), which signals via the Src family kinase Fyn to promote ECs apoptosis (Jimenez). A brief introduction of this ligand, TSP-1, is discussed below.

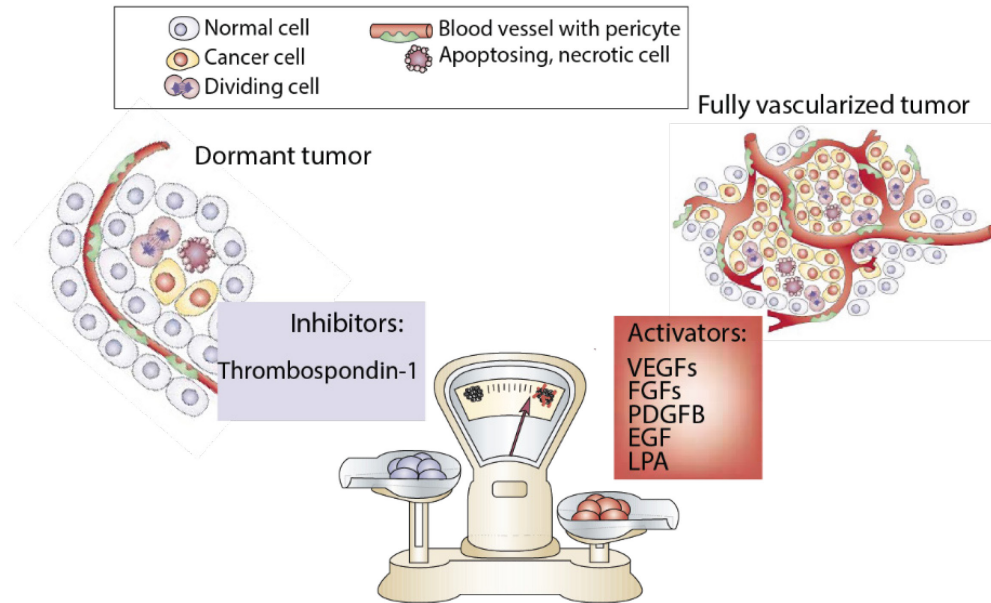


Figure 1-4: Angiogenic balance

Schematic representation of the angiogenic balance (adapted from (Bergers, Benjamin 2003)) governed by activators and inhibitors of angiogenesis. There is an intricate balance between inhibitors and activators of angiogenesis. Tumor cells skew this balance in favor of angiogenesis by downregulating inhibitors like thrombospondin-1 (TSP-1) and upregulating activators like vascular endothelial growth factor (VEGF), fibroblast growth factors (FGFs), platelet-derived growth factor (PDGF), epidermal growth factor (EGF) and lysophosphatic acid (LPA) to enhance their proliferation and survival.

Chapter 1– Introduction

1.2.3.2 *Thrombospondin-1*

TSP-1 belongs to thrombospondins (TSPs), a five-gene family (TSP-1 to 5) of extracellular matrix (ECM) calcium binding glycoproteins with a broad tissue distribution (Bentley, Adams 2010). TSP-1 was the first thrombospondin to be identified and was so named because thrombin stimulation of alpha granules of platelets caused its release from these cells (Baenziger, Brodie & Majerus 1971, Lawler, Slayter & Coligan 1978). TSP-1 and TSP-2 belongs to the group A thrombospondins (Carlson, Lawler & Mosher 2008), which form homotrimers, with the three monomers linked by disulfide bonds (Lawler et al. 1985). TSP-3, TSP-4 and TSP-5 belong to the group B of thrombospondins, and they form homopentamers (Carlson, Lawler & Mosher 2008). The disulfide bonds are not required for the formation of the TSP-1 trimers, but rather stabilize the trimers once formed (Sottile, Selegue & Mosher 1991, Carlson, Lawler & Mosher 2008), a phenomenon observed in another ECM protein, matrilin, which oligomerizes through a similar domain like TSP-1 (Dames et al. 1998, Carlson, Lawler & Mosher 2008).

TSP-1 trimer is a 450 kDa protein complex, with the monomer containing multiple domains including a N-terminal domain, an oligomerization domain (which forms disulfide bonds with the other monomers), a pro-collagen domain (also called von Willebrand Factor type C (VWC) domain), three type I repeats domain, three type II repeats domain, a calcium-binding type III repeats and a globular C-terminal domains (Figure 1-5). While TSP-2 has similar domains, thrombospondin group B members lack pro-collagen and type I repeat domains, but have additional type II repeat domain (Bentley, Adams 2010, Carlson, Lawler & Mosher 2008, Adams, Lawler 2004).

Chapter 1– Introduction

TSP-1 multiple domains enable it to bind to various proteins like histidine-rich glycoprotein (HRGP) (Silverstein, Febbraio 2007), CD36 (Asch et al. 1987), CD47 (also known as integrin-associated protein, IAP) (Brown, Frazier 2001), β_1 - (Short et al. 2005) and β_3 - (Lawler, Weinstein & Hynes 1988) integrins and its interactome continues to grow (Resovi et al. 2014). The discovery of soluble TSP-1 as an inhibitor of ECs proliferation and motility *in vivo* and *in vitro* opened doors for further research as to how it achieves this (Good et al. 1990). TSP-1 is now known to curtail angiogenesis mainly through CD36, a signaling pathway that initially activates the kinase, Fyn (Dawson et al. 1997, Jimenez et al. 2000). A brief introduction of this kinase, Fyn, is discussed below.

Thrombospondin-1 (TSP-1)

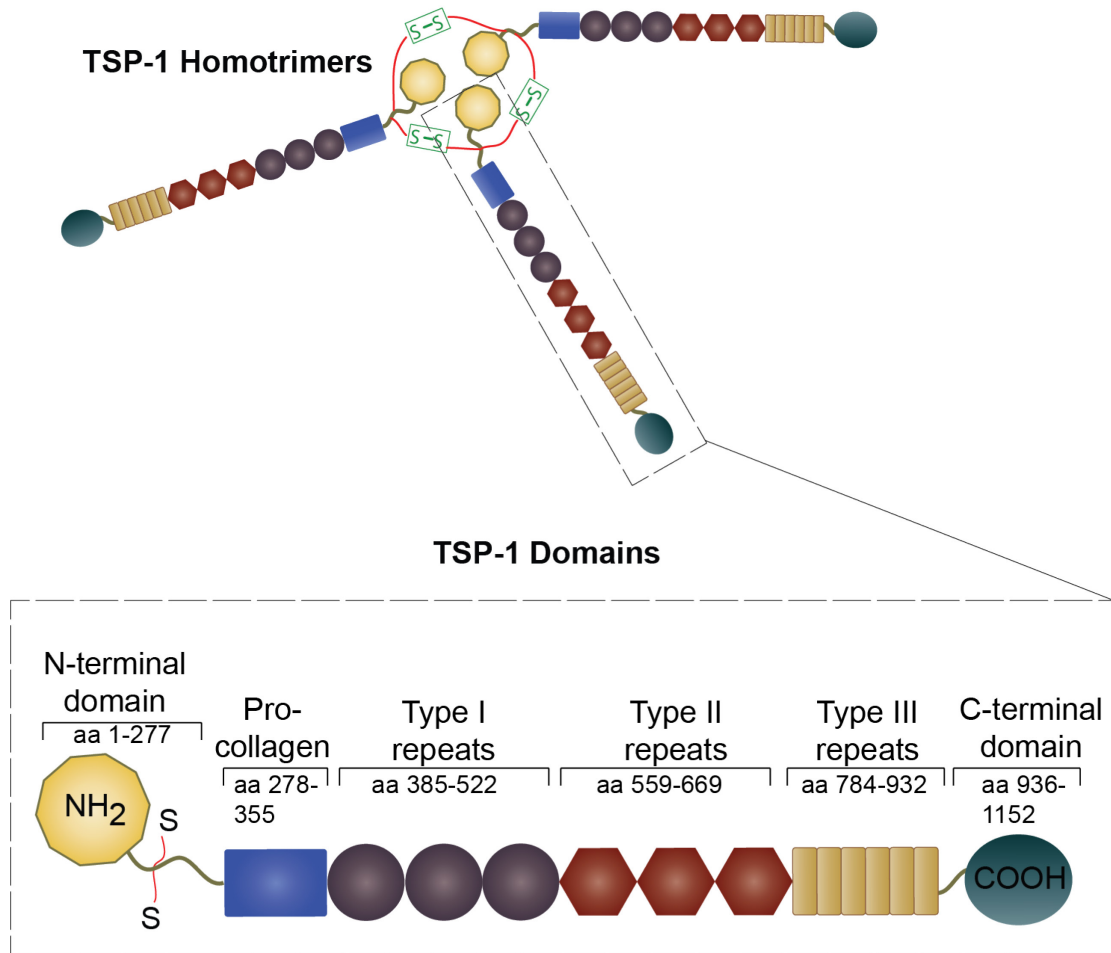


Figure 1-5: Schematic linear representation of TSP-1 structure

Schematic representation of TSP-1 homotrimers and the domains making up a monomer (adapted from (Zhang, Lawler 2007)). Three TSP-1 monomers are linked by intermolecular disulfide bridges to form the homotrimer. The domains of TSP-1 are highlighted with their corresponding amino acids positions.

Chapter 1– Introduction

1.2.3.3 *Fyn*

Fyn belongs to the Src Family Kinases (SFKs), a non-receptor tyrosine kinase family, composed of ten members, Src, *Fyn*, Yes, Frk, Lck, Lyn, Blk, Hck, Yrk and Fgr (Amata, Maffei & Pons 2014). Src, *Fyn* and Yes are ubiquitously expressed (Thomas, Brugge 1997). All members are myristoylated on Glycine 2 on the N-terminal, with most members having additional palmitate acylation on Cysteine 3 or Cysteine 3 and 6 within the N-terminus (Resh 1994). These lipid modifications help anchor them to the plasma membrane (Resh 1999). SFKs are generally considered oncogenes and are key signal transduction regulators under intense investigation, with Src being the first proto-oncogene discovered (Martin 2001, Parsons, Parsons 2004).

Fyn contains a myristoylated and dual palmitoylated Src Homology 4 domain (SH4) which anchors it to the inner leaflet of the plasma membrane, a unique domain, an SH3 domain, an SH2 domain, a protein-tyrosine kinase SH1 domain, and a C-terminal regulatory tail (Saito et al. 2010) (Figure 1-6A). The SH1-4 domains are conserved within the SFKs members, with the unique domain conferring the differences between members (Boggon, Eck 2004). *Fyn* was initially identified as Syn and was shown to belong to SFKs due to its high homology to Src and Yes (Semba et al. 1986). Autophosphorylation of *Fyn*'s tyrosine 420 results in the kinase activation while phosphorylation of tyrosine 531 results in an auto-inhibition conformation (Saito et al. 2010) (Figure 1-6B). Just like other SFK members, *Fyn* activation and deactivation is regulated by phosphorylation and dephosphorylation events by kinases and phosphatases respectively (Roskoski 2005). For example, inhibition can occur through phosphorylation of tyrosine 531 by C-terminal Src kinase (Csk), while activation can occur through tyrosine 531 dephosphorylation by phosphatases PTP1B (protein-tyrosine phosphatase 1B), Shp1, Shp2 (Src

Chapter 1– Introduction

homology 2 domain-containing tyrosine phosphatase 1 or 2), CD45, PTP α , PTP ϵ or PTP λ (protein-tyrosine phosphatase α , ϵ or λ) (Roskoski 2005, Thomas, Brugge 1997, Boggon, Eck 2004).

Fyn's biological functions are diverse, and have been implicated in growth factor and cytokine receptor signaling, integrin-mediated signaling, cell-cell adhesion, T-cell and B-cell receptor signaling, flotillin endocytosis and differentiation of natural killer cells, oligodendrocytes, and keratinocytes (Saito et al. 2010). Upon TSP-1 binding to CD36 in ECs, Fyn was shown to be activated and indispensable in the TSP-1 ability to induce anti-angiogenic responses in ECs (Jimenez et al. 2000). In light of this, my thesis is focused on the TSP-1-CD36-Fyn anti-angiogenic pathway discussed next.

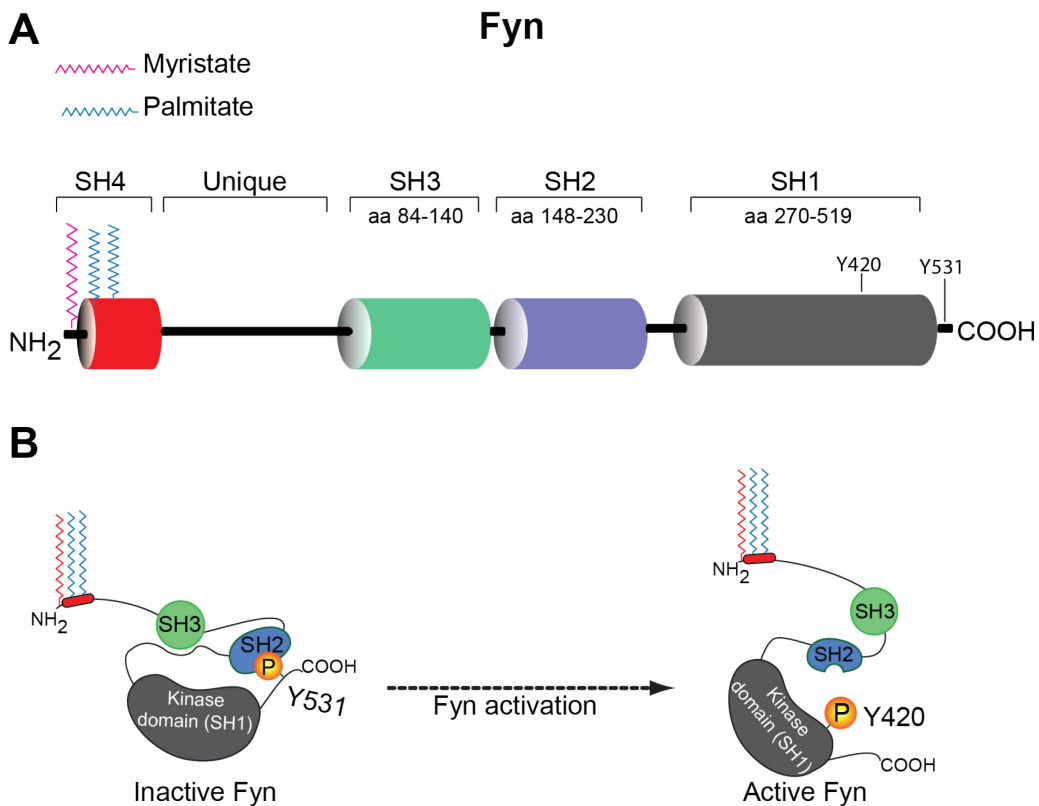


Figure 1-6: Schematic representation of Fyn structure

(A) Schematic linear representation of Fyn and its domains (adapted from (Saito et al. 2010)). From N-terminal, Fyn domains are; membrane targeting SH4 domain (Src Homology 4 domain) which is myristoylated on glycine 2 and dual palmitoylated on cysteine 3 and 6, unique domain, SH3 domain, SH2 domain, a protein-tyrosine kinase SH1 domain, and a C-terminal regulatory tail. (B) Phosphorylation of tyrosine 420 results in the kinase activation while phosphorylation of tyrosine 531 keeps it in an auto-inhibition conformation.

1.2.3.4 TSP-1-CD36-Fyn pathway in anti-angiogenesis

Earlier observations of TSP-1's ability to inhibit ECs proliferation led to a search for the receptor mediating this anti-angiogenic effect (Good et al. 1990). CD36 was identified as the TSP-1 receptor mediating this anti-angiogenesis by inducing a pathway that eventually led to apoptosis of ECs (Dawson et al. 1997, Jimenez et al. 2000). This is initiated through TSP-1's type I repeats domain binding to CD36 CLESH domain (Figure 1-7) (Guo et al. 1997, Crombie, Silverstein 1998). TSP-1 anti-angiogenic effect was lost in CD36 null mice in corneal neovascularization assays emphasizing CD36 indispensability in initiation of this pathway (Jimenez et al. 2000).

CD36 is associated with the SFK, Fyn (Bull, Brickell & Dowd 1994, Huang et al. 1991). Upon TSP-1 binding, Fyn was activated in a pathway that eventually led to activation of caspase-3, hence anti-angiogenesis through ECs apoptosis (Figure 1-7) (Jimenez et al. 2000, Volpert et al. 2002, Nor et al. 2000). This pathway was completely abrogated both in Fyn knockout mice as well as in ECs microinjected with Fyn neutralizing antibodies, underscoring the specificity of

Chapter 1– Introduction

Fyn involvement in TSP-1-CD36 anti-angiogenic pathway (Jimenez et al. 2000, Volpert et al. 2002). Fyn activation upon TSP-1 binding CD36 led to activation of p38 mitogen-activated protein kinases (p38MAPK) and c-Jun N-terminal kinase (JNK) (Jimenez et al. 2000, Jimenez et al. 2001). TSP-1-CD36 induced apoptosis, hence anti-angiogenic activity, was severely compromised in JNK-1 null mice (Jimenez et al. 2001) and under p38MAPK inhibition using the SB203580 inhibitor (Jimenez et al. 2000). Interestingly, decavalent mouse monoclonal anti CD36 IgM (clone SM ϕ) and TSP-1 were shown to inhibit ECs migration and induce their apoptosis to a similar extent, while divalent mouse monoclonal anti CD36 (clone FA6-152) could not (Dawson et al. 1997, Jimenez et al. 2000). This hinted to the possibility of this pathway being initiated by CD36 clustering.

This TSP-1-CD36-Fyn pathway is highly selective, targeting only remodeling ECs, such as tumor vasculature where new vessels are induced by tumorigenesis (Mirochnik, Kwiatek & Volpert 2008). In adults, resting, quiescent microvascular ECs have very low if any CD95 (also known as Fas receptor) on their plasma membrane. Remodeling ECs upon angiogenic stimuli, as in the case for tumor vasculature induction, increases plasma membrane CD95 levels in nascent ECs. On the other hand, TSP-1-CD36-Fyn-p38MAPK signaling cascade, leads to a p38MAPK mediated CD95L (CD95 ligand, also known as Fas) mRNA and protein elevation. Binding of CD95L to CD95 in these remodeling ECs triggers the canonical extrinsic apoptotic pathway where caspase-8 and subsequently caspase-3 are activated to orchestrate cell death (Taylor, Cullen & Martin 2008). TSP-1 anti-angiogenic effects are lost in either CD95 or CD95L null mice (Volpert et al. 2002).

Chapter 1– Introduction

Angiogenic stimuli has also been shown to activate the NFATc2 (Nuclear Factor of the Activated T-cells (Crabtree, Olson 2002)) transcription factor induced expression of anti-apoptosis regulator c-FLIP (cellular FLICE (FADD-like IL-1 β -converting enzyme)-inhibitory protein (Safa 2012)) to ensure ECs survival during ECs remodeling (Zaichuk et al. 2004, Hernandez et al. 2001). The aforementioned activation of JNK-1 by TSP-1-CD36-Fyn pathway has been shown to lead to cytoplasmic retention of NFATc2 through its re-phosphorylation, hence suppressing c-FLIP expression, allowing apoptosis to proceed (Zaichuk et al. 2004). Indeed, specific JNK inhibitor, SP-600125 suppresses NFATc2 phosphorylation and abolishes TSP-1-dependent apoptosis and anti-angiogenic activity in ECs (Zaichuk et al. 2004).

Taken all together, these observations make the TSP-1-CD36-Fyn pathway suitable for anti-angiogenic therapy in tumorigenesis as it would target exclusively remodeling endothelium, without any adverse effects to the quiescent vasculature. Indeed, TSP-1 based peptide mimetics have been designed and gone on to clinical trials (Henkin, Volpert 2011), as discussed in the next section.

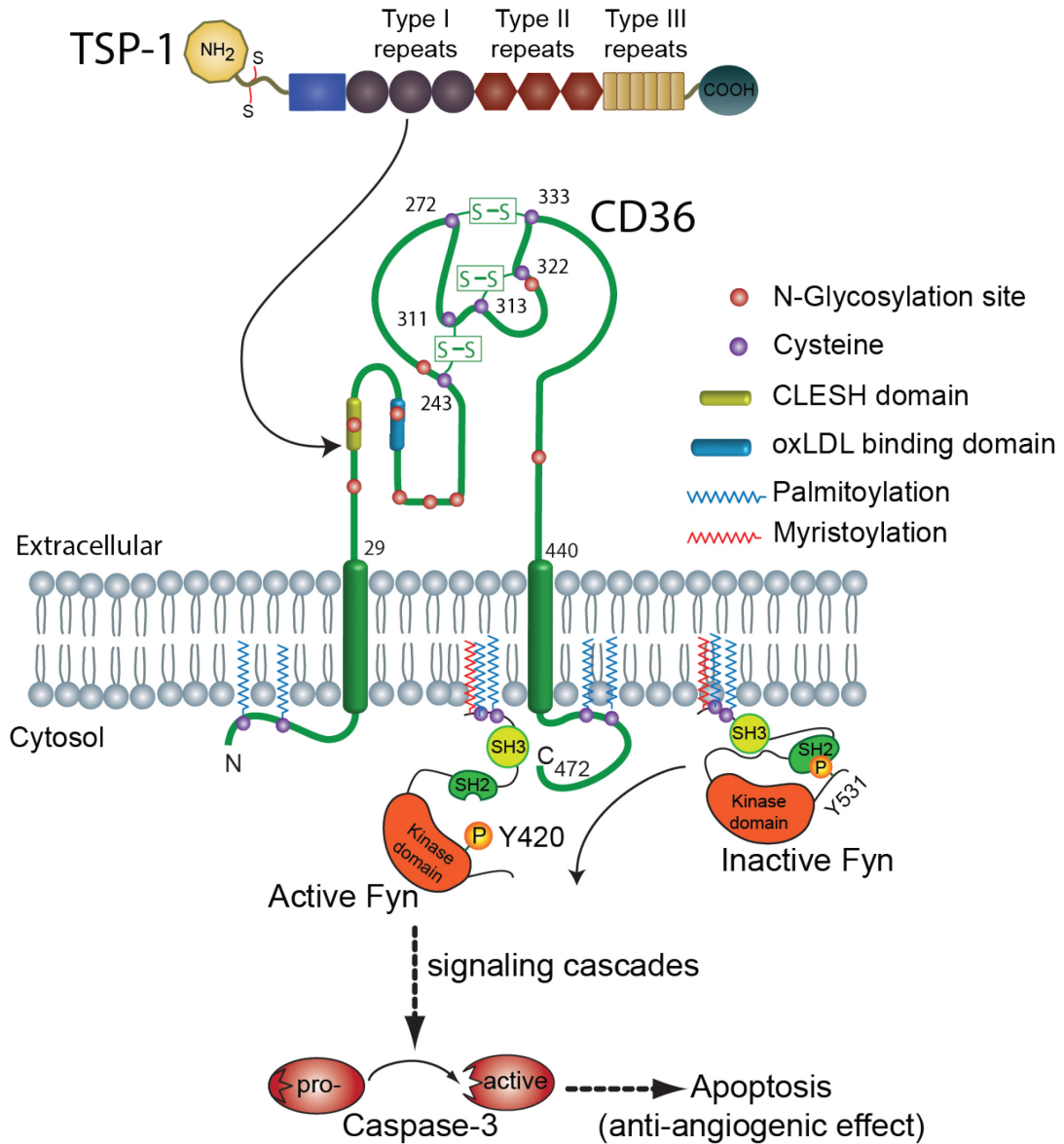


Figure 1-7: Schematic of TSP-1-CD36-Fyn anti-angiogenic pathway initiation
 CD36 ligand, TSP-1, binds to CLESH domain of CD36 through type I repeats. This binding results in activation of kinase Fyn through dephosphorylation of inhibitory tyrosine 531 and phosphorylation of activatory tyrosine 420. Fyn activation leads to a signaling cascade that eventually results in apoptosis of remodeling ECs through caspase-3 activation.

1.2.3.5 Clinical Trials of TSP-1 mimetics

TSP-1 amino acid sequence responsible for binding the CD36 CLESH domain has been mapped to the type I repeats, with the minimal sequence being GVITRIR (Mirochnik, Kwiatek & Volpert 2008, Haviv et al. 2005). This has allowed peptide based TSP-1 mimetics design by Abbott Laboratories, who developed two peptides, ABT-510 and ABT-526 (Haviv et al. 2005). ABT-510 was preferred as it showed increased water solubility and slower clearance in monkey and dog trials (Haviv et al. 2005). Clinical trial results for TSP-1 mimetics for anti-angiogenic cancer therapy have not been overwhelming and researchers have called for trial combinations with cytotoxic therapies and better understanding of the initial steps governing this anti-angiogenic pathway activation (Markovic et al. 2007, Hoekstra et al. 2006, Ebbinghaus et al. 2007). In addition, Abbott Laboratories' patented combination of ABT-510 with a histone deacetylase inhibitor, valproic acid (Jack 2008), which also inhibits angiogenesis independently (Michaelis et al. 2004), makes it harder to assess to what extent the anti-tumor activity of this combination is due to TSP-1 peptide mimicry.

The use of TSP-1 and its mimetics faces two challenges: 1) A soluble endogenous decoy, Histidine-Rich Glycoprotein (HRGP), which also contains a CLESH domain like CD36 could potentially bind TSP-1 and TSP-1 mimetics, abrogating the anti-angiogenic effect (Silverstein, Febbraio 2007, Simantov, Febbraio & Silverstein 2005); 2) Potential CD36 phosphorylation at threonine 92 by protein kinase C (PKC) intracellularly before translocating to the plasma membrane suppresses TSP-1 binding, and this could abrogate the anti-angiogenic effect as well (Asch et al. 1993, Chu, Silverstein 2012). Gaining more insight into the initial step of ligand-receptor ligation that leads to activation and signal transduction could potentially overcome these challenges. Interestingly, a multivalent mouse anti-CD36 IgM (SM ϕ) inhibited HMVECs

Chapter 1– Introduction

migration and induced their apoptosis to a similar extent as TSP-1, while divalent mouse anti-CD36 IgG (FA6-152) could not (Jimenez et al. 2000, Dawson et al. 1997). This suggested CD36 clustering was critical in the initiation of this pathway. The need to better define the initial molecular mechanism of TSP-1-CD36 signaling in ECs is the goal of my thesis.

1.2.3.6 Elucidating TSP-1-CD36 signaling in ECs

CD36 promiscuity in mediating a vast number of unrelated signaling pathways depending on cell type and ligand bound has always been a mystery (Ge, Elghetany 2005). Even more so because of the short cytosolic tails with no canonical signaling motifs, accounting for only approximately 4% of the total protein length (Kralisz 2001). While the modelled CD36 3D structure gives leads as to how CD36 might facilitate fatty acid uptake by cells, it does not give hints as to how the binding of TSP-1 on the extracellular space could activate Fyn in the cytoplasm.

There has been speculation that plasma membrane environment and CD36 organization in the plasma membrane is key to its functions. Indeed plasma membrane organization and the apposed cortical skeleton have been shown to affect membrane proteins spatial distribution, diffusion, interaction as well as their function (Jaqaman, Grinstein 2012). Recently, a cytoskeleton controlled CD36 priming model was proposed in macrophages, suggesting its organization at the plasma membrane might hold the key to its ability to mediate these different pathways (Jaqaman et al. 2011). In this model, CD36 diffusion on macrophage plasma membrane was controlled by cortical cytoskeleton, with some of the CD36 receptors being confined within linear cortical cytoskeleton facilitated troughs. This facilitated CD36 diffusion along one axis, increases the probability of CD36 molecules interacting and clustering.

Perturbing the cytoskeleton disrupted this CD36 plasma membrane organization and subsequently suppressed CD36 signaling as well as its endocytosis (Jaqaman et al. 2011).

We tested if a similar CD36 priming mechanism was employed in the TSP-1-CD36-Fyn pathway that results in anti-angiogenesis cues in ECs. We therefore set out to investigate CD36 organization on the plasma membrane at steady state, TSP-1's effect on this organization upon binding CD36, and whether the cortical cytoskeleton was involved in this as earlier observed in macrophages. The endocytic mechanism through which CD36 gets internalized in ECs, with or without TSP-1 stimulation was also investigated.

1.3 Rationale, hypothesis and objectives

According to the world health organization (WHO), cancer remains the world's leading cause of death (WHO 2015). In an effort to curb it, much research has been dedicated to elucidating its hallmarks. Induction of angiogenesis is one of the hallmarks of cancer (Hanahan, Weinberg 2011). Tumor cells' heavy dependence on angiogenesis to survive has resulted in development of angiogenesis inhibitors (Loges, Roncal & Carmeliet 2009). Among these anti-angiogenic factors is TSP-1 (Good et al. 1990), whose mechanism was shown to be induction of apoptosis in nascent ECs. CD36 was shown to be the TSP-1's receptor mediating this cell death. Interestingly, CD36 multivalent ligands like anti-CD36 IgM (decavalent, clone SM ϕ) antibodies are able to induce ECs apoptosis while anti-CD36 IgG (divalent, clone FA6-152) antibodies do not (Jimenez et al. 2000). These observations suggest that the dynamic organization of CD36 into multimeric complexes in the plasma membrane is key in the initiation of HMVECs apoptosis. We therefore hypothesized that plasma membrane organization regulates CD36 clustering as well as endocytosis, and this is essential for signaling upon TSP-1 binding in ECs.

Chapter 1– Introduction

The aims of this work were 1) to investigate how plasma membrane organization regulates TSP-1-CD36-Fyn activation and 2) to define the endocytic pathway of CD36-TSP-1 internalization, findings that would provide means to decipher its potential role in signaling. These findings will play a role in providing clues to design effective and better-targeted TSP-1 based anti-angiogenic compounds. *Chapter 2* details all the materials and methods employed in this thesis. *Chapter 3* reports data that gives us insights into CD36 organization on the plasma membrane, its association with its downstream effector kinase Fyn, and TSP-1's effect on this upon binding. *Chapter 4* describes the role actin and lipid rafts play in priming CD36-Fyn association and how this facilitates the TSP-1-CD36-Fyn pathway. *Chapter 5* highlights the possible endocytic pathway, through which CD36 is internalized. *Chapter 6* summarizes the results from our data, giving perspective to the initiation of TSP-1-CD36-Fyn pathway and future direction.

References

- Abumrad, N.A. 2005, "CD36 may determine our desire for dietary fats", *The Journal of clinical investigation*, vol. 115, no. 11, pp. 2965-2967.
- Adams, J.C. & Lawler, J. 2004, "The thrombospondins", *The international journal of biochemistry & cell biology*, vol. 36, no. 6, pp. 961-968.
- Albert, M.L., Pearce, S.F., Francisco, L.M., Sauter, B., Roy, P., Silverstein, R.L. & Bhardwaj, N. 1998, "Immature dendritic cells phagocytose apoptotic cells via alphavbeta5 and CD36, and cross-present antigens to cytotoxic T lymphocytes", *The Journal of experimental medicine*, vol. 188, no. 7, pp. 1359-1368.
- Alkhatatbeh, M.J., Mhaidat, N.M., Enjeti, A.K., Lincz, L.F. & Thorne, R.F. 2011, "The putative diabetic plasma marker, soluble CD36, is non-cleaved, non-soluble and entirely associated with microparticles", *Journal of thrombosis and haemostasis : JTH*, vol. 9, no. 4, pp. 844-851.
- Amata, I., Maffei, M. & Pons, M. 2014, "Phosphorylation of unique domains of Src family kinases", *Frontiers in Genetics*, vol. 5, pp. 10.3389/fgene.2014.00181.
- Anderson, J.M. 2000, "Multinucleated giant cells", *Current opinion in hematology*, vol. 7, no. 1, pp. 40-47.
- Andrews, N.L., Lidke, K.A., Pfeiffer, J.R., Burns, A.R., Wilson, B.S., Oliver, J.M. & Lidke, D.S. 2008, "Actin restricts FcepsilonRI diffusion and facilitates antigen-induced receptor immobilization", *Nature cell biology*, vol. 10, no. 8, pp. 955-963.
- Asch, A.S., Barnwell, J., Silverstein, R.L. & Nachman, R.L. 1987, "Isolation of the thrombospondin membrane receptor.", *Journal of Clinical Investigation*, vol. 79, no. 4, pp. 1054-1061.
- Asch, A.S., Liu, I., Briccetti, F.M., Barnwell, J.W., Kwakye-Berko, F., Dokun, A., Goldberger, J. & Pernambuco, M. 1993, "Analysis of CD36 binding domains: ligand specificity controlled by dephosphorylation of an ectodomain", *Science (New York, N.Y.)*, vol. 262, no. 5138, pp. 1436-1440.
- Babuke, T., Ruonala, M., Meister, M., Amaddii, M., Genzler, C., Esposito, A. & Tikkanen, R. 2009, "Hetero-oligomerization of reggie-1/flotillin-2 and reggie-2/flotillin-1 is required for their endocytosis", *Cellular signalling*, vol. 21, no. 8, pp. 1287-1297.
- Babuke, T. & Tikkanen, R. 2007, "Dissecting the molecular function of reggie/flotillin proteins", *European journal of cell biology*, vol. 86, no. 9, pp. 525-532.

Chapter 1– Introduction

- Baenziger, N.L., Brodie, G.N. & Majerus, P.W. 1971, "A thrombin-sensitive protein of human platelet membranes", *Proceedings of the National Academy of Sciences of the United States of America*, vol. 68, no. 1, pp. 240-243.
- Baillie, A.G., Coburn, C.T. & Abumrad, N.A. 1996, "Reversible binding of long-chain fatty acids to purified FAT, the adipose CD36 homolog", *The Journal of membrane biology*, vol. 153, no. 1, pp. 75-81.
- Barreiro, O., Zamai, M., Yanez-Mo, M., Tejera, E., Lopez-Romero, P., Monk, P.N., Gratton, E., Caiolfa, V.R. & Sanchez-Madrid, F. 2008, "Endothelial adhesion receptors are recruited to adherent leukocytes by inclusion in preformed tetraspanin nanoplateforms", *The Journal of cell biology*, vol. 183, no. 3, pp. 527-542.
- Baruch, D.I., Gormely, J.A., Ma, C., Howard, R.J. & Pasloske, B.L. 1996, "Plasmodium falciparum erythrocyte membrane protein 1 is a parasitized erythrocyte receptor for adherence to CD36, thrombospondin, and intercellular adhesion molecule 1", *Proceedings of the National Academy of Sciences of the United States of America*, vol. 93, no. 8, pp. 3497-3502.
- Baruch, D.I., Pasloske, B.L., Singh, H.B., Bi, X., Ma, X.C., Feldman, M., Taraschi, T.F. & Howard, R.J. 1995, "Cloning the P. falciparum gene encoding PfEMP1, a malarial variant antigen and adherence receptor on the surface of parasitized human erythrocytes", *Cell*, vol. 82, no. 1, pp. 77-87.
- Bentley, A.A. & Adams, J.C. 2010, "The evolution of thrombospondins and their ligand-binding activities.", *Molecular Biology & Evolution*, vol. 27, no. 9, pp. 2187-2197.
- Berditchevski, F. 2001, "Complexes of tetraspanins with integrins: more than meets the eye", *Journal of cell science*, vol. 114, no. Pt 23, pp. 4143-4151.
- Berendt, A.R., Ferguson, D.J. & Newbold, C.I. 1990, "Sequestration in Plasmodium falciparum malaria: sticky cells and sticky problems", *Parasitology today (Personal ed.)*, vol. 6, no. 8, pp. 247-254.
- Bergers, G. & Benjamin, L.E. 2003, "Tumorigenesis and the angiogenic switch", *Nature Reviews.Cancer*, vol. 3, no. 6, pp. 401-410.
- Berridge, M.J. 1984, "Inositol trisphosphate and diacylglycerol as second messengers", *The Biochemical journal*, vol. 220, no. 2, pp. 345-360.
- Boggon, T.J. & Eck, M.J. 2004, "Structure and regulation of Src family kinases", *Oncogene*, vol. 23, no. 48, pp. 7918-7927.
- Braccia, A., Villani, M., Immerdal, L., Niels-Christiansen, L.L., Nystrom, B.T., Hansen, G.H. & Danielsen, E.M. 2003, "Microvillar membrane microdomains exist at physiological

Chapter 1– Introduction

- temperature. Role of galectin-4 as lipid raft stabilizer revealed by "superrafts", *The Journal of biological chemistry*, vol. 278, no. 18, pp. 15679-15684.
- Brown, D.A. 2006, "Lipid rafts, detergent-resistant membranes, and raft targeting signals", *Physiology (Bethesda, Md.)*, vol. 21, pp. 430-439.
- Brown, D.A. & Rose, J.K. 1992, "Sorting of GPI-anchored proteins to glycolipid-enriched membrane subdomains during transport to the apical cell surface", *Cell*, vol. 68, no. 3, pp. 533-544.
- Brown, E.J. & Frazier, W.A. 2001, "Integrin-associated protein (CD47) and its ligands", *Trends in cell biology*, vol. 11, no. 3, pp. 130-135.
- Bull, H.A., Brickell, P.M. & Dowd, P.M. 1994, "Src-related protein tyrosine kinases are physically associated with the surface antigen CD36 in human dermal microvascular endothelial cells", *FEBS letters*, vol. 351, no. 1, pp. 41-44.
- Cabrera, A., Neculai, D. & Kain, K.C. 2014, "CD36 and malaria: friends or foes? A decade of data provides some answers", *Trends in parasitology*, vol. 30, no. 9, pp. 436-444.
- Callahan, M.K., Williamson, P. & Schlegel, R.A. 2000, "Surface expression of phosphatidylserine on macrophages is required for phagocytosis of apoptotic thymocytes", *Cell death and differentiation*, vol. 7, no. 7, pp. 645-653.
- Calvo, D., Gomez-Coronado, D., Suarez, Y., Lasuncion, M.A. & Vega, M.A. 1998, "Human CD36 is a high affinity receptor for the native lipoproteins HDL, LDL, and VLDL", *Journal of lipid research*, vol. 39, no. 4, pp. 777-788.
- Carlson, C.B., Lawler, J. & Mosher, D.F. 2008, "Structures of thrombospondins", *Cellular and molecular life sciences : CMLS*, vol. 65, no. 5, pp. 672-686.
- Cerneus, D.P., Ueffing, E., Posthuma, G., Strous, G.J. & van der Ende, A. 1993, "Detergent insolubility of alkaline phosphatase during biosynthetic transport and endocytosis. Role of cholesterol", *The Journal of biological chemistry*, vol. 268, no. 5, pp. 3150-3155.
- Chen, Y., Veracini, L., Benistant, C. & Jacobson, K. 2009, "The transmembrane protein CBP plays a role in transiently anchoring small clusters of Thy-1, a GPI-anchored protein, to the cytoskeleton", *Journal of cell science*, vol. 122, no. Pt 21, pp. 3966-3972.
- Chu, L.Y. & Silverstein, R.L. 2012, "CD36 Ectodomain Phosphorylation Blocks Thrombospondin-1 Binding: Structure-Function Relationships and Regulation by Protein Kinase C", *Arteriosclerosis, Thrombosis, and Vascular Biology*, vol. 32, no. 3, pp. 760-767.
- Clague, M.J., Urbe, S. & de Lartigue, J. 2009, "Phosphoinositides and the endocytic pathway", *Experimental cell research*, vol. 315, no. 9, pp. 1627-1631.

Chapter 1– Introduction

- Clark, H.C. 1915, "The Diagnostic Value of the Placental Blood Film in Æstivo-Autumnal Malaria", *The Journal of experimental medicine*, vol. 22, no. 4, pp. 427-444.
- Clemetson, K.J., Pfueller, S.L., Luscher, E.F. & Jenkins, C.S. 1977, "Isolation of the membrane glycoproteins of human blood platelets by lectin affinity chromatography", *Biochimica et biophysica acta*, vol. 464, no. 3, pp. 493-508.
- Coraci, I.S., Husemann, J., Berman, J.W., Hulette, C., Dufour, J.H., Campanella, G.K., Luster, A.D., Silverstein, S.C. & El-Khoury, J.B. 2002, "CD36, a class B scavenger receptor, is expressed on microglia in Alzheimer's disease brains and can mediate production of reactive oxygen species in response to beta-amyloid fibrils", *The American journal of pathology*, vol. 160, no. 1, pp. 101-112.
- Crabtree, G.R. & Olson, E.N. 2002, "NFAT signaling: choreographing the social lives of cells", *Cell*, vol. 109 Suppl, pp. S67-79.
- Cremona, M.L., Matthies, H.J.G., Pau, K., Bowton, E., Speed, N., Lute, B.J., Anderson, M., Sen, N., Robertson, S.D., Vaughan, R.A., Rothman, J.E., Galli, A., Javitch, J.A. & Yamamoto, A. 2011, "Flotillin-1 is essential for PKC-triggered endocytosis and membrane microdomain localization of DAT", *Nature neuroscience*, vol. 14, no. 4, pp. 469-477.
- Crombie, R. & Silverstein, R. 1998, "Lysosomal integral membrane protein II binds thrombospondin-1. Structure-function homology with the cell adhesion molecule CD36 defines a conserved recognition motif.", *Journal of Biological Chemistry*, vol. 273, no. 9, pp. 4855-4863.
- Dames, S.A., Kammerer, R.A., Wiltschek, R., Engel, J. & Alexandrescu, A.T. 1998, "NMR structure of a parallel homotrimeric coiled coil", *Nature structural biology*, vol. 5, no. 8, pp. 687-691.
- Daviet, L., Malvoisin, E., Wild, T.F. & McGregor, J.L. 1997, "Thrombospondin induces dimerization of membrane-bound, but not soluble CD36", *Thrombosis and haemostasis*, vol. 78, no. 2, pp. 897-901.
- Dawson, D.W., Pearce, S.F., Zhong, R., Silverstein, R.L., Frazier, W.A. & Bouck, N.P. 1997, "CD36 mediates the In vitro inhibitory effects of thrombospondin-1 on endothelial cells.", *Journal of Cell Biology*, vol. 138, no. 3, pp. 707-717.
- Dervichian, D. & Macheboeuf, M. 1938, "The existence of a unimolecular layer of lipoidal substances on the surface of the red blood cells", *The Journal of experimental medicine*, vol. 206, no. 4, pp. 1511-1514.
- Dinic, J., Ashrafzadeh, P. & Parmryd, I. 2013, "Actin filaments attachment at the plasma membrane in live cells cause the formation of ordered lipid domains", *Biochimica et biophysica acta*, vol. 1828, no. 3, pp. 1102-1111.

Chapter 1– Introduction

- Dowhan, W., Bogdanov, M. & Mileykovskaya, E. 2008, "CHAPTER 1 - Functional roles of lipids in membranes" in *Biochemistry of Lipids, Lipoproteins and Membranes (Fifth Edition)*, ed. D.E.V.E. Vance, Elsevier, San Diego, pp. 1-37.
- Drover, V.A., Nguyen, D.V., Bastie, C.C., Darlington, Y.F., Abumrad, N.A., Pessin, J.E., London, E., Sahoo, D. & Phillips, M.C. 2008, "CD36 mediates both cellular uptake of very long chain fatty acids and their intestinal absorption in mice", *The Journal of biological chemistry*, vol. 283, no. 19, pp. 13108-13115.
- Dulhunty, A.F. & Franzini-Armstrong, C. 1975, "The relative contributions of the folds and caveolae to the surface membrane of frog skeletal muscle fibres at different sarcomere lengths", *The Journal of physiology*, vol. 250, no. 3, pp. 513-539.
- Ebbinghaus, S., Hussain, M., Tannir, N., Gordon, M., Desai, A.A., Knight, R.A., Humerickhouse, R.A., Qian, J., Gordon, G.B. & Figlin, R. 2007, "Phase 2 study of ABT-510 in patients with previously untreated advanced renal cell carcinoma", *Clinical cancer research : an official journal of the American Association for Cancer Research*, vol. 13, no. 22 Pt 1, pp. 6689-6695.
- Eddidin, M. 2003, "Lipids on the frontier: a century of cell-membrane bilayers", *Nature reviews.Molecular cell biology*, vol. 4, no. 5, pp. 414-418.
- Eddidin, M., Zuniga, M.C. & Sheetz, M.P. 1994, "Truncation mutants define and locate cytoplasmic barriers to lateral mobility of membrane glycoproteins", *Proceedings of the National Academy of Sciences of the United States of America*, vol. 91, no. 8, pp. 3378-3382.
- Endemann, G., Stanton, L.W., Madden, K.S., Bryant, C.M., White, R.T. & Protter, A.A. 1993, "CD36 is a receptor for oxidized low density lipoprotein", *The Journal of biological chemistry*, vol. 268, no. 16, pp. 11811-11816.
- Espenel, C., Margeat, E., Dosset, P., Arduise, C., Le Grimellec, C., Royer, C.A., Boucheix, C., Rubinstein, E. & Milhiet, P.E. 2008, "Single-molecule analysis of CD9 dynamics and partitioning reveals multiple modes of interaction in the tetraspanin web", *The Journal of cell biology*, vol. 182, no. 4, pp. 765-776.
- Fadok, V.A., Warner, M.L., Bratton, D.L. & Henson, P.M. 1998, "CD36 is required for phagocytosis of apoptotic cells by human macrophages that use either a phosphatidylserine receptor or the vitronectin receptor (alpha v beta 3)", *Journal of immunology (Baltimore, Md.: 1950)*, vol. 161, no. 11, pp. 6250-6257.
- Febbraio, M., Hajjar, D.P. & Silverstein, R.L. 2001, "CD36: a class B scavenger receptor involved in angiogenesis, atherosclerosis, inflammation, and lipid metabolism", *The Journal of clinical investigation*, vol. 108, no. 6, pp. 785-791.

Chapter 1– Introduction

- Febbraio, M., Podrez, E.A., Smith, J.D., Hajjar, D.P., Hazen, S.L., Hoff, H.F., Sharma, K. & Silverstein, R.L. 2000, "Targeted disruption of the class B scavenger receptor CD36 protects against atherosclerotic lesion development in mice", *The Journal of clinical investigation*, vol. 105, no. 8, pp. 1049-1056.
- Feder, T.J., Brust-Mascher, I., Slattery, J.P., Baird, B. & Webb, W.W. 1996, "Constrained diffusion or immobile fraction on cell surfaces: a new interpretation.", *Biophysical journal*, vol. 70, no. 6, pp. 2767-2773.
- Feng, J., Han, J., Pearce, S.F., Silverstein, R.L., Gotto, A.M., Jr, Hajjar, D.P. & Nicholson, A.C. 2000, "Induction of CD36 expression by oxidized LDL and IL-4 by a common signaling pathway dependent on protein kinase C and PPAR-gamma", *Journal of lipid research*, vol. 41, no. 5, pp. 688-696.
- Fernandez-Real, J.M., Handberg, A., Ortega, F., Hojlund, K., Vendrell, J. & Ricart, W. 2009, "Circulating soluble CD36 is a novel marker of liver injury in subjects with altered glucose tolerance", *The Journal of nutritional biochemistry*, vol. 20, no. 6, pp. 477-484.
- Fernandis, A.Z. & Wenk, M.R. 2007, "Membrane lipids as signaling molecules", *Current opinion in lipidology*, vol. 18, no. 2, pp. 121-128.
- Fletcher, D.A. & Mullins, R.D. 2010, "Cell mechanics and the cytoskeleton", *Nature*, vol. 463, no. 7280, pp. 485-492.
- Folkman, J. 1971, "Tumor angiogenesis: therapeutic implications", *The New England journal of medicine*, vol. 285, no. 21, pp. 1182-1186.
- Forstner, M., Gohl, T., Gondesén, I., Raming, K., Breer, H. & Krieger, J. 2008, "Differential expression of SNMP-1 and SNMP-2 proteins in pheromone-sensitive hairs of moths", *Chemical senses*, vol. 33, no. 3, pp. 291-299.
- Franc, N.C., Dimarcq, J.L., Lagueux, M., Hoffmann, J. & Ezekowitz, R.A. 1996, "Croquemort, a novel Drosophila hemocyte/macrophage receptor that recognizes apoptotic cells", *Immunity*, vol. 4, no. 5, pp. 431-443.
- Franc, N.C., Heitzler, P., Ezekowitz, R.A. & White, K. 1999, "Requirement for croquemort in phagocytosis of apoptotic cells in Drosophila", *Science (New York, N.Y.)*, vol. 284, no. 5422, pp. 1991-1994.
- Frick, M., Bright, N.A., Riento, K., Bray, A., Merrified, C. & Nichols, B.J. 2007, "Coassembly of flotillins induces formation of membrane microdomains, membrane curvature, and vesicle budding", *Current biology : CB*, vol. 17, no. 13, pp. 1151-1156.
- Friedrichson, T. & Kurzchalia, T.V. 1998, "Microdomains of GPI-anchored proteins in living cells revealed by crosslinking", *Nature*, vol. 394, no. 6695, pp. 802-805.

Chapter 1– Introduction

- Fujiwara, T., Ritchie, K., Murakoshi, H., Jacobson, K. & Kusumi, A. 2002, "Phospholipids undergo hop diffusion in compartmentalized cell membrane.", *Journal of Cell Biology*, vol. 157, no. 6, pp. 1071-1081.
- Futerman, A.H. & Hannun, Y.A. 2004, "The complex life of simple sphingolipids", *EMBO reports*, vol. 5, no. 8, pp. 777-782.
- Garcia-Monzon, C., Lo Iacono, O., Crespo, J., Romero-Gomez, M., Garcia-Samaniego, J., Fernandez-Bermejo, M., Dominguez-Diez, A., Rodriguez de Cia, J., Saez, A., Porrero, J.L., Vargas-Castrillon, J., Chavez-Jimenez, E., Soto-Fernandez, S., Diaz, A., Gallego-Duran, R., Madejon, A. & Miquilena-Colina, M.E. 2014, "Increased soluble CD36 is linked to advanced steatosis in nonalcoholic fatty liver disease", *European journal of clinical investigation*, vol. 44, no. 1, pp. 65-73.
- Garcia-Parajo, M.F., Cambi, A., Torreno-Pina, J.A., Thompson, N. & Jacobson, K. 2014, "Nanoclustering as a dominant feature of plasma membrane organization", *Journal of cell science*, vol. 127, no. 23, pp. 4995-5005.
- Garner, O.B. & Baum, L.G. 2008, "Galectin–glycan lattices regulate cell-surface glycoprotein organization and signalling", *Biochemical Society transactions*, vol. 36, no. Pt 6, pp. 1472-1477.
- Ge, Y. & Elghetany, M.T. 2005, "CD36: a multiligand molecule", *Laboratory hematology : official publication of the International Society for Laboratory Hematology*, vol. 11, no. 1, pp. 31-37.
- Goncalves, A., Margier, M., Roi, S., Collet, X., Niot, I., Goupy, P., Caris-Veyrat, C. & Reboul, E. 2014, "Intestinal scavenger receptors are involved in vitamin k1 absorption", *The Journal of biological chemistry*, vol. 289, no. 44, pp. 30743-30752.
- Good, D.J., Polverini, P.J., Rastinejad, F., Le Beau, M.M., Lemons, R.S., Frazier, W.A. & Bouck, N.P. 1990, "A tumor suppressor-dependent inhibitor of angiogenesis is immunologically and functionally indistinguishable from a fragment of thrombospondin.", *Proceedings of the National Academy of Sciences of the United States of America*, vol. 87, no. 17, pp. 6624-6628.
- Gorelick, P.B., Scuteri, A., Black, S.E., Decarli, C., Greenberg, S.M., Iadecola, C., Launer, L.J., Laurent, S., Lopez, O.L., Nyenhuis, D., Petersen, R.C., Schneider, J.A., Tzourio, C., Arnett, D.K., Bennett, D.A., Chui, H.C., Higashida, R.T., Lindquist, R., Nilsson, P.M., Roman, G.C., Sellke, F.W., Seshadri, S. & American Heart Association Stroke Council, Council on Epidemiology and Prevention, Council on Cardiovascular Nursing, Council on Cardiovascular Radiology and Intervention, and Council on Cardiovascular Surgery and Anesthesia 2011, "Vascular contributions to cognitive impairment and dementia: a statement for healthcare professionals from the american heart association/american stroke association", *Stroke; a journal of cerebral circulation*, vol. 42, no. 9, pp. 2672-2713.

Chapter 1– Introduction

- Gorter, E. & Grendel, F. 1925, "On Bimolecular Layers of Lipoids on the Chromocytes of the Blood", *The Journal of experimental medicine*, vol. 41, no. 4, pp. 439-443.
- Goswami, D., Gowrishankar, K., Bilgrami, S., Ghosh, S., Raghupathy, R., Chadda, R., Vishwakarma, R., Rao, M. & Mayor, S. 2008, "Nanoclusters of GPI-anchored proteins are formed by cortical actin-driven activity", *Cell*, vol. 135, no. 6, pp. 1085-1097.
- Gowrishankar, K., Ghosh, S., Saha, S., C, R., Mayor, S. & Rao, M. 2012, "Active remodeling of cortical actin regulates spatiotemporal organization of cell surface molecules", *Cell*, vol. 149, no. 6, pp. 1353-1367.
- Grecco, H.E., Schmick, M. & Bastiaens, P.I. 2011, "Signaling from the living plasma membrane", *Cell*, vol. 144, no. 6, pp. 897-909.
- Greenberg, M.E., Sun, M., Zhang, R., Febbraio, M., Silverstein, R. & Hazen, S.L. 2006, "Oxidized phosphatidylserine–CD36 interactions play an essential role in macrophage-dependent phagocytosis of apoptotic cells", *The Journal of experimental medicine*, vol. 203, no. 12, pp. 2613-2625.
- Guo, N., Krutzsch, H.C., Inman, J.K. & Roberts, D.D. 1997, "Thrombospondin 1 and type I repeat peptides of thrombospondin 1 specifically induce apoptosis of endothelial cells.", *Cancer research*, vol. 57, no. 9, pp. 1735-1742.
- Hanahan, D. & Weinberg, R. 2011, *Hallmarks of Cancer: The Next Generation*, Cell Press.
- Hancock, J.F. 2006, "Lipid rafts: contentious only from simplistic standpoints", *Nature reviews.Molecular cell biology*, vol. 7, no. 6, pp. 456-462.
- Handberg, A., Levin, K., Hojlund, K. & Beck-Nielsen, H. 2006, "Identification of the oxidized low-density lipoprotein scavenger receptor CD36 in plasma: a novel marker of insulin resistance", *Circulation*, vol. 114, no. 11, pp. 1169-1176.
- Handberg, A., Skjelland, M., Michelsen, A.E., Sagen, E.L., Krohg-Sorensen, K., Russell, D., Dahl, A., Ueland, T., Oie, E., Aukrust, P. & Halvorsen, B. 2008, "Soluble CD36 in plasma is increased in patients with symptomatic atherosclerotic carotid plaques and is related to plaque instability", *Stroke; a journal of cerebral circulation*, vol. 39, no. 11, pp. 3092-3095.
- Hansen, C.G. & Nichols, B.J. 2009, "Molecular mechanisms of clathrin-independent endocytosis", *Journal of cell science*, vol. 122, no. Pt 11, pp. 1713-1721.
- Harmon, C.M. & Abumrad, N.A. 1993, "Binding of sulfosuccinimidyl fatty acids to adipocyte membrane proteins: isolation and amino-terminal sequence of an 88-kD protein implicated in transport of long-chain fatty acids", *The Journal of membrane biology*, vol. 133, no. 1, pp. 43-49.

Chapter 1– Introduction

- Haviv, F., Bradley, M.F., Kalvin, D.M., Schneider, A.J., Davidson, D.J., Majest, S.M., McKay, L.M., Haskell, C.J., Bell, R.L., Nguyen, B., Marsh, K.C., Surber, B.W., Uchic, J.T., Ferrero, J., Wang, Y.C., Leal, J., Record, R.D., Hodde, J., Badylak, S.F., Lesniewski, R.R. & Henkin, J. 2005, "Thrombospondin-1 mimetic peptide inhibitors of angiogenesis and tumor growth: design, synthesis, and optimization of pharmacokinetics and biological activities", *Journal of medicinal chemistry*, vol. 48, no. 8, pp. 2838-2846.
- Helming, L. & Gordon, S. 2007, "The molecular basis of macrophage fusion", *Immunobiology*, vol. 212, no. 9-10, pp. 785-793.
- Helming, L., Winter, J. & Gordon, S. 2009, "The scavenger receptor CD36 plays a role in cytokine-induced macrophage fusion", *Journal of cell science*, vol. 122, no. Pt 4, pp. 453-459.
- Hemler, M.E. 2014, "Tetraspanin proteins promote multiple cancer stages", *Nature reviews.Cancer*, vol. 14, no. 1, pp. 49-60.
- Hemler, M.E. 2003, "Tetraspanin proteins mediate cellular penetration, invasion, and fusion events and define a novel type of membrane microdomain", *Annual Review of Cell and Developmental Biology*, vol. 19, pp. 397-422.
- Henkin, J. & Volpert, O.V. 2011, "Therapies using anti-angiogenic peptide mimetics of thrombospondin-1", *Expert opinion on therapeutic targets*, vol. 15, no. 12, pp. 1369-1386.
- Hernandez, G.L., Volpert, O.V., Iniguez, M.A., Lorenzo, E., Martinez-Martinez, S., Grau, R., Fresno, M. & Redondo, J.M. 2001, "Selective inhibition of vascular endothelial growth factor-mediated angiogenesis by cyclosporin A: roles of the nuclear factor of activated T cells and cyclooxygenase 2", *The Journal of experimental medicine*, vol. 193, no. 5, pp. 607-620.
- Himoto, T., Tani, J., Miyoshi, H., Morishita, A., Yoneyama, H., Kurokohchi, K., Inukai, M., Masugata, H., Goda, F., Senda, S., Haba, R., Ueno, M., Yamaoka, G. & Masaki, T. 2013, "Investigation of the factors associated with circulating soluble CD36 levels in patients with HCV-related chronic liver disease", *Diabetology & metabolic syndrome*, vol. 5, no. 1, pp. 51-5996-5-51.
- Hishikawa, D., Hashidate, T., Shimizu, T. & Shindou, H. 2014, "Diversity and function of membrane glycerophospholipids generated by the remodeling pathway in mammalian cells", *Journal of lipid research*, vol. 55, no. 5, pp. 799-807.
- Hoeben, A., Landuyt, B., Highley, M.S., Wildiers, H., Van Oosterom, A.T. & De Bruijn, E.A. 2004, "Vascular Endothelial Growth Factor and Angiogenesis", *Pharmacological reviews*, vol. 56, no. 4, pp. 549-580.
- Hoekstra, R., de Vos, F.Y., Eskens, F.A., de Vries, E.G., Uges, D.R., Knight, R., Carr, R.A., Humerickhouse, R., Verweij, J. & Gietema, J.A. 2006, "Phase I study of the

Chapter 1– Introduction

- thrombospondin-1-mimetic angiogenesis inhibitor ABT-510 with 5-fluorouracil and leucovorin: a safe combination", *European journal of cancer (Oxford, England : 1990)*, vol. 42, no. 4, pp. 467-472.
- Holtzman, D.M., Morris, J.C. & Goate, A.M. 2011, "Alzheimer's disease: the challenge of the second century", *Science translational medicine*, vol. 3, no. 77, pp. 77sr1.
- Hooke, R. 1665, *Micrographia, or, Some physiological descriptions of minute bodies made by magnifying glasses: With observations and inquiries thereupon*, Jo. Martyn and Ja. Allestry, printers to the Royal Society, London.
- Hoosdally, S.J., Andress, E.J., Wooding, C., Martin, C.A. & Linton, K.J. 2009, "The Human Scavenger Receptor CD36: glycosylation status and its role in trafficking and function", *The Journal of biological chemistry*, vol. 284, no. 24, pp. 16277-16288.
- Howard, R.J., Barnwell, J.W., Rock, E.P., Neequaye, J., Ofori-Adjei, D., Maloy, W.L., Lyon, J.A. & Saul, A. 1988, "Two approximately 300 kilodalton Plasmodium falciparum proteins at the surface membrane of infected erythrocytes", *Molecular and biochemical parasitology*, vol. 27, no. 2-3, pp. 207-223.
- Huang, M.M., Bolen, J.B., Barnwell, J.W., Shattil, S.J. & Brugge, J.S. 1991, "Membrane glycoprotein IV (CD36) is physically associated with the Fyn, Lyn, and Yes protein-tyrosine kinases in human platelets", *Proceedings of the National Academy of Sciences of the United States of America*, vol. 88, no. 17, pp. 7844-7848.
- Hviid, L. & Jensen, A.T. 2015, "PfEMP1 - A Parasite Protein Family of Key Importance in Plasmodium falciparum Malaria Immunity and Pathogenesis", *Advances in Parasitology*, vol. 88, pp. 51-84.
- Iadecola, C. 2010, "The overlap between neurodegenerative and vascular factors in the pathogenesis of dementia", *Acta Neuropathologica*, vol. 120, no. 3, pp. 287-296.
- Isshiki, M., Ando, J., Korenaga, R., Kogo, H., Fujimoto, T., Fujita, T. & Kamiya, A. 1998, "Endothelial Ca²⁺ waves preferentially originate at specific loci in caveolin-rich cell edges", *Proceedings of the National Academy of Sciences of the United States of America*, vol. 95, no. 9, pp. 5009-5014.
- Jack, H. 2008, *Antitumorigenic drug combination comprising an hdac inhibitor and a tsp-1 peptidomimetic*, Google Patents.
- Jaqaman, K. & Grinstein, S. 2012, "Regulation from within: the cytoskeleton in transmembrane signaling", *Trends in cell biology*, vol. 22, no. 10, pp. 515-526.
- Jaqaman, K., Kuwata, H., Touret, N., Collins, R., Trimble, W.S., Danuser, G. & Grinstein, S. 2011, "Cytoskeletal control of CD36 diffusion promotes its receptor and signaling function", *Cell*, vol. 146, no. 4, pp. 593-606.

Chapter 1– Introduction

- Jay, A.G., Chen, A.N., Paz, M.A., Hung, J.P. & Hamilton, J.A. 2015, "CD36 binds oxidized low density lipoprotein (LDL) in a mechanism dependent upon fatty acid binding", *The Journal of biological chemistry*, vol. 290, no. 8, pp. 4590-4603.
- Jensen, M.D. 2002, "Adipose tissue and fatty acid metabolism in humans", *Journal of the Royal Society of Medicine*, vol. 95 Suppl 42, pp. 3-7.
- Jimenez, B., Volpert, O.V., Crawford, S.E., Febbraio, M., Silverstein, R.L. & Bouck, N. 2000, "Signals leading to apoptosis-dependent inhibition of neovascularization by thrombospondin-1", *Nature medicine*, vol. 6, no. 1, pp. 41-48.
- Jimenez, B., Volpert, O.V., Reiher, F., Chang, L., Munoz, A., Karin, M. & Bouck, N. 2001, "c-Jun N-terminal kinase activation is required for the inhibition of neovascularization by thrombospondin-1", *Oncogene*, vol. 20, no. 26, pp. 3443-3448.
- Kadamur, G. & Ross, E.M. 2013, "Mammalian phospholipase C", *Annual Review of Physiology*, vol. 75, pp. 127-154.
- Kagan, V.E., Gleiss, B., Tyurina, Y.Y., Tyurin, V.A., Elenstrom-Magnusson, C., Liu, S.X., Serinkan, F.B., Arroyo, A., Chandra, J., Orrenius, S. & Fadeel, B. 2002, "A role for oxidative stress in apoptosis: oxidation and externalization of phosphatidylserine is required for macrophage clearance of cells undergoing Fas-mediated apoptosis", *Journal of immunology (Baltimore, Md.: 1950)*, vol. 169, no. 1, pp. 487-499.
- Kent, W.S. 1881, *A Manual of the Infusoria: Including a Description of All Known Flagellate, Ciliate, and Tentaculiferous Protozoa, British and Foreign, and an Account of the Organization and the Affinities of the Sponges*, D. Bogue.
- Khan, N.A. & Besnard, P. 2009, "Oro-sensory perception of dietary lipids: new insights into the fat taste transduction", *Biochimica et biophysica acta*, vol. 1791, no. 3, pp. 149-155.
- Kimberly, W.T., Gilson, A., Rost, N.S., Rosand, J., Viswanathan, A., Smith, E.E. & Greenberg, S.M. 2009, "Silent ischemic infarcts are associated with hemorrhage burden in cerebral amyloid angiopathy", *Neurology*, vol. 72, no. 14, pp. 1230-1235.
- Kozera, L., White, E. & Calaghan, S. 2009, "Caveolae act as membrane reserves which limit mechanosensitive I(Cl,swell) channel activation during swelling in the rat ventricular myocyte", *PLoS one*, vol. 4, no. 12, pp. e8312.
- Kralisz, U. 2001, "Structure and functions of CD36 protein", *Postepy biochemii*, vol. 47, no. 4, pp. 307-317.
- Krogh, A., Larsson, B., von Heijne, G. & Sonnhammer, E.L. 2001, "Predicting transmembrane protein topology with a hidden Markov model: application to complete genomes", *Journal of Molecular Biology*, vol. 305, no. 3, pp. 567-580.

Chapter 1– Introduction

- Kropshofer, H., Spindeldreher, S., Rohn, T.A., Platania, N., Grygar, C., Daniel, N., Wolpl, A., Langen, H., Horejsi, V. & Vogt, A.B. 2002, "Tetraspan microdomains distinct from lipid rafts enrich select peptide-MHC class II complexes", *Nature immunology*, vol. 3, no. 1, pp. 61-68.
- Kusumi, A., Nakada, C., Ritchie, K., Murase, K., Suzuki, K., Murakoshi, H., Kasai, R.S., Kondo, J. & Fujiwara, T. 2005, "Paradigm shift of the plasma membrane concept from the two-dimensional continuum fluid to the partitioned fluid: high-speed single-molecule tracking of membrane molecules", *Annual Review of Biophysics and Biomolecular Structure*, vol. 34, pp. 351-378.
- Kusumi, A. & Sako, Y. 1996, "Cell surface organization by the membrane skeleton", *Current opinion in cell biology*, vol. 8, no. 4, pp. 566-574.
- Lajoie, P. & Nabi, I.R. 2010, "Lipid rafts, caveolae, and their endocytosis", *International review of cell and molecular biology*, vol. 282, pp. 135-163.
- Lakshminarayan, R., Wunder, C., Becken, U., Howes, M.T., Benzing, C., Arumugam, S., Sales, S., Ariotti, N., Chambon, V., Lamaze, C., Loew, D., Shevchenko, A., Gaus, K., Parton, R.G. & Johannes, L. 2014, "Galectin-3 drives glycosphingolipid-dependent biogenesis of clathrin-independent carriers", *Nature cell biology*, vol. 16, no. 6, pp. 595-606.
- Langmuir, I. 1917, "THE CONSTITUTION AND FUNDAMENTAL PROPERTIES OF SOLIDS AND LIQUIDS. II. LIQUIDS.1", *Journal of the American Chemical Society*, vol. 39, no. 9, pp. 1848-1906.
- Laugerette, F., Passilly-Degrace, P., Patris, B., Niot, I., Febbraio, M., Montmayeur, J.P. & Besnard, P. 2005, "CD36 involvement in orosensory detection of dietary lipids, spontaneous fat preference, and digestive secretions", *The Journal of clinical investigation*, vol. 115, no. 11, pp. 3177-3184.
- Lawler, J., Derick, L.H., Connolly, J.E., Chen, J.H. & Chao, F.C. 1985, "The structure of human platelet thrombospondin.", *Journal of Biological Chemistry*, vol. 260, no. 6, pp. 3762-3772.
- Lawler, J., Weinstein, R. & Hynes, R.O. 1988, "Cell attachment to thrombospondin: the role of ARG-GLY-ASP, calcium, and integrin receptors.", *Journal of Cell Biology*, vol. 107, no. 6 Pt 1, pp. 2351-2361.
- Lawler, J.W., Slayter, H.S. & Coligan, J.E. 1978, "Isolation and characterization of a high molecular weight glycoprotein from human blood platelets", *The Journal of biological chemistry*, vol. 253, no. 23, pp. 8609-8616.
- Lee, A.G., Birdsall, N.J., Metcalfe, J.C., Toon, P.A. & Warren, G.B. 1974, "Clusters in lipid bilayers and the interpretation of thermal effects in biological membranes", *Biochemistry*, vol. 13, no. 18, pp. 3699-3705.

Chapter 1– Introduction

- Lee, J. & Schmid-Schonbein, G.W. 1995, "Biomechanics of skeletal muscle capillaries: hemodynamic resistance, endothelial distensibility, and pseudopod formation", *Annals of Biomedical Engineering*, vol. 23, no. 3, pp. 226-246.
- Leslie, M. 2011, "Do Lipid Rafts Exist?", *Science*, vol. 334, no. 6059, pp. 1046-1047.
- Levy, S. & Shoham, T. 2005, "The tetraspanin web modulates immune-signalling complexes", *Nature reviews.Immunology*, vol. 5, no. 2, pp. 136-148.
- Lillemeier, B.F., Pfeiffer, J.R., Surviladze, Z., Wilson, B.S. & Davis, M.M. 2006, "Plasma membrane-associated proteins are clustered into islands attached to the cytoskeleton", *Proceedings of the National Academy of Sciences of the United States of America*, vol. 103, no. 50, pp. 18992-18997.
- Lingwood, D., Kaiser, H.J., Levental, I. & Simons, K. 2009, "Lipid rafts as functional heterogeneity in cell membranes", *Biochemical Society transactions*, vol. 37, no. Pt 5, pp. 955-960.
- Lingwood, D. & Simons, K. 2010, "Lipid rafts as a membrane-organizing principle", *Science*, vol. 327, no. 5961, pp. 46-50.
- Lingwood, D. & Simons, K. 2007, "Detergent resistance as a tool in membrane research", *Nature protocols*, vol. 2, no. 9, pp. 2159-2165.
- Lisanti, M.P., Scherer, P.E., Vidugiriene, J., Tang, Z., Hermanowski-Vosatka, A., Tu, Y.H., Cook, R.F. & Sargiacomo, M. 1994, "Characterization of caveolin-rich membrane domains isolated from an endothelial-rich source: implications for human disease.", *Journal of Cell Biology*, vol. 126, no. 1, pp. 111-126.
- Liu, L., He, B., Liu, W.M., Zhou, D., Cox, J.V. & Zhang, X.A. 2007, "Tetraspanin CD151 promotes cell migration by regulating integrin trafficking", *The Journal of biological chemistry*, vol. 282, no. 43, pp. 31631-31642.
- Lodish, H.F., Berk, A., Zipursky, S.L., Matsudaira, P., Baltimore, D. & Darnell, J. 2000, "Chapter 15, Transport across Cell Membranes" in *Molecular cell biology*, 4th edition edn, W. H. Freeman, New York.
- Loges, S., Roncal, C. & Carmeliet, P. 2009, "Development of targeted angiogenic medicine", *Journal of Thrombosis & Haemostasis*, vol. 7, no. 1, pp. 21-33.
- Lombard, J. 2014, "Once upon a time the cell membranes: 175 years of cell boundary research", *Biology direct*, vol. 9, no. 1, pp. 32.
- Lusis, A.J. 2000, "Atherosclerosis", *Nature*, vol. 407, no. 6801, pp. 233-241.

Chapter 1– Introduction

- Marchiafava, E. & Bignami, A. 1894, *On summer-autumn malarial fevers. In: Marchiafava E, editor. Two monographs on malaria and the parasites of malarial fevers*, New Sydenham Society, London.
- Marengo, B., De Ciucis, C., Ricciarelli, R., Pronzato, M.A., Marinari, U.M. & Domenicotti, C. 2011, "Protein Kinase C: An Attractive Target for Cancer Therapy", *Cancers*, vol. 3, no. 1, pp. 531.
- Marino, G. & Kroemer, G. 2013, "Mechanisms of apoptotic phosphatidylserine exposure", *Cell research*, vol. 23, no. 11, pp. 1247-1248.
- Markovic, S.N., Suman, V.J., Rao, R.A., Ingle, J.N., Kaur, J.S., Erickson, L.A., Pitot, H.C., Croghan, G.A., McWilliams, R.R., Merchan, J., Kottschade, L.A., Nevala, W.K., Uhl, C.B., Allred, J. & Creagan, E.T. 2007, "A phase II study of ABT-510 (thrombospondin-1 analog) for the treatment of metastatic melanoma", *American journal of clinical oncology*, vol. 30, no. 3, pp. 303-309.
- Martin, G.S. 2001, "The hunting of the Src", *Nature reviews.Molecular cell biology*, vol. 2, no. 6, pp. 467-475.
- McGilvray, I.D., Serghides, L., Kapus, A., Rotstein, O.D. & Kain, K.C. 2000, "Nonopsonic monocyte/macrophage phagocytosis of Plasmodium falciparum-parasitized erythrocytes: a role for CD36 in malarial clearance", *Blood*, vol. 96, no. 9, pp. 3231-3240.
- Meltzer, S.J. 1906, "The Dynamics of Living Matter", *Science (New York, N.Y.)*, vol. 24, no. 605, pp. 145-147.
- Michaelis, M., Michaelis, U.R., Fleming, I., Suhan, T., Cinatl, J., Blaheta, R.A., Hoffmann, K., Kotchetkov, R., Busse, R., Nau, H. & Cinatl, J., Jr 2004, "Valproic acid inhibits angiogenesis in vitro and in vivo", *Molecular pharmacology*, vol. 65, no. 3, pp. 520-527.
- Min, G., Wang, H., Sun, T.T. & Kong, X.P. 2006, "Structural basis for tetraspanin functions as revealed by the cryo-EM structure of uroplakin complexes at 6-A resolution", *The Journal of cell biology*, vol. 173, no. 6, pp. 975-983.
- Min, K.J., Um, H.J., Cho, K.H. & Kwon, T.K. 2013, "Curcumin inhibits oxLDL-induced CD36 expression and foam cell formation through the inhibition of p38 MAPK phosphorylation", *Food and chemical toxicology : an international journal published for the British Industrial Biological Research Association*, vol. 58, pp. 77-85.
- Miquilena-Colina, M.E., Lima-Cabello, E., Sanchez-Campos, S., Garcia-Mediavilla, M.V., Fernandez-Bermejo, M., Lozano-Rodriguez, T., Vargas-Castrillon, J., Buque, X., Ochoa, B., Aspichueta, P., Gonzalez-Gallego, J. & Garcia-Monzon, C. 2011, "Hepatic fatty acid translocase CD36 upregulation is associated with insulin resistance, hyperinsulinaemia and increased steatosis in non-alcoholic steatohepatitis and chronic hepatitis C", *Gut*, vol. 60, no. 10, pp. 1394-1402.

Chapter 1– Introduction

- Mirochnik, Y., Kwiatek, A. & Volpert, O.V. 2008, "Thrombospondin and apoptosis: molecular mechanisms and use for design of complementation treatments", *Current Drug Targets*, vol. 9, no. 10, pp. 851-862.
- Mishra, S. & Joshi, P.G. 2007, "Lipid raft heterogeneity: an enigma", *Journal of neurochemistry*, vol. 103 Suppl 1, pp. 135-142.
- Moore, K.J. & Freeman, M.W. 2006, "Scavenger receptors in atherosclerosis: beyond lipid uptake", *Arteriosclerosis, Thrombosis, and Vascular Biology*, vol. 26, no. 8, pp. 1702-1711.
- Mouritsen, O.G. & Zuckermann, M.J. 2004, "What's so special about cholesterol?", *Lipids*, vol. 39, no. 11, pp. 1101-1113.
- Munro, S. 2003, "Lipid rafts: elusive or illusive?", *Cell*, vol. 115, no. 4, pp. 377-388.
- Nabi, I.R., Shankar, J. & Dennis, J.W. 2015, "The galectin lattice at a glance", *Journal of cell science*, vol. 128, no. 13, pp. 2213-2219.
- Nassir, F., Wilson, B., Han, X., Gross, R.W. & Abumrad, N.A. 2007, "CD36 is important for fatty acid and cholesterol uptake by the proximal but not distal intestine", *The Journal of biological chemistry*, vol. 282, no. 27, pp. 19493-19501.
- Neculai, D., Schwake, M., Ravichandran, M., Zunke, F., Collins, R.F., Peters, J., Neculai, M., Plumb, J., Loppnau, P., Pizarro, J.C., Seitova, A., Trimble, W.S., Saftig, P., Grinstein, S. & Dhe-Paganon, S. 2013, "Structure of LIMP-2 provides functional insights with implications for SR-BI and CD36", *Nature*, vol. 504, no. 7478, pp. 172-176.
- Ng, D.P., Poulsen, B.E. & Deber, C.M. 2012, "Membrane protein misassembly in disease", *Biochimica et Biophysica Acta (BBA) - Biomembranes*, vol. 1818, no. 4, pp. 1115-1122.
- Nichols, Z. & Vogt, R.G. 2008, "The SNMP/CD36 gene family in Diptera, Hymenoptera and Coleoptera: *Drosophila melanogaster*, *D. pseudoobscura*, *Anopheles gambiae*, *Aedes aegypti*, *Apis mellifera*, and *Tribolium castaneum*", *Insect biochemistry and molecular biology*, vol. 38, no. 4, pp. 398-415.
- Nicholson, A.C., Frieda, S., Pearce, A. & Silverstein, R.L. 1995, "Oxidized LDL binds to CD36 on human monocyte-derived macrophages and transfected cell lines. Evidence implicating the lipid moiety of the lipoprotein as the binding site", *Arteriosclerosis, Thrombosis, and Vascular Biology*, vol. 15, no. 2, pp. 269-275.
- Nor, J.E., Mitra, R.S., Sutorik, M.M., Mooney, D.J., Castle, V.P. & Polverini, P.J. 2000, "Thrombospondin-1 induces endothelial cell apoptosis and inhibits angiogenesis by activating the caspase death pathway", *Journal of vascular research*, vol. 37, no. 3, pp. 209-218.

Chapter 1– Introduction

- Nydegger, S., Khurana, S., Kremontsov, D.N., Foti, M. & Thali, M. 2006, "Mapping of tetraspanin-enriched microdomains that can function as gateways for HIV-1", *The Journal of cell biology*, vol. 173, no. 5, pp. 795-807.
- Ochola, L.B., Siddondo, B.R., Ocholla, H., Nkya, S., Kimani, E.N., Williams, T.N., Makale, J.O., Liljander, A., Urban, B.C., Bull, P.C., Szeszak, T., Marsh, K. & Craig, A.G. 2011, "Specific receptor usage in Plasmodium falciparum cytoadherence is associated with disease outcome", *PloS one*, vol. 6, no. 3, pp. e14741.
- Okumura, T. & Jamieson, G.A. 1976, "Platelet glycolalicin. I. Orientation of glycoproteins of the human platelet surface", *The Journal of biological chemistry*, vol. 251, no. 19, pp. 5944-5949.
- Oquendo, P., Hundt, E., Lawler, J. & Seed, B. 1989, "CD36 directly mediates cytoadherence of Plasmodium falciparum parasitized erythrocytes.", *Cell*, vol. 58, no. 1, pp. 95-101.
- Otto, G.P. & Nichols, B.J. 2011, "The roles of flotillin microdomains--endocytosis and beyond", *Journal of cell science*, vol. 124, no. Pt 23, pp. 3933-3940.
- Pani, B., Ong, H.L., Brazer, S.C., Liu, X., Rauser, K., Singh, B.B. & Ambudkar, I.S. 2009, "Activation of TRPC1 by STIM1 in ER-PM microdomains involves release of the channel from its scaffold caveolin-1", *Proceedings of the National Academy of Sciences of the United States of America*, vol. 106, no. 47, pp. 20087-20092.
- Park, L., Zhou, J., Zhou, P., Pistick, R., El Jamal, S., Younkin, L., Pierce, J., Arreguin, A., Anrather, J., Younkin, S.G., Carlson, G.A., McEwen, B.S. & Iadecola, C. 2013, "Innate immunity receptor CD36 promotes cerebral amyloid angiopathy", *Proceedings of the National Academy of Sciences of the United States of America*, vol. 110, no. 8, pp. 3089-3094.
- Parsons, S.J. & Parsons, J.T. 2004, "Src family kinases, key regulators of signal transduction", *Oncogene*, vol. 23, no. 48, pp. 7906-7909.
- Parton, R.G. & del Pozo, M.A. 2013, "Caveolae as plasma membrane sensors, protectors and organizers", *Nature reviews.Molecular cell biology*, vol. 14, no. 2, pp. 98-112.
- Pike, L.J. 2004, "Lipid rafts: heterogeneity on the high seas", *The Biochemical journal*, vol. 378, no. Pt 2, pp. 281-292.
- Pluddemann, A., Neyen, C. & Gordon, S. 2007, "Macrophage scavenger receptors and host-derived ligands", *Methods (San Diego, Calif.)*, vol. 43, no. 3, pp. 207-217.
- Podrez, E.A., Poliakov, E., Shen, Z., Zhang, R., Deng, Y., Sun, M., Finton, P.J., Shan, L., Gugiu, B., Fox, P.L., Hoff, H.F., Salomon, R.G. & Hazen, S.L. 2002, "Identification of a novel family of oxidized phospholipids that serve as ligands for the macrophage scavenger receptor CD36", *The Journal of biological chemistry*, vol. 277, no. 41, pp. 38503-38516.

Chapter 1– Introduction

- Poon, I.K., Lucas, C.D., Rossi, A.G. & Ravichandran, K.S. 2014, "Apoptotic cell clearance: basic biology and therapeutic potential", *Nature reviews.Immunology*, vol. 14, no. 3, pp. 166-180.
- Pownall, H. & Moore, K. 2014, "Commentary on fatty acid wars: the diffusionists versus the translocatists", *Arteriosclerosis, Thrombosis, and Vascular Biology*, vol. 34, no. 5, pp. e8-9.
- Raghupathy, R., Anilkumar, A.A., Polley, A., Singh, P.P., Yadav, M., Johnson, C., Suryawanshi, S., Saikam, V., Sawant, S.D., Panda, A., Guo, Z., Vishwakarma, R.A., Rao, M. & Mayor, S. 2015, "Transbilayer lipid interactions mediate nanoclustering of lipid-anchored proteins", *Cell*, vol. 161, no. 3, pp. 581-594.
- Rahaman, S.O., Lennon, D.J., Febbraio, M., Podrez, E.A., Hazen, S.L. & Silverstein, R.L. 2006, "A CD36-dependent signaling cascade is necessary for macrophage foam cell formation", *Cell metabolism*, vol. 4, no. 3, pp. 211-221.
- Rajendran, L., Masilamani, M., Solomon, S., Tikkanen, R., Stuermer, C.A., Plattner, H. & Illges, H. 2003, "Asymmetric localization of flotillins/reggies in preassembled platforms confers inherent polarity to hematopoietic cells", *Proceedings of the National Academy of Sciences of the United States of America*, vol. 100, no. 14, pp. 8241-8246.
- Rasmussen, J.T., Berglund, L., Rasmussen, M.S. & Petersen, T.E. 1998, "Assignment of disulfide bridges in bovine CD36", *European journal of biochemistry / FEBS*, vol. 257, no. 2, pp. 488-494.
- Resh, M.D. 1999, "Fatty acylation of proteins: new insights into membrane targeting of myristoylated and palmitoylated proteins", *Biochimica et biophysica acta*, vol. 1451, no. 1, pp. 1-16.
- Resh, M.D. 1994, "Myristylation and palmitoylation of Src family members: the fats of the matter", *Cell*, vol. 76, no. 3, pp. 411-413.
- Resovi, A., Pinessi, D., Chiorino, G. & Taraboletti, G. 2014, "Current understanding of the thrombospondin-1 interactome", *Matrix biology : journal of the International Society for Matrix Biology*, vol. 37, pp. 83-91.
- Ricciarelli, R., D'Abramo, C., Zingg, J.M., Giliberto, L., Markesbery, W., Azzi, A., Marinari, U.M., Pronzato, M.A. & Tabaton, M. 2004, "CD36 overexpression in human brain correlates with beta-amyloid deposition but not with Alzheimer's disease", *Free radical biology & medicine*, vol. 36, no. 8, pp. 1018-1024.
- Richter, T., Floetenmeyer, M., Ferguson, C., Galea, J., Goh, J., Lindsay, M.R., Morgan, G.P., Marsh, B.J. & Parton, R.G. 2008, "High-resolution 3D quantitative analysis of caveolar ultrastructure and caveola-cytoskeleton interactions", *Traffic (Copenhagen, Denmark)*, vol. 9, no. 6, pp. 893-909.

Chapter 1– Introduction

- Riento, K., Frick, M., Schafer, I. & Nichols, B.J. 2009, "Endocytosis of flotillin-1 and flotillin-2 is regulated by Fyn kinase", *Journal of cell science*, vol. 122, no. Pt 7, pp. 912-918.
- Rigotti, A., Acton, S.L. & Krieger, M. 1995, "The class B scavenger receptors SR-BI and CD36 are receptors for anionic phospholipids", *The Journal of biological chemistry*, vol. 270, no. 27, pp. 16221-16224.
- Robertson, J.D. 1960, "The molecular structure and contact relationships of cell membranes", *Progress in biophysics and molecular biology*, vol. 10, pp. 343-418.
- Robertson, J.D. 1959, "The ultrastructure of cell membranes and their derivatives", *Biochemical Society symposium*, vol. 16, pp. 3-43.
- Roskoski, R., Jr 2005, "Src kinase regulation by phosphorylation and dephosphorylation", *Biochemical and biophysical research communications*, vol. 331, no. 1, pp. 1-14.
- Rowe, J.A., Claessens, A., Corrigan, R.A. & Arman, M. 2009, "Adhesion of Plasmodium falciparum-infected erythrocytes to human cells: molecular mechanisms and therapeutic implications", *Expert reviews in molecular medicine*, vol. 11, pp. e16.
- Rucevic, M., Hixson, D. & Josic, D. 2011, "Mammalian plasma membrane proteins as potential biomarkers and drug targets", *Electrophoresis*, vol. 32, no. 13, pp. 1549-1564.
- Ryeom, S.W., Silverstein, R.L., Scotto, A. & Sparrow, J.R. 1996, "Binding of anionic phospholipids to retinal pigment epithelium may be mediated by the scavenger receptor CD36", *The Journal of biological chemistry*, vol. 271, no. 34, pp. 20536-20539.
- Safa, A.R. 2012, "c-FLIP, a master anti-apoptotic regulator", *Experimental oncology*, vol. 34, no. 3, pp. 176-184.
- Saito, Y.D., Jensen, A.R., Salgia, R. & Posadas, E.M. 2010, "Fyn: a novel molecular target in cancer", *Cancer*, vol. 116, no. 7, pp. 1629-1637.
- Sala-Valdes, M., Ursa, A., Charrin, S., Rubinstein, E., Hemler, M.E., Sanchez-Madrid, F. & Yanez-Mo, M. 2006, "EWI-2 and EWI-F link the tetraspanin web to the actin cytoskeleton through their direct association with ezrin-radixin-moesin proteins", *The Journal of biological chemistry*, vol. 281, no. 28, pp. 19665-19675.
- Scherer, P.E. 2006, "Adipose tissue: from lipid storage compartment to endocrine organ", *Diabetes*, vol. 55, no. 6, pp. 1537-1545.
- Schlormann, W., Steiniger, F., Richter, W., Kaufmann, R., Hause, G., Lemke, C. & Westermann, M. 2010, "The shape of caveolae is omega-like after glutaraldehyde fixation and cup-like after cryofixation", *Histochemistry and cell biology*, vol. 133, no. 2, pp. 223-228.

Chapter 1– Introduction

- Schroeder, R., London, E. & Brown, D. 1994, "Interactions between saturated acyl chains confer detergent resistance on lipids and glycosylphosphatidylinositol (GPI)-anchored proteins: GPI-anchored proteins in liposomes and cells show similar behavior", *Proceedings of the National Academy of Sciences of the United States of America*, vol. 91, no. 25, pp. 12130-12134.
- Schwann, T. 1847, *Microscopical researches into the accordance in the structure and growth of animals and plants*, Sydenham Society.
- Segawa, K. & Nagata, S. 2015, "An Apoptotic 'Eat Me' Signal: Phosphatidylserine Exposure", *Trends in cell biology*, .
- Semba, K., Nishizawa, M., Miyajima, N., Yoshida, M.C., Sukegawa, J., Yamanashi, Y., Sasaki, M., Yamamoto, T. & Toyoshima, K. 1986, "Yes-Related Protooncogene, Syn, Belongs to the Protein-Tyrosine Kinase Family", *Proceedings of the National Academy of Sciences of the United States of America*, vol. 83, no. 15, pp. 5459-5463.
- Serghides, L., Smith, T.G., Patel, S.N. & Kain, K.C. 2003, "CD36 and malaria: friends or foes?", *Trends in parasitology*, vol. 19, no. 10, pp. 461-469.
- Sharma, P., Ghavami, S., Stelmack, G.L., McNeill, K.D., Mutawe, M.M., Klonisch, T., Unruh, H. & Halayko, A.J. 2010, "beta-Dystroglycan binds caveolin-1 in smooth muscle: a functional role in caveolae distribution and Ca²⁺ release", *Journal of cell science*, vol. 123, no. Pt 18, pp. 3061-3070.
- Shaw, S. 1987, "Characterization of human leukocyte differentiation antigens", *Immunology today*, vol. 8, no. 1, pp. 1-3.
- Shiju, T.M., Mohan, V., Balasubramanyam, M. & Viswanathan, P. 2015, "Soluble CD36 in plasma and urine: a plausible prognostic marker for diabetic nephropathy", *Journal of diabetes and its complications*, vol. 29, no. 3, pp. 400-406.
- Short, S.M., Derrien, A., Narsimhan, R.P., Lawler, J., Ingber, D.E. & Zetter, B.R. 2005, "Inhibition of endothelial cell migration by thrombospondin-1 type-1 repeats is mediated by beta1 integrins", *Journal of Cell Biology*, vol. 168, no. 4, pp. 643-653.
- Silverstein, R.L. & Febbraio, M. 2009, "CD36, a scavenger receptor involved in immunity, metabolism, angiogenesis, and behavior", *Science signaling*, vol. 2, no. 72, pp. re3.
- Silverstein, R.L. & Febbraio, M. 2007, "CD36-TSP-HRGP interactions in the regulation of angiogenesis", *Current pharmaceutical design*, vol. 13, no. 35, pp. 3559-3567.
- Silverstein, R.L., Li, W., Park, Y.M. & Rahaman, S.O. 2010, "Mechanisms of Cell Signaling by the Scavenger Receptor CD36: Implications in Atherosclerosis and Thrombosis", *Transactions of the American Clinical and Climatological Association*, vol. 121, pp. 206-220.

Chapter 1– Introduction

- Simantov, R., Febbraio, M. & Silverstein, R.L. 2005, "The antiangiogenic effect of thrombospondin-2 is mediated by CD36 and modulated by histidine-rich glycoprotein", *Matrix biology : journal of the International Society for Matrix Biology*, vol. 24, no. 1, pp. 27-34.
- Simons, K. & Gerl, M.J. 2010, "Revitalizing membrane rafts: new tools and insights", *Nature Reviews Molecular Cell Biology*, vol. 11, no. 10, pp. 688-699.
- Simons, K. & Ikonen, E. 1997, "Functional rafts in cell membranes", *Nature*, vol. 387, no. 6633, pp. 569-572.
- Simons, K. & Sampaio, J.L. 2011, "Membrane organization and lipid rafts", *Cold Spring Harbor perspectives in biology*, vol. 3, no. 10, pp. a004697.
- Simons, K. & van Meer, G. 1988, "Lipid sorting in epithelial cells", *Biochemistry*, vol. 27, no. 17, pp. 6197-6202.
- Simons, P.J., Kummer, J.A., Luiken, J.J. & Boon, L. 2011, "Apical CD36 immunolocalization in human and porcine taste buds from circumvallate and foliate papillae", *Acta Histochemica*, vol. 113, no. 8, pp. 839-843.
- Singer, S.J. & Nicolson, G.L. 1972, "The fluid mosaic model of the structure of cell membranes.", *Science*, vol. 175, no. 4023, pp. 720-731.
- Sinha, B., Koster, D., Ruez, R., Gonnord, P., Bastiani, M., Abankwa, D., Stan, R.V., Butler-Browne, G., Védie, B., Johannes, L., Morone, N., Parton, R.G., Raposo, G., Sens, P., Lamaze, C. & Nassoy, P. 2011, "Cells respond to mechanical stress by rapid disassembly of caveolae", *Cell*, vol. 144, no. 3, pp. 402-413.
- Slaughter, N., Laux, I., Tu, X., Whitelegge, J., Zhu, X., Effros, R., Bickel, P. & Nel, A. 2003, "The flotillins are integral membrane proteins in lipid rafts that contain TCR-associated signaling components: implications for T-cell activation", *Clinical immunology (Orlando, Fla.)*, vol. 108, no. 2, pp. 138-151.
- Smith, J.D., Chitnis, C.E., Craig, A.G., Roberts, D.J., Hudson-Taylor, D.E., Peterson, D.S., Pinches, R., Newbold, C.I. & Miller, L.H. 1995, "Switches in expression of Plasmodium falciparum var genes correlate with changes in antigenic and cytoadherent phenotypes of infected erythrocytes", *Cell*, vol. 82, no. 1, pp. 101-110.
- Solis, G.P., Hoegg, M., Munderloh, C., Schrock, Y., Malaga-Trillo, E., Rivera-Milla, E. & Stuermer, C.A. 2007, "Reggie/flotillin proteins are organized into stable tetramers in membrane microdomains", *The Biochemical journal*, vol. 403, no. 2, pp. 313-322.
- Sottile, J., Selegue, J. & Mosher, D.F. 1991, "Synthesis of truncated amino-terminal trimers of thrombospondin", *Biochemistry*, vol. 30, no. 26, pp. 6556-6562.

Chapter 1– Introduction

- Storm, J. & Craig, A.G. 2014, "Pathogenesis of cerebral malaria--inflammation and cytoadherence", *Frontiers in cellular and infection microbiology*, vol. 4, pp. 100.
- Su, X.Z., Heatwole, V.M., Wertheimer, S.P., Guinet, F., Herrfeldt, J.A., Peterson, D.S., Ravetch, J.A. & Wellems, T.E. 1995, "The large diverse gene family var encodes proteins involved in cytoadherence and antigenic variation of Plasmodium falciparum-infected erythrocytes", *Cell*, vol. 82, no. 1, pp. 89-100.
- Suzuki, K., Ritchie, K., Kajikawa, E., Fujiwara, T. & Kusumi, A. 2005, "Rapid hop diffusion of a G-protein-coupled receptor in the plasma membrane as revealed by single-molecule techniques.", *Biophysical journal*, vol. 88, no. 5, pp. 3659-3680.
- Tandon, N.N., Kralisz, U. & Jamieson, G.A. 1989, "Identification of glycoprotein IV (CD36) as a primary receptor for platelet-collagen adhesion", *The Journal of biological chemistry*, vol. 264, no. 13, pp. 7576-7583.
- Tandon, N.N., Lipsky, R.H., Burgess, W.H. & Jamieson, G.A. 1989, "Isolation and characterization of platelet glycoprotein IV (CD36)", *The Journal of biological chemistry*, vol. 264, no. 13, pp. 7570-7575.
- Tanford, C. 1978, "The hydrophobic effect and the organization of living matter", *Science (New York, N.Y.)*, vol. 200, no. 4345, pp. 1012-1018.
- Tarhda, Z. & Ibrahim, A. 2015, "Insight into the mechanism of lipids binding and uptake by CD36 receptor", *Bioinformation*, vol. 11, no. 6, pp. 302-306.
- Taylor, R.C., Cullen, S.P. & Martin, S.J. 2008, "Apoptosis: controlled demolition at the cellular level", *Nature Reviews Molecular Cell Biology*, vol. 9, no. 3, pp. 231-241.
- Thatcher, J.D. 2010, "The Inositol Trisphosphate (IP3) Signal Transduction Pathway", *Science Signaling*, vol. 3, no. 119, pp. tr3-tr3.
- Thomas, S.M. & Brugge, J.S. 1997, "Cellular functions regulated by Src family kinases", *Annual Review of Cell & Developmental Biology*, vol. 13, pp. 513-609.
- Thorne, R.F., Ralston, K.J., de Bock, C.E., Mhaidat, N.M., Zhang, X.D., Boyd, A.W. & Burns, G.F. 2010, "Palmitoylation of CD36/FAT regulates the rate of its post-transcriptional processing in the endoplasmic reticulum", *Biochimica et biophysica acta*, vol. 1803, no. 11, pp. 1298-1307.
- Tontonoz, P., Nagy, L., Alvarez, J.G., Thomazy, V.A. & Evans, R.M. 1998, "PPARgamma promotes monocyte/macrophage differentiation and uptake of oxidized LDL", *Cell*, vol. 93, no. 2, pp. 241-252.
- Travis, J. 2011, "Mysteries of the Cell", *Science*, vol. 334, no. 6059, pp. 1046-1046.

Chapter 1– Introduction

- Treanor, B., Depoil, D., Gonzalez-Granja, A., Barral, P., Weber, M., Dushek, O., Bruckbauer, A. & Batista, F.D. 2010, "The membrane skeleton controls diffusion dynamics and signaling through the B cell receptor", *Immunity*, vol. 32, no. 2, pp. 187-199.
- Tsuji, T. & Osawa, T. 1986, "Purification and chemical characterization of human platelet membrane glycoprotein IV", *Journal of Biochemistry*, vol. 100, no. 4, pp. 1077-1085.
- Unternaehrer, J.J., Chow, A., Pypaert, M., Inaba, K. & Mellman, I. 2007, "The tetraspanin CD9 mediates lateral association of MHC class II molecules on the dendritic cell surface", *Proceedings of the National Academy of Sciences of the United States of America*, vol. 104, no. 1, pp. 234-239.
- van Bennekum, A., Werder, M., Thuahnai, S.T., Han, C.H., Duong, P., Williams, D.L., Wettstein, P., Schulthess, G., Phillips, M.C. & Hauser, H. 2005, "Class B scavenger receptor-mediated intestinal absorption of dietary beta-carotene and cholesterol", *Biochemistry*, vol. 44, no. 11, pp. 4517-4525.
- van den Bogaart, G., Meyenberg, K., Risselada, H.J., Amin, H., Willig, K.I., Hubrich, B.E., Dier, M., Hell, S.W., Grubmuller, H., Diederichsen, U. & Jahn, R. 2011, "Membrane protein sequestering by ionic protein-lipid interactions", *Nature*, vol. 479, no. 7374, pp. 552-555.
- van Meer, G., Voelker, D.R. & Feigenson, G.W. 2008, "Membrane lipids: where they are and how they behave", *Nature reviews.Molecular cell biology*, vol. 9, no. 2, pp. 112-124.
- Volpert, O.V., Zaichuk, T., Zhou, W., Reiher, F., Ferguson, T.A., Stuart, P.M., Amin, M. & Bouck, N.P. 2002, "Inducer-stimulated Fas targets activated endothelium for destruction by anti-angiogenic thrombospondin-1 and pigment epithelium-derived factor", *Nature medicine*, vol. 8, no. 4, pp. 349-357.
- von Heijne, G. 2006, "Membrane-protein topology", *Nature reviews.Molecular cell biology*, vol. 7, no. 12, pp. 909-918.
- WHO, M.c. 2015, , *Cancer* [Homepage of WHO Media centre], [Online]. Available: <http://www.who.int/mediacentre/factsheets/fs297/en/> [2015, 03/25].
- Willems, B.A.G., Vermeer, C., Reutelingsperger, C.P.M. & Schurgers, L.J. 2014, "The realm of vitamin K dependent proteins: Shifting from coagulation toward calcification", *Molecular Nutrition & Food Research*, vol. 58, no. 8, pp. 1620-1635.
- Wunderlich, F., Ronai, A., Speth, V., Seelig, J. & Blume, A. 1975, "Thermotropic lipid clustering in tetrahymena membranes", *Biochemistry*, vol. 14, no. 17, pp. 3730-3735.
- Yamamoto, K., Furuya, K., Nakamura, M., Kobatake, E., Sokabe, M. & Ando, J. 2011, "Visualization of flow-induced ATP release and triggering of Ca²⁺ waves at caveolae in vascular endothelial cells", *Journal of cell science*, vol. 124, no. Pt 20, pp. 3477-3483.

Chapter 1– Introduction

- Yanez-Mo, M., Barreiro, O., Gordon-Alonso, M., Sala-Valdes, M. & Sanchez-Madrid, F. 2009, "Tetraspanin-enriched microdomains: a functional unit in cell plasma membranes", *Trends in cell biology*, vol. 19, no. 9, pp. 434-446.
- Yanez-Mo, M., Mittelbrunn, M. & Sanchez-Madrid, F. 2001, "Tetraspanins and intercellular interactions", *Microcirculation (New York, N.Y.: 1994)*, vol. 8, no. 3, pp. 153-168.
- Yang, H., Yan, L., Qian, P., Duan, H., Wu, J., Li, B. & Wang, S. 2015, "Icariin inhibits foam cell formation by down-regulating the expression of CD36 and up-regulating the expression of SR-BI", *Journal of cellular biochemistry*, vol. 116, no. 4, pp. 580-588.
- Yazgan, B., Ustunsoy, S., Karademir, B. & Kartal-Ozer, N. 2014, "CD36 as a biomarker of atherosclerosis", *Free radical biology & medicine*, vol. 75 Suppl 1, pp. S10.
- Ye, J. & DeBose-Boyd, R.A. 2011, "Regulation of cholesterol and fatty acid synthesis", *Cold Spring Harbor perspectives in biology*, vol. 3, no. 7, pp. 10.1101/cshperspect.a004754.
- Yoshizaki, F., Nakayama, H., Iwahara, C., Takamori, K., Ogawa, H. & Iwabuchi, K. 2008, "Role of glycosphingolipid-enriched microdomains in innate immunity: Microdomain-dependent phagocytic cell functions", *Biochimica et Biophysica Acta (BBA) - General Subjects*, vol. 1780, no. 3, pp. 383-392.
- Zaichuk, T.A., Shroff, E.H., Emmanuel, R., Filleur, S., Nelius, T. & Volpert, O.V. 2004, "Nuclear factor of activated T cells balances angiogenesis activation and inhibition", *The Journal of experimental medicine*, vol. 199, no. 11, pp. 1513-1522.
- Zhang, X. & Lawler, J. 2007, "Thrombospondin-based antiangiogenic therapy", *Microvascular research*, vol. 74, no. 2-3, pp. 90-99.

Chapter 2 - Materials and methods

2.1 Cell culture, molecular cloning and stable expression of CD36

2.1.1 Cell culture

Two cell lines were used, primary human microvascular endothelial cell line (HMVECs) and its immortalized version, human dermal microvascular endothelial cell line (HMEC-1) (Ades et al. 1992). HMEC-1 cells (Centers for Disease Control and Prevention, Atlanta, GA, USA) were cultured as earlier described (Ades et al. 1992) in MCDB-131 media (Gibco, Life Technologies, Burlington, ON, Canada) supplemented with 10% FBS (Wisent Bioproducts, St-Bruno, Quebec, Canada), 10 mM L-Glutamate (Gibco), 10 ng/mL Epidermal Growth Factor (BD Biosciences, Mississauga, ON, Canada), and 1 µg/mL hydrocortisone (Sigma-Aldrich, St Louis, MO, USA). Primary HMVECs (Lonza, Mississauga, ON, Canada) were cultured in EBM-2 basal medium (Lonza) supplemented with endothelial cells EGM-2 MV BulletKit (Lonza). Stable expression of CD36 constructs in HMEC-1 cells was done using viral transfection as described below. All transient transfections were performed using FugeneHD (Promega, Fitchburg, WI, USA) following the manufacturer instructions.

2.1.2 DNA plasmids and stable expression of the constructs

The CD36 open reading frame was obtained from the human cDNA ORF CD36 (Myc-DDK-tagged) clone purchased from Origene (OriGene Technologies, Inc., Rockville, MD, USA). The coding sequence was amplified with a 5' primer containing a BspEI site and a 3' primer with an EcoRI site. The purified PCR fragment was then digested with these enzymes and ligated in frame at the 5' end of the coding sequence of the following fluorescent proteins: mApple and PAmCherry. The same strategy was used to generate Fyn-mEmerald and Fyn-PAGFP vectors, in which case the human Fyn cDNA was obtained from Harvard Medical

Chapter 2- Materials and methods

School plasmid repository PlasmidID (Boston, MA, USA). Each CD36 construct, CD36-myc, mApple-CD36 and PAmCherry-CD36, was then subcloned into retroviral vector pFB-Neo using AgeI and NotI restriction sites (Stratagene, Santa Clara, CA, USA). These were then co-transfected with pVPack-VSV-G and pVPack-GP vectors in HEK 293T cells for production of virus. The viral supernatant was used to transduce HMEC-1 cells for 24hrs. The next day, 1mg/ml G418 (Sigma-Aldrich) was added to the culture media for selection of stable cell lines. Selection was performed for 14 days to get HMEC-CD36-myc, HMEC-mApple-CD36 and HMEC-PAmCherry-CD36 stable cell lines. Expression was confirmed with western-blot and immunofluorescence analysis.

Truncated Fyn-GFP expression vectors were a gift from Dr. Luc Berthiaume (Department of Cell Biology, University of Alberta) (Alland et al. 1994).

2.2 Western Blotting

Active state of Fyn, p38MAPK and p130Cas were analyzed by rabbit anti-P-Y420 (Invitrogen, Carlsbad, CA, USA), rabbit anti-phospho-p38MAPK (Cell Signaling, Boston, MA, USA) and rabbit anti-phospho-p130Cas (Cell Signaling), respectively. Anti-Fyn (Upstate, EMD Millipore, Billerica, MA, USA) and anti-tubulin (Sigma-Aldrich) were used to probe for total Fyn and tubulin, respectively, as loading controls. Cells were grown on a 6 well plate coated with $1\mu\text{g}/\text{cm}^2$ fibronectin (BD Biosciences). Serum Starvation was done for 3 hours using MBCD-131 media, after which thrombospondin-1 (TSP-1; Protein Sciences Meriden, CT, USA) was added for the intended time point. Cells were then lysed using phosphorylation lysis buffer (20mM MOPS, 1% Triton X-100, 1mM sodium orthovanadate, 2mM EGTA, 5mM EDTA, pH 7.0) supplemented with phosphatase inhibitor, PhosSTOP (Roche Applied Science, Laval, QC,

Chapter 2- Materials and methods

Canada) and protease inhibitor (Sigma-Aldrich). The lysates were resolved on SDS-PAGE gels, transferred to nitrocellulose membranes and immunoblotted with the antibodies above. The membranes were then incubated with the appropriate IRDye-coupled secondary antibodies (LI-COR Biosciences, Lincoln, NE, USA). Odyssey Infrared Imaging System scanner (LI-COR Biosciences) was used to scan for immunoblotted proteins in 700 and 800 nm channels. Quantification of the band intensities was performed using ImageJ and the relative amount of phosphorylation was normalized either to the total amount of the protein (for Fyn) or to the loading control tubulin (for p38MAPK and p130CAS). Statistical analyses were performed using Graphpad Prism (GraphPad Software, Inc., La Jolla, CA, USA) and MatLab (MathWorks, Natick, MA, USA).

2.3 Drug Treatment

Cells were incubated with 0.5 μ M PTP-CD45 (N-(9,10-dioxophenanthren-2-yl)-2,2-dimethylpropanamide) inhibitor (Calbiochem, EMD Millipore, Billerica, MA, USA), 200nM Latrunculin B (Sigma-Aldrich) or 2mM Methyl- β -CycloDextrin (Sigma-Aldrich) in basal MBCD-131 media for 15 minutes. To ensure that the drug disruption was maintained during TSP-1 stimulation, the treatments were immediately followed by another incubation period with the same drug with or without TSP-1 for the specified time points.

2.4 Chemical Crosslinking

Cells grown on a 6 well plate were stimulated with TSP-1 in basal MBCD-131 media at different timepoints after which they were washed twice with cold PBS. 2mM membrane-insoluble DTSSP (3,3'-dithiobis(sulfosuccinimidyl propionate)) (Thermo Fisher Scientific Inc, Waltham, MA, USA) in PBS was added on ice for 2 hours for extracellular crosslinking. The

Chapter 2- Materials and methods

reaction was stopped using 20mM Tris, pH 7.5 after which cells were lysed and processed for western blotting analysis. As a control of DTSSP ability to crosslink CD36, β -Mercaptoethanol (β ME; Sigma-Aldrich) was used to cleave DTSSP in 30% of the lysates volume.

2.5 CD36 Knockdown

HMVEC_s were grown to about 80% confluency. CD36 on-Target SMARTpool siRNA (Thermo Scientific) was diluted in nuclease-free water to a working concentration of 10 μ M. 90pmol of the siRNA was mixed with RNAiMAX reagent (Life Technologies) at 1:1 volume ratio in Opti-MEM medium (Gibco, Life Technologies). The complexes were incubated for 10 minutes at room temperature. The siRNA-reagent complex was added to cells and incubated for 48 hours before intended experiment was performed. The amount of knockdown was quantified by western blot analysis and estimated to ~90% efficacy.

2.6 Immunofluorescence

2.6.1 TSP-1 labelling

TSP-1 was labeled using fluorescent dyes (Cy3b or Atto647N) NHS esters (GE healthcare, Mississauga, ON, Canada, and Sigma-Aldrich, respectively). Lyophilized 0.02mg of the dye was dissolved in 10 μ L anhydrous DMSO. 10 μ g of TSP-1 was added to 20 μ L of 0.5M NaHCO₃ (pH 8.5) and 5 μ L of the dye solution added to the reaction.

The reaction was incubated for 1 hour in the dark rocking gently at room temperature. After the reaction, labeled TSP-1 was separated and recovered in the void volume of a NAP-5 column (GE Healthcare). TSP-1 conjugation with the dye was confirmed using NanoDrop Spectrophotometer (Thermo Scientific) and immunofluorescence microscopy.

2.6.2 Fab fragment generation and labeling

Fab fragments were generated from monoclonal mouse anti-CD36 IgG (clone 131.2, gift from Dr. N. Tandon, Otsuka America Pharmaceutical, Inc.) using Pierce™ Fab Preparation Kit. Briefly, 1mg of IgG was incubated with immobilized papain for 3 hours with constant end-over-end mixer at 37⁰C. The antibody digest was the passed through protein-A resin, and the fab eluant collected. Fab purity was verified using anti-Fc and anti-Fab antibodies on western blot. Only fab eluants positive of anti-Fab binding and negative of anti-Fc binding were used for dye labeling.

The anti-CD36 fabs were labeled using fluorescent dyes (Cy3b or Atto647N) NHS esters (GE healthcare, Mississauga, ON, Canada, and Sigma-Aldrich, respectively). Lyophilized 0.02mg of the dye was dissolved in 10μL anhydrous DMSO. 50μg of antibody was added to 10μL of 0.5M NaHCO₃ (pH 8.5) and 2μL of the dye solution added to the reaction.

The reaction was incubated for 0.5 hour in the dark rocking gently at room temperature. After the reaction, labeled Fab was separated and recovered in the void volume of a NAP-5 column (GE Healthcare). Fab conjugation with the dye was confirmed using NanoDrop Spectrophotometer (Thermo Scientific) and immunofluorescence microscopy.

2.6.3 Immunostaining

Cells were grown on Lab-Tek chambers (Fisher Scientific) coated with 1μg/cm² Fibronectin (BD Biosciences). Serum starvation was done for three hours using the basal MCB 131 media before stimulation with or without 10 nM TSP-1, 10μg/ml FA6-152 (Santa Cruz Biotechnology, Dallas, TX, USA) or 10μg/ml SMφ (Santa Cruz Biotechnology) for the intended

Chapter 2- Materials and methods

timepoints. These concentrations were maintained in all other stimulation experiments using these ligands.

This was followed by fixation with 3% Paraformaldehyde (Canemco, Canton de Gore, QC, Canada) and 0.1% Glutaraldehyde (Canemco) in PBS for 10 minutes at room temperature. Quenching was done with fresh 0.1% Sodium borohydride (Sigma-Aldrich) in PBS for 7 minutes. To stain for surface CD36, cells were blocked with 3% BSA in PBS for 30 minutes then incubated with 1:1000 monoclonal mouse anti CD36 IgG (clone FA6-152) in blocking buffer for 30 minutes, followed by incubation with anti-mouse antibody conjugated to AlexaFluor 488, Cy3 or AlexaFluor 647 (Jackson ImmunoResearch Laboratories Inc., West Grove, PA, USA) diluted in blocking buffer. For intracellular staining, 0.1% Triton X-100 in PBS was used to permeabilize the cells. Active Fyn was stained with directly coupled anti-P-Y420 AlexaFluor 488 (Invitrogen, Carlsbad, CA, USA) in blocking buffer after intracellular blocking. Actin was labeled with Phalloidin AlexaFluor 488, AlexaFluor 555 or AlexaFluor 647 (Invitrogen) depending on the experiment. DAPI (Sigma-Aldrich) was used to highlight cell nuclei.

2.7 Immunofluorescence Imaging

2.7.1 Confocal Imaging

Confocal imaging was done on Quorum Technologies (Guelph, ON, Canada) WaveFx spinning-disk microscope with a 60x, 1.42 numerical aperture oil objective, using EM-CDD camera (Hamamatsu, Hamamatsu City, Japan) and Volocity software (PerkinElmer, Waltham, MA, USA) set up on Olympus IX-81 inverted stand (Olympus, Shinjuku, Tokyo, Japan).

2.7.2 TIRFM Imaging

Total Internal Reflection Fluorescence microscopy (TIRFM) imaging was performed on an Olympus IX-81 motorized inverted base installed by Quorum Technologies (Guelph, ON Canada). Acquisition was done using 100x, 1.45 numerical aperture oil objective lens, with a Hamamatsu EM-CDD camera (ImageEM91013, Hamamatsu) using Volocity software (PerkinElmer, Waltham, MA, USA).

2.7.3 PALM Imaging

For super-resolution imaging, PhotoActivated Localization Microscopy (PALM) technique was employed using TIRFM Imaging. The coverslips to be imaged were incubated with multichannel tetraspec beads (Invitrogen) as fiducial markers to correct for any lateral drift. Low UV-laser, 20 μ W of 405 nm (Spectral Applied Research, Richmond Hill, On, Canada), was used to photo-activate PAmCherry-CD36 molecules of which the fluorescent signal was acquired at 605nm after excitation with 1mW of 561nm laser (Spectral Applied Research, Richmond Hill, On, Canada) at 100ms exposure time until all molecules were photobleached. For dual PALM imaging, Fyn-PA-GFP was acquired first, using 1mW of 491nm laser (Spectral Applied Research, Richmond Hill, On, Canada) to simultaneously photo-activate and image it at 100ms exposure time until all molecules were photobleached as earlier described (Sengupta et al., 2011). PAmCherry-CD36 was then imaged as above. Tetraspec beads were used to correct any lateral drift in individual channels and to align the two channels. Image analysis was performed using MatLab (MathWorks), as described next.

For spt-PALM, HMEC-mEos2-CD36 cells were used. Approximately 1 μ W of 405 nm UV-laser was used to randomly activate a subset of mEos2-CD36 molecules during the start of

Chapter 2- Materials and methods

acquisition and the fluorescent signal acquired at 605nm after excitation with 0.2 mW of 561nm laser. These activated molecules were acquired at 50ms and followed until all initially activated were photobleached. Tetraspec beads were used as described above.

2.7.4 FRAP Imaging

FRAP was performed on HMEC-mApple-CD36 cells with an Andor Discovery imaging system (Andor Technology Ltd., Belfast, UK) in TIRFM mode and using Andor Mosaic system for targeted photobleaching controlled by Metamorph (Molecular Devices, Sunnyvale, CA, USA). An area of $\sim 8.3 \mu\text{m}^2$ in the cell periphery was photobleached using 1 second exposure to a 405 nm laser.

2.7.5 FRET Imaging

Förster resonance energy transfer (FRET) was performed on cells expressing caspase 3 biosensor, mCerulean-DEVD-Ypet on a Quorum Technologies (Guelph, ON, Canada) WaveFx spinning-disk microscope with a 60x, 1.42 numerical aperture oil objective, using EM-CDD camera (Hamamatsu, Hamamatsu City, Japan) and Volocity software (PerkinElmer, Waltham, MA, USA) set up on Olympus IX-81 inverted stand (Olympus, Shinjuku, Tokyo, Japan).

2.8 Immunofluorescence Image Analysis

All immunofluorescence image analysis was done on MatLab (MathWorks, Natick, MA, USA) and Image-J (Schneider, Rasband & Eliceiri 2012).

2.8.1 *Miscellaneous image analysis*

Any contrast adjustment on images for visual purposes only was applied linearly. Confocal 3D image reconstruction was done using Image-J volume viewer. Spt-PALM analysis was done using uTrack software (Jaqaman et al. 2008). Endocytosed vesicle detection was achieved using à trous wavelet transform decomposition method (Olivo-Marin 2002).

2.8.2 *FRAP image analysis*

Analysis and quantification of all the FRAP images was done with MatLab (MathWorks, Natick, MA, USA). The average intensity of the photobleached area was measured overtime, background subtracted and corrected for photobleaching and normalized to the initial intensity. The resulting FRAP data was fitted with exponential equation 1 below for the time period post FRAP region photobleaching

$$f(t) = A(1 - e^{-\tau t}) \quad \text{Equation 1}$$

τ is the time constant, t is the FRAP time and A is the normalized intensity of fluorescence in the image.

To compute diffusion coefficient, the halftime of the exponential recovery curve was determined using equation 2 below, derived from equation 1 above. The halftime was then used in equation 3 as earlier described to estimate the diffusion coefficient (Axelrod et al. 1976).

$$\text{Halftime, } t_{1/2} = \frac{\ln 0.5}{-\tau} \quad \text{Equation 2}$$

$$\text{Diffusion Coefficient, } D = \frac{0.88r^2}{4t_{1/2}} \quad \text{Equation 3}$$

r is the radius of the photobleached ROI circle and $t_{1/2}$ is the halftime of maximal recovery.

2.8.3 PALM image analysis

PALM images were analyzed using Gaussian mixture-model fitting (Jaqaman et al. 2008), which yielded the molecular positions and their standard deviations (20.24 nm on average) in each image of the PALM sequence. Localizations with standard deviation above 50 nm (~0.0003% of localizations) were eliminated from further analysis of the identified localizations. To avoid molecule over-counting, the localized molecules were then tracked using our previously developed particle tracking algorithm (u-track; (Jaqaman et al. 2008)), using a search radius of 1 pixel and a gap closing time window of 3 frames. This strategy accounted for repeated emission and potential short-term blinking, but not any potential long-term blinking, which was however expected to be minimal for PAmcherry and PAGFP (Durisic et al. 2014). This effectiveness of this analysis to eliminate localization multi-appearances was tested with pair-correlation function (PCF) calculated as earlier described (Puchner et al. 2013).

For molecules that appeared in more than one frame, the final position was taken as the average position within each of their tracks, thus yielding a more accurate position in addition to avoiding over-counting. Any lateral drift was corrected using fiducial markers localization and tracking.

2.8.4 Spatial pattern analysis

This analysis is based on the work of Owen *et al.* (Owen et al. 2010, Williamson et al. 2011), to which we added a robust method to determine the threshold for identifying clusters

from local density maps (described below). In brief, three to four non-overlapping 4 μ m x 4 μ m regions of interest (ROI) were cropped from each imaged cell, within which Ripley's K function $K(r)$ was used to analyze overall CD36 molecule clustering. $K(r)$ was calculated using the Equation 3 below with Ripley's edge correction applied (Ripley 1977).

$$K(r) = \frac{A}{n} \sum_{i=1}^n \sum_{j \neq i}^n \left(\frac{\delta_{ij}}{n-1} \right) \text{ where } \delta_{ij}=1 \text{ if } d_{ij} < r, \text{ else } 0 \quad \text{Equation 4}$$

r is the radius of the concentric ring, n is number of points (coordinates) in the ROI, A is the ROI area, and d_{ij} is the distance between points i and j . For easier interpretation, $K(r)$ was linearized to the H-function, $H(r)$:

$$H(r) = L(r) - r = \sqrt{K(r)/\pi} - r \quad \text{Equation 5}$$

The radius $rMax$ that gives maximum $H(r)$ value was taken as the radius of maximal clustering. The higher the maximum $H(r)$ value, the higher the degree of clustering (Kiskowski, Hancock & Kenworthy 2009). $rMax$ is directly proportional to the average cluster radius R (Lagache et al. 2013):

$$R \approx \frac{rMax}{1.3} \quad \text{Equation 6}$$

To generate cluster spatial maps, second order neighborhood value $L_i(r)$ for each coordinate i , i.e. ignoring the i -sum in equation 4, was calculated at radius 50 nm as earlier described in (Getis, Franklin 1987). For visualization purposes only, the cluster spatial maps were converted to cluster heat maps through interpolation (MatLab 'v4' interpolation method) using the $L_i(r)$ value of each coordinate as its third dimension on a 20 nm resolution grid

Chapter 2- Materials and methods

To obtain cluster properties, we then developed a robust and unbiased thresholding approach to segment the local density spatial maps and identify receptor clusters. Specifically, we first randomized the receptor positions, assigned each randomized receptor a local density using the 50 nm radius used on the real data, and then took the average local density for the randomized receptors as the threshold. Any coordinate i in the clustered dataset with an $L_i(\mathbf{r})$ value higher than the maximum $L(\mathbf{r})$ value of corresponding randomized coordinates was considered to be in a cluster. Based on this threshold, binary spatial maps were generated and cluster features were extracted using MatLab.

The accuracy of this analysis in extracting cluster properties was assessed using simulated cluster data. Coordinates with known cluster properties and varying numbers of clusters per area, numbers of molecules per cluster, and density inside versus density outside clusters were generated. Cluster size heterogeneity was varied between 40 nm and 180 nm within same ROI. The range of these cluster properties was based on CD36 raw data obtained from both with and without TSP-1, with and without drug perturbation. The calculated cluster properties were compared to the simulation ground truth properties using 150 simulations. Dividing the calculated property values by the ground truth values, the method's accuracy was expressed as a ratio between 0 and 1. Our analysis gave high ratios, above 0.95, validating the approach.

2.8.5 Puncta-continuum colocalization analysis

The colocalization of full length or truncated Fyn with CD36 in multi-color immunofluorescence images was quantified as the average ratio of mean Fyn pixel intensity within CD36 spots to mean Fyn pixel intensity outside these spots. This approach allowed us to tackle the challenge that the CD36 images were punctate while the Fyn images were more

Chapter 2- Materials and methods

continuous, for which there are no standard colocalization analysis approaches. On the CD36 side, the centers of CD36 spots (each likely representing a CD36 cluster) were detected using Gaussian mixture-model fitting, as described previously (Jaqaman et al. 2008). Each CD36 spot was then taken as a circular area of radius 3 pixels around the center position, reflecting the size of the CD36 spots. On the Fyn side, the Fyn intensity was corrected for non-uniform background, which was estimated by filtering the image with a wide Gaussian (Gaussian standard deviation of 10 pixels). In order to avoid dividing by zero in the ratio calculation, the average raw image intensity value was added back after background image subtraction.

CD36 spots within the cell mask (see next section “Cell mask segmentation” for details) were mapped to the Fyn channel, and the corresponding mean Fyn intensity per CD36 spot was calculated. The mean Fyn intensity outside of CD36 spots was then simply the average intensity within the mask outside the CD36 spots. With this, the Fyn intensity ratio was calculated per spot, as the ratio of the mean intensity inside each spot to the mean Fyn intensity outside. For 2-way colocalization analysis (e.g. CD36 and Fyn), the average ratio for all spots was then taken as a measure of colocalization. The average ratio would be equal to 1 in instances of no colocalization, while ratios > 1 would indicate colocalization. To distinguish true colocalization from perchance colocalization simply due to molecular abundance, the mean ratio was also calculated for each dataset after randomizing the CD36 spot positions within the cell mask.

This methodology was extended to 3-way colocalization to analyze the relationships between CD36, Fyn/phospho-SFK, and F-actin. First, spot detection and mapping as described above was applied between CD36 and Fyn/phospho-SFK, and between CD36 and F-actin to obtain their ratios inside vs. outside CD36 spots. In order to identify CD36 spots strongly associated with actin, the mean F-actin intensity ratio after CD36 spot randomization was taken

Chapter 2- Materials and methods

as the divider to separate CD36 spots in 'high intensity' actin (F-actin ratio $>$ randomization mean) and in 'low intensity' actin (actin ratio \leq randomization mean). Once classified in this manner, the two populations of CD36 spots were used to separately average the Fyn/phospho-SFK ratio values in high intensity actin vs. low intensity actin areas, yielding CD36-Fyn colocalization measures in high vs. low actin intensity regions. In all of the intensity ratios for the data, to calculate the percent enrichment of the channel, we subtracted 1 from this intensity ratio and expressed it as a percentage.

2.8.6 Cell mask segmentation

Cell mask segmentation was based on the Fyn channel, as it had a continuum signal. Since multiple levels of intensity were often present due to Fyn forming loose clusters throughout the cell on top of a diffuse distribution, the MatLab function `multithresh` was used to separate these levels. The function `multithresh` uses a generalized Otsu approach to determine n thresholds for an image, together with a metric that measures the confidence of using these n thresholds. For any given image, the number of thresholds n with the highest confidence metric was selected. Among these n thresholds, the threshold value which had the greatest distance from the preceding threshold was taken as the cell mask threshold. The latter choice was motivated by the fact that the largest intensity level difference within an image is the difference between inside and outside the cell.

2.9 Endocytosis-Exocytosis Assay

HMEC-CD36-myc cells were grown on Lab-Tek chambers coated with $1\mu\text{g}/\text{cm}^2$ Fibronectin. To measure CD36 endocytosis in TSP-1 stimulated and unstimulated conditions, monovalent Cy3b labelled anti-CD36 fab fragments were used (see section 2.6.2 Fab fragment

Chapter 2- Materials and methods

generation and labeling). The anti-CD36 Cy3b fabs were bound to CD36-myc cells on ice followed by 10 minutes incubation at 37°C with or without TSP-1. Surface bound antibodies were acid washed on ice (acid wash solution: 500mM glacial acetic acid, 150mM NaCl, pH 2.5) for 2 minutes followed by 2 minutes recovery with basal MBCD-131 media and additional 2 minutes incubation in the acid wash solution. Cells were fixed as outlined in immunofluorescence protocol. Cells were immunostained with AlexaFluor-488 anti-mouse secondary antibody following the normal Immunofluorescence protocol. The extent of CD36 endocytosis was determined from epi-fluorescence microscopy imaging by measuring the amount of anti-CD36 Cy3b fab internalized.

To measure CD36 exocytosis, all surface CD36 was bound with the monoclonal mouse anti-CD36 fabs in MBCB 131 media on ice using a saturating antibody concentration. Unbound antibodies were washed off with cold MBCB 131 media, followed by 10 minutes incubation at 37°C with or without TSP-1. Cells were then fixed using normal immunofluorescence protocol. Pre-bound CD36 fab antibodies were detected using AlexaFluor-488 anti-mouse antibody. The unbound CD36 fraction (exocytosed fraction) was then labeled with monoclonal mouse anti-CD36 Cy3b fabs. The extent of CD36 exocytosis was determined from TIRF microscopy imaging by measuring the amount of anti-CD36 Cy3b fab bound.

2.10 Triton X-100 extraction

Cells grown on a 6 well plate were incubated with Lat B or M β CD or no drug for 25 minutes at 37°C. Triton X-100 extraction was done at 4°C where cells were incubated with ice cold 1% Triton X-100 in PBS for 20 min, then washed into 2% PFA in PBS, and fixed using the normal immunofluorescence protocol.

2.11 Cholesterol assay

Cholesterol assay kit (abcam) was used to assay effect of Lat B or M β CD treatment on cholesterol levels. HMEC-1 cells were treated with 200nM Lat B or 2mM M β CD for 15 minutes. The cells were then fixed with the kit's cell-based assay fixative solution for 10 minutes at room temperature. This was followed by 3 times washes, 5 minutes each, with the kit's cholesterol detection wash buffer. The cells were then incubated for 60 minutes in the dark with Filipin-III, diluted to 1:100 in the kit's cholesterol detection assay buffer. Two, 5 minutes washes were done with the cholesterol detection wash buffer. The cells were then imaged using Fura-2 excitation filter and 440/20 emission filter.

2.12 Flow cytometry

For comparative assessment of cell surface CD36 in HMVECs and the stable cell lines (HMEC-CD36-myc, HMEC-mApple-CD36 and HMEC-PAmCherry-CD36. HMEC-1 was used as a negative control), flow cytometry was employed. Briefly, cells in a 10cm dish were washed 3 times with PBS followed by addition of 1 ml Accutase to each dish and a 5 minutes incubation at 37°C. Cells were harvested through centrifugation (800rpm for 4 minutes), and the pellet resuspended in PBS. Cell fixation was done using 4% PFA for 10 minutes, after which, they were blocked with 3%BSA in PBS. Each cell line was partitioned into two. One portion was incubated with 1:1000 monoclonal mouse anti CD36 IgG (clone FA6-152) in blocking buffer for 30 minutes while the other one was not. This was followed by incubation, for both portions, with an anti-mouse antibody conjugated to AlexaFluor 647. Each antibody incubation was followed by two washes with PBS. Cell surface stained CD36 was determined using an Accuri C6 flow cytometer (BD Accuri) in the FL-4H channel. The control cells were used to gate CD36

expressing cells and the median fluorescence of the resultant fluorescence histogram compared to determine CD36 expression levels in all cell lines used.

2.13 Graphing and statistical analysis

Bar graphs were done on GraphPad prism (Graphpad Software, La Jolla, CA, USA). All other graphing and statistical analysis outlined below was done on MatLab (MathWorks, Natick, MA, USA). Unless otherwise stated, all error bars in bar graphs are represented as mean \pm standard deviation (SD). For the boxplots, the red central mark is the median, the edges of the box are the 25th and 75th percentiles, the whiskers extend to the most extreme data points not considered outliers, and outliers are plotted individually as red pluses (Figure 2-1). Measurement's mean (circle) and standard error of the mean (error bars) are overlaid on boxplot (Figure 2-1). For all western blots data and flow cytometry data, statistical significance for two groups was calculated using two-tailed unpaired t-test, with the alpha (α) set at 0.05. For three or more groups of western blots data, analysis of variance (ANOVA) was used to determine if statistical significant difference existed between the groups. For these data sets, Dunnett's post hoc test was computed to test differences between control untreated and treated group pairs and obtain the adjusted p-value (Dunnett 1955).

For all the other data (i.e. all other data besides western blots and flow cytometry data), nonparametric Wilcoxon rank sum test was used to test two paired groups, with the α set at 0.05 (Wilcoxon 1945). For three or more groups, to circumvent assumptions of ANOVA (Armstrong, Slade & Eperjesi 2000), rank-based nonparametric Kruskal-Wallis test was employed to determine if statistically significant differences existed between the groups (Kruskal, Wallis 1952). This was followed by pairwise the two-sided Wilcoxon rank sum test to compare pairs of

the groups. The resultant p-value in this was assessed for significance compared to Dunn-Šidák's adjusted α (α^* , equation 7 below) (Dunn 1964, Šidák 1967). In all these statistical approaches, if significant, the actual p-value is given, up to four decimal places, otherwise, ns = not significant.

For $\alpha=0.05$, Dunn-Šidák's $\alpha^* = 1 - (1 - \alpha)^{1/n}$, where n =number of groups **Equation 7**

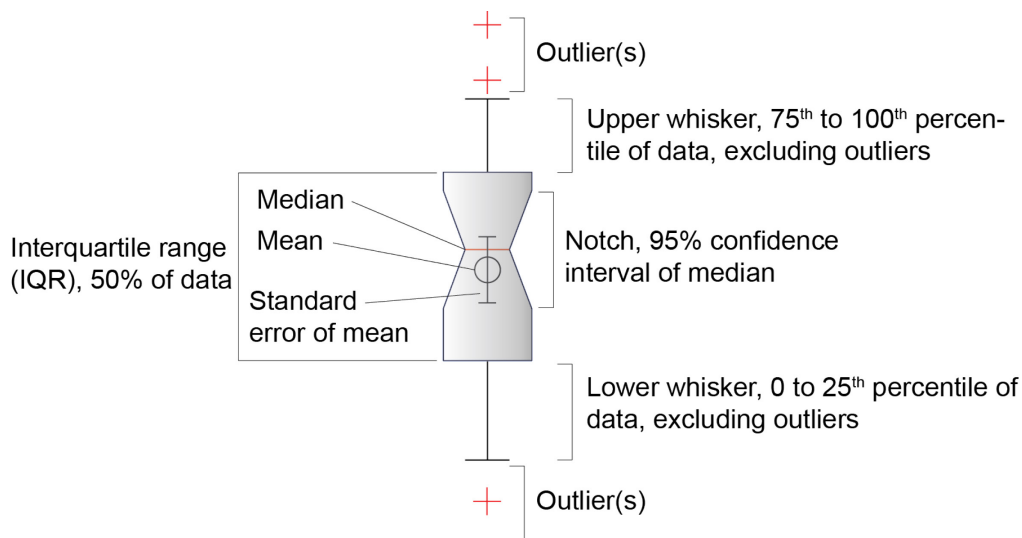


Figure 2-1: Representative boxplot features

Description of boxplot features used in data representation. For each box, the red central mark is the median, the edges of the box are the 25th and 75th percentiles with the mean (circle) and standard error of the mean (error bar) overlaid on the box. The box notch indicates the 95% confidence interval of the median. The whiskers extend to the most extreme data points not considered outliers, and outliers are plotted individually as red pluses

References

- Ades, E.W., Candal, F.J., Swerlick, R.A., George, V.G., Summers, S., Bosse, D.C. & Lawley, T.J. 1992, "HMEC-1: establishment of an immortalized human microvascular endothelial cell line.", *Journal of Investigative Dermatology*, vol. 99, no. 6, pp. 683-690.
- Alland, L., Peseckis, S.M., Atherton, R.E., Berthiaume, L. & Resh, M.D. 1994, "Dual myristylation and palmitoylation of Src family member p59fyn affects subcellular localization.", *Journal of Biological Chemistry*, vol. 269, no. 24, pp. 16701-16705.
- Armstrong, R.A., Slade, S.V. & Eperjesi, F. 2000, "An introduction to analysis of variance (ANOVA) with special reference to data from clinical experiments in optometry", *Ophthalmic and Physiological Optics*, vol. 20, no. 3, pp. 235-241.
- Axelrod, D., Koppel, D.E., Schlessinger, J., Elson, E. & Webb, W.W. 1976, "Mobility measurement by analysis of fluorescence photobleaching recovery kinetics", *Biophysical journal*, vol. 16, no. 9, pp. 1055-1069.
- Dunn, O.J. 1964, "Multiple Comparisons Using Rank Sums", *Technometrics*, vol. 6, no. 3, pp. 241-252.
- Dunnett, C.W. 1955, "A Multiple Comparison Procedure for Comparing Several Treatments with a Control", *Journal of the American Statistical Association*, vol. 50, no. 272, pp. 1096-1121.
- Durisic, N., Laparra-Cuervo, L., Sandoval-Alvarez, A., Borbely, J.S. & Lakadamyali, M. 2014, "Single-molecule evaluation of fluorescent protein photoactivation efficiency using an in vivo nanotemplate", *Nature methods*, vol. 11, no. 2, pp. 156-162.
- Getis, A. & Franklin, J. 1987, "Second-Order Neighborhood Analysis of Mapped Point Patterns", *Ecology*, vol. 68, no. 3, pp. 473-477.
- Jaqaman, K., Loerke, D., Mettlen, M., Kuwata, H., Grinstein, S., Schmid, S.L. & Danuser, G. 2008, "Robust single-particle tracking in live-cell time-lapse sequences", *Nat Meth*, vol. 5, no. 8, pp. 695-702.
- Kiskowski, M.A., Hancock, J.F. & Kenworthy, A.K. 2009, "On the Use of Ripley's K-Function and Its Derivatives to Analyze Domain Size", *Biophysical journal*, vol. 97, no. 4, pp. 1095-1103.
- Kruskal, W.H. & Wallis, W.A. 1952, "Use of Ranks in One-Criterion Variance Analysis", *Journal of the American Statistical Association*, vol. 47, no. 260, pp. 583-621.
- Lagache, T., Lang, G., Sauvonnnet, N. & Olivo-Marin, J.C. 2013, "Analysis of the spatial organization of molecules with robust statistics", *PloS one*, vol. 8, no. 12, pp. e80914.

Chapter 2- Materials and methods

- Olivo-Marin, J. 2002, "Extraction of spots in biological images using multiscale products", *Pattern Recognition*, vol. 35, no. 9, pp. 1989-1996.
- Owen, D.M., Rentero, C., Rossy, J., Magenau, A., Williamson, D., Rodriguez, M. & Gaus, K. 2010, "PALM imaging and cluster analysis of protein heterogeneity at the cell surface.", *Journal of Biophotonics*, vol. 3, no. 7, pp. 446-454.
- Puchner, E.M., Walter, J.M., Kasper, R., Huang, B. & Lim, W.A. 2013, "Counting molecules in single organelles with superresolution microscopy allows tracking of the endosome maturation trajectory", *Proceedings of the National Academy of Sciences of the United States of America*, vol. 110, no. 40, pp. 16015-16020.
- Ripley, B.D. 1977, "Modelling spatial patterns", *J. R. Stat. Soc. Series B Stat. Methodol.*, vol. 39, pp. 172–192.
- Schneider, C.A., Rasband, W.S. & Eliceiri, K.W. 2012, "NIH Image to ImageJ: 25 years of image analysis", *Nature methods*, vol. 9, no. 7, pp. 671-675.
- Šidák, Z. 1967, "Rectangular Confidence Regions for the Means of Multivariate Normal Distributions", *Journal of the American Statistical Association*, vol. 62, no. 318, pp. 626-633.
- Wilcoxon, F. 1945, "Individual Comparisons by Ranking Methods", *Biometrics Bulletin*, vol. 1, no. 6, pp. 80-83.
- Williamson, D.J., Owen, D.M., Rossy, J., Magenau, A., Wehrmann, M., Gooding, J.J. & Gaus, K. 2011, "Pre-existing clusters of the adaptor Lat do not participate in early T cell signaling events.", *Nature immunology*, vol. 12, no. 7, pp. 655-662.

**Chapter 3 - Insights into CD36-Fyn reorganization upon TSP-1
binding**

Some portions of this chapter are part of a manuscript under review, drafted by me and edited by Nicolas and Khuloud.

3.1 Introduction

Decavalent mouse monoclonal anti CD36 IgM (clone SM ϕ) and TSP-1 were shown to inhibit ECs migration and induce their apoptosis, while divalent mouse monoclonal anti CD36 (clone FA6-152) could not (Dawson et al. 1997, Jimenez et al. 2000). This hinted to a multivalency dependent pathway initiation of this signaling cascade, possibly through CD36 clustering. While the signaling pathway leading to this cell death downstream TSP-1-CD36-Fyn interaction has been vastly investigated and elucidated, the initial steps are poorly understood (Mirochnik, Kwiatek & Volpert 2008). Indeed, clinical trials for TSP-1 mimetics as anti-angiogenic cancer therapy called for better understanding of the initial steps governing this signal activation (Markovic et al. 2007). We sort to investigate if indeed there was any clustering of CD36 at the plasma membrane upon TSP-1 binding and if so, how these clusters played a role in activating the immediate downstream kinase Fyn. We show that in ECs at rest, unligated CD36 exists both in monomeric and clustered state, with Fyn colocalizing in CD36 clusters at all times. Upon 10 nM TSP-1 stimulation, the concentration used in previous antiangiogenic studies (Jimenez et al. 2000), CD36 clustering is enhanced, forming larger, more compact clusters, which lead to Fyn activation. Similar results are recapitulated under decavalent SM ϕ stimulation while divalent FA6-152 stimulation fails to compact CD36 clusters.

3.2 Results

3.2.1 Expression of CD36 in HMEC-1

Expression of CD36 in primary HMVECs and immortalized version, HMEC-1 (Ades et al. 1992), was tested by staining for surface (plasma membrane) CD36. While HMVECs expressed detectable levels of CD36, HMEC-1 did not express any detectable endogenous CD36 if any (Figure 3-1A). HMEC-1 therefore provided us with the opportunity to engineer stable cell lines expressing CD36 with various tags as needed for our imaging and biochemical studies. HMEC-1 cell lines stably expressing CD36-myc (HMEC-CD36-myc), mApple-CD36 (HMEC-mApple-CD36) and PAmCherry-CD36 (HMEC-PAmCherry-CD36) were developed and CD36 expression confirmed using immunofluorescence (Figure 3-1A). Next, we stained surface CD36 (plasma membrane CD36) using mouse anti CD36 or an isotype IgG as a control for flow cytometry analysis of CD36 expression levels (Figure 3-1B). Using HMVECs CD36 expression levels as a reference, all the stable cell lines we made expressed CD36 within ~1 to 2 fold (Figure 3-1C). As earlier observed, there was no detectable levels of CD36 in HMEC-1 cell line. However, not all cells in primary HMVECs and HMEC stable cell lines expressed CD36 (Figure 3-1D). To gain confidence in the use of our stable cell lines in this study, TSP-1 binding to CD36 and its ability to activate the kinase Fyn and induce apoptosis was tested.

Chapter 3- Insights into CD36-Fyn reorganization upon TSP-1 binding

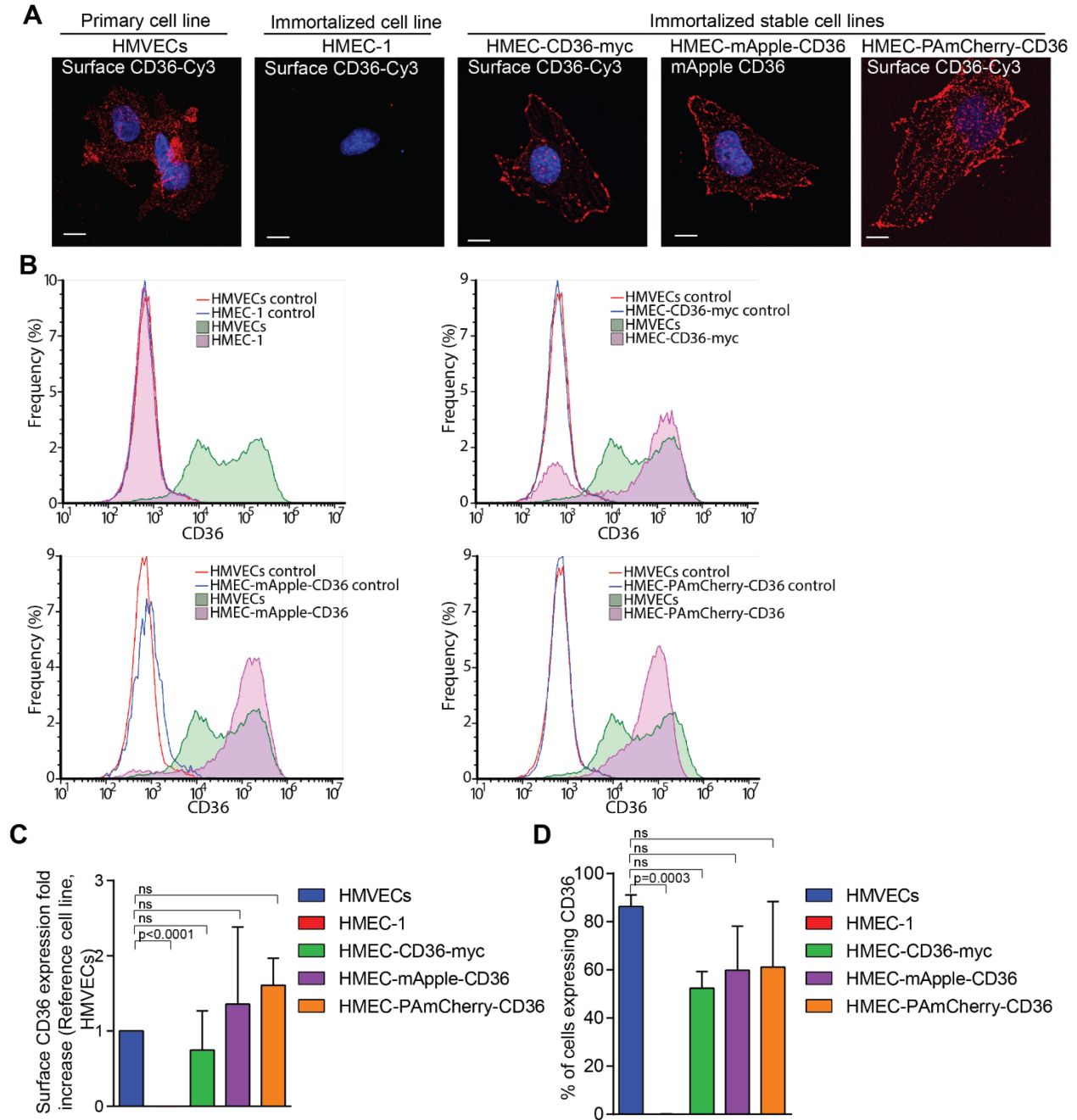


Figure 3-1: CD36 expression in HMVECs, HMEC-1 and HMEC-1 stable cell lines.

(A) Projections of z-stacks of confocal images of surface (plasma membrane) CD36 expression in HMVECs, HMEC-1, HMEC-CD36-myc, HMEC-mApple-CD36 and HMEC-PAmCherry-CD36 respectively (left to right order). Surface (plasma

Chapter 3- Insights into CD36-Fyn reorganization upon TSP-1 binding

membrane) CD36 was labeled using monoclonal mouse anti-human CD36 (FA6-152) and secondary donkey anti-mouse Cy3 (red). Cell nuclei was stained with DAPI (blue) in all cell lines. Scale bars (applicable to all images), 5 μ m. **(B)** Representative flow cytometry overlay histograms of surface CD36 staining with an anti-CD36 IgG and donkey anti-mouse AlexaFluor 647. Isotype mouse IgG was used as a control. In all the histograms, HMEC-1 and their stable cell lines are overlaid on HMVECs histograms. *x*-axis is CD36 fluorescence read out, *y*-axis is the count as percent frequency. **(C)** Fold expression levels of CD36 in HMEC-1 and their stable cell lines compared to HMVECs. **(D)** Percent of cells expressing CD36 in all the cell lines. Data from 3 independent experiments, all error bars, mean \pm SD. Statistical analysis as described in 2.13 Graphing and statistical analysis

3.2.2 TSP-1 binding in ECs depend heavily on CD36

TSP-1 has been shown to interact with different proteins and extracellular matrix components (Resovi et al. 2014). Pre-binding of monoclonal anti-CD36 antibodies (clone OKM5) to platelets drastically reduced these cells ability to bind TSP-1 (Asch et al. 1987). This suggested that CD36 was the main receptor for TSP-1 binding. To test this in ECs, Cy3b conjugated TSP-1 was incubated with HMVECs for 10 minutes, and surface CD36 stained after fixation. TSP-1 binding was significantly reduced in CD36 knockdown conditions compared to nonspecific siRNA conditions (Figure 3-2A, B), reiterating the earlier observation of CD36 being the main receptor for TSP-1. This was further confirmed by the rescue of HMEC-1 ability to bind TSP-1 upon CD36 expression (Figure 3-2C). We next investigated if TSP-1 binding to CD36 could activate caspase 3 as earlier reported (Jimenez et al. 2000, Volpert et al. 2002).

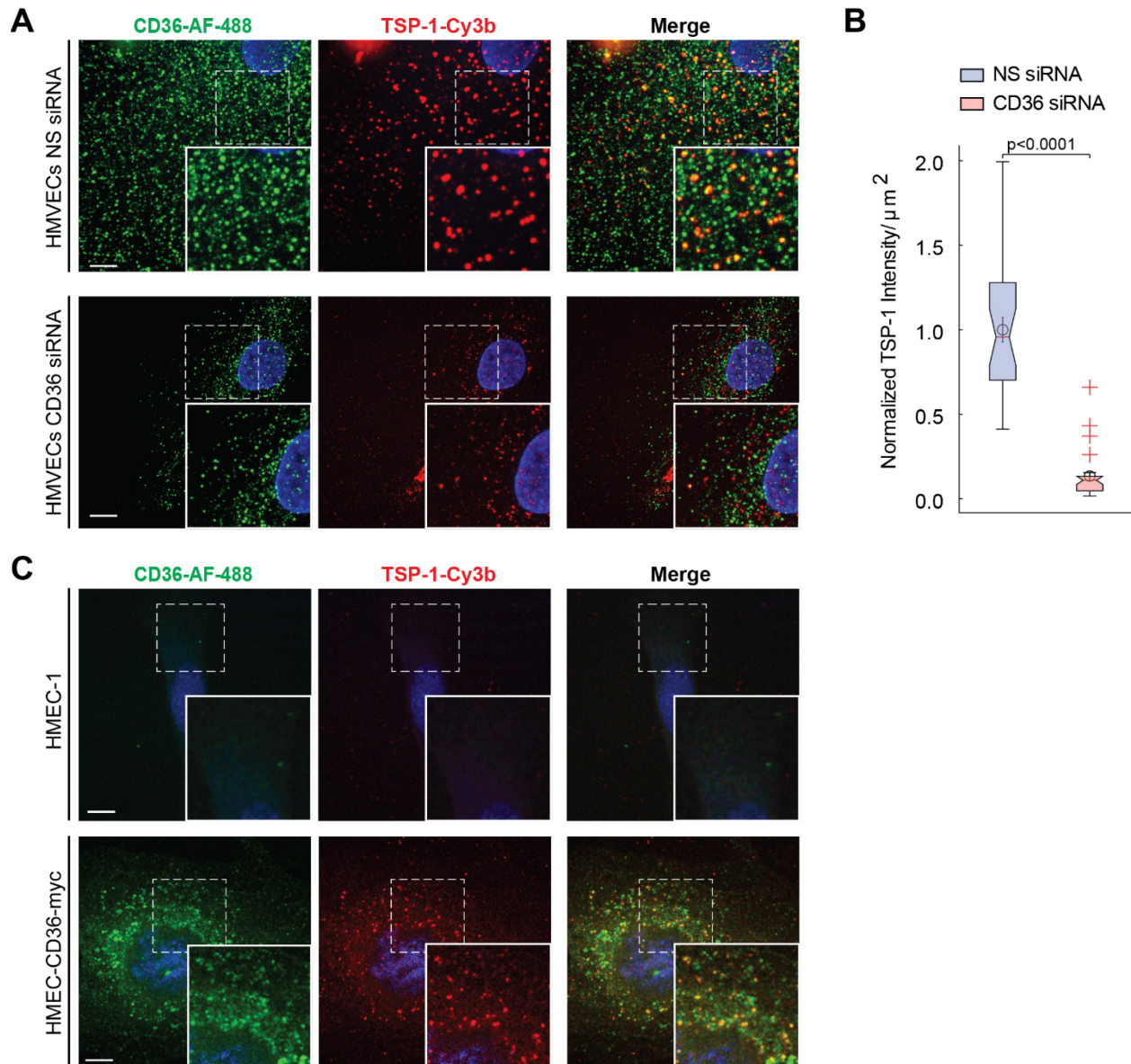


Figure 3-2: TSP-1 binding in ECs depends on CD36

(A) Projection of z-stacks of confocal images of TSP-1-Cy3b bound (10 minutes incubation) to HMVECs treated with non-specific siRNA (NS siRNA) or CD36 siRNA. Cells were fixed and stained for surface CD36 using mouse anti-human CD36 (FA6-152) and secondary donkey anti-mouse AlexaFluor 488 antibodies, and their nuclei were labeled with DAPI. Insets represent magnified areas underlined with dashed line boxes. (B) Levels of TSP-1 binding were determined as the mean TSP-1-Cy3b intensity within cells segmented using the CD36 signal. 30 data points

Chapter 3- Insights into CD36-Fyn reorganization upon TSP-1 binding

from 3 independent experiments were analyzed. Boxplots and statistical analysis as described in 2.13 Graphing and statistical analysis. Briefly, for the boxplots, the red central mark is the median, the edges of the box are the 25th and 75th percentiles, the whiskers extend to the most extreme data points not considered outliers, outliers are plotted individually as red pluses, measurement's mean (circle) and standard error of the mean (error bars) are overlaid on boxplot. (C) Projection of z-stacks of confocal images of TSP-1-Cy3b bound (10 minutes incubation) to HMEC-1 (no detectable CD36) and HMEC-CD36-myc cells. Immunostaining was done as described in (A) for HMVECs. Insets represent magnified areas underlined with dashed line boxes. Scale bars (applicable to all images), 5 μm .

3.2.3 TSP-1 activates caspase 3 in ECs

The end result of TSP-1 binding to CD36 in endothelial cells is activation of caspase 3, leading to cell death (Jimenez et al. 2000, Volpert et al. 2002, Mirochnik, Kwiatek & Volpert 2008). This was also emphasized by TSP-1's inability to trigger cell death in ECs treated with Ac-DEVD-CHO, an inhibitor of caspase-3/7 (DEVDase) activity (Jimenez et al. 2000). To verify this, we used an earlier described FRET caspase 3 biosensor to monitor caspase 3 activation in live cells (Nguyen, Daugherty 2005). This biosensor is made up of a FRET donor CyPet and acceptor Ypet, with a spacer between them containing caspase 3 cleavage site, DEVD. Besides CyPet poor folding at 37°C, the FRET pair has been shown to be prone to enhanced dimerization, hence artifacts in observed FRET signal (Shaner, Patterson & Davidson 2007). To circumvent these disadvantages of CyPet, we replaced it with a more photo-stable, non-dimerizing fluorescent protein Cerulean (Figure 3-3A). First, we used western blotting to test if the spacer could be cleaved by caspase activity. Incubating Hela cells expressing the biosensor, with staurosporine (STS), a known activator of caspase 3 resulted in cleaving of the spacer (Figure

Chapter 3- Insights into CD36-Fyn reorganization upon TSP-1 binding

3-3B). The cleavage of the spacer also occurred when lysates of HeLa cells expressing the biosensor were incubated with a recombinant active caspase 3 (Figure 3-3C). Next, we confirmed that the pair could FRET upon expression in living cells (Figure 3-3D). To check the sensitivity of the biosensor to detect caspase 3 activation using imaging, we computed normalized FRET/Donor ratio of the biosensor in HeLa cells expressing it, with or without STS. STS resulted in loss of FRET (decrease in FRET/Donor ratio) indicating cleavage of the biosensor (Figure 3-3E). Incubating HMEC-CD36-myc with TSP-1 resulted in loss of FRET, suggesting caspase 3 activation by TSP-1 in ECs as earlier reported (Figure 3-3F).

Chapter 3- Insights into CD36-Fyn reorganization upon TSP-1 binding

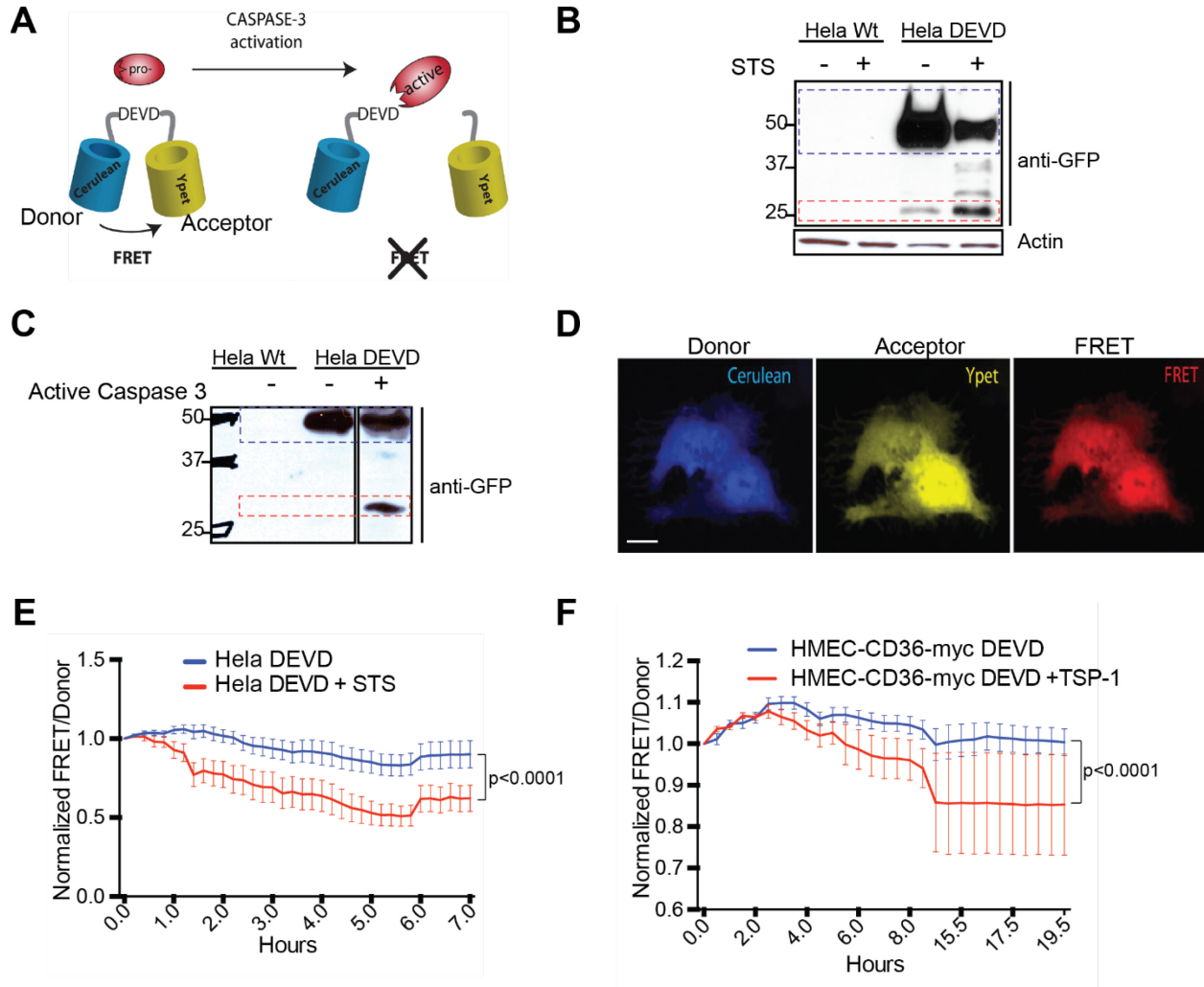


Figure 3-3: FRET Caspase 3 biosensor use in monitoring caspase 3 activation

(A) Caspase-3 biosensor design. FRET pair Cerulean and Ypet are separated by a linker containing caspase 3 cleavage site, DEVD. Caspase-3 activation cleaves the linker resulting in loss of FRET signal. (B) Cleavage of the linker was tested in HeLa cells expressing the biosensor (Hela DEVD, transiently transfected with the biosensor). Lysates were harvested after 4 hours incubation with or without STS (a known inducer of apoptosis through Caspase-3) and fluorescent protein probed on a western blot using anti-GFP antibody (detecting both the analogous protein Cerulean and Ypet). Actin was used as a loading control, while HeLa wild type cells, Hela Wt, were used to assess any non-specific binding of the anti-GFP antibody. STS resulted

Chapter 3- Insights into CD36-Fyn reorganization upon TSP-1 binding

in cleavage of the biosensor (red ROI) while majority of the biosensor remained full length in untreated condition (blue ROI). (C) To ascertain that caspase 3 was cleaving the biosensor, Hela DEVD lysates were incubated with a purified recombinant active caspase 3. Only lysates incubated with the caspase 3 resulted in a cleaved fragment. (D) Representative images of a single z-plane of donor (Cerulean), acceptor (Ypet) and FRET signals acquired on a spinning-disk confocal microscope. Scale bar, 5 μm . (E) Caspase-3 biosensor sensitivity in immunofluorescence was tested in live cell imaging. The signals in (D) for Hela DEVD were recorded every 10 minutes with or without STS. FRET/Donor ratio normalized to the initial ratio, was calculated to assay Caspase-3 activity. FRET/Donor ratio for STS treated cells (red) decreased with time (indicating activation of Caspase-3) compared to control (blue). (F) A similar experiment to (E) was performed using HMEC-CD36-myc cells with or without TSP-1 incubation. FRET/Donor ratio for TSP-1 treated cells (red) decreased with time (indicating activation of Caspase-3) compared to control (blue). Data from 30 data points of 3 independent experiments, all error bars, mean \pm SD. Statistical analysis as described in 2.13 Graphing and statistical analysis

3.2.4 Fyn activation in ECs is CD36 and multivalency dependent

CD36 has been shown by biochemical approaches to associate mainly with Fyn among other SFKs (Bull, Brickell & Dowd 1994, Huang et al. 1991). This SFK was shown to be key in the anti-angiogenic pathway as TSP-1 was unable to block angiogenesis of fibroblast growth factor (FGF) stimulated corneal neovascularization in Fyn-null mice (Jimenez et al. 2000). Though CD36 immunoprecipitated with Fyn in unstimulated conditions, TSP-1 was shown to increase recruitment of Fyn to immunoprecipitated CD36 complexes, resulting into an increase in the activation of the kinase (Jimenez et al. 2000). We tested the activation of Fyn and its dependency on CD36 by immunoblotting with an antibody recognizing Fyn's phosphorylated

Chapter 3- Insights into CD36-Fyn reorganization upon TSP-1 binding

tyrosine 420 form (referred to hereafter as P-Y420) (Saito et al. 2010). TSP-1 stimulation activated Fyn in the engineered cell lines stably expressing CD36, but not in the original HMEC-1 cells lacking CD36 (Figure 3-4A, B). The relative intensity of the anti P-Y420 signal normalized to the total amount of Fyn showed ~50% increase following 15 min of incubation with TSP-1 (Figure 3-4B), similar to the increase in primary HMVECs (Figure 3-4C, D). At the same time, siRNA mediated depletion of CD36 in primary HMVECs abrogated TSP-1 mediated Fyn activation (Figure 3-4C, D), rendering them similar to HMEC-1 cells not expressing CD36. These results pointed towards a CD36 dependent activation of Fyn by TSP-1.

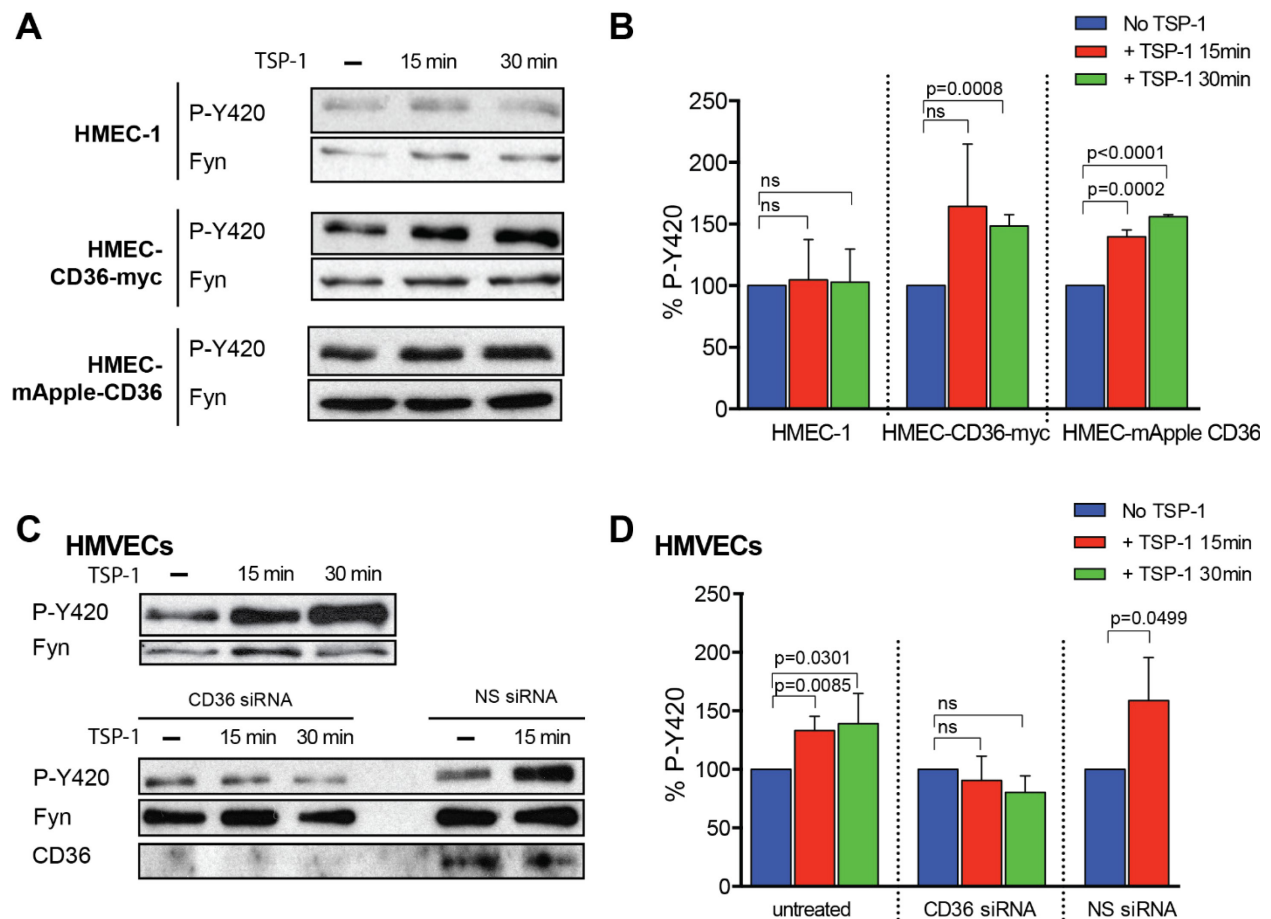


Figure 3-4: CD36 expression in HMEC-1 recapitulates TSP-1-CD36-Fyn

signaling

(A) HMEC-1, HMEC-CD36-myc and HMEC-mApple-CD36 cells were stimulated with TSP-1 for 15 or 30 minutes, and Fyn activation was probed using anti P-Y420 antibody on western blots, with total Fyn as loading control. All blots (throughout figure) are representative of three independent experiments each. (B) Percentage of P-Y420 quantified as the ratio of P-Y420 to total Fyn intensities from blots in (A) and normalized to the untreated value. Data from 3 independent experiments, all error bars (in all panels), mean \pm SD. Statistical analysis as described in 2.13 Graphing and statistical analysis. (C) HMVECs, and HMVECs treated with CD36 (CD36 siRNA) or non-specific siRNA (NS siRNA) were stimulated with TSP-1 for 15 or 30 minutes and analyzed by western blot as in (A). (D) Percentage of P-Y420 in HMVECs and HMVECs treated with siRNAs quantified as in (B).

Decavalent SM ϕ ability to induce HMVECs apoptosis and inhibit their migration to similar levels as TSP-1 while divalent FA6-152 couldn't (Jimenez et al. 2000, Dawson et al. 1997) suggested clustering of CD36 might play a role in signal transduction. To corroborate the dependence of Fyn activation on CD36 and its clustering, we examined by immunofluorescence staining the distribution of P-Y420 signal in HMEC-mApple-CD36 cells in the absence or presence of TSP-1. Since not all of HMEC-mApple-CD36 cells expressed the construct, we selected fields of view containing cells with and without mApple-CD36 (white and yellow ROIs respectively Figure 3-5). In agreement with the biochemical results, we found that addition of TSP-1 for 15 min resulted in increased P-Y420 signal only in the cells expressing mApple-CD36 (Figure 3-5A). Calculating the ratio of the P-Y420 signal in CD36 expressing cells to the signal in non-expressing cells, we also detected a 50% increase in P-Y420 signal levels (Figure 3-5D). Furthermore, in agreement with previous observations in primary cells (Jimenez et al. 2000, Dawson et al. 1997), our immunofluorescence analysis reported a significant increase in P-Y420

Chapter 3- Insights into CD36-Fyn reorganization upon TSP-1 binding

phosphorylation upon treatment with decavalent SM ϕ but not upon treatment with divalent FA6-152 (Figure 3-5B, D). As a positive control, we incubated cells with hydrogen peroxide (H₂O₂), which is known to activate SFKs (Sato et al. 2001). The kinase activation was to a similar extent in cells with or without CD36 (Figure 3-5C, D).

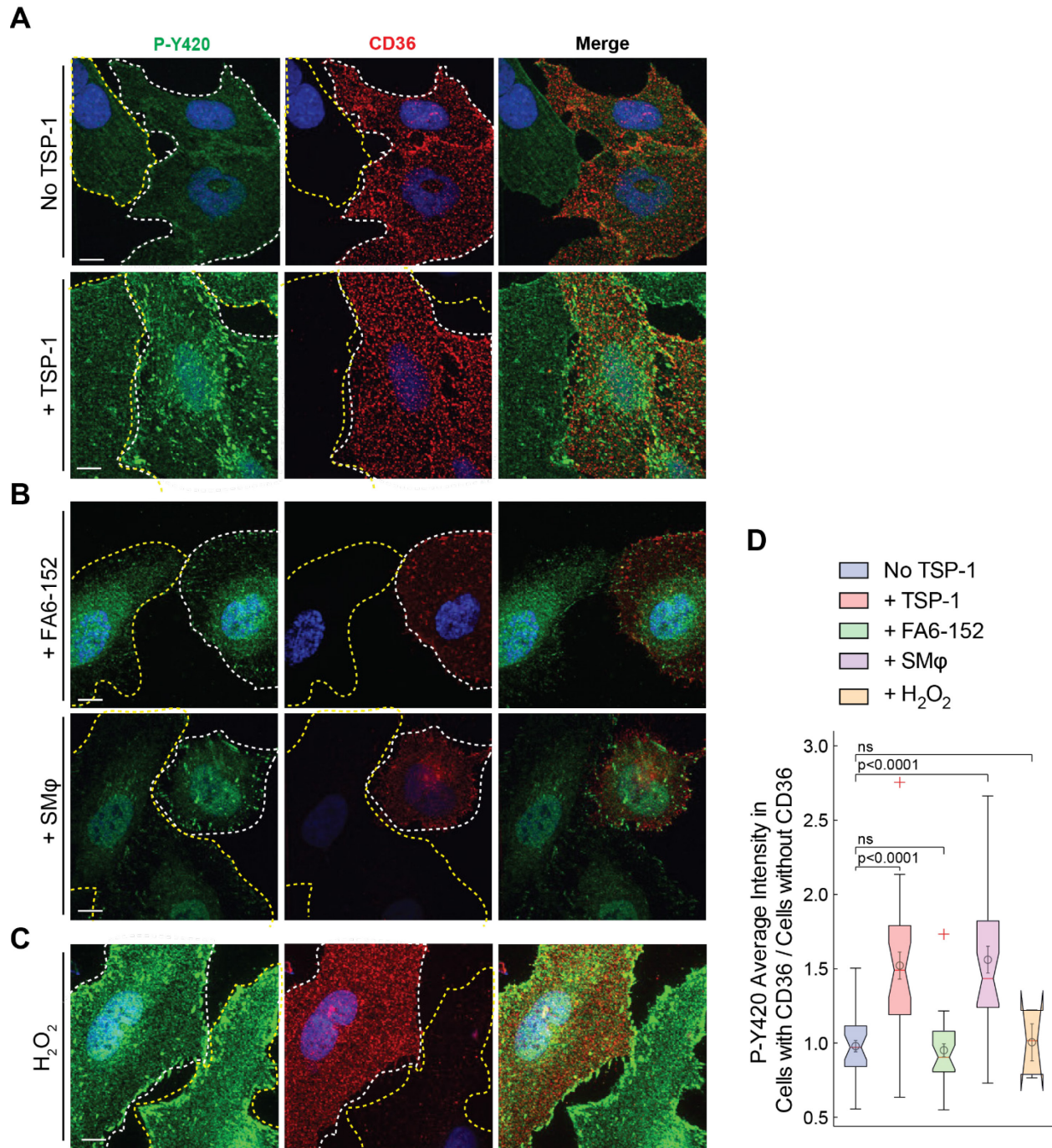


Figure 3-5: Fyn activation is CD36 and multivalency dependent

Z stack projection of confocal images. (A) HMEC-mApple-CD36 cells were untreated or incubated with TSP-1 for 15 minutes before fixation and immunostaining with anti-P-Y420 AlexaFluor 488 coupled antibody. Images were

Chapter 3- Insights into CD36-Fyn reorganization upon TSP-1 binding

collected by confocal microscopy, and fields of view were selected to contain cells expressing or not CD36 (white ROI and yellow ROI respectively). Nuclei of cells were highlighted using DAPI (blue). **(B)** Phosphorylation of SFK on Y420 imaged in HMEC-mApple-CD36 cells incubated with FA6-152 or SM ϕ for 15 minutes. Immunostaining and imaging done as in (A) above. **(C)** Phosphorylation of SFK on Y420 imaged in HMEC-mApple-CD36 cells incubated with H₂O₂ for 15 minutes. Immunostaining and imaging done as in (A) above. **(D)** Ratio of the average P-Y420 intensity in cells expression CD36 to the P-Y420 intensity in cells not expressing CD36 for the conditions in (A), (B) and (C). Data for all conditions from 3 independent experiments with data points ranging from 8 to 11 fields each. Statistical analysis as described in 2.13 Graphing and statistical analysis. Scale bars (applicable to all images), 5 μ m.

While the overall increase in P-Y420 signal upon TSP-1 or SM ϕ was CD36 dependent, we sort to investigate if P-Y420 signal increased specifically in CD36 enriched areas. We repeated the same immunofluorescence staining of P-Y420 signal in HMEC-mApple-CD36 cells in untreated or TSP-1, FA6-152 or SM ϕ treated conditions. We then imaged these cells using Total Internal Reflection Fluorescence microscopy (TIRFM) (Figure 3-6A), a technique that allows one to activate fluorescent molecules only at or very near the plasma membrane, hence eliminating background signal from the cytosol (Fish 2009). Computing percent P-Y420 enrichment in CD36 spots (see section 2.8.5 Puncta-continuum colocalization analysis) showed a significant increase in P-Y420 enrichment in CD36 spots upon TSP-1 or SM ϕ stimulation compared to unstimulated or FA6-152 treated conditions (Figure 3-6B). In all conditions, P-Y420 enrichment was significantly higher than in the randomized controls (Figure 3-6B). This verified the earlier observation of P-Y420 activation being dependent on CD36 and also points to activation of the kinase happening in CD36 spots. This is in line with the biochemical data of

Chapter 3- Insights into CD36-Fyn reorganization upon TSP-1 binding

TSP-1 increasing Fyn recruitment to immunoprecipitated CD36 complexes for Fyn activation to take place (Jimenez et al. 2000).

The idea of CD36 clustering being involved in Fyn activation would imply an increase in P-Y420 enrichment in CD36 spots as the amount of CD36 in these spots increased. To test this, we binned CD36 channel intensity ratio between inside and outside of CD36 spots, with the corresponding average percent P-Y420 enrichment per bin (Figure 3-6C). Quadratic fits of the corresponding data points for the different conditions showed an increase in percent P-Y420 enrichment as the amount of CD36 in spots increased in TSP-1 and SM ϕ treated conditions (Figure 3-6C). This suggested that the increase number of CD36 molecules in these spots under multivalent ligand binding, was possibly key in Fyn activation.

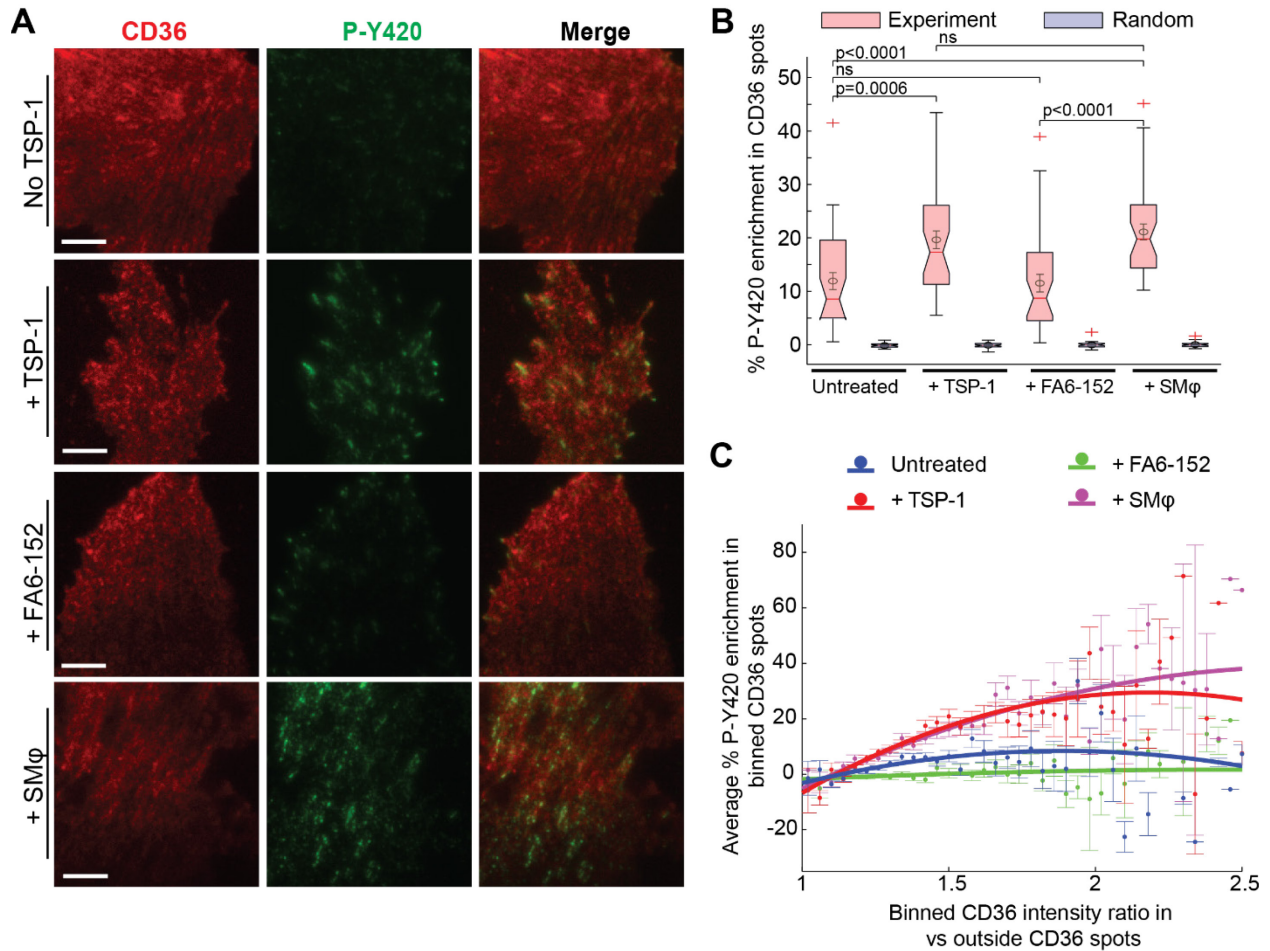


Figure 3-6: P-Y420 activation increases with CD36 enrichment upon multivalent ligand binding

(A) TIRFM imaging of HMEC-mApple-CD36 cells unstimulated or stimulated with TSP-1, FA6-152 or SMφ for 10 min, fixed and labeled for P-Y420 using anti-P-Y420 coupled to AlexaFluor 488. (B) Average percent P-Y420 enrichment within mApple-CD36 spots in experimental raw data or randomized CD36 spots for all the conditions (light red versus light blue boxplots respectively). Boxplots and statistical analysis as described in 2.13 Graphing and statistical analysis. (C) Binned CD36 intensity ratio between inside and outside of CD36 spots, with the corresponding average percent P-Y420 enrichment per bin marked by the dots. Error bars, mean \pm SD. Quadratic lines fits of the corresponding (similar color) data points for the different conditions are superimposed.

Chapter 3- Insights into CD36-Fyn reorganization upon TSP-1 binding

Data from 3 independent experiments each containing ~15 images acquired with identical settings. Scale bars (applicable to all images), 5 μm .

While Fyn was shown to be the specific kinase activated by TSP-1 binding CD36 in ECs (Jimenez et al. 2000), the antibody we used for probing P-Y420 could potentially crossreact and detect activated Src. To test if TSP-1 activated specifically Fyn in our ECs system, we knocked down either Fyn or Src in HMEC-mApple-CD36 cells, stained and imaged the cells as described above, in untreated or TSP-1, FA6-152 or SM ϕ treated conditions. In no siRNA and non-specific siRNA treated cells, the amount of Fyn or Src was relatively the same (Figure 3-7A, B). While both Fyn and Src siRNAs knocked down ~80% of their respective target, they did also knockdown ~50% of either Src or Fyn respectively (Figure 3-7A, B). However, P-Y420 activation by TSP-1 or SM ϕ was significantly abrogated in Fyn siRNA conditions compared to, untreated, non-specific siRNA or Src siRNA treated conditions (Figure 3-7A, B), reiterating the earlier observation of Fyn being the kinase TSP-1 activated upon binding CD36.

Taken all together, these results established our engineered HMEC-1 lines expressing CD36 as a good model system to study the TSP-1-CD36-Fyn signaling pathway. They also hinted to initiation of the pathway through CD36 clustering by the ligand.

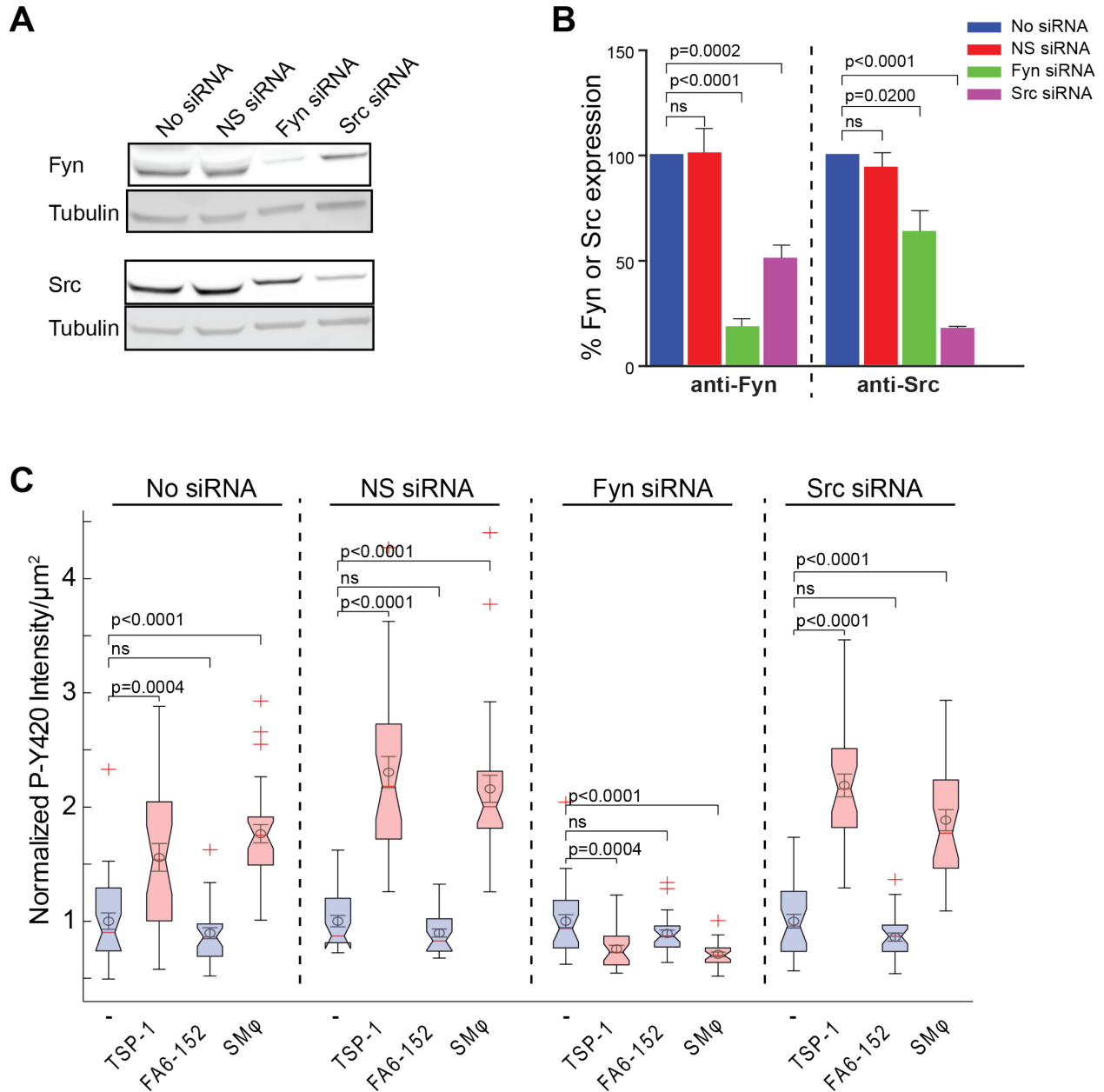


Figure 3-7: P-Y420 activation by CD36 multivalent ligands is specific for Fyn

(A) HMEC-mApple-CD36 cells were untreated or treated with non-specific siRNA (NS siRNA), Fyn siRNA or Src siRNA. Total Fyn or Src was probed using rabbit anti Fyn or rabbit anti Src antibody respectively on western blots, with total tubulin (probed with mouse anti-tubulin) as loading control. All blots (throughout figure) are representative of three independent experiments each. (B) Percentage of total Fyn or

Chapter 3- Insights into CD36-Fyn reorganization upon TSP-1 binding

Src in each condition quantified as the ratio of the total kinase signal to total tubulin intensities from blots in (A) and normalized to the untreated condition. Error bars (in all panels) show SD. Data from 3 independent experiments, statistical analysis as described in 2.13 Graphing and statistical analysis. (C) HMEC-mApple-CD36 untreated or treated with the siRNAs in (A) were stained and imaged with TIRFM as described in (Figure 3-6A), and the P-Y420 levels normalized to untreated condition quantified. Boxplots and statistical analysis as described in 2.13 Graphing and statistical analysis. Data from 3 independent experiments each containing ~10 images acquired with identical settings.

3.2.5 CD36 is clustered at steady state; TSP-1 induces further clustering

3.2.5.1 TSP-1 induces more clustering of CD36

Since the activation of Fyn in microvascular endothelial cells was dependent on CD36 as well as multivalency of CD36 ligand, we tested if TSP-1 clustered plasma membrane CD36 by membrane proteins crosslinking. HMEC-CD36-myc cells were stimulated with TSP-1 for 5, 10 and 15 minutes before incubation with a cell membrane impermeant DTSSP (3,3'-dithiobis (sulfosuccinimidyl propionate)), the amino-reactive molecule used to crosslink membrane proteins. Cells were then lysed and blotted with an anti myc antibody to detect CD36-myc. The ratio of clustered to monomeric CD36 molecules (as indicated on the right side of the blot) in the plasma membrane was then quantified by densitometry (Figure 3-8A, B). We found that plasma membrane bound CD36 existed as monomers and clusters even when unligated, but that the cluster:monomer ratio increased upon TSP-1 incubation (Figure 3-8A, B). Cleavage of the crosslinker disulfide bridge with β -mercaptoethanol (β ME) reduced all CD36 to monomeric form (Figure 3-8A).

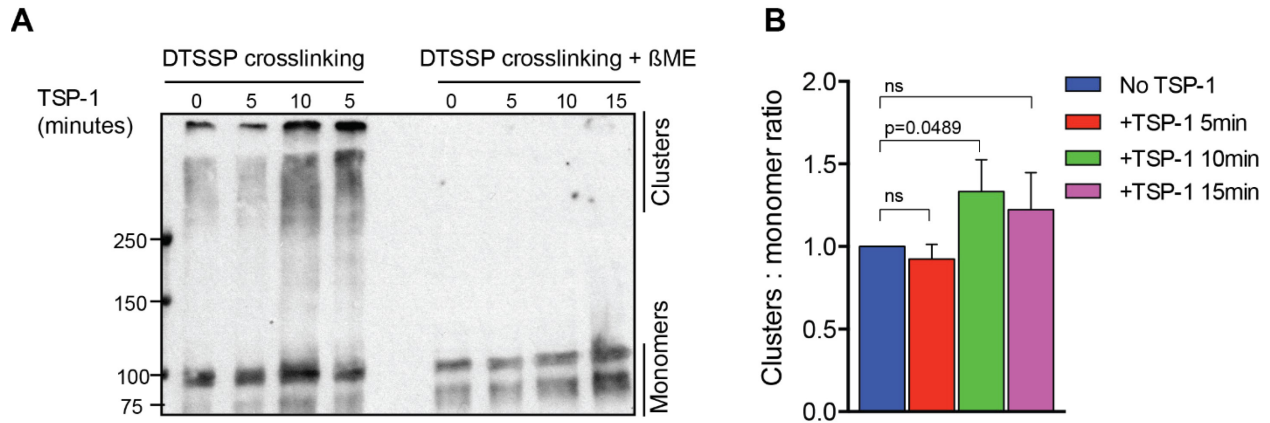


Figure 3-8: TSP-1 induces more clustering of CD36 in ECs

(A) HMEC-CD36-myc cells were incubated with TSP-1 at different time points and crosslinked immediately with membrane impermeant DTSSP on ice. CD36 state was probed using anti-myc on western blots. As a control, β ME was used to cleave off the crosslinker which reduced all clusters to monomers. (B) Quantification of clusters to monomers ratio from (A) at different time points. Data from 3 independent experiments. Data from 3 independent experiments, all error bars, mean \pm SD. Statistical analysis as described in 2.13 Graphing and statistical analysis.

To gain insight into the properties of these CD36 clusters, we employed super resolution imaging (SRI) using PhotoActivated Localization Microscopy (PALM) of HMEC-PAmCherry-CD36 cells by Total Internal Reflection Fluorescence microscopy (TIRFM). The 10 minutes, 10 nM TSP-1 incubation time point was used since it gave the highest CD36 clusters to monomer ratio (Figure 3-8B). First, we verified if TSP-1-CD36 complexes were still at the plasma membrane at the 10 minutes time point. Cy3b conjugated TSP-1 colocalized with plasma membrane CD36 at 10 minutes and eventually got internalized at 30 minutes time point (Figure 3-9). Next, we optimized the spatial pattern analysis we used to quantify the PALM images to gain confidence in our analysis.

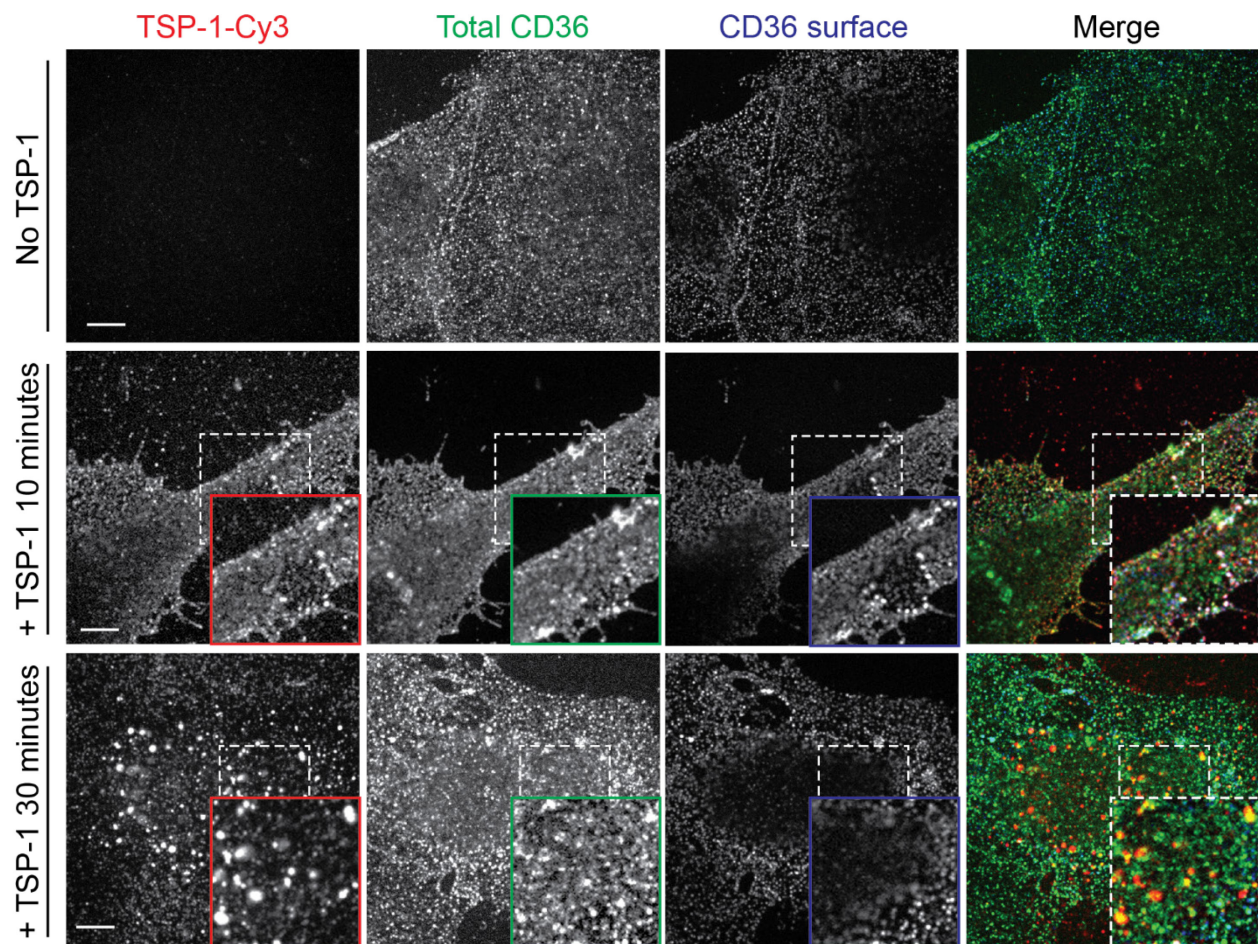


Figure 3-9: TSP-1-CD36 complex is at the plasma membrane at 10 minutes time point

Z slice of confocal imaging of HMEC-CD36-myc cells untreated or incubated with TSP-1-Cy3b for 10 minutes or 30 minutes before fixation and immunostaining for plasma membrane CD36 (blue CD36 surface) and total CD36 (green total CD36). While most of the TSP-1-CD36 complexes were internalized by 30 minutes time point, most TSP-1 colocalized with surface CD36 at 10 minutes. Insets represent magnified areas underlined with dashed line boxes. Images representative of 3 independent experiments. Scale bars (applicable to all images), 5 μ m.

3.2.5.2 Spatial Pattern Analysis optimization

To investigate the clustering of CD36 from PALM SRI data, we employed Ripley's K function, $K(r)$, a powerful spatial pattern analysis method employed to determine the degree of clustering in a given data set (see 2.8.4 Spatial pattern analysis) (Owen et al. 2010, Williamson et al. 2011). For easier interpretation, $K(r)$ is linearized to H-function, $H(r)$, and the radius that gives maximum $H(r)$ value, referred to hereafter as r_{Max} , is taken as the radius of maximal aggregation (Kiskowski, Hancock & Kenworthy 2009). The higher the r_{Max} , the higher the degree of clustering. While this spatial analysis has gained momentum in its use in biophysics, we sort to address two challenges that faced it. These challenges were:

- 1) The relationship between r_{Max} and average cluster radius was not fully investigated.
- 2) The accuracy of this method to extract the real properties of the clusters was not previously optimized.

To address the first challenge, we determined if r_{Max} could predict differences in cluster radius using cluster simulations (see 2.8.4 Spatial pattern analysis). While some have attempted to use r_{Max} as the average clusters radius (Zhang et al. 2006, Hancock, Prior 2005), it was noted by others that r_{Max} is not equal to the average cluster radius, R , and that r_{Max} is always between R and $2R$ (Kiskowski, Hancock & Kenworthy 2009). This is due to the accumulative nature of this function where at larger concentric rings radius, $K(r)$ values are confounded with the $K(r)$ values at shorter radius. A derivative of $H(r)$, $H'(r)$, which measures the rate of change of $H(r)$ had been shown to determine cluster radius with high precision (Kiskowski, Hancock & Kenworthy 2009), where the radius that gives minimum $H'(r)$, $H'(r)_{min}$, was found to be equal to $2R$ (Figure 3-10A). However, this was done on simulated clusters which were all separated by

Chapter 3- Insights into CD36-Fyn reorganization upon TSP-1 binding

equal distance, a pattern that is not likely to be representative of plasma membrane receptor organization. The authors also noted that “In irregular distribution in which the monomer density fluctuates non-randomly outside domains, using this method to identify the domain radius would be biased by this second level of aggregation” (Kiskowski, Hancock & Kenworthy 2009). It was no surprise that this method had challenges to predict R on our simulated clusters (Figure 3-10B). Obtaining r_{Max} from H-function plots (Figure 3-10C), we observed a linear correlation between r_{Max} and already known ground truth average cluster radius R of our simulations (Figure 3-10D). This linear relationship has since been determined in a more robust spatial pattern statistical analysis (see 2.8.4 Spatial pattern analysis, equation 6) (Lagache et al. 2013). While this correlation validated the use of r_{Max} to predict cluster sizes, it was observed on constant cluster radius simulations (homogeneous simulations (Figure 3-10D)). Varying the cluster radii in heterogeneous simulations greatly reduced the ability of r_{Max} to predict cluster sizes (Figure 3-10E). This calls for re-evaluation of r_{Max} as a predictor of cluster radial sizes as they tend to be heterogeneous in nature.

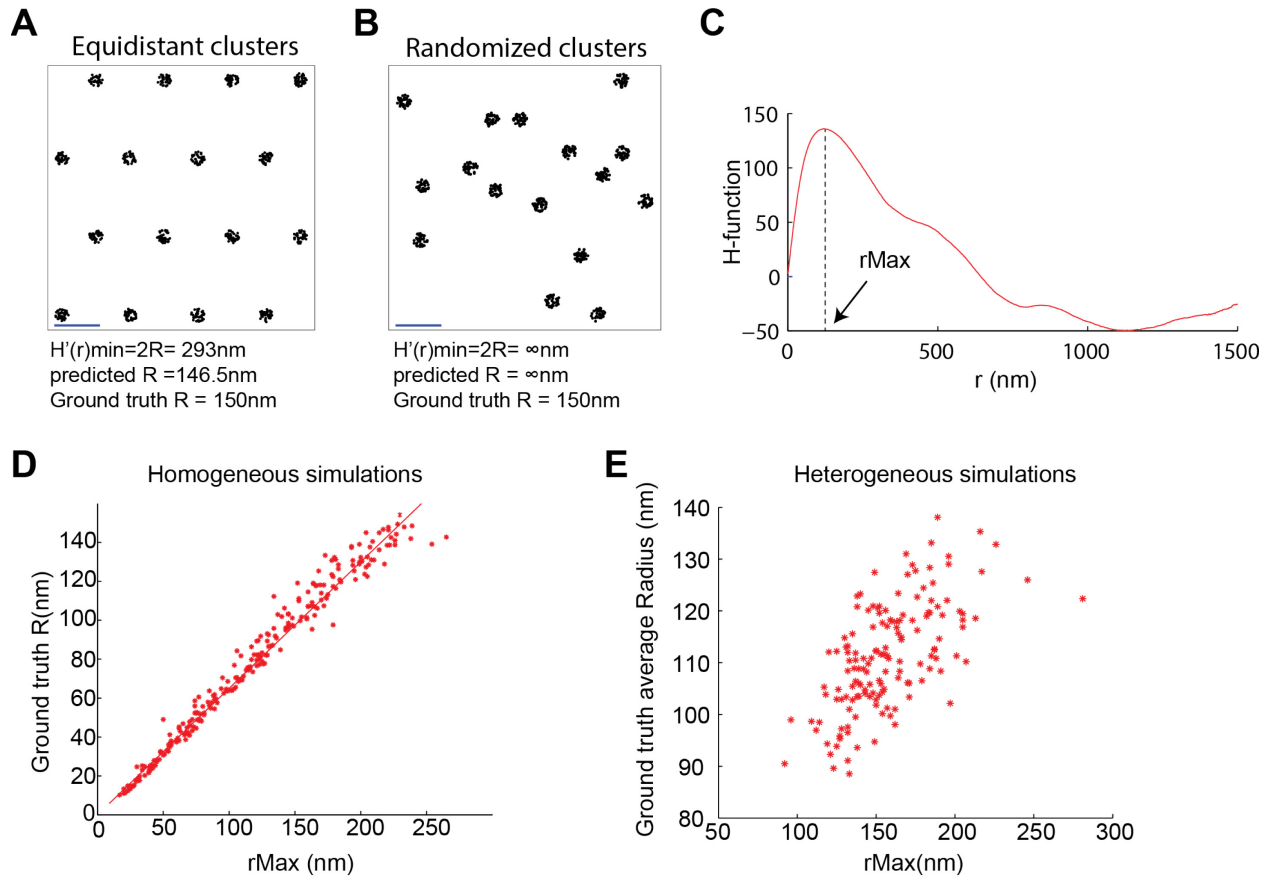


Figure 3-10: Cluster radius R and H-function rMax correlation

$H(r)$ derivative, $H'(r)$, ability to predict the actual simulation cluster radius (Ground truth R) was tested and correlation between H-function r_{Max} and Ground truth R determined. (A) $H'(r)$ predicted cluster radius R was very close to the Ground truth R in equidistant cluster simulations. (B) $H'(r)$ failed to predict cluster radius in randomized cluster simulations, ∞ = infinity. (C) A representative H-function plot, with r_{Max} being the radius that gives maximum $H(r)$ value. (D) 150 homogeneous simulations (same cluster radius per ROI) showed a linear correlation between Ground truth R and H-function r_{Max} . (E) Linear correlation between Ground truth R and H-function's r_{Max} is lost in heterogeneous 150 simulations.

To address the second challenge, which would include an alternative method for predicting cluster radius, we used simulated cluster data to determine if we could extract the

Chapter 3- Insights into CD36-Fyn reorganization upon TSP-1 binding

clusters properties with high accuracy using our analysis. Coordinates with known cluster properties and varying numbers of clusters per area, numbers of molecules per cluster, and density inside versus density outside clusters were generated. Cluster radial size heterogeneity was varied between 40 nm and 180 nm within same ROI (red ROI Figure 3-11A). The range of these cluster properties was based on CD36 raw data obtained. Following the work of (Owen et al. 2010, Williamson et al. 2011), Getis and Franklin's second order neighborhood analysis (see 2.8.4 Spatial pattern analysis) was computed at 50 nm, and used to assign a "local density" for each detected receptor, yielding a spatial map of local receptor densities, as portrayed in the heat maps (Figure 3-11C). We then developed a robust and unbiased thresholding approach to segment the local density spatial maps and identify the receptors present in clusters in order to measure the cluster characteristics. Specifically, we randomized equal number of receptor positions (blue ROI Figure 3-11A). While H-function plot of a clustered simulation is greater than zero (red plot Figure 3-11B), the one for randomized points was near zero (blue plot Figure 3-11B). For the randomized data, we assigned each randomized receptor a local density using the same 50 nm as the real data, then took the maximum local density for the randomized receptors as the threshold. Receptors in the real data with local density larger than this threshold were considered clustered. This yielded cluster binary maps from which cluster properties could be calculated (Figure 3-11D). To validate our spatial pattern analysis, we applied it to 150 different heterogeneous cluster simulations. Ratios of the calculated clustering parameters to the initial ground truth characteristics were consistently above 0.95 demonstrating the accuracy of this approach, including better prediction of cluster radius sizes (Figure 3-11E) compared to $H'(r)_{\min}$ (see Figure 3-10).

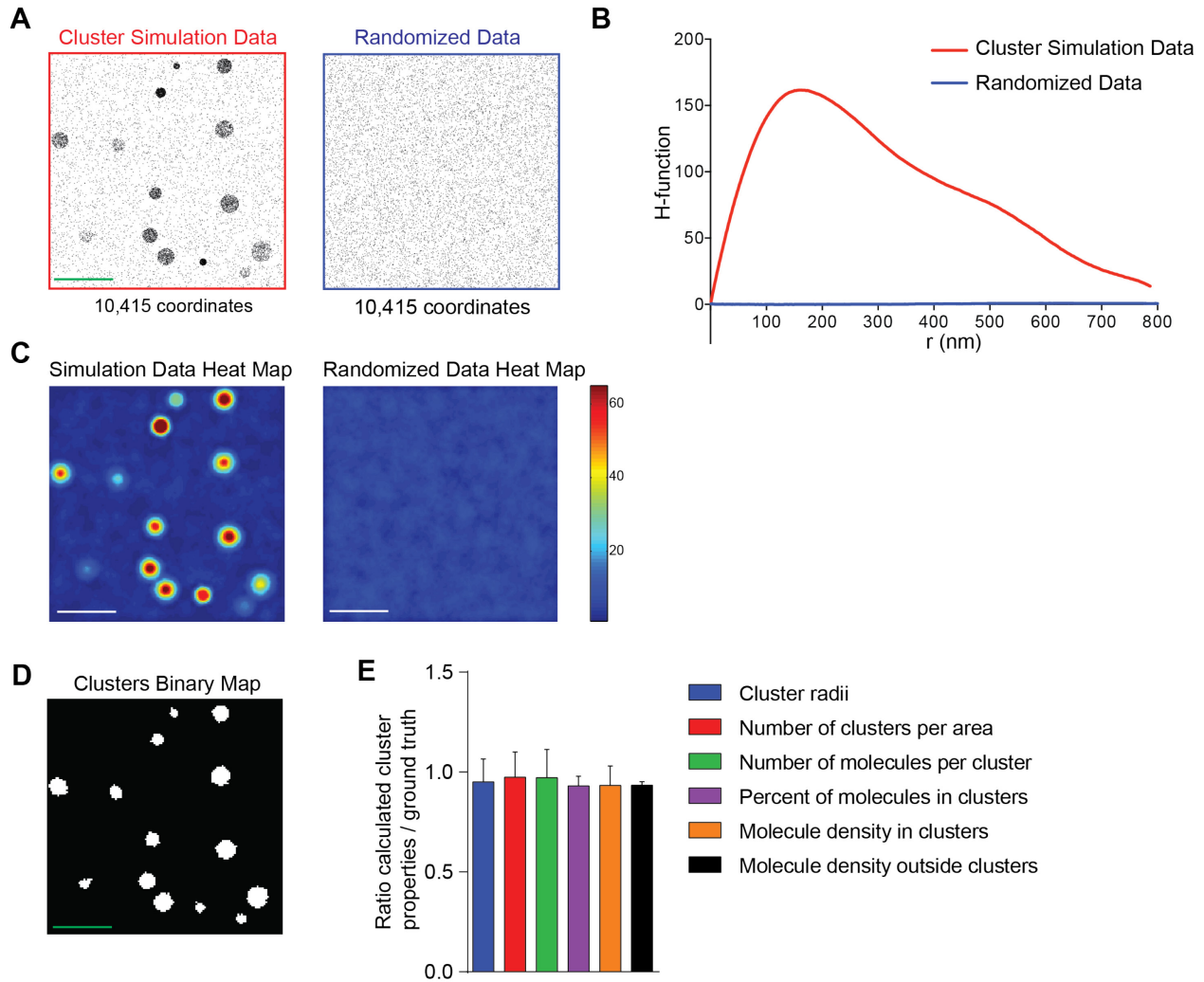


Figure 3-11: Cluster properties extraction validation using simulations

(A) Example field of simulated clusters (red ROI) and randomization of equal number of coordinates within an ROI of same size (blue ROI) (see 2.8.4 Spatial pattern analysis). (B) H-function plot of the simulated data in (A) as a function of the radius r (nm). For randomized dataset (blue plot), H-function is approximately zero for all radii. For clustered coordinate set (red plot), H-function is above zero. (C) Cluster heat maps computed by interpolating simulations in (A). Pseudo-colors indicate local density values at 50nm. (D) Binary map of clusters detected in simulated data in (A) using the threshold derived from the randomization control (see 2.8.4 Spatial pattern analysis). (E) Ratio of the cluster properties calculated from the

Chapter 3- Insights into CD36-Fyn reorganization upon TSP-1 binding

binary maps to the simulation ground truth (GT) properties. The graph represents results from 150 heterogeneous simulations (see 2.8.4 Spatial pattern analysis). All error bars, mean \pm SD.

Scale bars (applicable to all images), 1 μ m.

3.2.5.3 TSP-1 induces compaction of CD36 clusters

As described above, CD36 molecules pre-exist in clusters in the plasma membrane of ECs, in agreement with previous observations in macrophages (Jaqaman et al. 2011), and adds another layer of complexity to the regulation of CD36 clustering and Fyn activation in this signaling pathway.

To dissect this complexity, we turned to PhotoActivated Localization Microscopy (PALM), which would allow us to determine the nanometer scale characteristics and spatial organization of membrane-bound CD36. Following treatment with or without TSP-1, HMEC-PAmCherry-CD36 cells were fixed and imaged by TIRFM. PAmCherry fluorescent proteins were photo-activated using low intensity 405 nm light excitation, and their fluorescence signal at 600 ± 20 nm was recorded over time (at 10 fps) upon 561 nm excitation (Figure 3-12A). The acquisition was stopped when all the fluorescent molecules were exhausted, which corresponded typically to 5000 frame sequences (Figure 3-12 B). Fiducial markers were used to correct for any lateral drift during imaging (see green arrows Figure 3-12B).

Single fluorescent molecules were detected and localized using Gaussian mixture model fitting, which allowed us to localize molecules with overlapping signals even below the resolution limit (Jaqaman et al. 2008, Thomann et al. 2002). This allowed high resolution mapping of CD36 molecules coordinates separated by time (Figure 3-12C, D), with the

Chapter 3- Insights into CD36-Fyn reorganization upon TSP-1 binding

localization precision of our PALM system before multi-appearance correction averaging 20 nm (Figure 3-12E). To avoid molecule over-counting due to repeated emission by the same molecule in consecutive frames, we employed our previously developed particle tracking algorithm to link molecules appearing within 1 pixel of each other within a time window of 3 frames (Jaqaman et al. 2008) (see 2.8.3 PALM image analysis). Having tracked each molecule, its average position within each track was taken as the final position, thus yielding a more accurate position in addition to avoiding over-counting. This strategy did not eliminate over-counting resulting from blinking over longer periods of time; however, PAmCherry undergoes very little blinking, thus minimizing this artifact (Durisic et al. 2014). To confirm the capacity of the tracking algorithm to remove multiple appearances by the same molecule, we measured the pair-correlation function for absolute densities for the localized molecular coordinates (Puchner et al. 2013) within the super-resolution images. The large decrease in the pair-correlation peak at small distances indicates efficient correction (Figure 3-12F). The overall density of CD36 molecules at the ECs plasma membrane was found to be ~ 600 molecules/ μm^2 at rest, and significantly higher after 10 minutes of TSP-1 stimulation (Figure 3-12G).

Chapter 3- Insights into CD36-Fyn reorganization upon TSP-1 binding

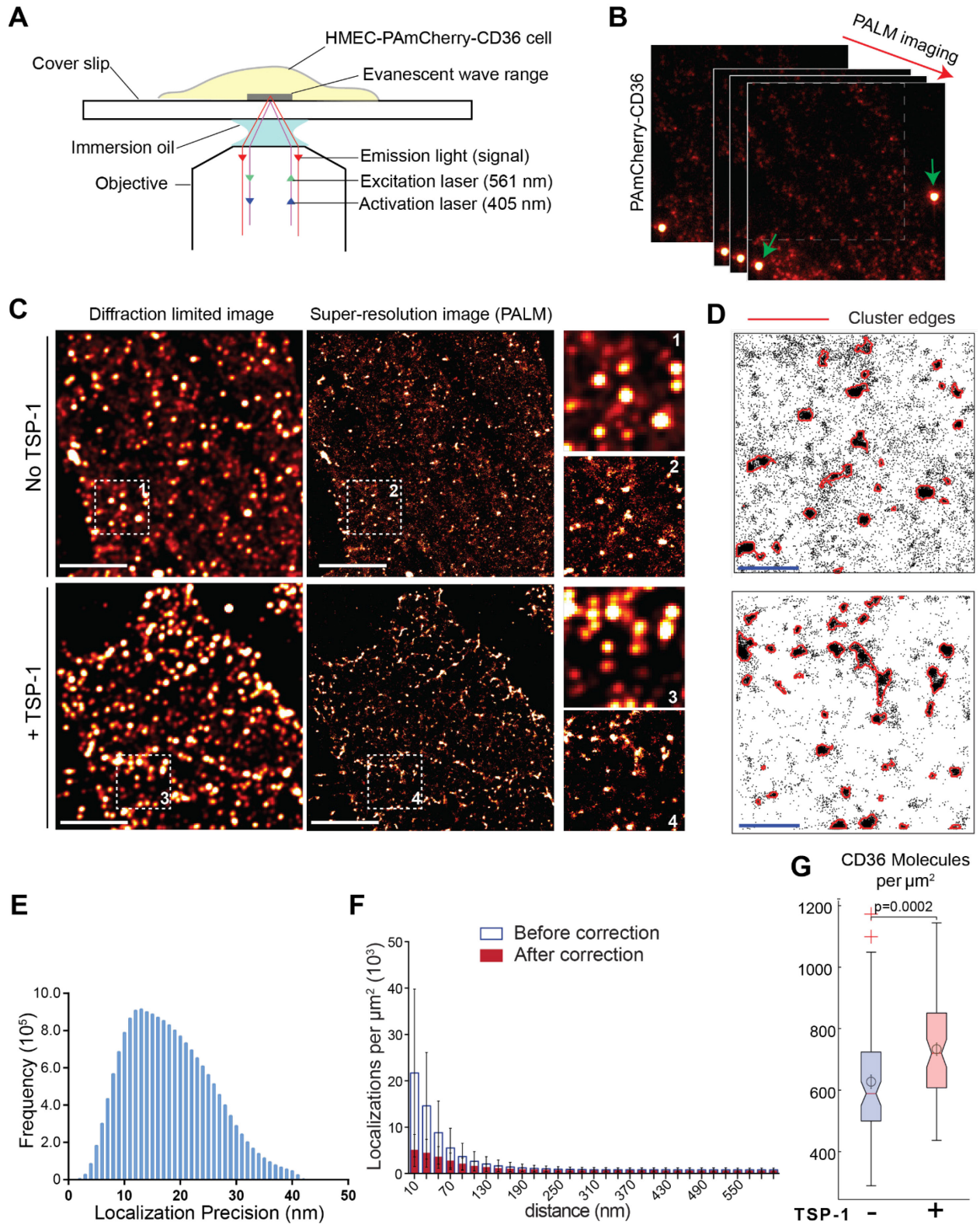


Figure 3-12: SRI of CD36 in HMEC-PAmCherryCD36

(A) TIRFM setup (not drawn to scale) for PALM imaging of CD36. TIRFM's evanescent wave enables plasma membrane localized imaging. PAmCherry-CD36 was activated by 405 nm laser and excited by a 561 nm laser. (B) PALM image sequences (typically 5000 frames recorded at 10 fps) of HMEC-PAmCherry-CD36 cells were acquired by TIRFM. Fiducial markers (indicated by green arrows) were used to correct for any lateral drift. (C) Diffraction limited image (left side) and the corresponding PALM super-resolution image (middle) of HMEC-PAmCherry-CD36 with or without TSP-1 stimulation. Insets in C, zoom-in areas from the corresponding ROI highlighting the improved resolution of the PALM image. Scale bars, 5 μm . (D) CD36 molecular coordinates plot from regions 2 and 4 in (C), with clusters edges, determined from spatial pattern analysis, outlined in red. Scale bar, 1 μm . (E) Histogram of the localization precision in nanometers of PALM imaging of PAmCherry-CD36. (F) Histograms of absolute densities of localization before (blue histogram) and after (red histogram) multi-appearance correction of CD36 coordinates, calculated using pair-correlation function. Data from 21 movies. Error bars indicate SD. (G) Density of CD36 molecules localized at the surface of HMEC-PAmCherry-CD36 cells measured after treatment with or without TSP-1. Data points used represents the result of a 4 x 4 μm ROI (81 ROIs in NoTSP-1 data, 70 ROIs in +TSP-1 data). Boxplots and statistical analysis as described in 2.13 Graphing and statistical analysis. Data from 3 independent experiments, each containing 7 to 10 different cells.

As aforementioned, the PALM data showed a slightly higher density of CD36 molecules at the ECs surface upon TSP-1 stimulation. To test whether this increase was due to newly exocytosed molecules populating the surface or due to reduced receptor internalization, we measured each process independently during TSP-1 stimulation. The level of endocytosis was to be determined in a protocol utilizing acid wash of extracellular bound antibodies. The acid wash

Chapter 3- Insights into CD36-Fyn reorganization upon TSP-1 binding

was quite effective, stripping off approximately 90% of extracellular bound antibodies (Figure 3-13A, B). Endocytosis was determined by first saturating all the surface CD36 molecules with Cy3b-conjugated anti-CD36 Fab fragments. Following 10 min incubation with TSP-1, remaining membrane-bound antibodies were removed by an acid wash before fixation (Figure 3-13C, D). The level of endocytosis was normalized to the average intensity value of the untreated condition. On the other hand, The level of exocytosis was determined by first saturating all the surface CD36 molecules with (unconjugated) anti-CD36 Fab fragments (from a monoclonal antibody) before addition of TSP-1, fixing the cells after TSP-1 addition, and then labeling newly exposed receptors using the same Fab fragments but coupled to Cy3b (Figure 3-13E, F). Measuring the amount of surviving fluorescence in both cases indicated that the amount of exocytosis was not altered upon TSP-1 stimulation, rather the level of endocytosis was reduced (Figure 3-13D, F), leading to higher CD36 density on the cell surface.

Chapter 3- Insights into CD36-Fyn reorganization upon TSP-1 binding

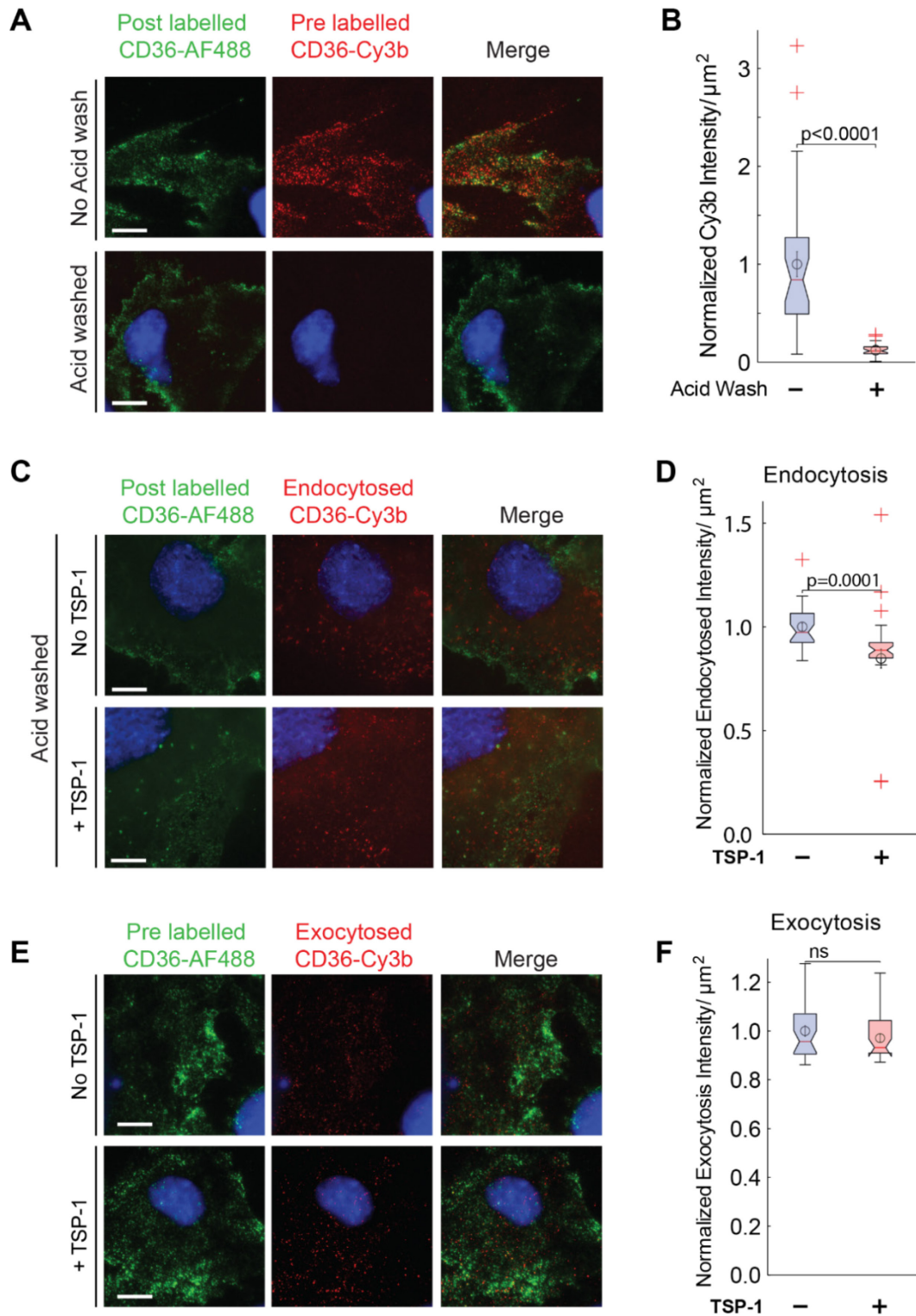


Figure 3-13: TSP-1 effect on CD36 endocytosis-exocytosis axis at 10 minutes

time point.

(A) Representative widefield images used to determine the effectiveness of acid wash to strip off plasma membrane bound antibodies. HMEC-CD36-myc cells were pre labelled with anti-CD36 Cy3b Fab on ice. Acid wash of the antibody was followed on ice and cells fixed. CD36 expressing cells were labelled with anti CD36 AlexaFuor-488 and imaged. No acid wash condition was used as a control of the acid wash effectiveness. (B) Normalized levels of Cy3b intensity detected with or without acid wash, the difference of which indicates effectiveness of the acid wash. (C) Representative widefield images used to determine extent of endocytosis. HMEC-CD36-myc cells were pre labelled with anti-CD36 Cy3b Fab on ice. Cells were then incubated with or without TSP-1 for 10 minutes at 37⁰C after which acid wash of the antibody was followed on ice and cells fixed. CD36 expressing cells were labelled with anti CD36 AlexaFuor-488. (D) Normalized levels of Cy3b intensity detected from (C), the difference of which indicates any change in extent of endocytosis with or without TSP-1. (E) Representative TIRFM images used to determine extent of exocytosis. HMEC-CD36-myc cells were bound with monoclonal mouse anti-CD36 AlexaFluor-488 on ice, using a high antibody concentration to ensure all CD36 molecules are bound. Cells were then incubated with or without TSP-1 for 10 minutes at 37⁰C, after which they were fixed. Unbound CD36 fraction (i.e. exocytosed CD36 molecules) were labeled using anti-CD36 Cy3b fab and imaged. (F) Normalized levels of Cy3b intensity detected from (E), the difference of which indicates any change in extent of exocytosis with or without TSP-1.

30 data points from 3 independent experiments were analyzed for all conditions. In all images, cell nuclei was stained with DAPI (blue). Boxplots and statistical analysis as described in 2.13 Graphing and statistical analysis. Scale bars (applicable to all images), 5 μ m.

To quantitatively characterize the clustering properties of CD36 and its possible reorganization by TSP-1, receptor coordinates obtained by PALM were analyzed by spatial

pattern analysis (Owen et al. 2010, Williamson et al. 2011), with a robust optimized approach to gain confidence in our cluster properties extraction analysis (see 3.2.5.2 Spatial Pattern Analysis optimization). As suspected from the cross-linking assay results (see Figure 3-8), the spatial distribution of CD36 revealed by PALM was neither homogenous monomers in the presence of TSP-1 nor in its absence. At steady state, ~40% of the CD36 molecules in the membrane resided in clusters, with a median cluster radius of 70 nm (Figure 3-14A, B). Upon addition of TSP-1, cluster radius increased to an average value of 90 nm (Figure 3-14A) with the percentage of receptors in clusters going up to ~60% (Figure 3-14B). These larger CD36 clusters observed upon TSP-1 stimulation had more CD36 molecules per cluster (Figure 3-14C), while the overall number of individual clusters per surface area remained the same (Figure 3-14D). Interestingly, within these larger clusters, CD36 molecules became more “concentrated” or compact, with increase in CD36 density in them and a decreased CD36 density outside clusters upon TSP-1 stimulation (Figure 3-14E-G). Since CD36 density on plasma membrane was slightly higher upon TSP-1 stimulation (see Figure 3-12G), we tested if there was any correlation between the degree of clustering (ratio of density inside versus outside clusters) and CD36 density on the membrane. Pearson's correlation coefficient of ratio of CD36 density inside/outside clusters versus CD36 density on membrane revealed no correlation (Figure 3-14H), attributing the changes to cluster properties due to TSP-1 binding. While the results of the chemical crosslinking of CD36 hinted to the presence of pre-existing clusters becoming reinforced upon CD36 ligation by TSP-1, the super-resolution imaging and spatial pattern analysis provided quantitative molecular information of the re-arrangement of the receptors induced by TSP-1.

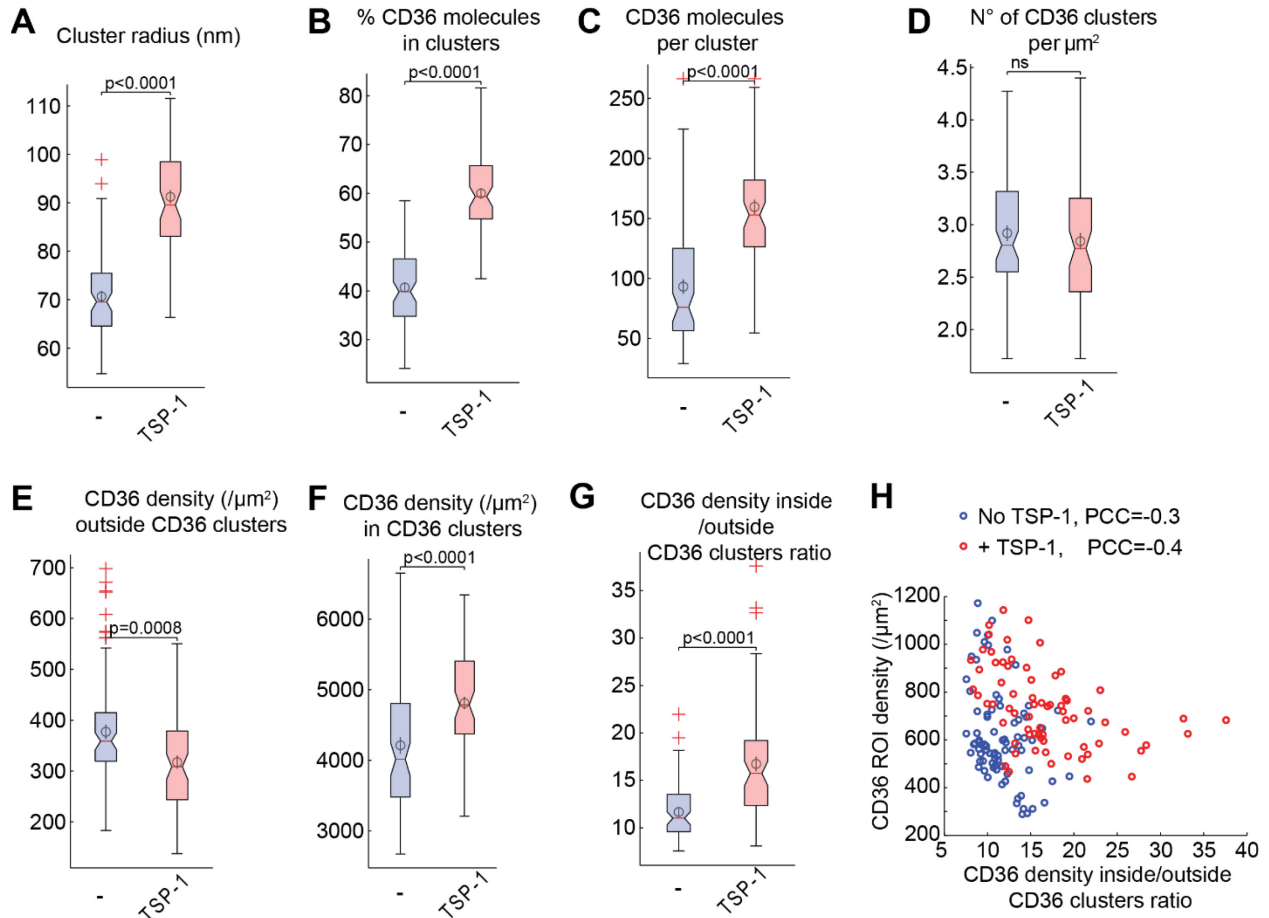


Figure 3-14: CD36 is clustered at steady state; TSP-1 induces further clustering

(A-G) Average cluster radius (A), percentage of CD36 molecules present in clusters (B), average number of CD36 molecules per cluster (C), number of CD36 clusters per μm^2 (D), CD36 density outside CD36 clusters per μm^2 (E), CD36 density in CD36 clusters per μm^2 (F) and ratio of corresponding densities inside versus outside CD36 clusters (G). All properties are calculated from same ROIs as in (Figure 3-12G), i.e. 81 ROIs in NoTSP-1 data, 70 ROIs in +TSP-1 data. (H) Scatterplot of the density ratios versus CD36 density with computed Pearson's correlation coefficient (PCC), with or without TSP-1. Boxplots and statistical analysis as described in 2.13 Graphing and statistical analysis. Data from 3 independent experiments, each containing 7 to 10 different cells.

3.2.5.4 Compaction of CD36 clusters is multivalency dependent

The observed recruitment and compaction of CD36 in clusters by TSP-1 indicated a multivalency dependent mechanism. To further validate this, and given that multivalent TSP-1 and SM ϕ activated Fyn while divalent FA6-152 could not (see Figure 3-5, Figure 3-6 and Figure 3-7), we extended our PALM imaging and analysis by looking at CD36 clusters under FA6-152 or SM ϕ stimulation. In line with our previous results, SM ϕ stimulation recruited more molecules into clusters just like TSP-1, resulting in larger and denser clusters, while FA6-152 failed to increase clustering (Figure 3-15A-C). Indeed, SM ϕ was also able to induce compaction of these clusters with increased cluster density to a similar extent as TSP-1 (Figure 3-15D). Taken all together, these results demonstrated a clustering dependent response of TSP-1-CD36-Fyn pathway initiation, achieved only under multivalency ligand stimulation.

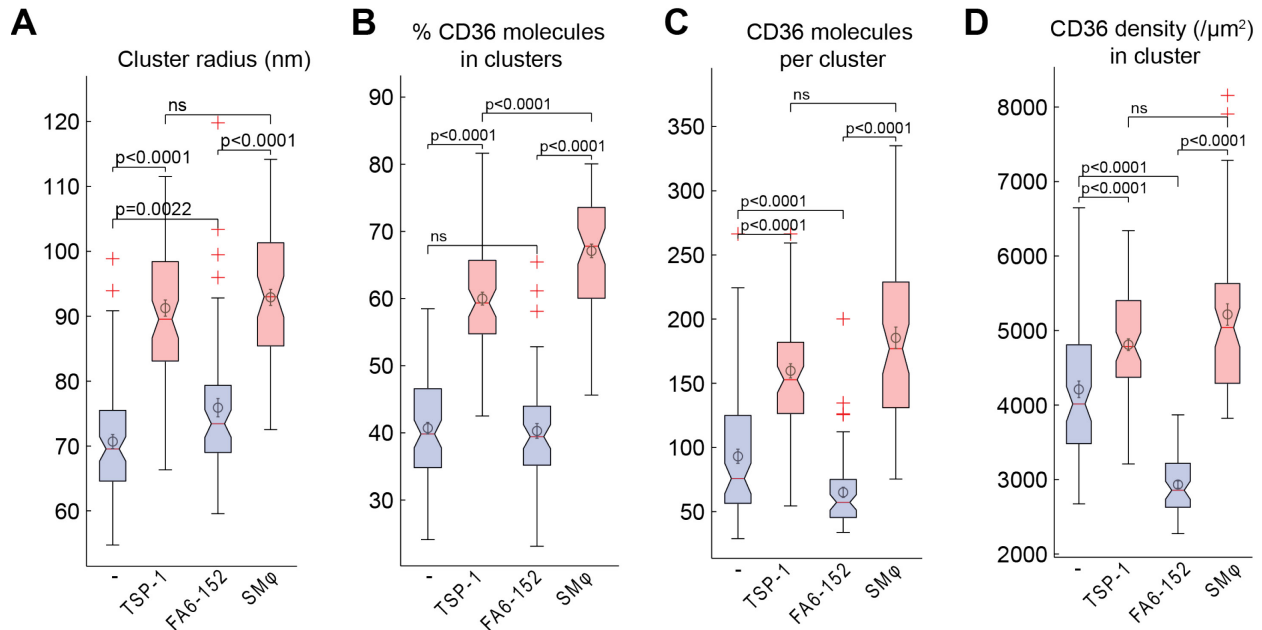


Figure 3-15: CD36 clusters compaction is multivalency dependent

(A-D) Average cluster radius (A), percentage of CD36 molecules present in clusters (B), average number of CD36 molecules per cluster (C) and CD36 density in CD36 clusters per μm^2 (D). All properties are calculated as described earlier (Figure 3-14). Boxplots and statistical analysis as described in 2.13 Graphing and statistical analysis. Data from 3 independent experiments, each containing 7 to 10 different cells. Data points used, 81 ROIs in untreated data, 70 ROIs in +TSP-1 data, 59 ROIs in +FA6-152 data and 63 ROIs in +SMφ data.

3.2.6 CD36 clusters are enriched with Fyn at all times

Since CD36 ligation by TSP-1 activates Fyn, we next investigated the spatial relationship between CD36 clusters and Fyn. For this, we developed a 2-color PALM imaging method to quantify the Fyn and CD36 distributions simultaneously. HMEC-PAmCherry-CD36 cells were transiently transfected with a Fyn-PAGFP construct, imaged by TIRFM, and then each channel

Chapter 3- Insights into CD36-Fyn reorganization upon TSP-1 binding

was analyzed separately as described above for CD36. The coordinates of Fyn and CD36 molecules were aligned using fiduciary markers easily identifiable in both channels. Visual inspection of the Fyn superresolution images suggested that Fyn had an anisotropic (elongated) spatial distribution (Figure 3-16A, yellow ROI), which is incompatible with our spatial pattern analysis technique (Sengupta, Jovanovic-Talisman & Lippincott-Schwartz 2013). To circumvent this challenge, we analyzed Fyn localization in relation to CD36 clusters before and after TSP-1 stimulation. Specifically, following the identification of CD36 clusters using spatial pattern analysis as described above, the spatial properties of Fyn molecules inside vs. outside these clusters were measured (Figure 3-16B). We tested the significance of any measured Fyn properties inside CD36 clusters by randomizing the CD36 cluster positions (50 times) and measuring the same Fyn spatial properties in the randomized clusters (Figure 3-16C).

Our analysis revealed that, while the density of Fyn molecules at the membrane remained the same before and after addition of TSP-1 (Figure 3-16D), the percentage of Fyn molecules in CD36 clusters increased upon TSP-1 stimulation (Figure 3-16E). Randomizing CD36 clusters significantly reduced the percentage of Fyn molecules found within the clusters in both conditions (Figure 3-16E), indicating that Fyn enrichment in CD36 clusters was specific to these clusters both in the absence and presence of ligand. The increase in the percentage of Fyn molecules within CD36 clusters upon TSP-1 stimulation was most likely due to the increased area covered by the clusters, as the percentage also increased for the randomized cluster positions (Figure 3-16E). While the density of Fyn molecules per μm^2 outside CD36 clusters remained the same in experimental and randomized states (Figure 3-16F), the density present in CD36 clusters was higher, indicative of Fyn enrichment in CD36 clusters (Figure 3-16G). These results suggest that CD36 and Fyn molecules associate with each other at all times, in agreement

Chapter 3- Insights into CD36-Fyn reorganization upon TSP-1 binding

with previous biochemical studies (Bull, Brickell & Dowd 1994, Huang et al. 1991). Stimulation with TSP-1 then recruits CD36 together with its associated Fyn into bigger and more compact clusters that likely play a key role in Fyn activation. Interestingly, our dual PALM data analysis also showed a CD36:Fyn stoichiometry change from 1:1 to 3:2 (Figure 3-16H), suggesting possible recruitment of other signaling molecules by CD36 into the clusters besides Fyn.

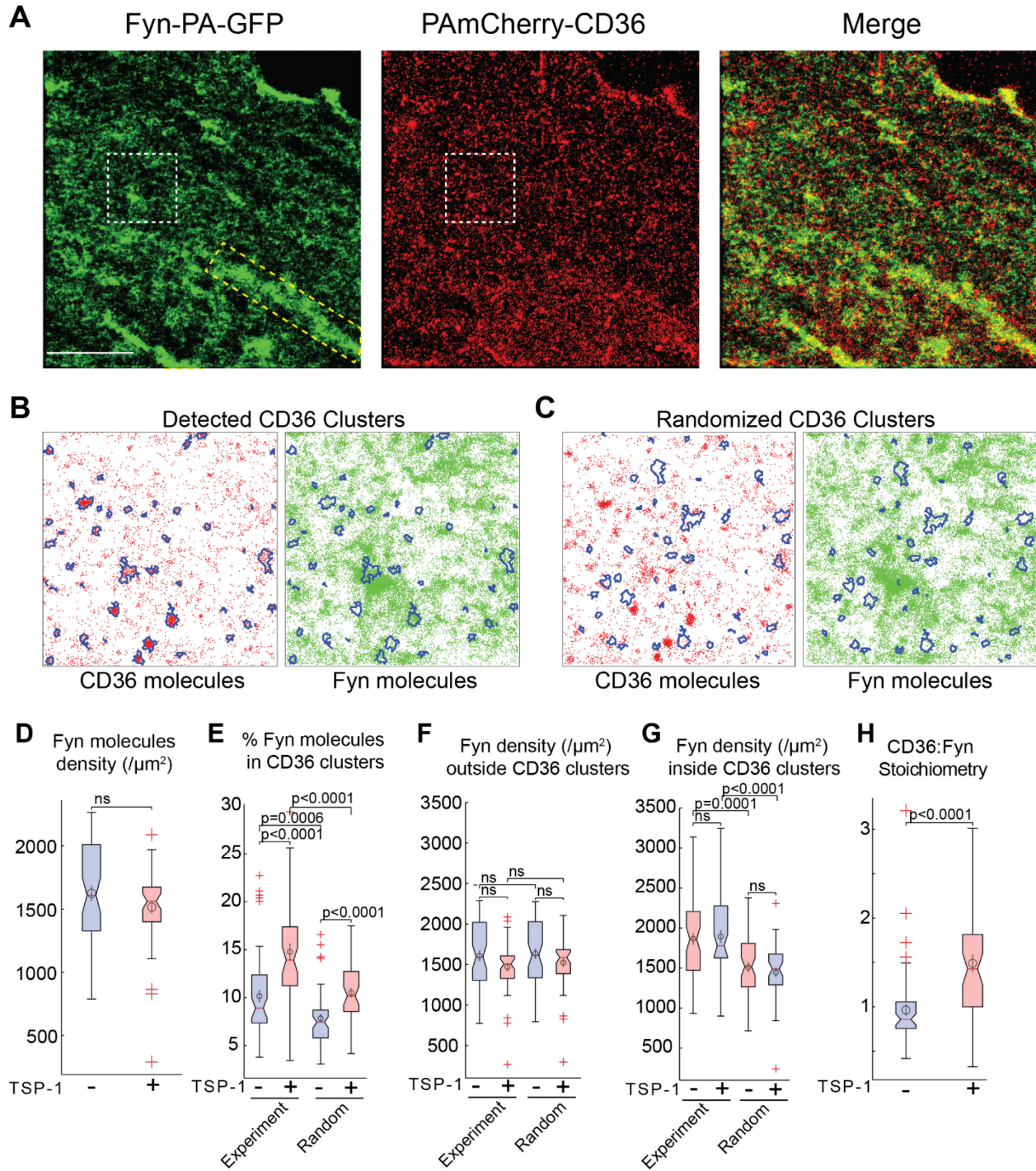


Figure 3-16: CD36 clusters are enriched with Fyn at all times

(A) Dual PALM imaging of PAmCherry-CD36 and Fyn-PA-GFP. Fyn exhibited anisotropic elongated morphology (yellow ROIs). Scale bars, 5 μm . (B) Example of

Chapter 3- Insights into CD36-Fyn reorganization upon TSP-1 binding

a ROI containing CD36 (left) and Fyn (right) localized molecules. Cluster regions, determined by spatial pattern analysis of CD36 (cluster edges outlined in blue), are overlaid on both channels in order to measure Fyn's properties in those regions. Scale bar, 1 μm . (C) Positions of CD36 cluster regions from B were randomized in order to measure Fyn's properties in random cellular locations. (D) Density of Fyn molecules obtained from HMEC-PAmCherry-CD36 cells treated or not with TSP-1 for 10 min. (E) Percentage of Fyn molecules in CD36 clusters determined from the experimental data (left) or from 50 randomized cluster position (right). (F) Fyn molecules density, per μm^2 outside CD36 clusters determined from the experimental data (left) or from 50 randomized cluster position (right). (G) Fyn molecules density, per μm^2 inside CD36 clusters determined from the experimental data (left) or from 50 randomized cluster position (right). (H) CD36:Fyn stoichiometry from dual PALM experimental data.

Data in (D-H) from cropped ROIs of 3 independent experiments (untreated: 59 ROIs from 15 cells; +TSP-1: 50 ROIs from 15 cells). Boxplots and statistical analysis as described in 2.13 Graphing and statistical analysis.

One accessory protein commonly associated with SFKs activation and deactivation is the protein tyrosine phosphatase (PTP) CD45 (Rhee, Veillette 2012). It has been postulated that CD45 could activate SFKs like Fyn by dephosphorylating its inhibitory tyrosine residue Y531, or alternatively inhibit Fyn activation by dephosphorylating its activation tyrosine Y420. Western blot analysis of Fyn activation in the presence of a CD45 inhibitor (PTP-CD45 inhibitor) suggested that CD45-mediated dephosphorylation of Y531 is necessary for Fyn activation (Figure 3-17A, B). TIRFM imaging of CD45 and mApple-CD36 showed striking spatial pattern similarities between the two proteins, along elongated morphology, reminiscent of cytoskeleton involvement (Figure 3-17C).

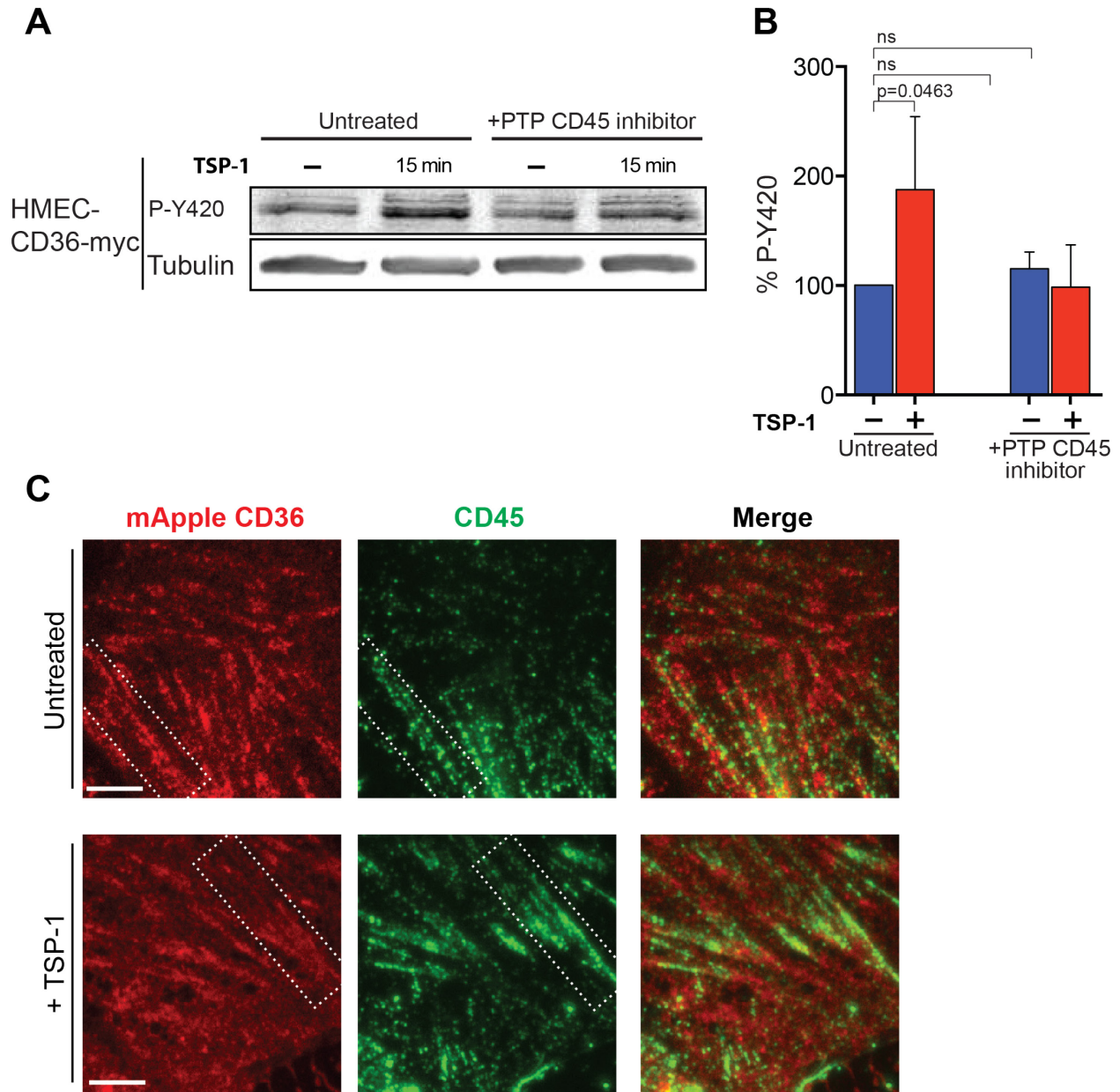


Figure 3-17: CD45 helps in activation of Fyn in TSP-1-CD36-Fyn pathway

(A) Levels of P-Y420 in HMEC-CD36-myc stimulated or not for 15 min with TSP-1 after addition or not of a PTP-CD45 inhibitor. Tubulin is shown as a loading control. Each blot is a representative of three independent similar experiments. (B) Percentage of P-Y420 levels quantified from blots in (A) and normalized to the level of tubulin. Error bars indicate mean \pm SD. Statistical analysis as described in 2.13 Graphing and statistical analysis. (C) TIRFM imaging of CD45 in HMEC-mApple-

CD36 cells, with or without TSP-1. White dashed ROIs highlight sample cytoskeleton like elongated morphology exhibited by CD45 and CD36.

Scale bars (applicable to all images), 5 μm .

3.3 Discussion

Nanoclustering is emerging as a prominent feature of membrane-associated protein organization (Garcia-Parajo et al. 2014), in contrast to the classical fluid mosaic model of the plasma membrane (Singer, Nicolson 1972). Multiple factors are thought to mediate this organization, including lipid-lipid, lipid-protein and protein-protein interactions within the plane of the membrane (Simons, Gerl 2010), as well as plasma membrane-cortical cytoskeleton interactions (Jaqaman, Grinstein 2012, Morone et al. 2006). Much however remains to be determined about the specific mechanisms leading to nanoclustering, the nature of the nanoclustering, and, most importantly, its functional consequences for receptor signaling (Garcia-Parajo et al. 2014).

Using super-resolution imaging and spatial pattern analysis, we have explored nanoclustering of CD36 in ECs. We found that at steady state, ~40% of CD36 on the plasma membrane exists in clusters ~70 nm in radius (Figure 3-14). TSP-1 stimulation induces larger, ~90 nm in radius, compact clusters, a trend mirrored in decavalent SM α stimulation but not in divalent FA6-152 condition. Importantly, Fyn is enriched in these unligated CD36 nanoclusters, as well as in ligand stimulated condition (Figure 3-16).

Unligated receptor clustering has been invoked in several previous studies as a mechanism to prime the cell to respond when exposed to ligand (Cambi et al. 2004, Cambi et al.

Chapter 3- Insights into CD36-Fyn reorganization upon TSP-1 binding

2006, Itano et al. 2012, Veatch et al. 2012, Mattila et al. 2013, Lillemeier et al. 2010). In the case of multivalent ligands, it would increase the efficiency of receptor clustering upon binding, as the ligand would encounter multiple receptors in a shorter period of time. Since TSP-1 and SM ϕ are multivalent, the unligated CD36 clusters observed in our study most likely contribute to such a mechanism, as previously also observed for CD36 in macrophages in the context of oxLDL binding (Jaqaman et al. 2011). However, since CD36 itself lacks any canonical intracellular signaling domains and rather signals through the SFK Fyn, multivalent ligand binding and signaling would only be efficient if Fyn is in the close vicinity of CD36. The enrichment of Fyn in unligated CD36 nanoclusters potentially serves exactly this purpose, keeping the receptor (CD36) and its signaling partner (Fyn) close to each other, ready to signal when exposed to ligand. Modeling efforts have indeed previously suggested that clustering reduces the effective dissociation constant between receptors and their downstream effectors due to enhanced rebinding (Hsieh et al. 2010). We suspect that a co-clustering based mechanism, as observed here for CD36 and Fyn, may be a general mechanism to increase the signaling efficiency of receptors that lack signaling domains and instead signal through associated kinases, such as cytokine and immuno-receptors (Garcia-Parajo et al. 2014, O'Shea, Murray 2008).

We envision two main, not mutually exclusive mechanisms to explain the activation of Fyn upon TSP-1 binding. First, the compaction of CD36 clusters may lead to reduction in the intermolecular distance between Fyn molecules, and this could facilitate in their trans autophosphorylation, a known phenomenon leading to SFK activation (Cooper, MacAuley 1988). Second, cluster remodeling could alter the interactions between Fyn and accessory proteins that also reside in the clusters. The inhibition of Fyn activation by inhibiting tyrosine phosphatase (PTP) CD45, commonly associated with SFKs (Rhee, Veillette 2012), suggests that

Chapter 3- Insights into CD36-Fyn reorganization upon TSP-1 binding

CD45 may be one of the accessory protein needed to drive TSP-1-CD36-Fyn pathway, possibly through dephosphorylation of Fyn's inhibitory Y-531 (Figure 3-17). It is very likely that CD36 recruitment into clusters upon multivalent ligand binding, brings along CD45 into these clusters to aid Fyn activation.

CD36 lacks any canonical signaling motif in its cytoplasmic tails, yet it associates with Fyn (Bull, Brickell & Dowd 1994, Huang et al. 1991). Fyn attachment to the inner leaflet of the plasma membrane is through dual palmitoylation and myristoylation (Resh 1994). One factor that might help bring Fyn and CD36 together is by a co-recruitment to similar lipid nanodomains (as CD36 cytoplasmic tails are each dual palmitoylation (Tao, Wagner & Lublin 1996)). Lipid modified proteins anchored to the membrane have a high affinity for these nanodomains (Levental et al. 2010). However, this alone cannot account for the clustering and spatial organization observed, in chapter 3, between CD36-Fyn interactions. One key factor in controlling the clustering and organization of receptors at the plasma membrane is the cortical cytoskeleton (Jaqaman, Grinstein 2012). The anisotropic elongated morphology observed in Fyn (yellow dotted ROIs, Figure 3-16A) as well as CD36 (white dotted ROIs, Figure 3-17C) pointed towards cortical cytoskeleton involvement. Indeed, cytoskeletal control of CD36 has been demonstrated in macrophages (Jaqaman et al. 2011, Jaqaman et al. 2008), though the universality of this regulation in other cell lines has not been explored. In light of our findings in chapter 3, we next investigated the involvement of cortical cytoskeleton and lipid rafts in controlling TSP-1-CD36-Fyn pathway in chapter 4.

References

- Ades, E.W., Candal, F.J., Swerlick, R.A., George, V.G., Summers, S., Bosse, D.C. & Lawley, T.J. 1992, "HMEC-1: establishment of an immortalized human microvascular endothelial cell line.", *Journal of Investigative Dermatology*, vol. 99, no. 6, pp. 683-690.
- Asch, A.S., Barnwell, J., Silverstein, R.L. & Nachman, R.L. 1987, "Isolation of the thrombospondin membrane receptor.", *Journal of Clinical Investigation*, vol. 79, no. 4, pp. 1054-1061.
- Bull, H.A., Brickell, P.M. & Dowd, P.M. 1994, "Src-related protein tyrosine kinases are physically associated with the surface antigen CD36 in human dermal microvascular endothelial cells", *FEBS letters*, vol. 351, no. 1, pp. 41-44.
- Cambi, A., de Lange, F., van Maarseveen, N.M., Nijhuis, M., Joosten, B., van Dijk, E.M., de Bakker, B.I., Fransen, J.A., Bovee-Geurts, P.H., van Leeuwen, F.N., Van Hulst, N.F. & Figdor, C.G. 2004, "Microdomains of the C-type lectin DC-SIGN are portals for virus entry into dendritic cells", *The Journal of cell biology*, vol. 164, no. 1, pp. 145-155.
- Cambi, A., Joosten, B., Koopman, M., de Lange, F., Beeren, I., Torensma, R., Fransen, J.A., Garcia-Parajo, M., van Leeuwen, F.N. & Figdor, C.G. 2006, "Organization of the integrin LFA-1 in nanoclusters regulates its activity", *Molecular biology of the cell*, vol. 17, no. 10, pp. 4270-4281.
- Cooper, J.A. & MacAuley, A. 1988, "Potential positive and negative autoregulation of p60c-src by intermolecular autophosphorylation", *Proceedings of the National Academy of Sciences of the United States of America*, vol. 85, no. 12, pp. 4232-4236.
- Dawson, D.W., Pearce, S.F., Zhong, R., Silverstein, R.L., Frazier, W.A. & Bouck, N.P. 1997, "CD36 mediates the In vitro inhibitory effects of thrombospondin-1 on endothelial cells.", *Journal of Cell Biology*, vol. 138, no. 3, pp. 707-717.
- Durisic, N., Laparra-Cuervo, L., Sandoval-Alvarez, A., Borbely, J.S. & Lakadamyali, M. 2014, "Single-molecule evaluation of fluorescent protein photoactivation efficiency using an in vivo nanotemplate", *Nature methods*, vol. 11, no. 2, pp. 156-162.
- Fish, K.N. 2009, "Total internal reflection fluorescence (TIRF) microscopy", *Current Protocols in Cytometry. Chapter 12:Unit12.18, 2009 Oct*, vol. Chapter 12, pp. Unit12.18.
- Garcia-Parajo, M.F., Cambi, A., Torreno-Pina, J.A., Thompson, N. & Jacobson, K. 2014, "Nanoclustering as a dominant feature of plasma membrane organization", *Journal of cell science*, vol. 127, no. 23, pp. 4995-5005.
- Hancock, J.F. & Prior, I.A. 2005, "Electron microscopic imaging of Ras signaling domains", *Methods (San Diego, Calif.)*, vol. 37, no. 2, pp. 165-172.

Chapter 3- Insights into CD36-Fyn reorganization upon TSP-1 binding

- Hsieh, M.Y., Yang, S., Raymond-Stinz, M.A., Edwards, J.S. & Wilson, B.S. 2010, "Spatio-temporal modeling of signaling protein recruitment to EGFR", *BMC systems biology*, vol. 4, pp. 57-0509-4-57.
- Huang, M.M., Bolen, J.B., Barnwell, J.W., Shattil, S.J. & Brugge, J.S. 1991, "Membrane glycoprotein IV (CD36) is physically associated with the Fyn, Lyn, and Yes protein-tyrosine kinases in human platelets", *Proceedings of the National Academy of Sciences of the United States of America*, vol. 88, no. 17, pp. 7844-7848.
- Itano, M.S., Steinhauer, C., Schmied, J.J., Forthmann, C., Liu, P., Neumann, A.K., Thompson, N.L., Tinnefeld, P. & Jacobson, K. 2012, "Super-resolution imaging of C-type lectin and influenza hemagglutinin nanodomains on plasma membranes using blink microscopy", *Biophysical journal*, vol. 102, no. 7, pp. 1534-1542.
- Jaqaman, K. & Grinstein, S. 2012, "Regulation from within: the cytoskeleton in transmembrane signaling", *Trends in cell biology*, vol. 22, no. 10, pp. 515-526.
- Jaqaman, K., Kuwata, H., Touret, N., Collins, R., Trimble, W.S., Danuser, G. & Grinstein, S. 2011, "Cytoskeletal control of CD36 diffusion promotes its receptor and signaling function", *Cell*, vol. 146, no. 4, pp. 593-606.
- Jaqaman, K., Loerke, D., Mettlen, M., Kuwata, H., Grinstein, S., Schmid, S.L. & Danuser, G. 2008, "Robust single-particle tracking in live-cell time-lapse sequences", *Nat Meth*, vol. 5, no. 8, pp. 695-702.
- Jimenez, B., Volpert, O.V., Crawford, S.E., Febbraio, M., Silverstein, R.L. & Bouck, N. 2000, "Signals leading to apoptosis-dependent inhibition of neovascularization by thrombospondin-1", *Nature medicine*, vol. 6, no. 1, pp. 41-48.
- Kiskowski, M.A., Hancock, J.F. & Kenworthy, A.K. 2009, "On the Use of Ripley's K-Function and Its Derivatives to Analyze Domain Size", *Biophysical journal*, vol. 97, no. 4, pp. 1095-1103.
- Lagache, T., Lang, G., Sauvonnnet, N. & Olivo-Marin, J.C. 2013, "Analysis of the spatial organization of molecules with robust statistics", *PloS one*, vol. 8, no. 12, pp. e80914.
- Levental, I., Lingwood, D., Grzybek, M., Coskun, U. & Simons, K. 2010, "Palmitoylation regulates raft affinity for the majority of integral raft proteins.", *Proceedings of the National Academy of Sciences of the United States of America*, vol. 107, no. 51, pp. 22050-22054.
- Lillemeier, B.F., Mortelmaier, M.A., Forstner, M.B., Huppa, J.B., Groves, J.T. & Davis, M.M. 2010, "TCR and Lat are expressed on separate protein islands on T cell membranes and concatenate during activation", *Nature immunology*, vol. 11, no. 1, pp. 90-96.
- Markovic, S.N., Suman, V.J., Rao, R.A., Ingle, J.N., Kaur, J.S., Erickson, L.A., Pitot, H.C., Croghan, G.A., McWilliams, R.R., Merchan, J., Kottschade, L.A., Nevala, W.K., Uhl, C.B.,

Chapter 3- Insights into CD36-Fyn reorganization upon TSP-1 binding

- Allred, J. & Creagan, E.T. 2007, "A phase II study of ABT-510 (thrombospondin-1 analog) for the treatment of metastatic melanoma", *American journal of clinical oncology*, vol. 30, no. 3, pp. 303-309.
- Mattila, P.K., Feest, C., Depoil, D., Treanor, B., Montaner, B., Otipoby, K.L., Carter, R., Justement, L.B., Bruckbauer, A. & Batista, F.D. 2013, "The actin and tetraspanin networks organize receptor nanoclusters to regulate B cell receptor-mediated signaling", *Immunity*, vol. 38, no. 3, pp. 461-474.
- Mirochnik, Y., Kwiatek, A. & Volpert, O.V. 2008, "Thrombospondin and apoptosis: molecular mechanisms and use for design of complementation treatments", *Current Drug Targets*, vol. 9, no. 10, pp. 851-862.
- Morone, N., Fujiwara, T., Murase, K., Kasai, R.S., Ike, H., Yuasa, S., Usukura, J. & Kusumi, A. 2006, "Three-dimensional reconstruction of the membrane skeleton at the plasma membrane interface by electron tomography", *The Journal of cell biology*, vol. 174, no. 6, pp. 851-862.
- Nguyen, A.W. & Daugherty, P.S. 2005, "Evolutionary optimization of fluorescent proteins for intracellular FRET", *Nature biotechnology*, vol. 23, no. 3, pp. 355-360.
- O'Shea, J.J. & Murray, P.J. 2008, "Cytokine signaling modules in inflammatory responses", *Immunity*, vol. 28, no. 4, pp. 477-487.
- Owen, D.M., Rentero, C., Rossy, J., Magenau, A., Williamson, D., Rodriguez, M. & Gaus, K. 2010, "PALM imaging and cluster analysis of protein heterogeneity at the cell surface.", *Journal of Biophotonics*, vol. 3, no. 7, pp. 446-454.
- Puchner, E.M., Walter, J.M., Kasper, R., Huang, B. & Lim, W.A. 2013, "Counting molecules in single organelles with superresolution microscopy allows tracking of the endosome maturation trajectory", *Proceedings of the National Academy of Sciences of the United States of America*, vol. 110, no. 40, pp. 16015-16020.
- Resh, M.D. 1994, "Myristylation and palmitoylation of Src family members: the fats of the matter", *Cell*, vol. 76, no. 3, pp. 411-413.
- Resovi, A., Pinessi, D., Chiorino, G. & Taraboletti, G. 2014, "Current understanding of the thrombospondin-1 interactome", *Matrix biology : journal of the International Society for Matrix Biology*, vol. 37, pp. 83-91.
- Rhee, I. & Veillette, A. 2012, "Protein tyrosine phosphatases in lymphocyte activation and autoimmunity", *Nature immunology*, vol. 13, no. 5, pp. 439-447.
- Saito, Y.D., Jensen, A.R., Salgia, R. & Posadas, E.M. 2010, "Fyn: a novel molecular target in cancer", *Cancer*, vol. 116, no. 7, pp. 1629-1637.

Chapter 3- Insights into CD36-Fyn reorganization upon TSP-1 binding

- Sato, K., Ogawa, K., Tokmakov, A.A., Iwasaki, T. & Fukami, Y. 2001, "Hydrogen peroxide induces Src family tyrosine kinase-dependent activation of *Xenopus* eggs", *Development, growth & differentiation*, vol. 43, no. 1, pp. 55-72.
- Sengupta, P., Jovanovic-Taliman, T. & Lippincott-Schwartz, J. 2013, "Quantifying spatial organization in point-localization superresolution images using pair correlation analysis", *Nature protocols*, vol. 8, no. 2, pp. 345-354.
- Shaner, N.C., Patterson, G.H. & Davidson, M.W. 2007, "Advances in fluorescent protein technology", *Journal of cell science*, vol. 120, no. Pt 24, pp. 4247-4260.
- Simons, K. & Gerl, M.J. 2010, "Revitalizing membrane rafts: new tools and insights", *Nature Reviews Molecular Cell Biology*, vol. 11, no. 10, pp. 688-699.
- Singer, S.J. & Nicolson, G.L. 1972, "The fluid mosaic model of the structure of cell membranes.", *Science*, vol. 175, no. 4023, pp. 720-731.
- Tao, N., Wagner, S.J. & Lublin, D.M. 1996, "CD36 is palmitoylated on both N- and C-terminal cytoplasmic tails", *The Journal of biological chemistry*, vol. 271, no. 37, pp. 22315-22320.
- Thomann, D., Rines, D.R., Sorger, P.K. & Danuser, G. 2002, "Automatic fluorescent tag detection in 3D with super-resolution: application to the analysis of chromosome movement", *Journal of microscopy*, vol. 208, no. Pt 1, pp. 49-64.
- Veatch, S.L., Chiang, E.N., Sengupta, P., Holowka, D.A. & Baird, B.A. 2012, "Quantitative nanoscale analysis of IgE-FcepsilonRI clustering and coupling to early signaling proteins", *The journal of physical chemistry.B*, vol. 116, no. 23, pp. 6923-6935.
- Volpert, O.V., Zaichuk, T., Zhou, W., Reiher, F., Ferguson, T.A., Stuart, P.M., Amin, M. & Bouck, N.P. 2002, "Inducer-stimulated Fas targets activated endothelium for destruction by anti-angiogenic thrombospondin-1 and pigment epithelium-derived factor", *Nature medicine*, vol. 8, no. 4, pp. 349-357.
- Williamson, D.J., Owen, D.M., Rossy, J., Magenau, A., Wehrmann, M., Gooding, J.J. & Gaus, K. 2011, "Pre-existing clusters of the adaptor Lat do not participate in early T cell signaling events.", *Nature immunology*, vol. 12, no. 7, pp. 655-662.
- Zhang, J., Leiderman, K., Pfeiffer, J.R., Wilson, B.S., Oliver, J.M. & Steinberg, S.L. 2006, "Characterizing the topography of membrane receptors and signaling molecules from spatial patterns obtained using nanometer-scale electron-dense probes and electron microscopy", *Micron (Oxford, England : 1993)*, vol. 37, no. 1, pp. 14-34.

**Chapter 4 - Actin and lipid nanodomains control TSP-1-CD36-Fyn
pathway**

Some portions of this chapter are part of a manuscript under review, drafted by me and edited by Nicolas and Khuloud.

4.1 Introduction

Analyses from dual PALM revealed that CD36 and Fyn associate together at all times, independently of TSP-1. This leads to the question what mechanisms bring them together and what factors control the dynamic clustering of CD36 that shifts to compaction and Fyn activation upon TSP-1 stimulation. Both CD36 and Fyn are palmitoylated (Tao, Wagner & Lublin 1996, Alland et al. 1994), increasing their affinity for lipid nanodomains (Levental et al. 2010), a feature that might help bring the two proteins together. In addition, the anisotropic spatial distribution of Fyn observed hinted to cytoskeletal actin involvement. Indeed cytoskeletal control of plasma membrane CD36 in macrophages has been proposed to organize and aid CD36 signaling (Jaqaman et al. 2011, Jaqaman et al. 2008). Recently, it was shown that in CD36 mediated adhesion of infected red blood cells to HMVECs, SFKs are activated, which in turn phosphorylate and activate an adaptor protein, p130Cas causing actin rearrangement (Davis et al. 2011). CD36 has also been shown to signal to the actin cytoskeleton through p130Cas activation by Fyn activation in primary microglia and macrophages exposed to β A (Stuart et al. 2007).

In light of these reports and our earlier observations, we set out to investigate if actin and lipid nanodomains were involved in TSP-1-CD36-Fyn pathway. We show that in ECs, cortical actin and lipid nanodomains are linked and collaborate to spatially organize CD36-Fyn complexes, and aid in the TSP-1 mediated CD36 cluster reorganization and subsequent Fyn activation. Pharmacological perturbation of actin or lipid nanodomains resulted in:

- 1) Disrupted CD36-Fyn spatial distribution.
- 2) Reduced TSP-1 binding.
- 3) Abrogated Fyn activation by TSP-1-CD36.
- 4) Disrupted CD36 cluster enhancement by TSP-1.
- 5) Increased CD36 immobility.

In the following chapter, experiments demonstrating the role of the actin cytoskeleton and membrane integrity are presented and their potential control on CD36-Fyn signaling are further discussed.

4.2 Results

4.2.1 The membrane-targeting domain of Fyn is sufficient for its recruitment to CD36 clusters

Since all four intracellular cysteine residues of CD36 (C3, C7, C464 and C466) are palmitoylated (Tao, Wagner & Lublin 1996) and Fyn is myristoylated on G2 and dual palmitoylated on C3 and C6 (Resh 1994), we examined whether their membrane targeting co-partitioned them into specific membrane microdomains. Using TIRFM, we imaged HMEC-mApple-CD36 cells transiently transfected either with wild -type (WT) Fyn-mEmerald or with a truncated Fyn construct tagged with GFP (truncated Fyn-GFP), containing only the N-terminal membrane-targeting domain of Fyn (Figure 4-1A, B). In these images, the CD36 clusters were close to diffraction limited spots that we detected using Gaussian mixture-model fitting (Jaqaman et al. 2008). The colocalization of full length or truncated Fyn within the CD36 spots was then quantified as percent Fyn enrichment obtained from the ratio of the average Fyn pixel intensity within CD36 spots to the average Fyn pixel intensity outside these spots. This approach allowed us to tackle the challenge that the CD36 images were punctate while the Fyn images were rather

Chapter 4- Actin and lipid nanodomains control TSP-1-CD36-Fyn pathway

continuous, for which there are no standard colocalization analysis approaches (for details, see 2.8.5 Puncta-continuum colocalization analysis). Subtracting 1 from the ratio of Fyn intensities inside versus outside would be equal to 0 in instances of no colocalization, while > 0 would indicate colocalization. Expressing these values as a percentage would give percent enrichment of Fyn in CD36 spots. To test for the significance of any observed colocalization, the percent enrichment was also calculated for each dataset after randomizing the CD36 spot (i.e. cluster) positions, which would yield values close at 0. Subtracting ratio of randomization from experimental ratio, expressed as a percentage gave percent enrichment of Fyn in CD36 clusters.

Consistent with the dual-color PALM analysis (Figure 3-16), percent Fyn enrichment in CD36 spots from experimental data was significantly higher than that of the randomized control (Figure 4-1C, light red boxplots versus light blue boxplots respectively). TSP-1 stimulation did increase Fyn enrichment in CD36 spots, though this was not observed in truncated Fyn experiment. Importantly, the enrichments were relatively equivalent for the full length and truncated Fyn (Figure 4-1C), indicating that the N-terminal membrane-targeting domain of the kinase is sufficient for its colocalization within CD36 clusters.

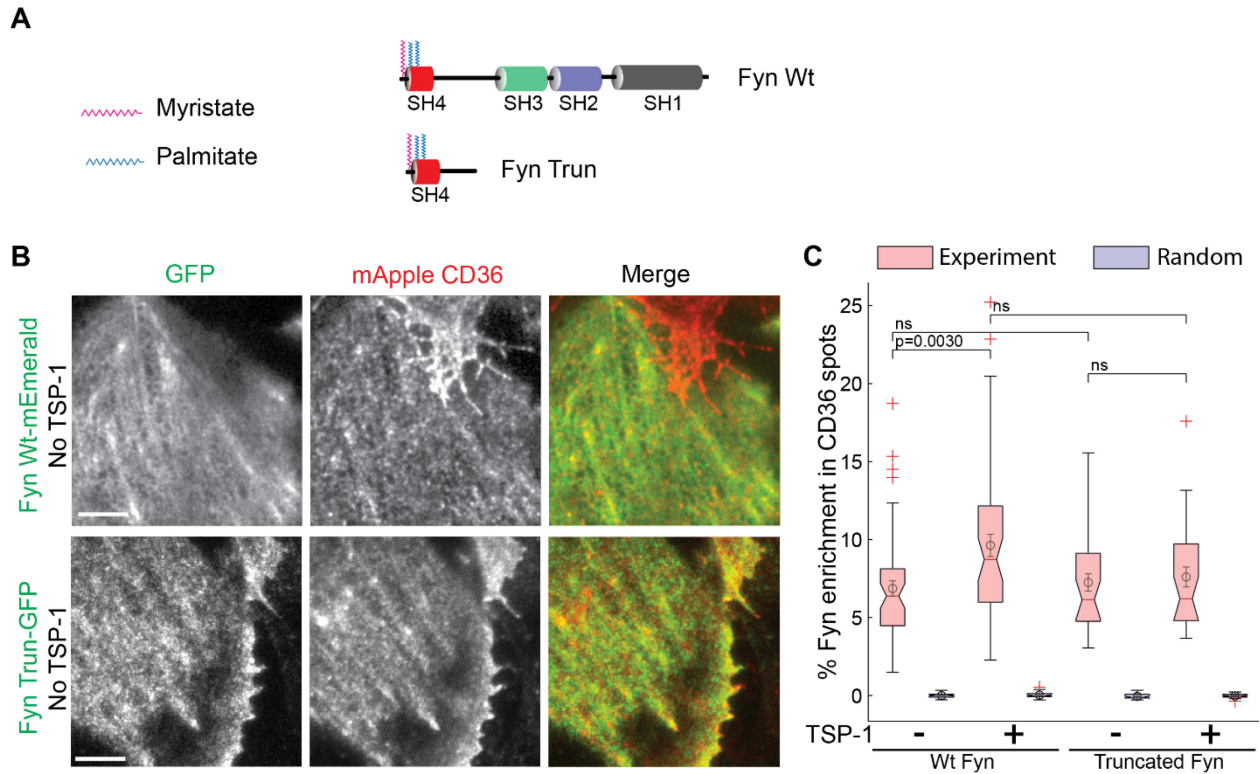


Figure 4-1: The membrane-targeting domain of Fyn is sufficient for its recruitment to CD36 clusters

(A) Schematic representation of the domains of WT Fyn or truncated Fyn. (B) Fixed cell TIRFM imaging of WT Fyn-mEmerald or truncated Fyn-GFP transfected in HMEC-mApple-CD36 cells. (C) Average percent Fyn enrichment (WT Fyn-mEmerald or truncated Fyn-GFP) within mApple-CD36 spots (light red boxplots) together with the randomized control (light blue boxplots). Boxplots and statistical analysis as described in 2.13 Graphing and statistical analysis.

All data from 3 independent experiments, each with at least 10 fields of view, all imaged with identical settings. Scale bars (applicable to all images), 5 μ m.

4.2.2 CD36-Fyn association is primarily along the actin cytoskeleton

While the membrane-targeting domain of Fyn seemed to be sufficient for its colocalization with CD36, the pattern of Fyn distribution on the membrane, even of truncated Fyn, was reminiscent of the actin cytoskeleton (Figure 4-1B). This actin-like pattern was also confirmed in steady state and TSP-1 stimulated cells, by visual inspection of sample Fyn images from the dual PALM SRI experiment (Figure 4-2).

Sample Fyn-PA-GFP superresolution images

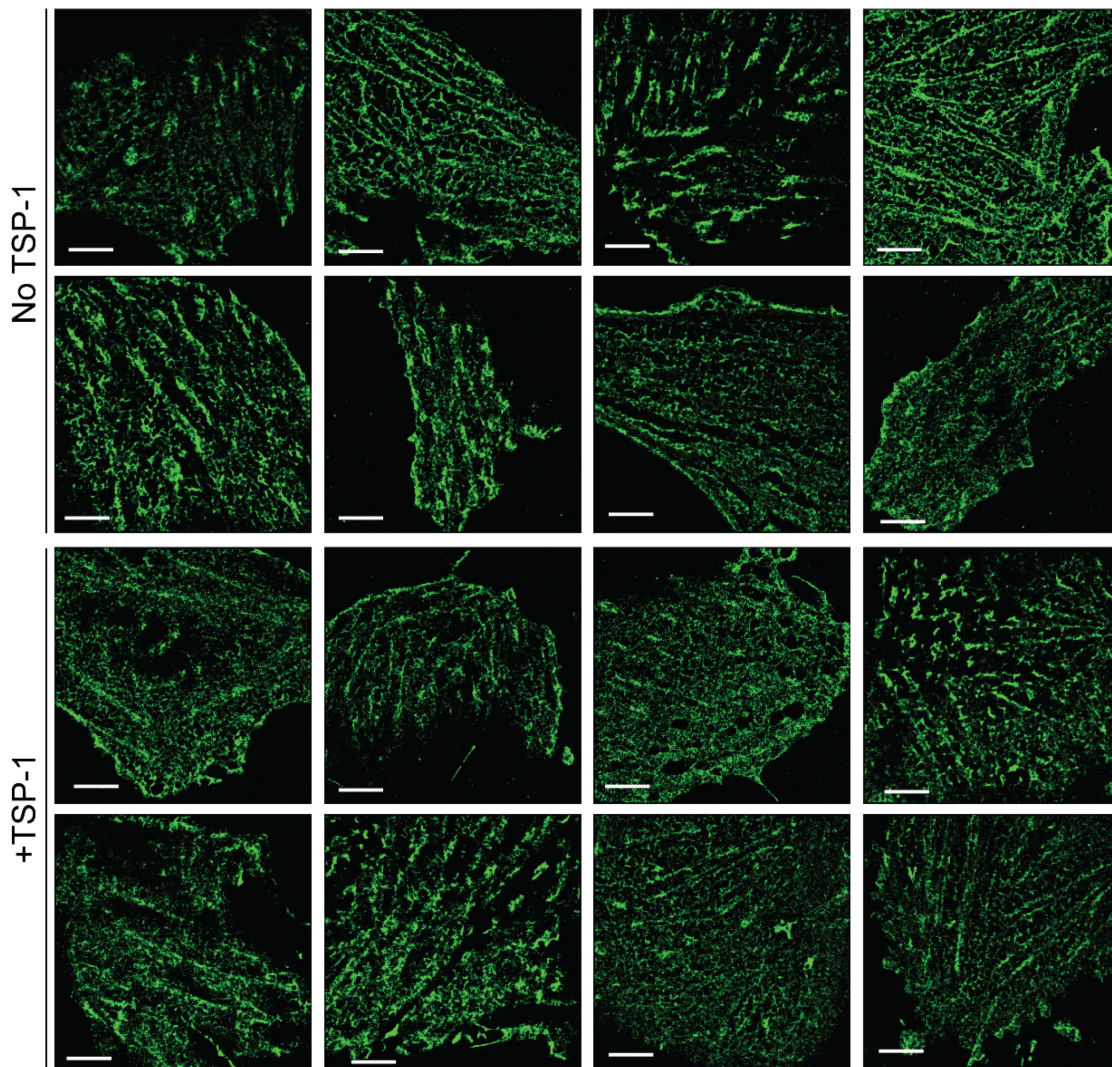


Figure 4-2: SRI of Fyn-PA-GFP showing its variable anisotropic spatial distribution

Sample images from dual PALM data were randomly picked to highlight the different anisotropic spatial distribution exhibited by Fyn. Scale bars (applicable to all images), 5 μm .

To test whether there was preferential CD36-Fyn colocalization along actin, we performed a 3-way colocalization analysis of CD36, Fyn and filamentous actin (F-actin). Specifically, the actin cytoskeleton was stained with phalloidin AlexaFluor 647 in HMEC-mApple-CD36 cells transfected with Fyn-mEmerald or truncated Fyn-GFP and imaged by TIRFM (Figure 4-3A). The same quantification of percent Fyn enrichment in CD36 spots was performed as above, but with the CD36 spots pre-classified as lying in high versus low actin intensity areas (see 2.8.5 Puncta-continuum colocalization analysis). From this classification, in unstimulated conditions, ~60% of the CD36 spots were on high actin areas, with TSP-1 stimulation causing that to increase to ~65% (Figure 4-3B). This analysis also revealed that percent Fyn enrichment in CD36 spots, in both WT and truncated version, in regions rich in F-actin was indeed much higher than in regions poor in F-actin (Figure 4-3, light red versus light blue boxplots respectively).

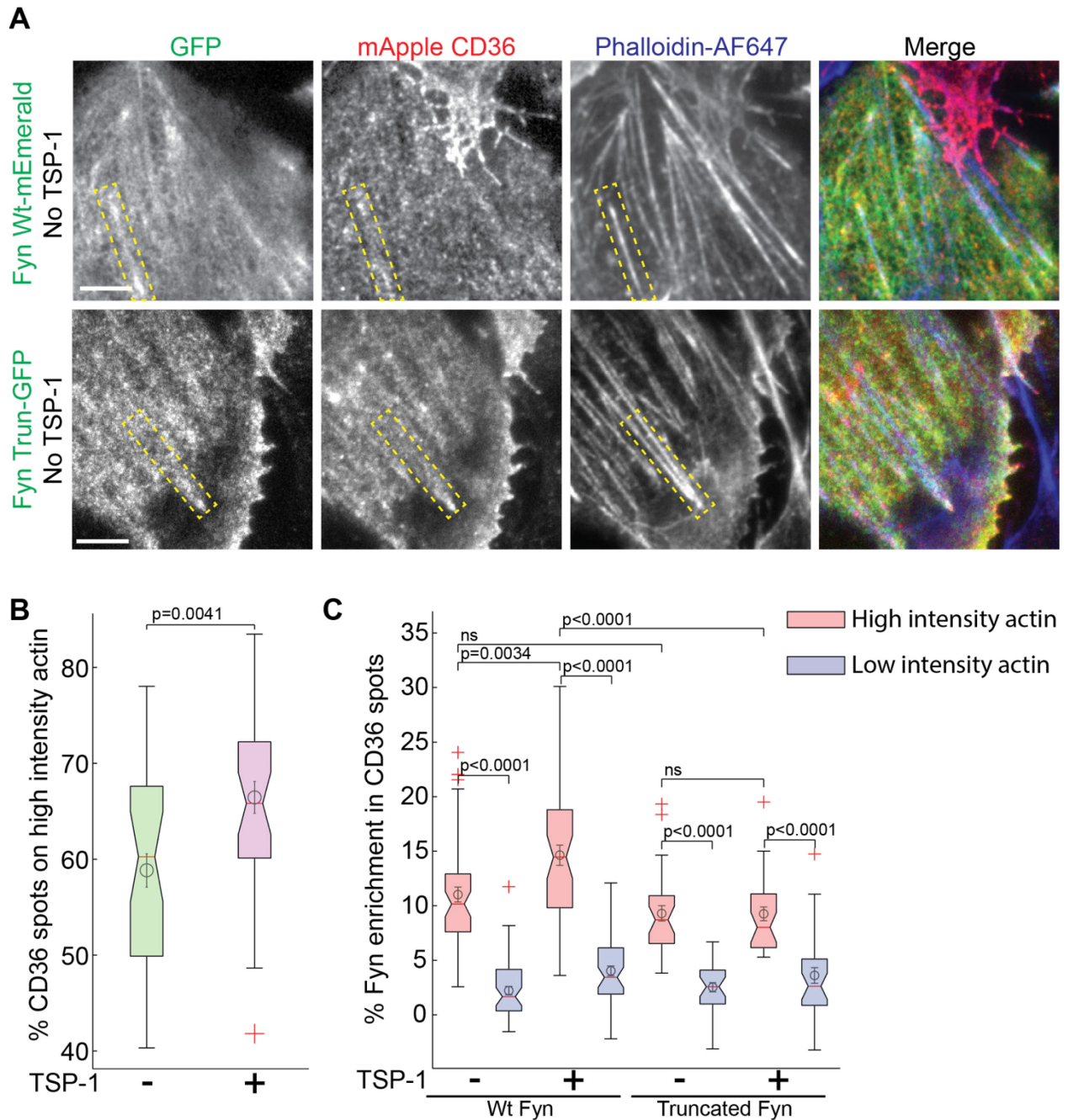


Figure 4-3: CD36-Fyn association is primarily along the actin cytoskeleton

(A) Fixed cell TIRFM imaging of WT Fyn-mEmerald or truncated Fyn-GFP transfected in HMEC-mApple-CD36 cells with F-actin stained with phalloidin AlexaFluor 647. (B) Quantification of percent of CD36 spots on high actin regions. (C) Average percent Fyn enrichment (WT Fyn-mEmerald or truncated Fyn-GFP)

within mApple-CD36 spots in high or low actin intensity regions (light red vs light blue boxplots respectively). Boxplots and statistical analysis as described in 2.13 Graphing and statistical analysis.

All data from 3 independent experiments, each with at least 10 fields of view, all imaged with identical settings. Scale bars (applicable to all images), 5 μ m.

4.2.3 CD36-Fyn associate in lipid nanodomains along the actin cytoskeleton

Since palmitoylated proteins have been shown to have a high affinity for cholesterol and sphingolipid enriched domains, commonly referred to as lipid rafts (Levental et al. 2010, Lingwood, Simons 2010), we tested whether these lipid nanodomains played a role in bringing CD36 and Fyn together and whether actin was involved. To achieve this, we measured percent Fyn enrichment in CD36 spots following pharmacological actin perturbation or lipid nanodomains perturbation. Two periods of 15 min incubation with 200 nM Latrunculin B (Lat B, inhibits actin polymerization) or 2 mM of methyl- β -cyclodextrin (M β CD, removes cholesterol from the membrane) were used to disrupt F-actin or lipid nanodomains respectively before fixation of HMEC-mApple-CD36 transfected with Fyn-mEmerald. The concentration of Lat B and M β CD used (200nM and 2mM respectively) was relatively low compared to concentrations reported in other studies (Peng, Wilson & Weiner 2011, Zidovetzki, Levitan 2007) and this helped in maintaining cell morphology. Importantly, Lat B disrupted actin filaments without perturbing cholesterol levels and similarly, M β CD removed cholesterol without perturbing actin filaments (Figure 4-4A, B, C).

Chapter 4- Actin and lipid nanodomains control TSP-1-CD36-Fyn pathway

To our surprise, even though TSP-1 stimulation did increase Fyn enrichment in CD36 spots (observed earlier in Figure 4-1C), neither Lat B nor M β CD treatment altered Fyn enrichment in CD36 spots either before or after TSP-1 stimulation, with the Fyn enrichments relatively equivalent to unperturbed conditions (Figure 4-4D). Put together, these data suggest that while the membrane-targeting domain of Fyn is sufficient for its colocalization within unligated CD36 clusters, this process does not seem to depend on actin or lipid nanodomains.

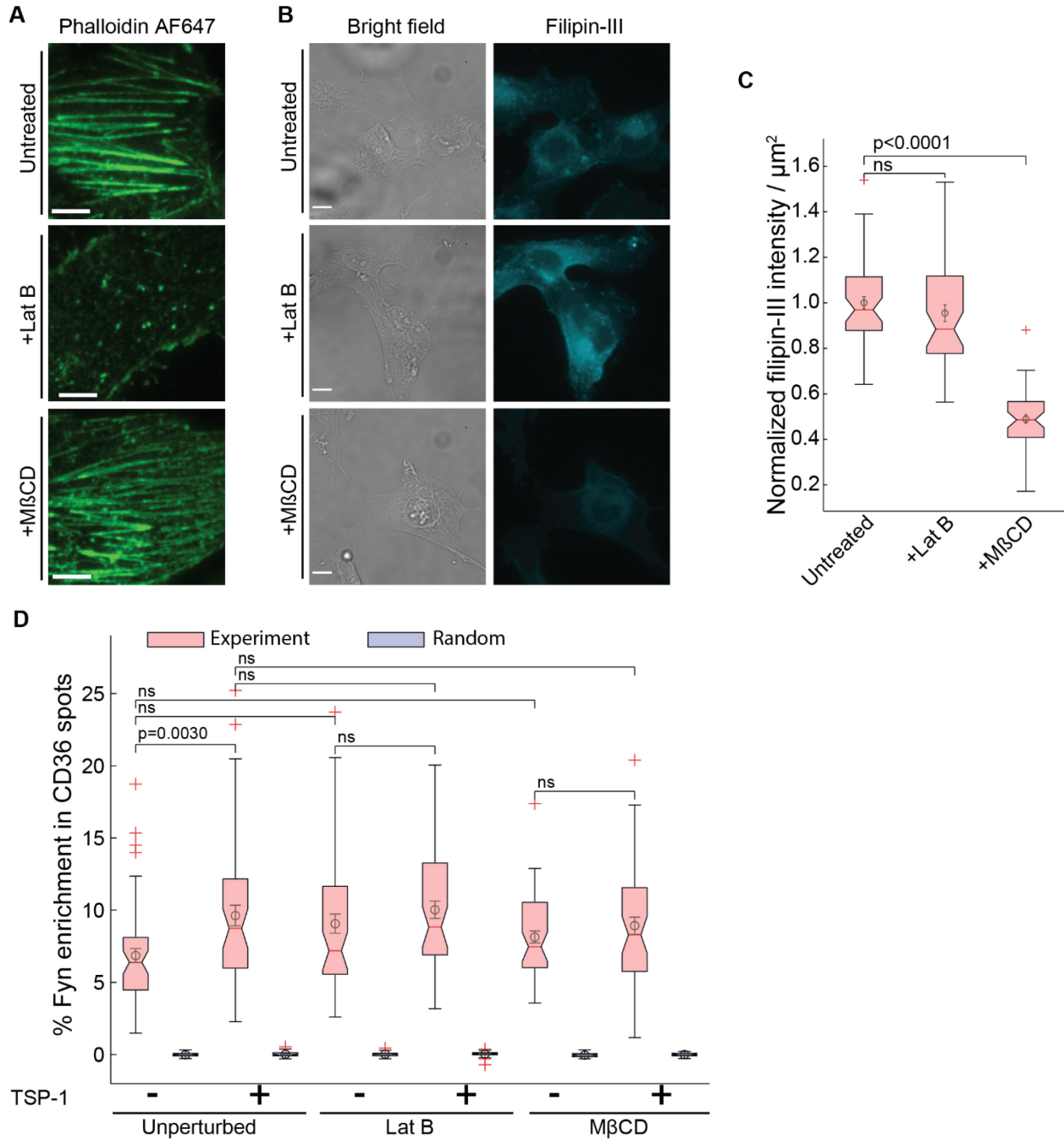


Figure 4-4: CD36-Fyn association is independent of actin and lipid nanodomains

(A) Actin staining using Phalloidin AlexaFluor 647 in untreated or Lat B or MβCD pretreated HMEC-mApple-CD36 cells. Only Lat B disrupts the actin filaments. (B) Cholesterol staining with Filipin-III in untreated or Lat B or MβCD pretreated

Chapter 4- Actin and lipid nanodomains control TSP-1-CD36-Fyn pathway

HMEC-mApple-CD36 cells. Corresponding bright field images are shown on the left. (C) Quantification of the amount of Filipin binding to HMEC-mApple-CD36 cells, indicative of relative cholesterol levels, in untreated or Lat B or M β CD treated conditions (from (B)). All data from 3 independent experiments, each with at least 10 fields of view, all imaged with identical settings. Boxplots and statistical analysis as described in 2.13 Graphing and statistical analysis. (D) Average percent WT Fyn-mEmerald enrichment within mApple-CD36 spots (light red boxplots) together with the randomized control (light blue boxplots) in cells stimulated or not for 10 min with TSP-1 and either unperturbed or pretreated with Lat B or M β CD. All data from 3 independent experiments (sample images in Figure 4-8A), each with at least 10 fields of view, all imaged with identical settings. Boxplots and statistical analysis as described in 2.13 Graphing and statistical analysis.

Scale bars (applicable to all images), 5 μ m.

While the association of CD36-Fyn seemed independent of actin and lipid nanodomains, we looked at whether CD36-Fyn partitioned into rafts, and whether actin had a role in this. Lipid nanodomains marker, Cholera toxin subunit B (CTxB), which binds to the sphingolipid, monosialotetrahexosylganglioside (GM1) (Merritt et al. 1994), exhibited similar actin like pattern like CD36 and Fyn (Figure 4-5A). Interestingly, CD36 partitioned into lipid nanodomains more in high actin areas than low actin areas (Figure 4-5B, C). As a control, we tested a non-raft resident, transferrin receptor (Harder et al. 1998), which associated with CD36 to similar extent in both high and low actin areas (Figure 4-5B, C). From these observations, CD36 and Fyn partitioned into lipid nanodomains and this association was on actin. This suggested a link between actin and lipid nanodomains, a phenomenon that has been proposed recently (Dinic, Ashrafzadeh & Parmryd 2013, Kraft 2013, Raghupathy et al. 2015).

Chapter 4- Actin and lipid nanodomains control TSP-1-CD36-Fyn pathway

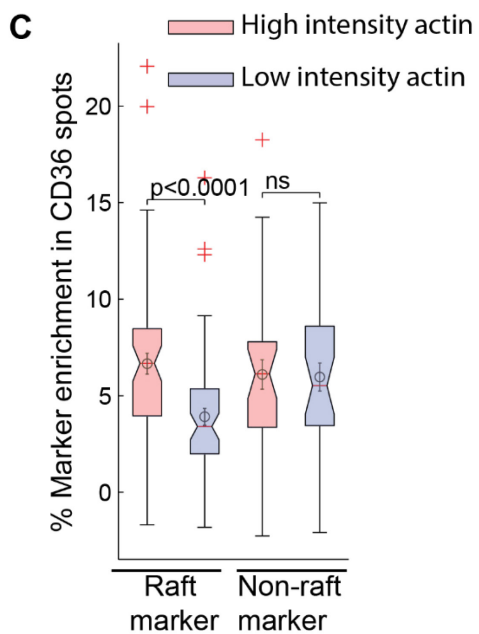
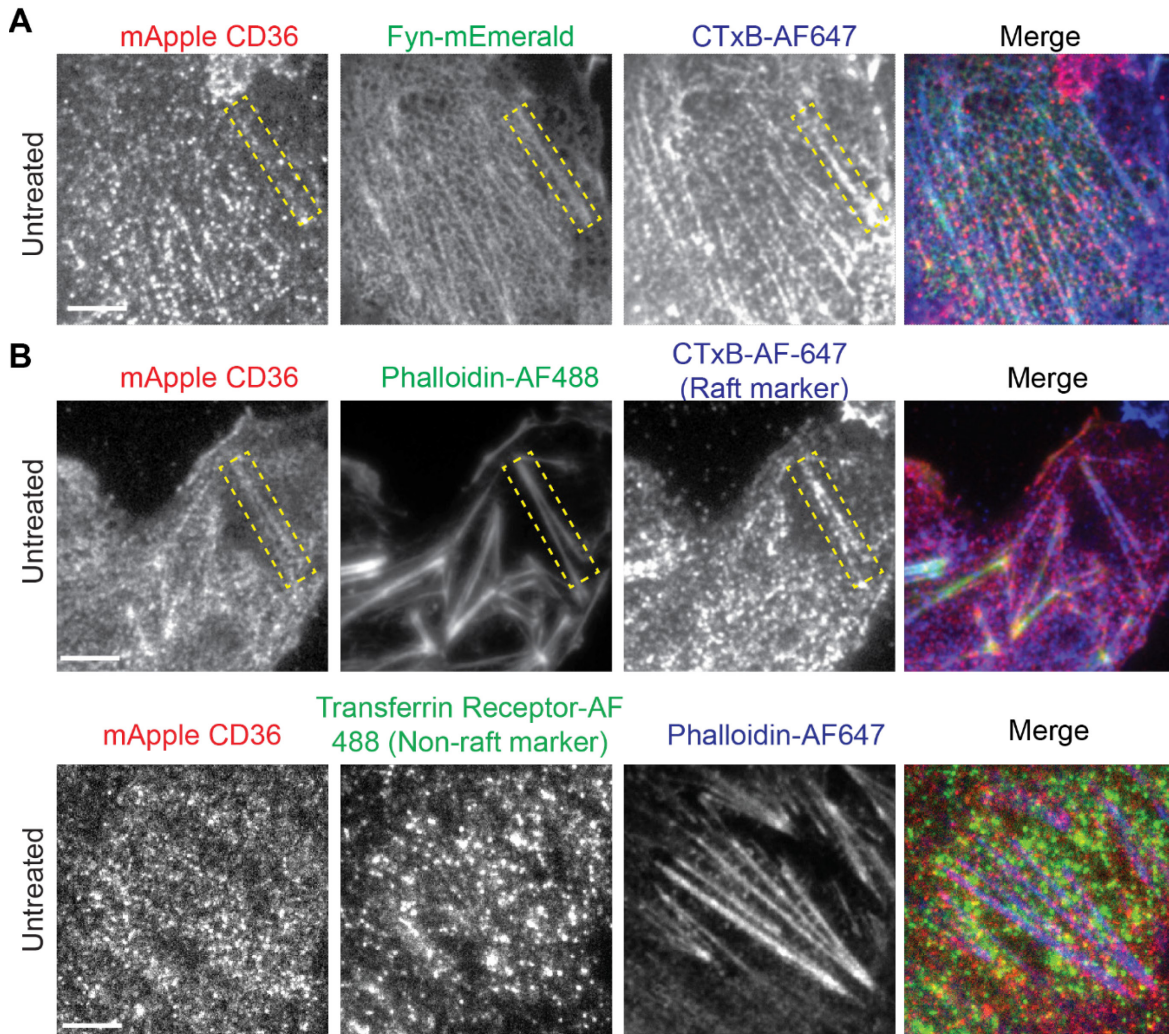


Figure 4-5: CD36 partitions in lipid nanodomains along the actin cytoskeleton

(A) TIRFM imaging of mApple-CD36, Fyn-mEmerald and raft resident GM1 (CTxB AlexaFluor 647) on fixed cells. Yellow ROI highlights actin like pattern observed. (B) Upper row, TIRFM imaging of mApple-CD36, actin and the raft resident GM1 (CTxB AlexaFluor 647 binds GM1). Lower row, TIRFM imaging of mApple-CD36, actin and non-raft resident, transferrin receptor. (C) Average percent CTxB AlexaFluor 647 enrichment (raft marker) within mApple-CD36 spots and average percent transferrin receptor enrichment (non-raft marker) within mApple-CD36 spots in high or low actin intensity regions. All data from 3 independent experiments, each with at least 10 fields of view, all imaged with identical settings. Boxplots and statistical analysis as described in 2.13 Graphing and statistical analysis. Scale bars (applicable to all images), 5 μm

Indeed, another raft marker, glycosylphosphatidylinositol anchor tagged GFP (GPI-GFP), which resides on the outer leaflet of the plasma membrane, showed a similar actin like pattern (Figure 4-6), reaffirming a connection between lipid raft domains and actin. In light of these observation, we investigated if CD36 partitioning into lipid nanodomains was actin driven.

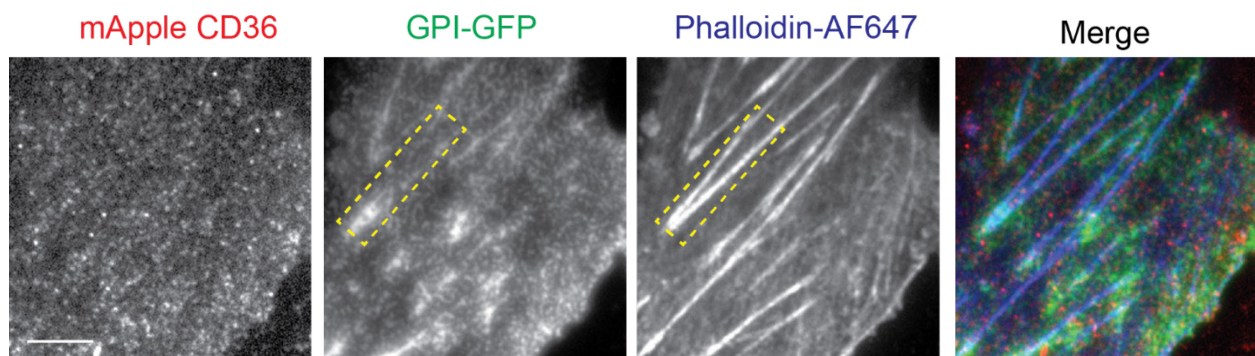


Figure 4-6: GPI anchor, a raft marker, partitions along actin

TIRFM imaging of mApple-CD36, transfected GPI-GFP and actin (phalloidin-

AlexaFluor 647) on fixed cells. Yellow ROI highlights actin like pattern observed in GPI-GFP. Images representative of 3 independent experiments. Scale bars (applicable to all images), 5 μm .

4.2.4 CD36 partitioning into rafts is actin dependent

In the classic biochemical method of identifying lipid rafts, proteins in the detergent resistant membranes (DRM) fractions are generally considered to be lipid rafts residents. CD36 has been shown to be enriched in 4°C Triton X-100 (TX-100) insoluble membranes (Gousset et al. 2002) as well as Fyn (van't Hof, Resh 1997). Since raft proteins don't dissolve in non-ionic detergents like Triton X-100 at 4°C (Brown 2006), we checked CD36 solubility in 1% Triton on ice, with or without actin or lipid-raft disruption. While some of the non-raft CD36 dissolved in 1% Triton, almost all CD36 was dissolved upon disruption of actin with Lat B or disruption of lipid rafts by M β CD (Figure 4-7). Specific CD36 solubilization in 1% Triton after actin perturbation, while lipid rafts membrane components, sphingolipids and cholesterol, remained insoluble, implied that actin was possibly controlling CD36 partitioning into lipid rafts. This is in line with the recent report that actin filaments causes formation of ordered lipid domains (Dinic, Ashrafzadeh & Parmryd 2013).

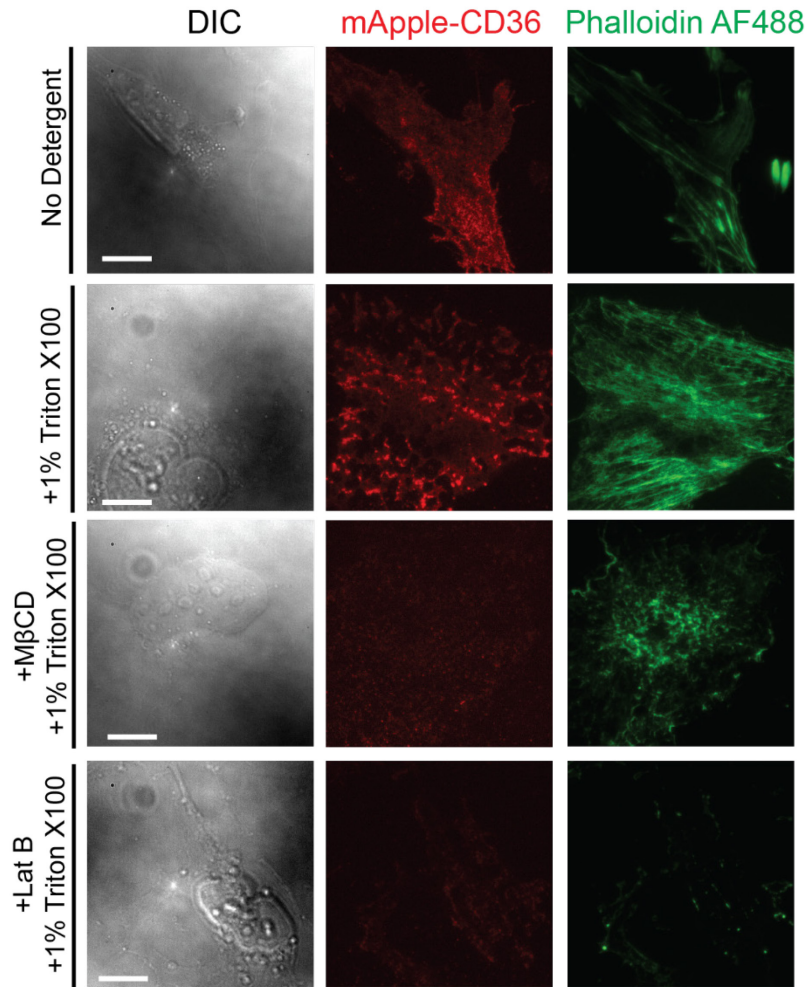


Figure 4-7: CD36 partitioning into rafts is actin dependent

Fixed cells TIRFM imaging of mApple-CD36 and actin (Phalloidin AlexaFluor 488) with or without Lat B or MβCD pre-treatment, with or without 1% Triton X100 extraction. DIC (Differential interference contrast) channel was used to highlight the cells imaged. Images representative of 3 independent experiments. Scale bars (applicable to all images), 5 μm.

4.2.5 Actin cytoskeleton and lipid nanodomains control CD36-Fyn spatial organization

While the link between actin and lipid nanodomains may be unclear and needs further investigation to outline their interdependency, we focused on ways in which both affected TSP-1-CD36-Fyn pathway. Actin or lipid raft perturbation with Lat B or M β CD respectively abrogated the actin like spatial organization of CD36-Fyn association observed earlier (Figure 4-8A). This actin like spatial pattern observed earlier with raft marker like GPI-GFP and GM1 (see Figure 4-6 and Figure 4-5A respectively), was abolished under these perturbations (Figure 4-8B). Besides spatial organization disruption of these proteins, we investigated what other effects these perturbations had on the pathway.

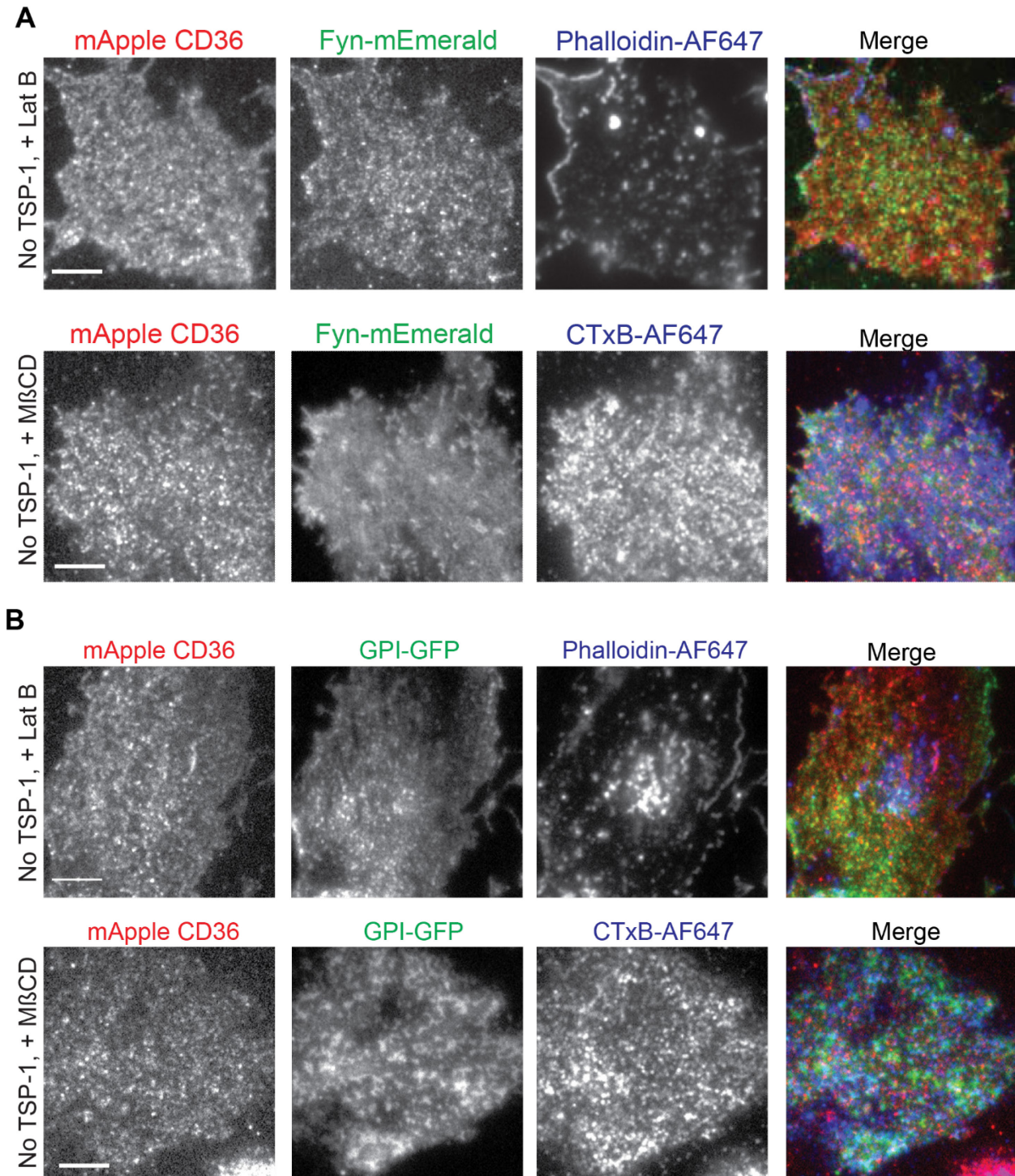


Figure 4-8: Actin cytoskeleton and lipid nanodomains control CD36-Fyn spatial organization

(A) Fixed cells TIRFM imaging of mApple-CD36, Fyn-mEmerald and phalloidin-

AlexaFluor 647 (upper panel, with Lat B treatment) or CTxB AlexaFluor 647 (lower panel, with M β CD treatment) in HMEC-mApple-CD36 cells. **(B)** Fixed cells TIRFM imaging of mApple-CD36, GPI-GFP and phalloidin AlexaFluor 647 (upper panel, with Lat B treatment) or CTxB AlexaFluor 647 (lower panel, with M β CD treatment) in HMEC-mApple-CD36 cells.

Images representative of 3 independent experiments. Scale bars (applicable to all images), 5 μ m.

4.2.6 TSP-1-CD36-Fyn signaling depends on the actin cytoskeleton and lipid nanodomains

While the role of lipid nanodomains and the actin cytoskeleton in bringing CD36 and Fyn together might be unclear, besides spatially organizing them on the membrane, further analysis of CD36-Fyn signaling indicated that lipid rafts and the actin cytoskeleton were nevertheless required for Fyn activation. First, we examined the localization of Fyn activation relative to CD36 and the actin cytoskeleton. Following 10 min incubation with TSP-1, HMEC-mApple-CD36 cells were fixed, permeabilized and stained with phalloidin AlexaFluor 647 and rabbit anti P-Y420 coupled to AlexaFluor 488 (Figure 4-9A). Subjecting these images to our aforementioned 3-way colocalization analysis revealed that P-Y420 was enriched in CD36 spots, and importantly its increase in the presence of TSP-1, was primarily in regions rich in F-actin (Figure 4-9B). Similar results to TSP-1 stimulation were observed under decavalent SM ϕ stimulation, while divalent FA6-152 failed to increase P-Y420 enrichment (Figure 4-9B). These data suggest that TSP-1-CD36-Fyn activation occurs primarily along the actin cytoskeleton in a multivalency dependent manner.

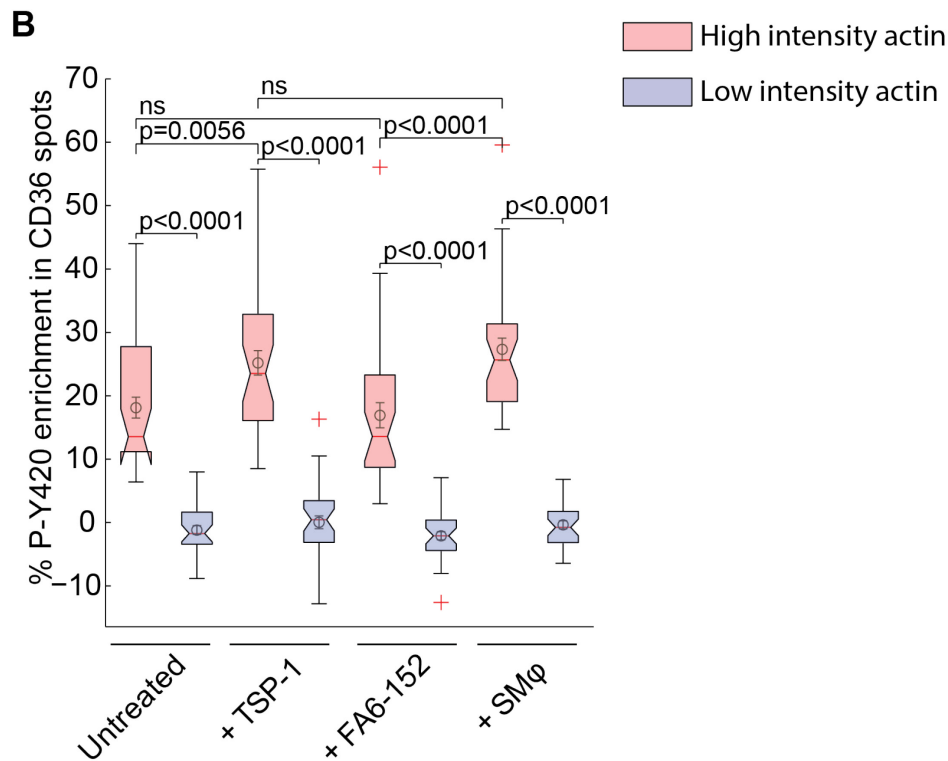
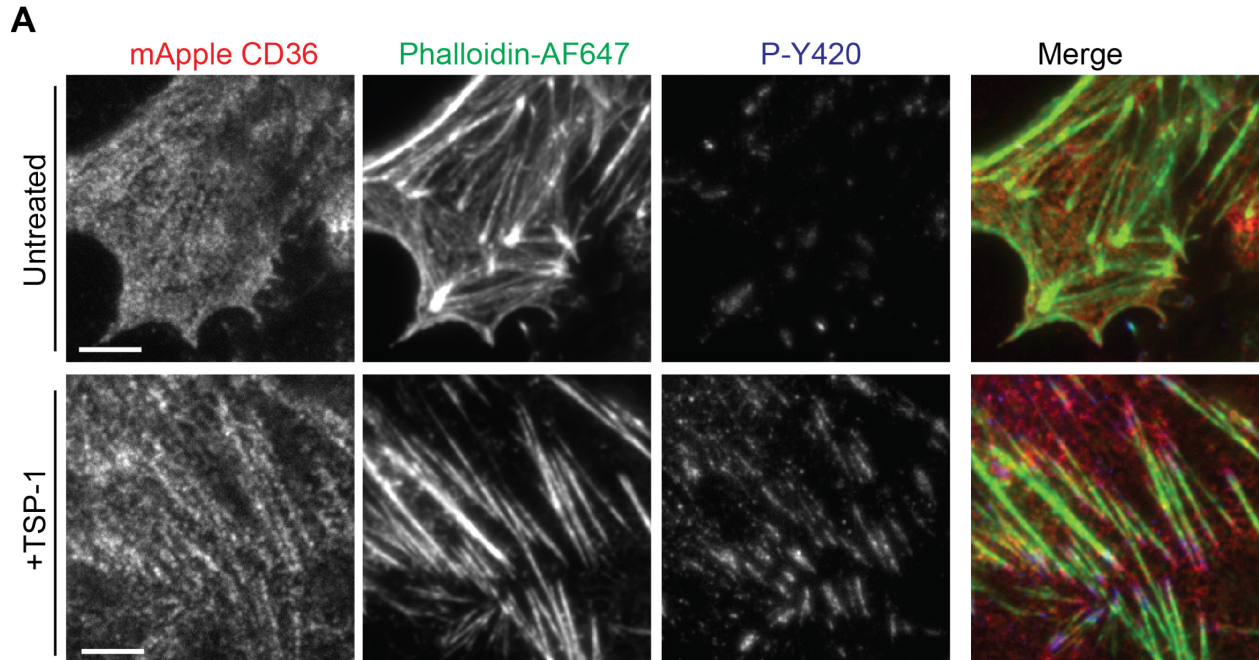


Figure 4-9: CD36-Fyn signaling is along the actin cytoskeleton

(A) TIRFM imaging of HMEC-mApple-CD36 cells stimulated or not with 10 nM

Chapter 4- Actin and lipid nanodomains control TSP-1-CD36-Fyn pathway

TSP-1 for 10 min and labeled for F-actin (phalloidin AlexaFluor 647) and P-Y420 using anti-PY420 coupled to AlexaFluor 488. **(B)** Average percent P-Y420 enrichment within mApple-CD36 spots in high or low actin intensity regions (light red versus light blue boxplots respectively) in untreated, TSP-1, FA6-152 or SM ϕ treated conditions. Boxplots and statistical analysis as described in 2.13 Graphing and statistical analysis.

Data from 3 independent experiments each containing ~15 images acquired with identical settings. Scale bars (applicable to all images), 5 μ m.

Second, we investigated the capacity of TSP-1 to induce signal transduction downstream of CD36 under actin or lipid raft perturbation. In unperturbed HMEC-CD36-myc cells, TSP-1 stimulated the phosphorylation of Fyn, p38MAPK (previously described in (Jimenez et al., 2000) and p130Cas (Figure 4-10A, B). Activation of p130Cas downstream of CD36 in this pathway has not been reported previously, although CD36 has been implicated in activating p130Cas in other pathways (Stuart et al., 2007; Davis et al., 2011). Importantly, actin or lipid raft disruption using Lat B or M β CD, respectively, blocked these phosphorylation events (Figure 4-10A, B), which was confirmed in primary HMVECs as well (Figure 4-10C, D). All in all, these data suggest that the actin cytoskeleton and lipid nanodomains are required for TSP-1-CD36-Fyn signaling.

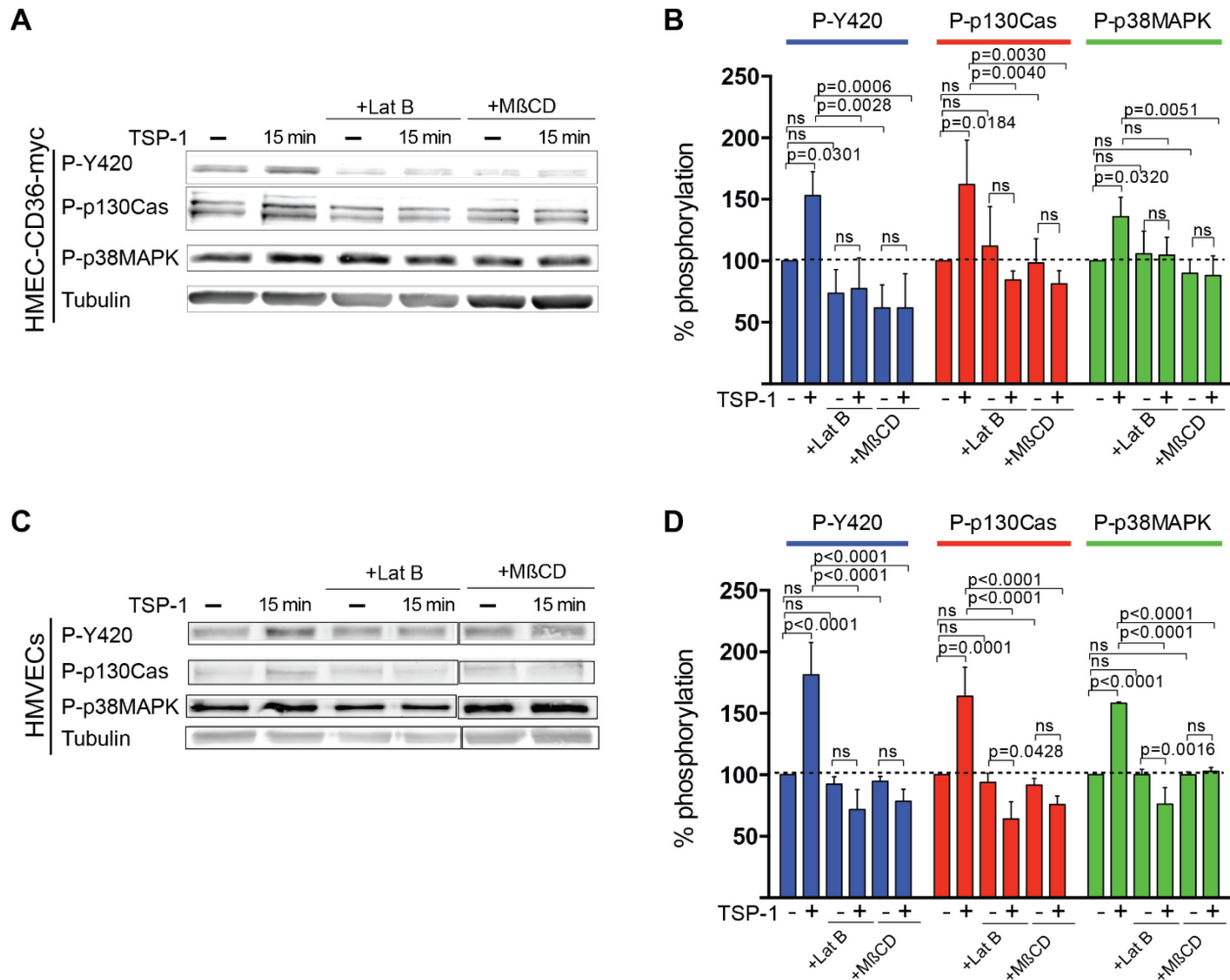


Figure 4-10: CD36-Fyn signaling depends on the actin cytoskeleton and membrane integrity.

(A) HMEC-CD36-myc cells were incubated with or without Lat B or MβCD for 15 minutes before stimulation with TSP-1 for 15 minutes. P-Y420, phospho-p38MAPK and phospho-p130Cas levels were determined by western blotting and tubulin was used as loading control. (B) Quantification of the percent phosphorylation (P-Y420, P-p130Cas and P-p38MAPK) in (A) normalized to level in untreated control. (C) HMVECs cells were incubated with or without Lat B or MβCD for 15 minutes before stimulation with TSP-1 for 15 minutes. P-Y420, phospho-p38MAPK and phospho-p130Cas levels were determined by western blotting and tubulin was used as loading control. (D) Quantification of the percent phosphorylation (P-Y420, P-p130Cas and P-p38MAPK) in (C) normalized to level in untreated control.

All data from 3 independent experiments. Statistical analysis as described in 2.13 Graphing and statistical analysis.

4.2.7 Actin cytoskeleton and lipid nanodomains controls TSP-1 binding to CD36

If disruption of the actin cytoskeleton or lipid nanodomains does not alter CD36-Fyn colocalization, then what leads to the drastic inhibition of TSP-1-CD36-Fyn signaling? We reasoned this inhibition could be due to reduced ligand binding capacity and/or due to a defect in CD36 reorganization on the cell surface upon TSP-1 binding. To quantify the binding of TSP-1 to HMEC-mApple-CD36 cells, cells pre-treated or not with Lat B or M β CD were fixed following 10 min incubation with TSP-1. The bound ligand was detected by immunostaining using goat anti-TSP-1 followed by Dylight649-donkey anti-goat antibodies and TIRFM imaging (Figure 4-11A). Cells expressing CD36 were masked and the amount of bound TSP-1 was defined as the mean intensity in the cell area. The measurements were normalized to the amount of binding in the unperturbed condition. This analysis indicated that treatment with Lat B or M β CD resulted in a significant decrease in the amount of TSP-1 binding (Figure 4-11A, B). While there was a stronger correlation between TSP-1 bound and CD36 density before perturbation (PCC~0.5), the reduced binding of TSP-1 under Lat B or M β CD was not due to decreased CD36 density as their correlation was almost equal to zero (PCC~0.1, PCC~0.1 respectively, Figure 4-11C).

However, while significant, this decrease in binding capacity could not account for the complete inhibition of signaling induced by these perturbations. Therefore, we next examined the

Chapter 4- Actin and lipid nanodomains control TSP-1-CD36-Fyn pathway

effect of drug perturbation on the capacity of TSP-1 to enhance CD36 clustering, using PALM imaging and spatial pattern analysis.

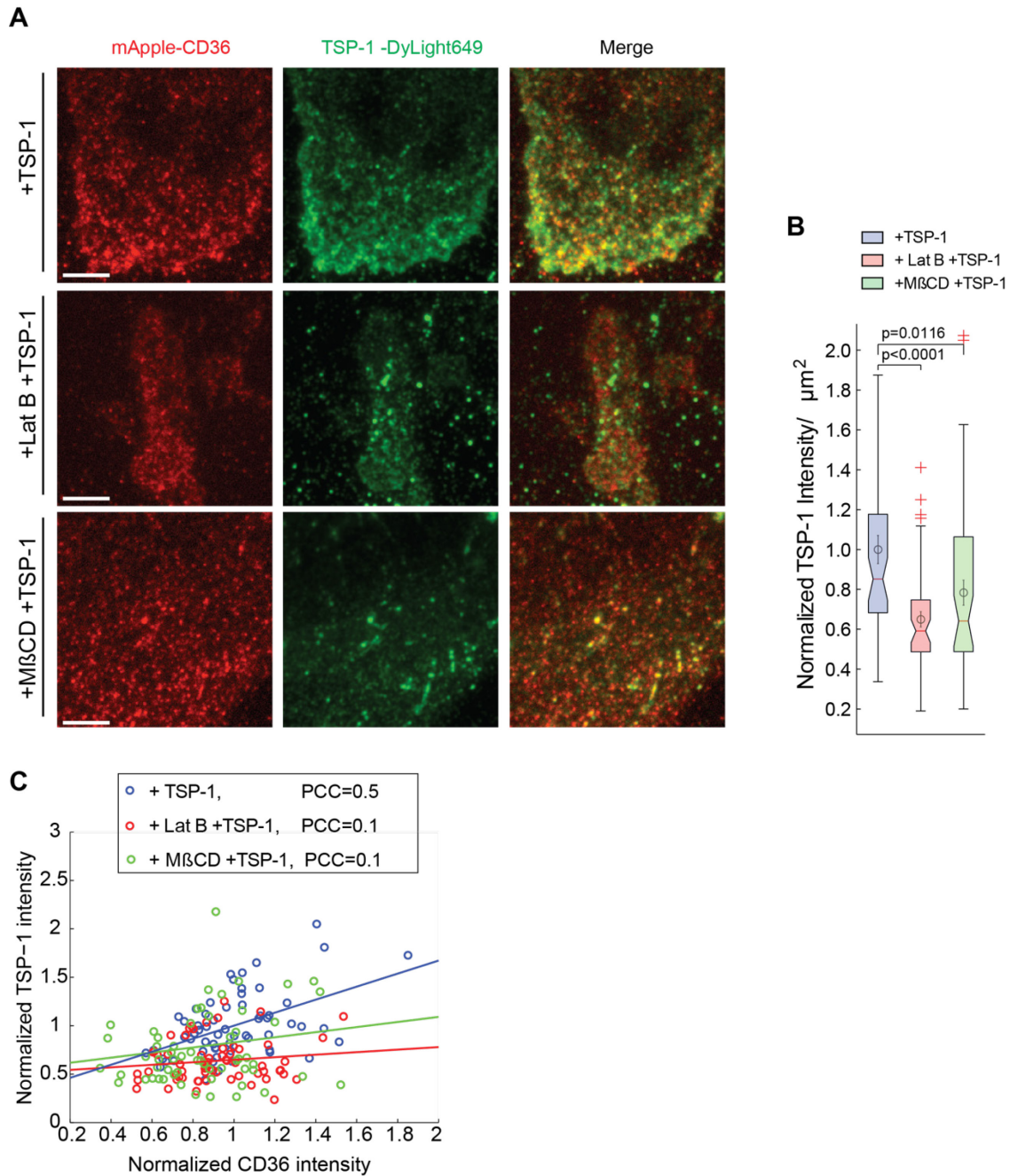


Figure 4-11: Actin cytoskeleton and lipid nanodomains control TSP-1 binding to CD36

(A) HMEC-mApple-CD36 cells were incubated with or without Lat B or M β CD for 15 minutes and then stimulated with TSP-1 for 10 minutes. Bound TSP-1 was immunostained with goat anti-human TSP-1 followed by donkey anti-goat Dylight-649. (B) Quantification of the amount of TSP-1 binding to HMEC-mApple-CD36 cells in unperturbed, or Lat B or M β CD treated conditions (from (A)). Boxplots and statistical analysis as described in 2.13 Graphing and statistical analysis. (C) Scatterplot of normalized bound TSP-1 intensity versus normalized CD36 intensity from images in (A) with computed Pearson's correlation coefficient (PCC). Least square fit lines of the corresponding (similar color) data points for the scatters of the different conditions are superimposed.

Data from 3 similar independent experiments. Scale bars (applicable to all images), 5 μ m.

4.2.8 CD36 cluster enhancement by TSP-1 depends on the actin cytoskeleton and lipid nanodomains

In addition to reducing the amount of CD36 molecules imaged at the plasma membrane of HMEC-PAmCherry-CD36 cells (Figure 4-12A; ~30% reduction), actin or lipid raft perturbations indeed altered the clustering of CD36 both at steady state and upon ligation. At steady state, CD36 cluster sizes in radius was relatively the same in unperturbed and perturbed conditions (Figure 4-12B). Upon TSP-1 stimulation, TSP-1's ability to induce larger (in radius) CD36 clusters was impaired in Lat B and M β CD conditions (Figure 4-12B). The number of CD36 molecules within the clusters was reduced under these perturbations in unstimulated and TSP-1 stimulated state (Figure 4-12C). Indeed, the density of CD36, per μ m², under actin and lipid nanodomains impairment was significantly lower at steady state and TSP-1 failed to compact these clusters (Figure 4-12D, E). DTSSP's ability to crosslink CD36 clusters, both at

Chapter 4- Actin and lipid nanodomains control TSP-1-CD36-Fyn pathway

steady state and TSP-1 stimulation condition, was reduced (red ROI Figure 4-12F), possibly due to the decreased compaction of these clusters under actin or lipid nanodomains disruption. These analyses suggest that Fyn activation and signaling by TSP-1 requires CD36 clusters that are both compact enough and contain a sufficient number of molecules, a rearrangement that depends on both the actin cytoskeleton and membrane cholesterol.

Chapter 4- Actin and lipid nanodomains control TSP-1-CD36-Fyn pathway

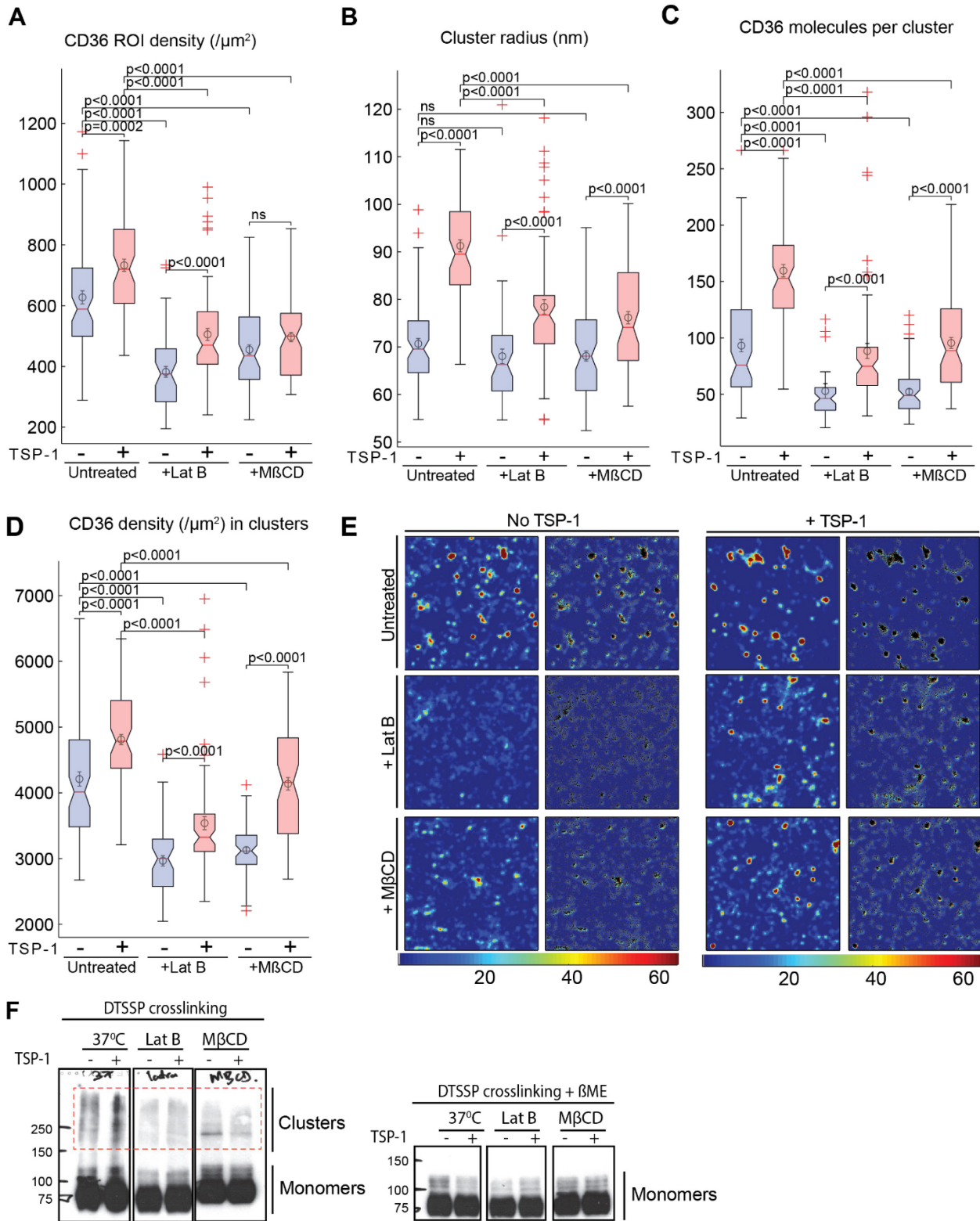


Figure 4-12: CD36 cluster enhancement by TSP-1 depends on the actin

cytoskeleton and lipid nanodomains

(A) Density of CD36 molecules localized by PALM imaging from HMEC-PAmCherry-CD36 cells unperturbed or treated with Lat B or M β CD and stimulated or not for 10 min with TSP-1. Data from 3 similar independent experiments, 51 to 81 data points per condition. Boxplots and statistical analysis as described in 2.13 Graphing and statistical analysis. (B) Cluster radius size (nm) of data in (A). (C) Average number of CD36 molecules per cluster from data described in (A). (D) CD36 density (per μm^2) within CD36 clusters from data described in (A). (E) Representative ROI density heat maps of CD36 molecules in conditions described in (A). Each heat map's corresponding CD36 molecules superimposed on it are shown on the right side of the heatmap. (F) HMEC-CD36-myc cells were incubated with TSP-1 for 10 minutes and crosslinked immediately with membrane impermeant DTSSP on ice. CD36 state was probed using anti-myc on western blots (blots on the left, red ROI encloses clusters regions). As a control, β ME was used to cleave off the crosslinker which reduced all clusters to monomers (blots on the right).

4.2.9 Actin cytoskeleton and lipid nanodomains control CD36 mobility necessary for TSP-1-CD36-Fyn pathway

The cortical cytoskeleton has been proposed to aid in organizing plasma membrane residents and controlling protein and lipid diffusion on this structure (Kusumi, Sako 1996, Feder et al. 1996). One of the models proposed, 'the picket and fence model', postulates a cytoskeleton mesh that compartmentalizes plasma membrane proteins, resulting in a spatial confinement that regulates signaling events (Morone et al. 2006). Indeed, this model proposes immobilization of the receptors in the confinements to enhance clustering and signaling, say, upon ligand binding. Our observation of CD36-Fyn partitioning into lipid nanodomains along actin filaments (see section 4.2.3 CD36-Fyn associate in lipid nanodomains along the actin cytoskeleton) is in

contrast with ‘picket and fence model’ of cytoskeletal mesh confinement of this receptor. It was recently shown that cortical cytoskeleton controls CD36 diffusion along the cytoskeleton troughs and increases the probability of CD36 interactions to form clusters in macrophages (Jaqaman et al. 2008, Jaqaman et al. 2011). We sort to investigate if CD36 diffuses along actin, whether observed CD36 clusters were along actin (as we earlier observed in Figure 4-3B) and the role of actin and lipid nanodomains in controlling CD36 mobile/immobile fractions and mobile fraction diffusivity.

Tracks from spt-PALM TIRFM live cell imaging of HMEC-PAmCherry-CD36 cells transfected with lifeAct-GFP (lifeAct binds actin (Riedl et al. 2008)) showed a confinement along the actin filaments (Figure 4-13A). Indeed, dual tracking of labelled TSP-1 and CD36 showed colocalizing linear tracks, deemed to be along actin (Figure 4-13B). PALM imaging of PAmCherry-CD36 showed CD36 clusters enrichment along actin filaments (Figure 4-13C), in agreement with our earlier diffraction limited imaging data (see Figure 4-3).

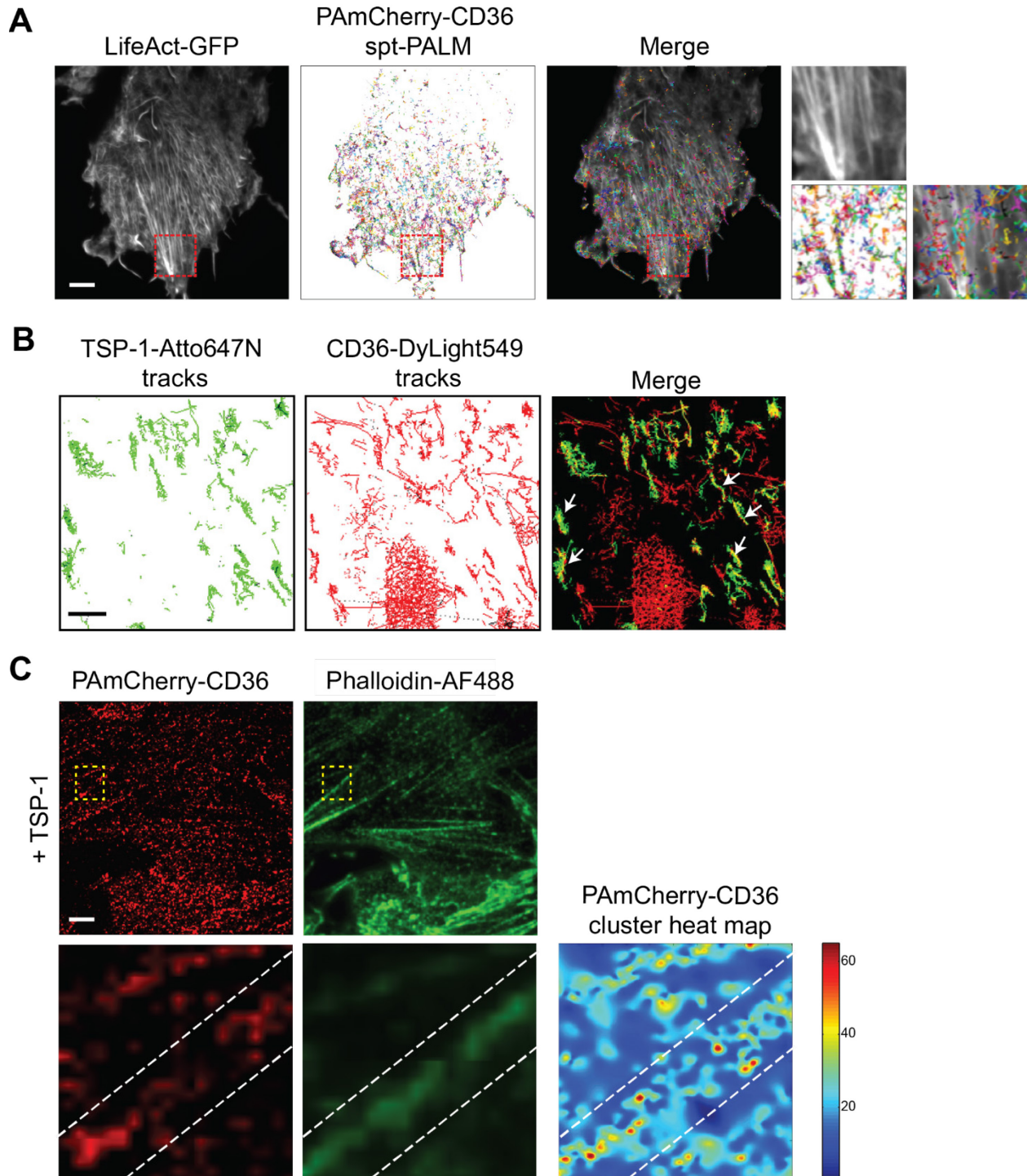


Figure 4-13: CD36 diffuses and forms clusters along actin

(A) Live spt-PALM imaging of HMEC-PAmCherry-CD36 cells using TIRFM, on cells transiently transfected with lifeact-GFP. Images on the right represent magnified areas underlined with dashed red line boxes. (B) Live single particle

Chapter 4- Actin and lipid nanodomains control TSP-1-CD36-Fyn pathway

tracking of Atto-647N labelled TSP-1 (green tracks) and dylight549 labelled anti CD36 Fab fragments (red tracks) on HMEC-CD36-myc cells using TIRFM. White arrows highlight some of the colocalized tracks (C) PALM imaging of HMEC-PAmCherry-CD36 cells, labelled with phalloidin AlexaFluor 488 post fixation. Lower panel represent magnified areas underlined with dashed yellow line boxes, and the corresponding cluster heat map obtained through interpolation of the PALM data. White dotted lines highlight the actin regions along which CD36 clusters are localized.

Data representative of 3 similar independent experiments. Scale bars (applicable to all images), 5 μm .

To dissect what role actin and lipid nanodomains played in controlling this CD36 diffusion, we turned to TIRFM FRAP experiments on HMEC-mApple-CD36 cells. An area of $\sim 8.3 \mu\text{m}^2$ in the cell membrane was photobleached using 1 second exposure to a 405 nm laser and mApple-CD36 signal was imaged for about 50 seconds (Figure 4-14A). This was done with or without TSP-1, in unperturbed or actin or lipid nanodomains perturbed conditions. The FRAP data was normalized between 0 and 1 and plotted against time (Figure 4-14B). Actin and lipid nanodomains perturbations resulted in an increase of CD36 immobile fraction such that it was not appropriately modeled by our FRAP exponential fit (Figure 4-14C). For this reason, movies with an R-squared (measure of goodness of fit) below 0.4 ($\sim 20\%$ of movies in these perturbed conditions) were eliminated from computation of CD36 immobile fractions and diffusivity estimations (Figure 4-14D). The immobile CD36 fraction in unperturbed conditions was $\sim 30\%$ (Figure 4-14E). Surprisingly, both Lat B and MBCD treatments doubled the immobile fraction ($\sim 60\%$ in all perturbed conditions, with or without TSP-1 Figure 4-14E). These perturbations also abrogated TSP-1's ability to increase CD36 diffusivity, a property that TSP-1 possibly exploits in enhancing CD36 clusters to enable signaling (Figure 4-14F).

Chapter 4- Actin and lipid nanodomains control TSP-1-CD36-Fyn pathway

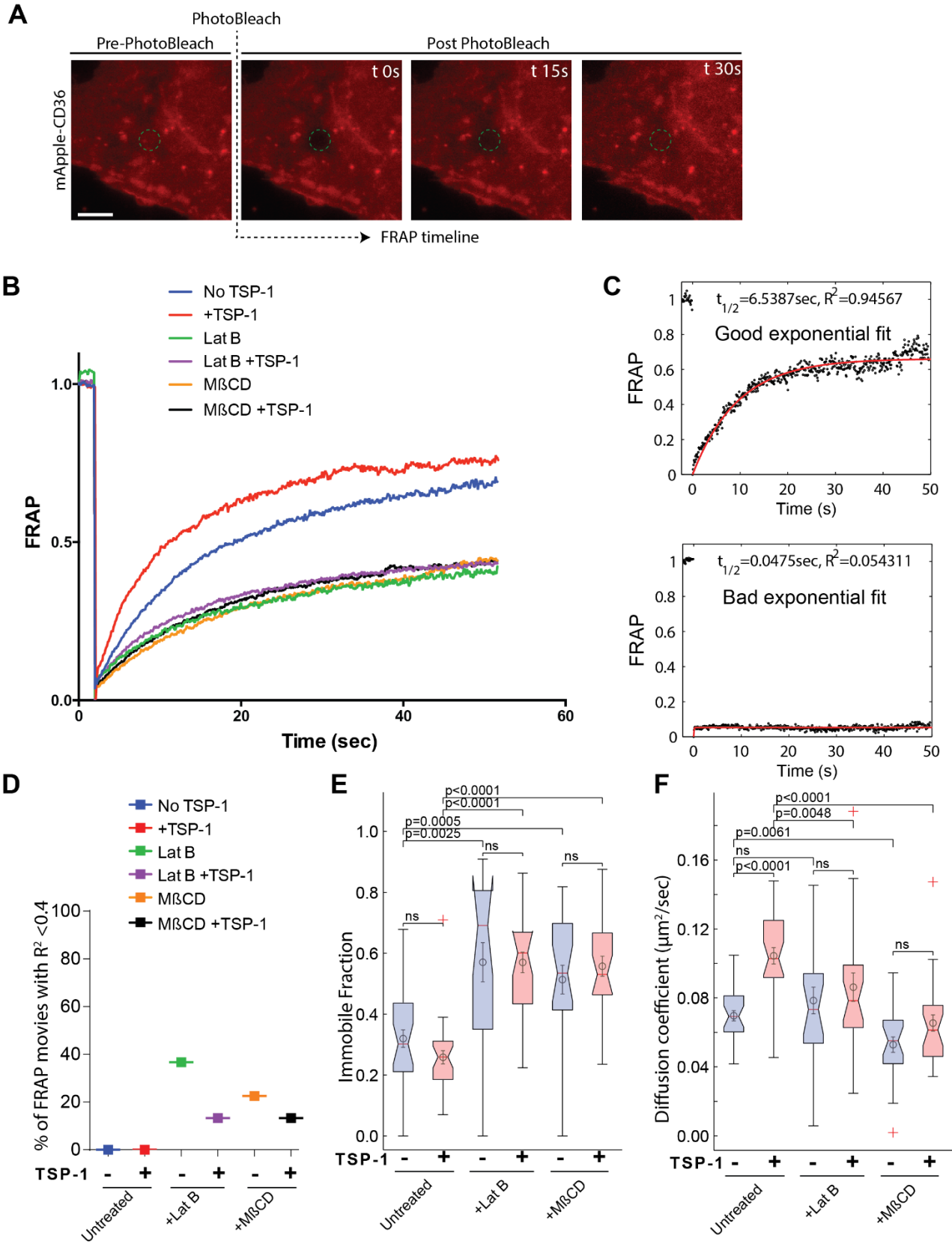


Figure 4-14: Actin cytoskeleton and lipid nanodomains control CD36 mobility

(A) Fluorescence recovery after photobleaching (FRAP) imaging by TIRFM on HMEC-mApple-CD36 showing pre and post photo bleaching of the FRAP area (green ROI). Scale bar, 5 μ m. (B) FRAP data represented as the mean normalized fluorescence intensity within the bleached area in unperturbed and Lat B or M β CD perturbed conditions, with or without TSP-1 over time (seconds). (C) Sample representation of FRAP data fit curves (red line), with the computed half-life, $t_{1/2}$, and goodness of fit, R^2 . Lack of recovery results in bad exponential fit. (D) Percentage of movies eliminated from further analysis due to bad exponential fit resulting from immobility of mApple-CD36 molecules (R^2 less than 0.4). (E) Immobile fractions determined from fitting of the FRAP data (see 2.8.2 FRAP image analysis). Boxplots and statistical analysis as described in 2.13 Graphing and statistical analysis. (F) Diffusion coefficients of the mobile fraction determined from the half-recovery time of the fitted FRAP data using equation 2 shown in section 2.8.2 FRAP image analysis. Box plots as in (E).

Data from 3 independent experiments, with 9-11 movies per condition and per experiment.

4.3 Discussion

In this chapter, we explored CD36-Fyn association and how actin and lipid nanodomains control TSP-1-CD36-Fyn pathway. We first asked what leads to basal CD36-Fyn co-clustering. Our study provides some mechanistic insight, although this question requires further investigation beyond the scope of our current work. First, we found that a Fyn truncation mutant containing only the membrane-targeting domain of Fyn colocalizes within CD36 clusters to the same extent as full length Fyn (Figure 4-1). This suggests that the fatty acid chains of Fyn and CD36 embedded in the inner leaflet of the membrane might segregate them into common plasma

membrane nanodomains. We were not able to test this model for CD36 as substitution of its intracellular cysteines with alanines, to prevent palmitoylation, drastically reduced its surface expression (Thorne et al. 2010). Cholesterol depletion experiments suggest that this process is however cholesterol-independent (Figure 4-4). Second, we found that Fyn (full length or truncated) colocalizes with CD36 primarily along actin filaments (Figure 4-3). Yet, actin depolymerization did not perturb overall CD36-Fyn colocalization (Figure 4-4). Put together, these observations suggest that Fyn is preferentially enriched in CD36 clusters aligned along actin filaments, although via a mechanism that primarily depends on intermolecular interactions within the plane of the membrane without direct actin involvement. CD36 has been indeed shown to promiscuously interact with many transmembrane molecules, such as integrins and tetraspanins, (Heit et al. 2013, Huang, Febbraio & Silverstein 2011, Thorne et al. 2000), which could contribute to this mechanism.

If CD36 and Fyn are co-clustered in the absence or presence of ligand, what prevents them from signaling at all times? The answer to this question is two-fold. First, our data suggest that prior to ligand binding, Fyn is in fact activated at a basal level, as demonstrated by the decreased level of phosphorylation following cluster disruption when the actin cytoskeleton or membrane cholesterol are perturbed (Figure 4-10). The levels of phospho-p38MAKP on the other hand remained unchanged after these perturbations, suggesting that this “tonic” Fyn activation is not propagated to more downstream effectors. Such basal-level tonic signaling has been observed previously, e.g. for the B cell receptor (Treanor et al. 2010). The mechanisms that limit signal propagation to downstream effectors remain however to be defined.

Chapter 4- Actin and lipid nanodomains control TSP-1-CD36-Fyn pathway

Second, our analyses also indicate that CD36-Fyn nanocluster remodeling upon TSP-1 binding, such that they grow in size and get more compact, is necessary for full-scale signaling. This is demonstrated by the abrogation of Fyn, p130Cas and p38MAPK activation by TSP-1 upon F-actin or cholesterol perturbation (Figure 4-10), both of which impede proper CD36 cluster remodeling (Figure 4-12). The inability of TSP-1 to increase cluster size after actin or cholesterol depletion suggests that actin and lipid nanodomains membrane aids in the recruitment of new CD36 molecules and/or in stabilizing the CD36 clusters to allow them to grow. In both perturbations, the inability of the CD36 clusters to get compacted by TSP-1 suggests that actin and lipid nanodomains are necessary for cluster compaction. Fluorescence recovery after photobleaching (FRAP) analysis suggests that CD36 molecules exchange dynamically between them and the rest of the membrane (Figure 4-14). The failure of proper cluster rearrangement after perturbing the actin cytoskeleton or lipid nanodomains might be in part due to the reduced receptor mobility under these conditions at steady state and TSP-1 stimulated state (Figure 4-14). It is worth noting that the reduced CD36 mobility under actin perturbation (Figure 4-14) is in contrast with the ‘picket and fence’ model (Morone et al. 2006), which predicts faster diffusion of membrane components upon disruption of actin (the fence). These results suggest that Fyn activation may only occur if the CD36-Fyn clusters cross specific thresholds in both compactness and size. Such a compound threshold may minimize spurious “tonic” signaling in the absence of ligand, as unligated clusters would only rarely cross both thresholds.

As aforementioned, unligated receptor clustering has been invoked in several previous studies as a mechanism to prime the cell to respond when exposed to ligand (Cambi et al. 2004, Cambi et al. 2006, Itano et al. 2012, Veatch et al. 2012, Mattila et al. 2013, Lillemeier et al. 2010). This would increase the efficiency of receptor clustering upon multivalent ligand binding,

Chapter 4- Actin and lipid nanodomains control TSP-1-CD36-Fyn pathway

as the ligand would encounter multiple receptors in a shorter period of time. In support of this notion, our experiments demonstrate that TSP-1 binding is reduced upon actin depolymerization or cholesterol removal from the membrane (Figure 4-11), both of which perturb membrane organization (Figure 4-8) and receptor nanoclustering (Figure 4-12).

The striking colocalization of activated SFK with CD36 along F-actin structures (Figure 4-9) suggests that the actin cytoskeleton not only plays a role in cluster reorganization upon TSP-1 binding, but also in controlling interactions with accessory proteins. As earlier observed in chapter 3, protein tyrosine phosphatase (PTP) CD45 was colocalized along actin like patterns together with CD36 (Figure 3-17). CD45 could serve as one of the accessory proteins as it has been postulated that it could activate Fyn by dephosphorylating the inhibitory tyrosine residue Y531, or that it could alternatively inhibit Fyn activation by dephosphorylating the activation tyrosine Y420 (Rhee, Veillette 2012). The former seems to be the case here as western blot analysis of Fyn activation in the presence of a CD45 inhibitor (PTP-CD45 inhibitor) suggested that CD45-mediated dephosphorylation of Y531 (Figure 3-17). Furthermore, transient expression of various lipid probes in HMEC-mApple-CD36 cells showed a shift from phosphatidylinositol 4,5-bisphosphate (PI(4,5)P₂) to phosphatidylinositol (3,4,5)-trisphosphate (PI(3,4,5)P₃) enrichment in CD36 clusters upon TSP-1 stimulation (Figure 4-15). This could suggest activation of phosphatidylinositide 3-kinases (PI3K) to phosphorylate PI(4,5)P₂ to PI(3,4,5)P₃ (Leervers, Vanhaesebroeck & Waterfield 1999). Though the significance of this in TSP-1-CD36 signaling remains to be determined, it could either be a mechanism to control TSP-1-CD36-Fyn pathway at the plasma membrane or aid in TSP-1-CD36 endocytosis. Actin has been shown to regulate lipid nanodomains formation through PI(4,5)P₂ (Dinic, Ashrafzadeh & Parmryd 2013), while PI3K-C2alpha has been shown to be necessary for dynamin independent endocytosis

pathways (Krag, Malmberg & Salcini 2010). Further investigation is needed to identify other accessory proteins and lipid modifications that control TSP-1-CD36-Fyn pathway that might be recruited or excluded from CD36 clusters during ligand stimulation.

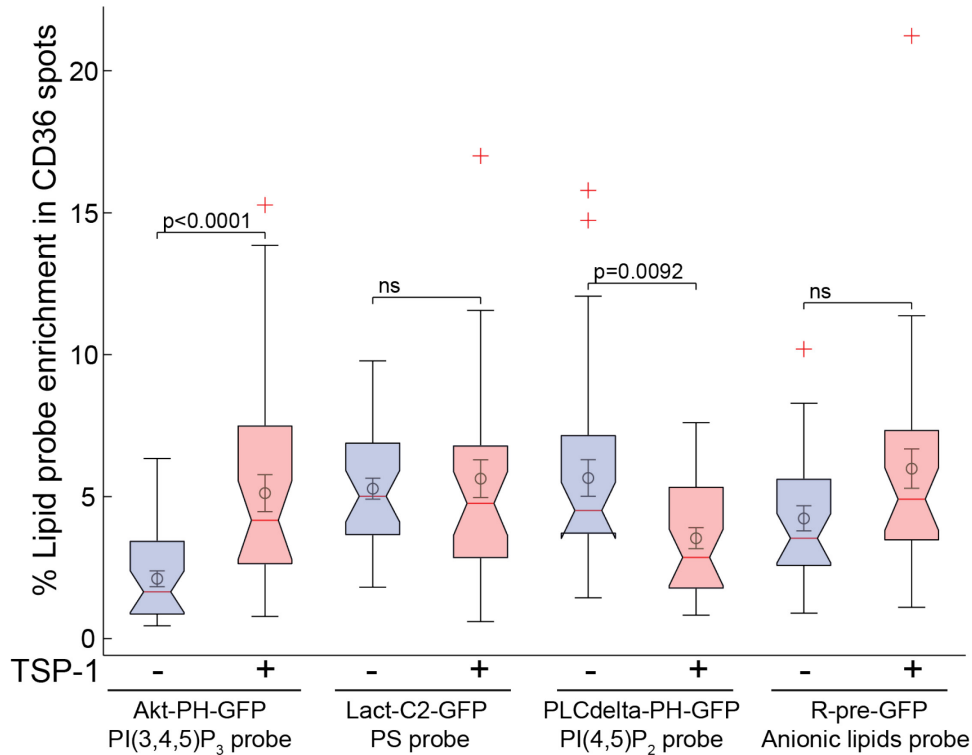


Figure 4-15: PI(4,5)P₂ is reduced while PI(3,4,5)P₃ is increased in CD36 spots

Different lipid probes (described below) were transiently expressed in HMEC-mApple-CD36 cells, fixed and imaged using TIRFM. Their percentage enrichment was determined as earlier described (see Figure 4-4). Akt-PH-GFP; Pleckstrin homology domain of protein kinase B (Akt) tagged to GFP, binds phosphatidylinositol (3,4,5)-trisphosphate (PI(3,4,5)P₃) (Kwon, Hofmann & Montell 2007). Lact-C2-GFP; A probe developed to bind phosphatidylserine (PS) (Yeung et al. 2008). PLCdelta-PH-GFP; Pleckstrin homology domain of phospholipase C delta 1 tagged to GFP, binds phosphatidylinositol 4,5-bisphosphate (PI(4,5)P₂) (Stauffer, Ahn & Meyer 1998). R-pre-GFP; A probe developed to bind anionic lipids (Yeung et

al. 2008).

Boxplots and statistical analysis as described in 2.13 Graphing and statistical analysis. Data from 3 independent experiments, with 10-15 images per condition and per experiment.

All plasma membrane proteins get endocytosed into the cell at some point in their lifetime, either through basal unligated state endocytosis or ligand induced endocytosis (Doherty, McMahon 2009). Indeed we observed CD36 endocytosis in unstimulated and TSP-1 stimulated state (Figure 3-9, Figure 3-13). Having worked on the dynamics and factors controlling TSP-1-CD36-Fyn pathway at the plasma membrane, in the next chapter 5, we investigated the mode of endocytosis through which unligated and TSP-1 ligated CD36 molecules are internalized.

References

- Alland, L., Peseckis, S.M., Atherton, R.E., Berthiaume, L. & Resh, M.D. 1994, "Dual myristylation and palmitoylation of Src family member p59fyn affects subcellular localization.", *Journal of Biological Chemistry*, vol. 269, no. 24, pp. 16701-16705.
- Brown, D.A. 2006, "Lipid rafts, detergent-resistant membranes, and raft targeting signals", *Physiology (Bethesda, Md.)*, vol. 21, pp. 430-439.
- Cambi, A., de Lange, F., van Maarseveen, N.M., Nijhuis, M., Joosten, B., van Dijk, E.M., de Bakker, B.I., Fransen, J.A., Bovee-Geurts, P.H., van Leeuwen, F.N., Van Hulst, N.F. & Figdor, C.G. 2004, "Microdomains of the C-type lectin DC-SIGN are portals for virus entry into dendritic cells", *The Journal of cell biology*, vol. 164, no. 1, pp. 145-155.
- Cambi, A., Joosten, B., Koopman, M., de Lange, F., Beeren, I., Torensma, R., Fransen, J.A., Garcia-Parajo, M., van Leeuwen, F.N. & Figdor, C.G. 2006, "Organization of the integrin LFA-1 in nanoclusters regulates its activity", *Molecular biology of the cell*, vol. 17, no. 10, pp. 4270-4281.
- Davis, S.P., Amrein, M., Gillrie, M.R., Lee, K., Muruve, D.A. & Ho, M. 2011, "Plasmodium falciparum-induced CD36 clustering rapidly strengthens cytoadherence via p130CAS-mediated actin cytoskeletal rearrangement", *The FASEB journal : official publication of the Federation of American Societies for Experimental Biology*, .
- Dinic, J., Ashrafzadeh, P. & Parmryd, I. 2013, "Actin filaments attachment at the plasma membrane in live cells cause the formation of ordered lipid domains", *Biochimica et biophysica acta*, vol. 1828, no. 3, pp. 1102-1111.
- Doherty, G.J. & McMahon, H.T. 2009, "Mechanisms of endocytosis", *Annual Review of Biochemistry*, vol. 78, pp. 857-902.
- Feder, T.J., Brust-Mascher, I., Slattery, J.P., Baird, B. & Webb, W.W. 1996, "Constrained diffusion or immobile fraction on cell surfaces: a new interpretation.", *Biophysical journal*, vol. 70, no. 6, pp. 2767-2773.
- Gousset, K., Wolkers, W.F., Tsvetkova, N.M., Oliver, A.E., Field, C.L., Walker, N.J., Crowe, J.H. & Tablin, F. 2002, "Evidence for a physiological role for membrane rafts in human platelets", *Journal of cellular physiology*, vol. 190, no. 1, pp. 117-128.
- Harder, T., Scheiffele, P., Verkade, P. & Simons, K. 1998, "Lipid Domain Structure of the Plasma Membrane Revealed by Patching of Membrane Components", *The Journal of cell biology*, vol. 141, no. 4, pp. 929-942.

Chapter 4- Actin and lipid nanodomains control TSP-1-CD36-Fyn pathway

- Heit, B., Kim, H., Cosio, G., Castano, D., Collins, R., Lowell, C.A., Kain, K.C., Trimble, W.S. & Grinstein, S. 2013, "Multimolecular Signaling Complexes Enable Syk-Mediated Signaling of CD36 Internalization", *Developmental cell*, vol. 24, no. 4, pp. 372-383.
- Huang, W., Febbraio, M. & Silverstein, R.L. 2011, "CD9 tetraspanin interacts with CD36 on the surface of macrophages: a possible regulatory influence on uptake of oxidized low density lipoprotein", *PLoS one*, vol. 6, no. 12, pp. e29092.
- Itano, M.S., Steinhauer, C., Schmied, J.J., Forthmann, C., Liu, P., Neumann, A.K., Thompson, N.L., Tinnefeld, P. & Jacobson, K. 2012, "Super-resolution imaging of C-type lectin and influenza hemagglutinin nanodomains on plasma membranes using blink microscopy", *Biophysical journal*, vol. 102, no. 7, pp. 1534-1542.
- Jaqaman, K., Kuwata, H., Touret, N., Collins, R., Trimble, W.S., Danuser, G. & Grinstein, S. 2011, "Cytoskeletal control of CD36 diffusion promotes its receptor and signaling function", *Cell*, vol. 146, no. 4, pp. 593-606.
- Jaqaman, K., Loerke, D., Mettlen, M., Kuwata, H., Grinstein, S., Schmid, S.L. & Danuser, G. 2008, "Robust single-particle tracking in live-cell time-lapse sequences", *Nat Meth*, vol. 5, no. 8, pp. 695-702.
- Kraft, M.L. 2013, "Plasma membrane organization and function: moving past lipid rafts", *Molecular biology of the cell*, vol. 24, no. 18, pp. 2765-2768.
- Krag, C., Malmberg, E.K. & Salcini, A.E. 2010, "PI3KC2alpha, a class II PI3K, is required for dynamin-independent internalization pathways", *Journal of cell science*, vol. 123, no. Pt 24, pp. 4240-4250.
- Kusumi, A. & Sako, Y. 1996, "Cell surface organization by the membrane skeleton", *Current opinion in cell biology*, vol. 8, no. 4, pp. 566-574.
- Kwon, Y., Hofmann, T. & Montell, C. 2007, "Integration of Phosphoinositide and Calmodulin Mediated Regulation of TRPC6", *Molecular cell*, vol. 25, no. 4, pp. 491-503.
- Leevers, S.J., Vanhaesebroeck, B. & Waterfield, M.D. 1999, "Signalling through phosphoinositide 3-kinases: the lipids take centre stage", *Current opinion in cell biology*, vol. 11, no. 2, pp. 219-225.
- Levental, I., Lingwood, D., Grzybek, M., Coskun, U. & Simons, K. 2010, "Palmitoylation regulates raft affinity for the majority of integral raft proteins.", *Proceedings of the National Academy of Sciences of the United States of America*, vol. 107, no. 51, pp. 22050-22054.
- Lillemeier, B.F., Mortelmaier, M.A., Forstner, M.B., Huppa, J.B., Groves, J.T. & Davis, M.M. 2010, "TCR and Lat are expressed on separate protein islands on T cell membranes and concatenate during activation", *Nature immunology*, vol. 11, no. 1, pp. 90-96.

Chapter 4- Actin and lipid nanodomains control TSP-1-CD36-Fyn pathway

- Lingwood, D. & Simons, K. 2010, "Lipid rafts as a membrane-organizing principle", *Science*, vol. 327, no. 5961, pp. 46-50.
- Mattila, P.K., Feest, C., Depoil, D., Treanor, B., Montaner, B., Otipoby, K.L., Carter, R., Justement, L.B., Bruckbauer, A. & Batista, F.D. 2013, "The actin and tetraspanin networks organize receptor nanoclusters to regulate B cell receptor-mediated signaling", *Immunity*, vol. 38, no. 3, pp. 461-474.
- Merritt, E.A., Sarfaty, S., van, d.A., L'Hoir, C., Martial, J.A. & Hol, W.G. 1994, "Crystal structure of cholera toxin B-pentamer bound to receptor GM1 pentasaccharide", *Protein Science : A Publication of the Protein Society*, vol. 3, no. 2, pp. 166-175.
- Morone, N., Fujiwara, T., Murase, K., Kasai, R.S., Ike, H., Yuasa, S., Usukura, J. & Kusumi, A. 2006, "Three-dimensional reconstruction of the membrane skeleton at the plasma membrane interface by electron tomography", *The Journal of cell biology*, vol. 174, no. 6, pp. 851-862.
- Peng, G.E., Wilson, S.R. & Weiner, O.D. 2011, "A pharmacological cocktail for arresting actin dynamics in living cells", *Molecular biology of the cell*, vol. 22, no. 21, pp. 3986-3994.
- Raghupathy, R., Anilkumar, A.A., Polley, A., Singh, P.P., Yadav, M., Johnson, C., Suryawanshi, S., Saikam, V., Sawant, S.D., Panda, A., Guo, Z., Vishwakarma, R.A., Rao, M. & Mayor, S. 2015, "Transbilayer lipid interactions mediate nanoclustering of lipid-anchored proteins", *Cell*, vol. 161, no. 3, pp. 581-594.
- Resh, M.D. 1994, "Myristylation and palmitoylation of Src family members: the fats of the matter", *Cell*, vol. 76, no. 3, pp. 411-413.
- Rhee, I. & Veillette, A. 2012, "Protein tyrosine phosphatases in lymphocyte activation and autoimmunity", *Nature immunology*, vol. 13, no. 5, pp. 439-447.
- Riedl, J., Crevenna, A.H., Kessenbrock, K., Yu, J.H., Neukirchen, D., Bista, M., Bradke, F., Jenne, D., Holak, T.A., Werb, Z., Sixt, M. & Wedlich-Soldner, R. 2008, "Lifeact: a versatile marker to visualize F-actin.", *Nature Methods*, vol. 5, no. 7, pp. 605-607.
- Stauffer, T.P., Ahn, S. & Meyer, T. 1998, "Receptor-induced transient reduction in plasma membrane PtdIns(4,5)P2 concentration monitored in living cells", *Current biology : CB*, vol. 8, no. 6, pp. 343-346.
- Stuart, L.M., Bell, S.A., Stewart, C.R., Silver, J.M., Richard, J., Goss, J.L., Tseng, A.A., Zhang, A., El Khoury, J.B. & Moore, K.J. 2007, "CD36 signals to the actin cytoskeleton and regulates microglial migration via a p130Cas complex", *The Journal of biological chemistry*, vol. 282, no. 37, pp. 27392-27401.
- Tao, N., Wagner, S.J. & Lublin, D.M. 1996, "CD36 is palmitoylated on both N- and C-terminal cytoplasmic tails", *The Journal of biological chemistry*, vol. 271, no. 37, pp. 22315-22320.

Chapter 4- Actin and lipid nanodomains control TSP-1-CD36-Fyn pathway

- Thorne, R.F., Marshall, J.F., Shafren, D.R., Gibson, P.G., Hart, I.R. & Burns, G.F. 2000, "The integrins alpha3beta1 and alpha6beta1 physically and functionally associate with CD36 in human melanoma cells. Requirement for the extracellular domain OF CD36.", *Journal of Biological Chemistry*, vol. 275, no. 45, pp. 35264-35275.
- Thorne, R.F., Ralston, K.J., de Bock, C.E., Mhaidat, N.M., Zhang, X.D., Boyd, A.W. & Burns, G.F. 2010, "Palmitoylation of CD36/FAT regulates the rate of its post-transcriptional processing in the endoplasmic reticulum", *Biochimica et biophysica acta*, vol. 1803, no. 11, pp. 1298-1307.
- Treanor, B., Depoil, D., Gonzalez-Granja, A., Barral, P., Weber, M., Dushek, O., Bruckbauer, A. & Batista, F.D. 2010, "The membrane skeleton controls diffusion dynamics and signaling through the B cell receptor", *Immunity*, vol. 32, no. 2, pp. 187-199.
- van't Hof, W. & Resh, M.D. 1997, "Rapid plasma membrane anchoring of newly synthesized p59fyn: selective requirement for NH2-terminal myristoylation and palmitoylation at cysteine-3", *The Journal of cell biology*, vol. 136, no. 5, pp. 1023-1035.
- Veatch, S.L., Chiang, E.N., Sengupta, P., Holowka, D.A. & Baird, B.A. 2012, "Quantitative nanoscale analysis of IgE-FcepsilonRI clustering and coupling to early signaling proteins", *The journal of physical chemistry.B*, vol. 116, no. 23, pp. 6923-6935.
- Yeung, T., Gilbert, G.E., Shi, J., Silvius, J., Kapus, A. & Grinstein, S. 2008, "Membrane phosphatidylserine regulates surface charge and protein localization", *Science (New York, N.Y.)*, vol. 319, no. 5860, pp. 210-213.
- Zidovetzki, R. & Levitan, I. 2007, "Use of cyclodextrins to manipulate plasma membrane cholesterol content: evidence, misconceptions and control strategies", *Biochimica et biophysica acta*, vol. 1768, no. 6, pp. 1311-1324.

Chapter 5 - Endocytosis of CD36 in endothelial cells

5.1 Introduction

Plasma membrane proteins get endocytosed into the cell, either at steady state or following ligand induced receptor internalization (Doherty, McMahon 2009). There are different endocytic pathways that are involved in membrane protein and ligand internalization (Doherty, McMahon 2009). As a multi-ligand receptor, CD36 has been extensively studied on its capacity to bind ligands and the resultant downstream signaling effects (Silverstein, Febbraio 2009). However, knowledge on the plasma membrane turnover of CD36 and the role of its endocytosis in signaling or even in fatty transport remain insufficient. Several reports that have surveyed CD36 endocytic pathways have come to contradicting conclusions. CD36 has been proposed to be endocytosed via caveolae pathway (Ring et al. 2006), caveolae independent CLIC/GEEC pathway (clathrin-independent carrier, GPI-anchored-proteins enriched early endosomal compartments pathway) (Zeng et al. 2003), clathrin mediated endocytosis (Shamsul et al. 2010) and actin-dependent-macropinocytosis-independent endocytosis (Collins et al. 2009). These contradicting results have been obtained in different cell lines and through the use of varying CD36 ligands. Having looked at CD36 signaling on the plasma membrane of ECs in chapter 3 and 4, we investigated the mode of endocytosis CD36 exhibited, with or without TSP-1 stimulation. We found CD36 to be internalized through the CLIC/GEEC pathway in ECs. This internalization was through polymorphous tubules and was dynamin, actin, cholesterol and Cdc42 dependent.

5.2 Results

5.2.1 CD36 is endocytosed through CLIC/GEEC pathway, with or without TSP-1

There are approximately ten different internalization pathways previously described for membrane proteins (Doherty, McMahon 2009). We focused on four different pathways because on their previous involvement in CD36 internalization or connection to downstream effectors:

- 1) Clathrin mediated endocytosis (CME), could account for over 95% of all endocytosis on the plasma membrane (Bitsikas, Correa & Nichols 2014), and has been shown to mediate CD36 internalization in murine macrophage cell line, RAW264.7 (Shamsul et al. 2010).
- 2) Caveolae mediated endocytosis has been proposed to mediate CD36 endocytosis. Caveolin-1 was proposed to be required for CD36 localization and function at the plasma membrane of mouse embryonic fibroblasts (Ring et al. 2006).
- 3) Flotillin mediated endocytosis, which was shown to be regulated specifically by SFK Fyn in NIH3T3 fibroblasts, SYF and HeLa cells (Riento et al. 2009), and as earlier demonstrated in Chapter 3 and 4, CD36 associates with Fyn always in ECs.
- 4) Clathrin-independent carrier, GPI-anchored-proteins enriched early endosomal compartments pathway (CLIC/GEEC) pathway, which is commonly involved in endocytosing lipid rafts residents and has been proposed to mediate CD36 endocytosis in chinese hamster ovary cells (Doherty, McMahon 2009, Zeng et al. 2003).

To evaluate whether CD36 was internalized via one of these pathways, we first developed a specific endocytic assay. We incubated HMEC-mApple-CD36 cells with or without

Chapter 5- Endocytosis of CD36 in endothelial cells

TSP-1 for 2 minutes and 5 minutes, and labelled different endocytic markers of endocytic pathways post-fixation using antibodies. For CLIC/GEEC pathway, transient GPI-GFP transfection was used. Colocalization of CD36 with the endocytic markers at these early stages time points would give a lead into the possible endocytic pathway involved. In all time points, with or without TSP-1, CD36 colocalized more with GPI-GFP, a CLIC/GEEC pathway marker (Lundmark et al. 2008), compared to clathrin heavy chain (CME marker (Godlee, Kaksonen 2013)), caveolin-1 (Caveolae dependent pathway marker (Kiss 2012)) and flotillin-1 (Flotillin dependent pathway marker (Riento et al. 2009)) (Figure 5-1A, B). The average 25th percentile of the Pearson correlation coefficient (PCC) of CD36 and GPI-GFP was well above the 75th percentile PCC of CD36 and the markers of all the other pathways (green dotted line, Figure 5-1B). This data hinted to a CLIC/GEEC pathway involvement in unligated and TSP-1 ligated CD36 endocytosis.

Chapter 5- Endocytosis of CD36 in endothelial cells

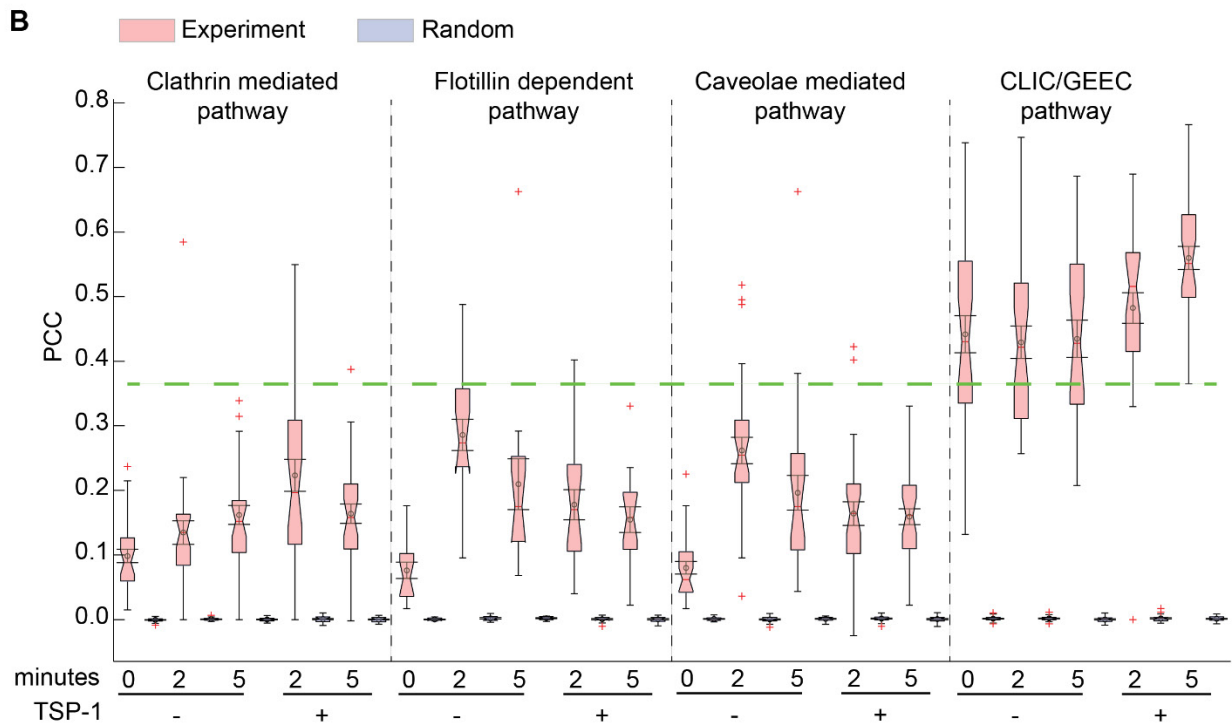
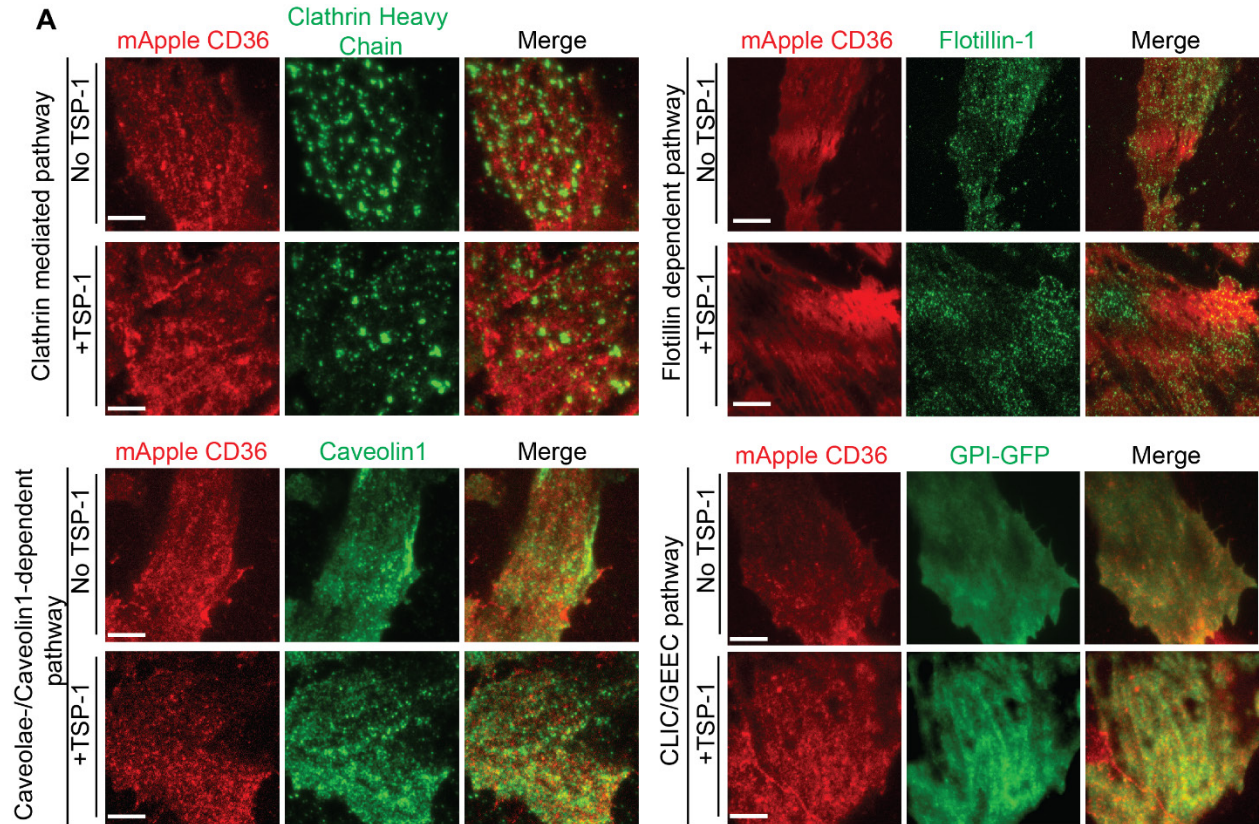


Figure 5-1: CD36 is endocytosed through CLIC/GEEC pathway

(A) TIRFM images of HMEC-mApple-CD36 cells with different endocytic pathways labeled post fixation. Cells were incubated with or without TSP-1 for different timepoints, followed by fixation and labeling of CME pathway (clathrin heavy chain), flotillin dependent pathway (flotillin-1), caveolae dependent pathway (caveolin-1) or transfected GPI-GFP (CLIC/GEEC pathway). Data representative of 3 similar independent experiments. Scale bars (applicable to all images), 5 μ m. (B) Pearson correlation coefficient (PCC) from data in (A) between CD36 and the different endocytic pathways markers at different time points, with or without TSP-1. Boxplots as described in 2.13 Graphing and statistical analysis. Green dotted line is the average 25th percentile of CD36-GPI-GFP PCC.

We then looked into the kinetics of CD36 endocytosis. Plasma membrane CD36 in HMEC-CD36-myc cells was pre-labelled with Cy3b-conjugated anti-CD36 Fab fragments on ice. This was then followed by time point incubation (10, 20 and 30 minutes) with or without TSP-1 at 37°C. At the end of each time point, before cell fixation, remaining membrane-bound antibodies were removed by an acid wash on ice, which we had earlier determined to be quite effective (see Figure 3-13). These cells were then fixed and imaged on a widefield microscope. Endocytosed CD36 vesicles, which contained Cy3b fluorophores, were identified using à trous wavelet transform decomposition method (Figure 5-2A) (Olivo-Marin 2002). As earlier observed (see Figure 3-13), looking at the number of CD36 vesicles per area, TSP-1 delayed CD36 endocytosis at 10 minutes time point (Figure 5-2B). However, similar number of vesicles per area were observed at 20 and 30 minutes (Figure 5-2B). These vesicles average intensity increased with time (Figure 5-2C), which was either due to endosomes merging or recruitment of more CD36 molecules to the endocytic pits with time before internalization. The size of these vesicles was relatively the same in all time points (Figure 5-2D). However, this size of vesicles

Chapter 5- Endocytosis of CD36 in endothelial cells

was within the diffraction limit of the microscope (~250nm), higher resolution would be needed to confirm if indeed these endosomes have the same size in all time points.

Taken all together, these results suggested CD36 was internalized through CLIC/GEEC pathway and although TSP-1 binding delayed part of CD36 endocytosis during the first 10 minutes of stimulation, the kinetics of unligated and TSP-1 ligated CD36 were relatively similar. To confirm CLIC/GEEC pathway was involved, we investigated other known properties of this pathway in the context of CD36 endocytosis.

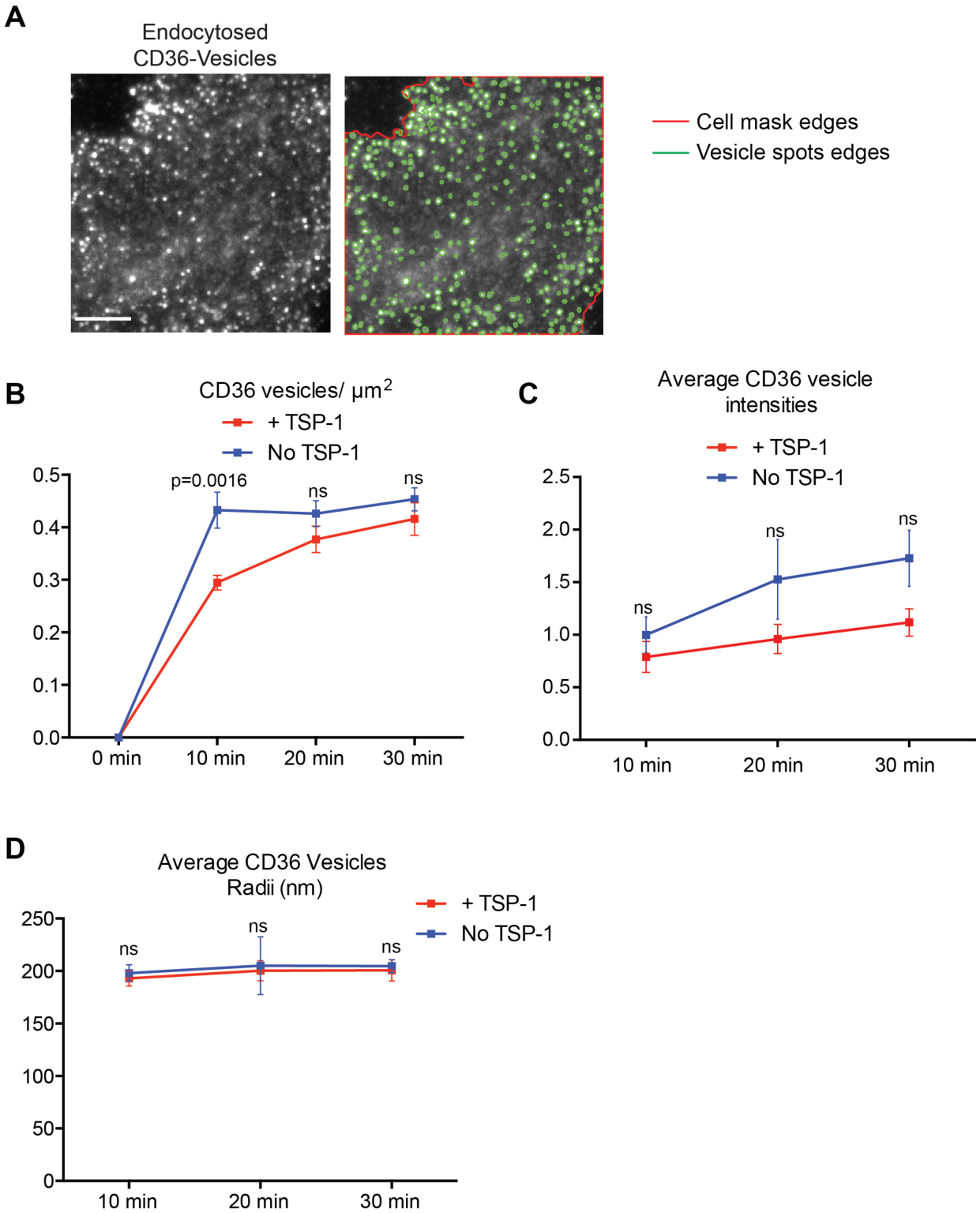


Figure 5-2: CD36 endocytosis kinetics

(A) Image representative of CD36 endosomes at 30 minutes time point in HMEC-CD36-myc cells post acid wash and fixation, with the cell ROI edges highlighted in red (see 2.8.6 Cell mask segmentation) and endosomes edges in green, identified by à trous wavelet transform decomposition. Scale bars, 5 μ m. (B) Number of CD36 vesicles per area calculated from data in (A) at different time points, with or without TSP-1 stimulation. (C) Average intensity per vesicle from data in (A) at different time points, with or without TSP-1 stimulation, normalized to no TSP-1 10 minute time point. (D) Estimated vesicle radii from data in (A) at different time points, with or without TSP-1 stimulation.

Data representative of 3 similar independent experiments, with 9-11 fields per time point and per experiment. All error bars, mean \pm SEM Statistical analysis as described in 2.13 Graphing and statistical analysis.

5.2.2 CD36 is endocytosed through polymorphous tubules

Morphological analysis of endocytic pits has recently reported tubular compartments, besides the canonical vesicular ones (Johannes et al. 2015). Earlier observation of these tubules may have been hampered by fixation conditions and user visualization bias in electron microscopy (EM) as tubules would appear spherical in a 2D cross-section (Doherty, McMahon 2009). These polymorphous tubules are reported, almost exclusively in CLIC/GEEC endocytic pathway (Johannes et al. 2015). To test if CD36 was internalized through tubular invaginations, HMEC-CD36-myc cells were pre-labelled with Cy3b-conjugated anti-CD36 Fab fragments on ice, followed by 5 minutes incubation at 37°C. At the end of the time point, before cell fixation, remaining membrane-bound antibodies were removed by an acid wash on ice. These cells were then fixed and imaged on a spinning-disc confocal microscope, with a 250 nm spacing between the different cross-section of the cell(s) along the z axis. 3D reconstruction of the endocytic

CD36 compartments revealed visible polymorphous tubular like structures (Figure 5-3), reminiscent of earlier reports of such endocytic pits (Hansen, Nichols 2009).

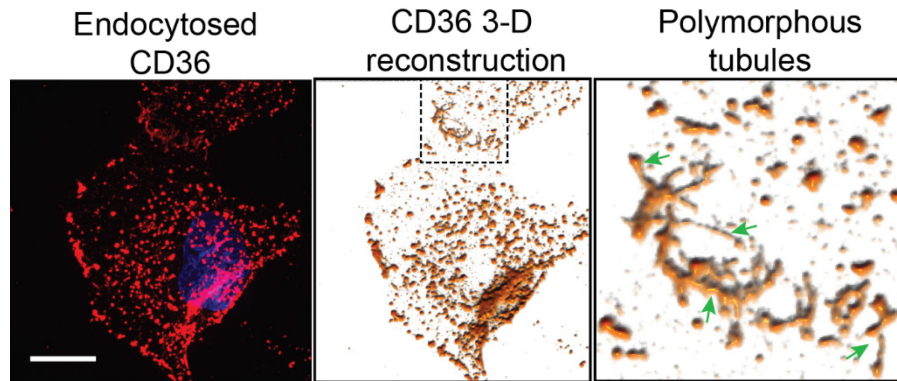


Figure 5-3: Polymorphous tubules formed during CD36 endocytosis

Projected z-stacks confocal images of CD36 endosomes after 5 minutes incubation of anti-CD36 Cy3b labelled HMEC-CD36-myc cells post acid wash and fixation. Cell nuclei was stained with DAPI (blue). 3-D reconstruction of the confocal images is shown in golden-yellow image. Inset represent magnified area underlined with dashed line boxes. Tubular structures are highlighted by green arrows Scale bar, 5 μm . Data representative of 3 similar independent experiments.

Next, we confirmed if other endocytic cargoes observed in tubular like compartments colocalized with CD36. Two cargo proteins endocytosed in such tubules were used, CD44 and CD147 (Dutta, Donaldson 2015, Hansen, Nichols 2009). HMEC-mApple-CD36 cells were pre-labelled with monoclonal mouse anti-CD44 or mouse anti-CD147 on ice, followed by 5 minutes incubation at 37°C. At the end of the time point, before cell fixation, remaining membrane-bound antibodies were removed by an acid wash on ice. Cells were then permeabilized and the internalized primary antibody labelled with a donkey anti-mouse AlexaFluor 488 antibody.

Chapter 5- Endocytosis of CD36 in endothelial cells

Confocal imaging of both mApple CD36 and CD44 or CD147 showed remarkable colocalization between CD36 and these cargo proteins in tubular structures (Figure 5-4A, B).

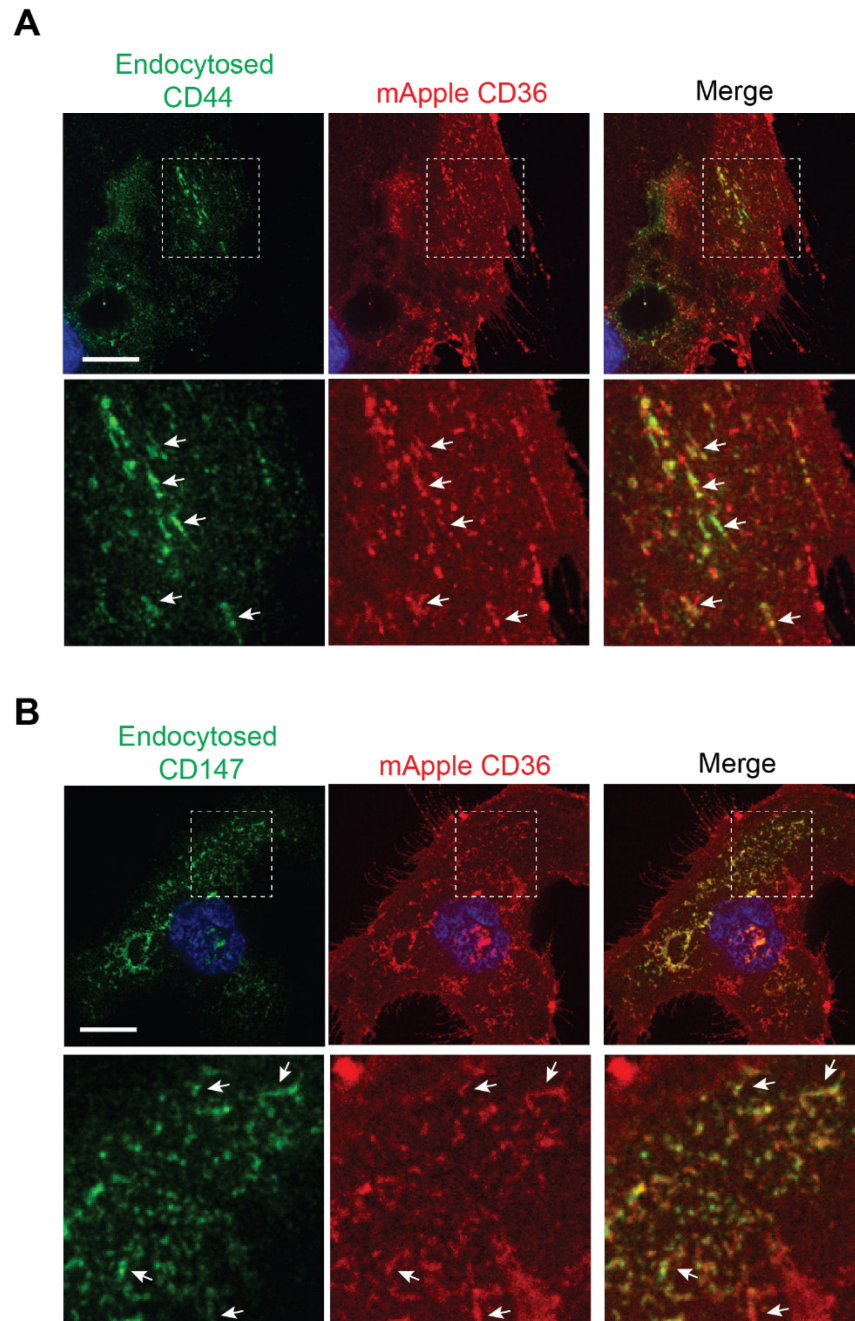


Figure 5-4: CD36 colocalizes with reported tubular structure compartments cargoes

(A) Projected z-stacks confocal images of CD44 endosomes after 5 minutes incubation of mouse anti-CD44 labelled HMEC-mApple-CD36 cells post acid wash and fixation. The endosomes are labelled with an anti-mouse AlexaFluor 488. Inset represent magnified area underlined with dashed line boxes. Colocalized tubular structures are highlighted by white arrows. Cell nuclei was stained with DAPI (blue) in all cell lines. Scale bar, 5 μ m. Data representative of 3 similar independent experiments. (B) Data for CD147, as demonstrated for CD44 in (A).

5.2.3: CD36 endocytosis is dynamin dependent

Endocytic vesicle scission from the plasma membrane, for most of the endocytosis pathways, is often achieved via dynamin, a GTPase protein (Doherty, McMahon 2009). There are three dynamin isoforms, dynamin 1 to 3, where dynamin 2 is ubiquitous, while dynamin 1 and 3 are expressed in the brain (Cao, Garcia & McNiven 1998, Cook, Urrutia & McNiven 1994, Tanifuji et al. 2013). Through GTP hydrolysis, dynamin forms a helical polymer around the neck of the endocytic pits, irreversibly detaching the vesicle off the plasma membrane (Morlot, Roux 2013). CLIC/GEEC pathway is primarily dynamin independent though dynamin dependent paths have been reported (Kirkham, Parton 2005, Lajoie, Nabi 2010, Ricci et al. 2000, Skretting et al. 1999, Nichols et al. 2001, Sabharanjak et al. 2002). To probe if CD36 endocytosis is dynamin dependent or not, we used a widely studied dynamin inhibitor, dynasore (Macia et al. 2006). Transferrin (Tf) endocytosis, a well characterized dynamin dependent internalization cargo (Tortorella, Karagiannis 2014), was used alongside CD59, a GPI-anchored protein whose internalization has been shown to be dynamin independent (Naslavsky, Weigert & Donaldson 2004, Krag, Malmberg & Salcini 2010). HMEC-CD36-myc cells were incubated with or without 80 μ M dynasore, before pre-labelling with Cy3b-conjugated anti-CD36 Fab fragments or mouse-anti-CD59 and AlexaFluor 488 conjugated Tf on ice, followed by 10 minutes incubation at 37°C.

Chapter 5- Endocytosis of CD36 in endothelial cells

At the end of this time point, remaining membrane-bound antibodies and Tf were removed by an acid wash on ice. These cells were then fixed, and in cells with mouse anti-CD59 antibodies, they were permeabilized and labelled with an anti-mouse Cy3. All these cells were mounted and imaged on a spinning disc confocal microscope (Figure 5-5A). The intensity measurements were normalized to the amount Tf or CD36 or CD59 endocytosed in the untreated condition. Dynamin inhibition significantly reduced the amount of CD36 and Tf endocytosed (Figure 5-5B) but had no significant effect on amount of CD59 endocytosed, underscoring a dynamin dependent CD36 internalization.

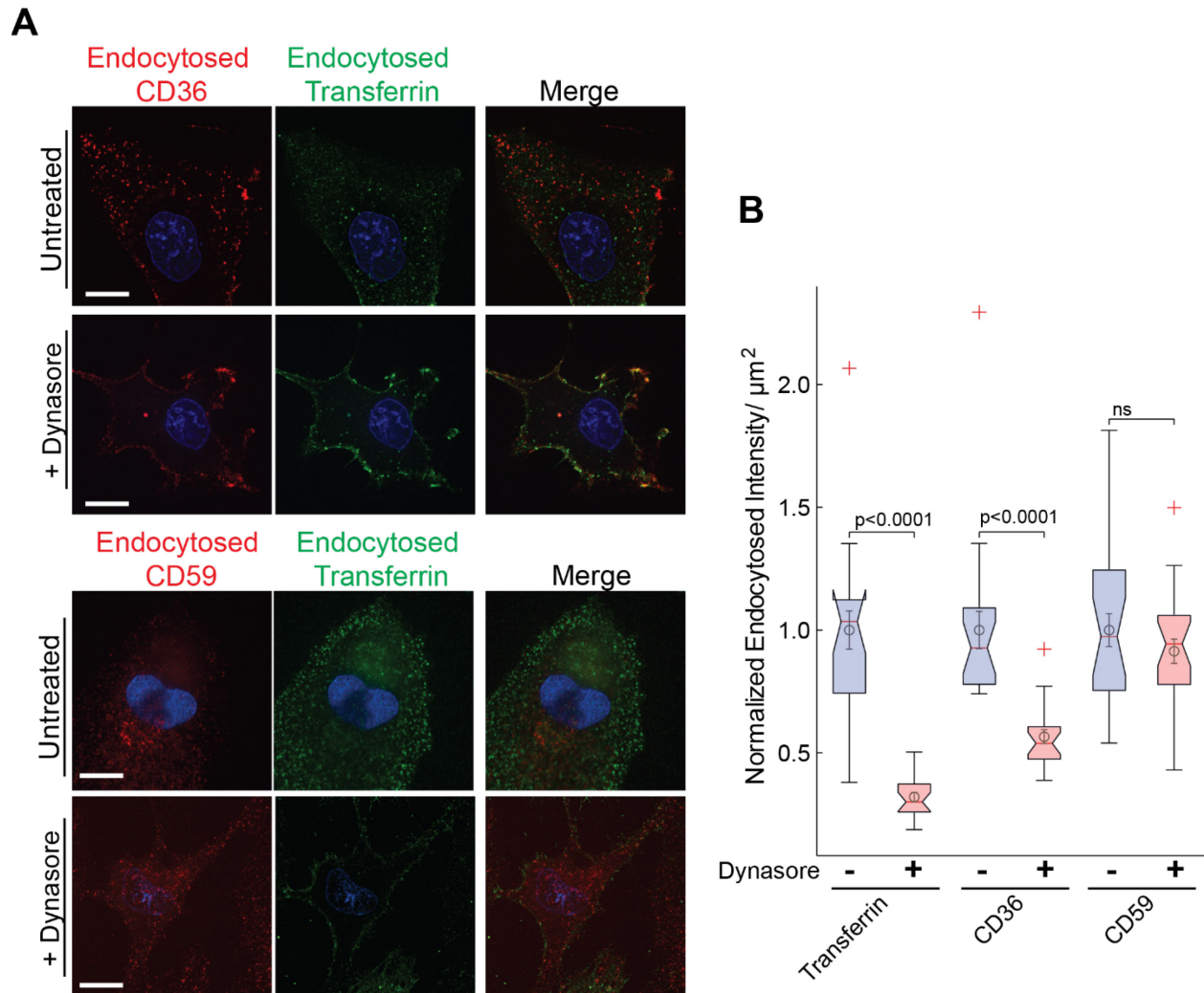


Figure 5-5: CD36 endocytosis is dynamin dependent

(A) Upper panel; Confocal image of endocytosed CD36 and transferrin (Tf) after 10 minutes incubation of anti-CD36 Cy3b, Tf AlexaFluor 488 labelled HMEC-CD36-myc cells, post acid wash and fixation. This was done with or without dynasore (80 μM) treatment. Lower panel: confocal images of endocytosed CD59 and Tf labelled as in upper panel, with endocytosed CD59 labelled instead of CD36. Scale bar for all images, 5 μm . Cell nuclei stained with DAPI (blue) in all cell lines. (B) Quantification of the amount of Tf, CD36 and CD59 endocytosed in untreated (light blue boxplots) and dynasore treated (light red boxplots) conditions (from (A)). Boxplots and statistical analysis as described in 2.13 Graphing and statistical

analysis. Data from 3 experiments, with 9-11 images per condition and per experiment.

5.2.4 CD36 endocytosis is dependent on actin, cholesterol and Cdc42

Lipid rafts have been shown to collaborate with the actin cytoskeleton and to promote Cdc42 activation resulting in actin polymerization necessary for the formation of the endosomal invaginations specific to CLIC/GEEC endocytosis (Chadda et al. 2007). Cholesterol depletion, actin polymerization perturbation or Cdc42 inhibition abrogates CLIC/GEEC endocytic machinery (Chadda et al. 2007, Mayor, Parton & Donaldson 2014, Johannes et al. 2015). To further validate that CLIC/GEEC pathway is indeed for the endocytic route of CD36 in ECs, we measured the amount of CD36 endocytosed under actin disruption, cholesterol depletion or Cdc42 inhibition.

Pre-treating HMEC-CD36-myc cells with the earlier optimized conditions of actin perturbation (with 200 nM Lat B) or lipid raft disruption (cholesterol depletion with 2mM M β CD) (see Figure 4-4), CD36 and Tf endocytosis was probed as described earlier (see Figure 5-5). Disrupting actin or depleting cholesterol significantly reduce the amount of CD36 endocytosed but had no significant effect on the amount Tf internalized (Figure 5-6A, B).

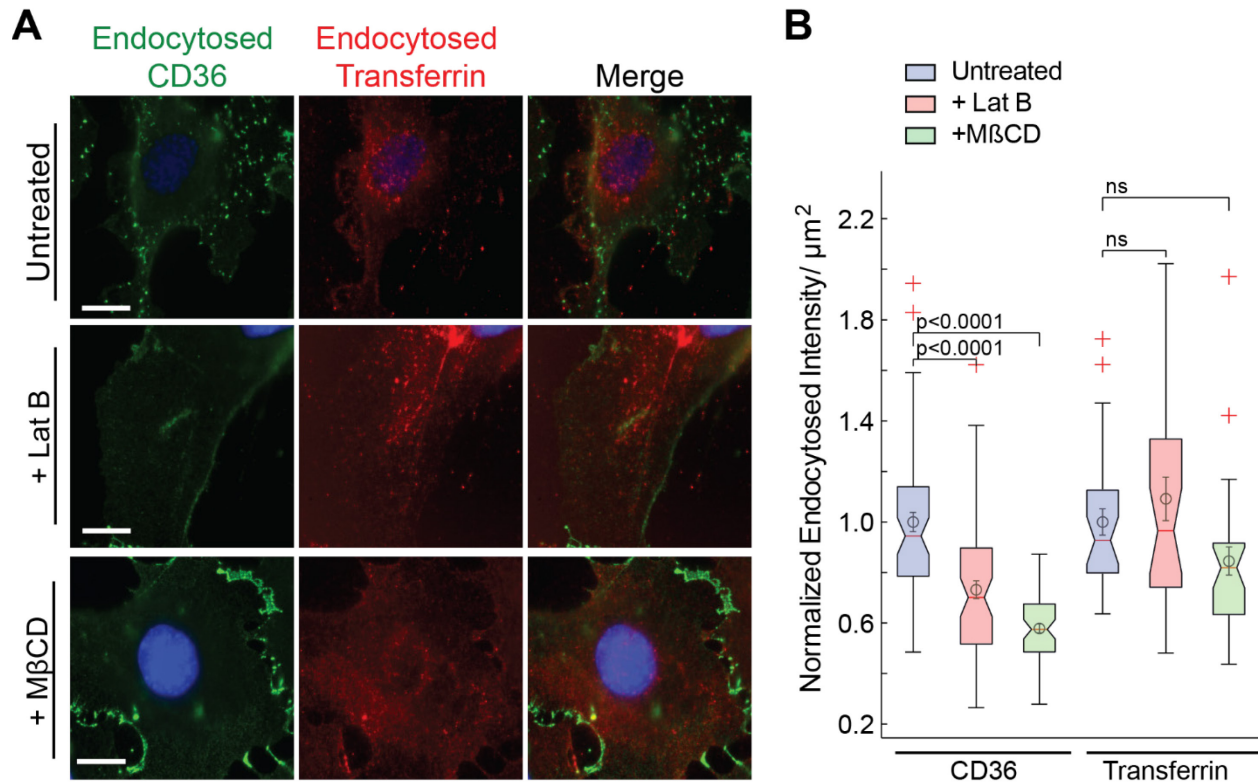


Figure 5-6: CD36 endocytosis is actin and cholesterol dependent

(A) Confocal image of endocytosed CD36 and Tf after 10 minutes incubation of anti-CD36 AlexaFluor 488, Tf AlexaFluor 647 labelled HMEC-CD36-myc cells, post acid wash and fixation. This was done with or without Lat B (200nM) or MβCD (2mM) treatment. Scale bar for all images, 5 μm. (B) Quantification of the amount of CD36 or Tf endocytosed, determined by the average intensity within cells area normalized to untreated condition, in untreated (light blue boxplots), Lat B treated (light red boxplots) or MβCD treated (light green boxplots) conditions (from (A)). Boxplots and statistical analysis as described in 2.13 Graphing and statistical analysis. Data from 3 experiments, with at least 10 images per condition and per experiment with the cell nuclei stained with DAPI (blue) in all cell lines.

As aforementioned, the Rho GTPase Cdc42 activation is necessary in actin reorganization to induced pit invagination in CLIC/GEEC endocytic pathway (Chadda et al.

2007). Recently, a potent, selective pharmacological inhibitor of Cdc42, ML141, has been developed (Surviladze et al. 2010). Using this inhibitor, we repeated the same experiment presented previously (Figure 5-5), pretreating the cells with 10 μ M ML141. Inhibition of Cdc42 significantly reduced the amount of CD36 endocytosed while the amount of Tf internalized was unaffected (Figure 5-7A, B). Taken all together, we determined that CD36 internalization was actin, cholesterol and Cdc42 dependent, a characteristic common in CLIC/GEEC pathway cargoes (Johannes et al. 2015).

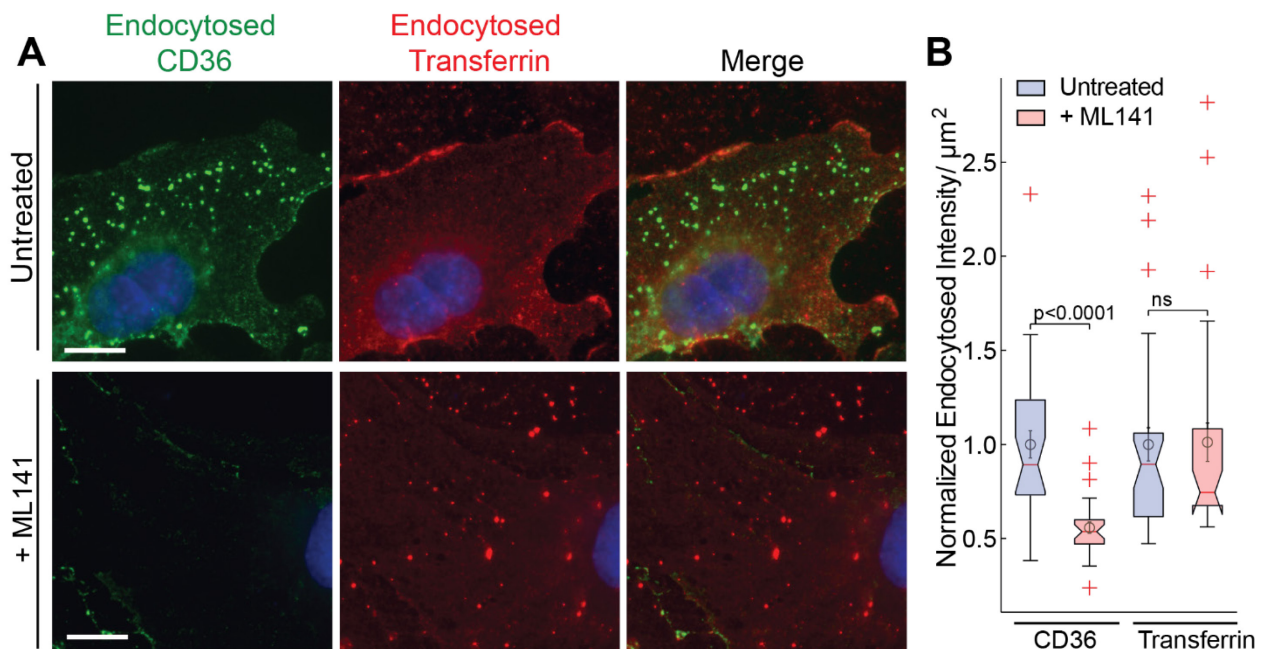


Figure 5-7: CD36 endocytosis is Cdc42 dependent

(A) Confocal images of endocytosed CD36 and Tf after 10 minutes incubation of anti-CD36 AlexaFluor 488, Tf AlexaFluor 647 labelled HMEC-CD36-myc cells, post acid wash and fixation. This was done with or without ML141 (10 μ M) treatment. Scale bar for all images, 5 μ m. Cell nuclei stained with DAPI (blue) in all cell lines. (B) Quantification of the amount of CD36 and Tf endocytosed in untreated (light blue boxplots) and ML141 treated (light red boxplots) conditions (from (A)).

Boxplots and statistical analysis as described in 2.13 Graphing and statistical analysis.

Data from 3 experiments, with at least 10 images per condition and per experiment.

5.3 Discussion

Endocytosis is a key regulator of plasma membrane components uptake and intracellular signaling (Miaczynska, Bar-Sagi 2010). In this chapter, we explored the endocytic pathway involved in the internalization of unligated and TSP-1 ligated CD36 in ECs. First, we found that CD36 colocalizes significantly more with the CLIC/GEEC pathway marker, GPI-GFP, at both steady state and TSP-1 stimulated state, suggesting involvement of this pathway in CD36 endocytosis (Figure 5-1). CD36 endocytosis was dependent on dynamin, actin, cholesterol and Cdc42, in line with previous observations of other specific cargoes of this pathway (Chadda et al. 2007, Doherty, McMahon 2009, Johannes et al. 2015).

CLIC/GEEC pathway has been implicated in oxLDL-CD36 endocytosis in CHO cells (Zeng et al. 2003), alongside CME in FSL-1 (a synthetic lipoprotein)-CD36 endocytosis in RAW264.7 cells (Shamsul et al. 2010) and actin-dependent-macropinocytosis-independent endocytosis in oxLDL-CD36 endocytosis in primary macrophages (Collins et al. 2009). Of note, all these reports used different cell lines in their investigations. This implies that CD36 endocytosis is possibly cell-type specific, a phenomenon reported in another plasma membrane protein, neurotensin receptor (Savdie et al. 2006). Two of the major factors that CLIC/GEEC pathway relies on are actin and lipid raft component, cholesterol (Chadda et al. 2007, Doherty, McMahon 2009, Johannes et al. 2015). Cholesterol depletion has been shown to inhibit Cdc42

activation, thereby, abrogating the necessary actin re-organization thought to mediate the tubular invaginations during endocytosis (Chadda et al. 2007, Johannes et al. 2015).

While CLIC/GEEC pathway is generally considered dynamin independent (Johannes et al. 2015), we found CD36 endocytosis to be dynamin dependent (Figure 5-5). Indeed, some have categorized CLIC/GEEC pathway as both dynamin dependent and independent (Doherty, McMahon 2009). For instance, GPI-anchored CD59 has been shown to be dynamin dependent in some reports and dynamin independent in others (Naslavsky, Weigert & Donaldson 2004, Krag, Malmberg & Salcini 2010, Kumari, Mg & Mayor 2010, Johannes et al. 2015). This highlights the need to better define CLIC/GEEC pathway as much of how it is regulated remains to be elucidated. There has been speculation of GPI-anchored proteins sorting mechanisms at the plasma membrane being the feature enabling them to enter the cell via multiple mechanisms (Mayor, Riezman 2004, Sharma et al. 2004, Bhagatji et al. 2009, Johannes, Mayor 2010).

The role of CLIC/GEEC endocytic pathway in the TSP-1-CD36-Fyn pathway remains to be elucidated. For a long time, endocytosis was viewed simply as a mean to downregulate signaling from the plasma membrane, by internalizing receptors or ligand-receptor complexes (Pálffy, Reményi & Korcsmáros 2012, Miaczynska, Bar-Sagi 2010). However, there is increasing evidence of instances where endocytosis perpetuates signaling, through the so called 'signaling endosomes'. Further investigations are needed to determine if TSP-1-CD36 internalization downregulates Fyn activation or perpetuates it.

References

- Bhagatji, P., Leventis, R., Comeau, J., Refa'ei, M. & Silvius, J.R. 2009, "Steric and not structure-specific factors dictate the endocytic mechanism of glycosylphosphatidylinositol-anchored proteins", *The Journal of cell biology*, vol. 186, no. 4, pp. 615-628.
- Bitsikas, V., Correa, I.R., Jr & Nichols, B.J. 2014, "Clathrin-independent pathways do not contribute significantly to endocytic flux", *eLife*, vol. 3, pp. e03970.
- Cao, H., Garcia, F. & McNiven, M.A. 1998, "Differential Distribution of Dynamin Isoforms in Mammalian Cells", *Molecular biology of the cell*, vol. 9, no. 9, pp. 2595-2609.
- Chadda, R., Howes, M.T., Plowman, S.J., Hancock, J.F., Parton, R.G. & Mayor, S. 2007, "Cholesterol-sensitive Cdc42 activation regulates actin polymerization for endocytosis via the GEEC pathway", *Traffic (Copenhagen, Denmark)*, vol. 8, no. 6, pp. 702-717.
- Collins, R.F., Touret, N., Kuwata, H., Tandon, N.N., Grinstein, S. & Trimble, W.S. 2009, "Uptake of oxidized low density lipoprotein by CD36 occurs by an actin-dependent pathway distinct from macropinocytosis", *The Journal of biological chemistry*, vol. 284, no. 44, pp. 30288-30297.
- Cook, T.A., Urrutia, R. & McNiven, M.A. 1994, "Identification of dynamin 2, an isoform ubiquitously expressed in rat tissues", *Proceedings of the National Academy of Sciences of the United States of America*, vol. 91, no. 2, pp. 644-648.
- Doherty, G.J. & McMahon, H.T. 2009, "Mechanisms of endocytosis", *Annual Review of Biochemistry*, vol. 78, pp. 857-902.
- Dutta, D. & Donaldson, J.G. 2015, "Sorting of Clathrin-Independent Cargo Proteins Depends on Rab35 Delivered by Clathrin-Mediated Endocytosis", *Traffic (Copenhagen, Denmark)*, vol. 16, no. 9, pp. 994-1009.
- Godlee, C. & Kaksonen, M. 2013, "Review series: From uncertain beginnings: initiation mechanisms of clathrin-mediated endocytosis", *The Journal of cell biology*, vol. 203, no. 5, pp. 717-725.
- Hansen, C.G. & Nichols, B.J. 2009, "Molecular mechanisms of clathrin-independent endocytosis", *Journal of cell science*, vol. 122, no. Pt 11, pp. 1713-1721.
- Johannes, L. & Mayor, S. 2010, "Induced domain formation in endocytic invagination, lipid sorting, and scission", *Cell*, vol. 142, no. 4, pp. 507-510.
- Johannes, L., Parton, R.G., Bassereau, P. & Mayor, S. 2015, "Building endocytic pits without clathrin", *Nature reviews.Molecular cell biology*, vol. 16, no. 5, pp. 311-321.

Chapter 5- Endocytosis of CD36 in endothelial cells

- Kirkham, M. & Parton, R.G. 2005, "Clathrin-independent endocytosis: new insights into caveolae and non-caveolar lipid raft carriers", *Biochimica et biophysica acta*, vol. 1746, no. 3, pp. 349-363.
- Kiss, A.L. 2012, "Caveolae and the regulation of endocytosis", *Advances in Experimental Medicine and Biology*, vol. 729, pp. 14-28.
- Krag, C., Malmberg, E.K. & Salcini, A.E. 2010, "PI3KC2alpha, a class II PI3K, is required for dynamin-independent internalization pathways", *Journal of cell science*, vol. 123, no. Pt 24, pp. 4240-4250.
- Kumari, S., Mg, S. & Mayor, S. 2010, "Endocytosis unplugged: multiple ways to enter the cell", *Cell research*, vol. 20, no. 3, pp. 256-275.
- Lajoie, P. & Nabi, I.R. 2010, "Lipid rafts, caveolae, and their endocytosis", *International review of cell and molecular biology*, vol. 282, pp. 135-163.
- Lundmark, R., Doherty, G.J., Howes, M.T., Cortese, K., Vallis, Y., Parton, R.G. & McMahon, H.T. 2008, "The GTPase-Activating Protein GRAF1 Regulates the CLIC/GEEC Endocytic Pathway", *Current Biology*, vol. 18, no. 22-2, pp. 1802-1808.
- Macia, E., Ehrlich, M., Massol, R., Boucrot, E., Brunner, C. & Kirchhausen, T. 2006, "Dynasore, a cell-permeable inhibitor of dynamin", *Developmental cell*, vol. 10, no. 6, pp. 839-850.
- Mayor, S., Parton, R.G. & Donaldson, J.G. 2014, "Clathrin-independent pathways of endocytosis", *Cold Spring Harbor perspectives in biology*, vol. 6, no. 6, pp. 10.1101/cshperspect.a016758.
- Mayor, S. & Riezman, H. 2004, "Sorting GPI-anchored proteins", *Nature reviews.Molecular cell biology*, vol. 5, no. 2, pp. 110-120.
- Miaczynska, M. & Bar-Sagi, D. 2010, "Signaling endosomes: seeing is believing", *Current opinion in cell biology*, vol. 22, no. 4, pp. 535-540.
- Morlot, S. & Roux, A. 2013, "Mechanics of dynamin-mediated membrane fission", *Annual review of biophysics*, vol. 42, pp. 629-649.
- Naslavsky, N., Weigert, R. & Donaldson, J.G. 2004, "Characterization of a Nonclathrin Endocytic Pathway: Membrane Cargo and Lipid Requirements", *Molecular biology of the cell*, vol. 15, no. 8, pp. 3542-3552.
- Nichols, B.J., Kenworthy, A.K., Polishchuk, R.S., Lodge, R., Roberts, T.H., Hirschberg, K., Phair, R.D. & Lippincott-Schwartz, J. 2001, "Rapid cycling of lipid raft markers between the cell surface and Golgi complex", *The Journal of cell biology*, vol. 153, no. 3, pp. 529-541.

Chapter 5- Endocytosis of CD36 in endothelial cells

- Olivo-Marin, J. 2002, "Extraction of spots in biological images using multiscale products", *Pattern Recognition*, vol. 35, no. 9, pp. 1989-1996.
- Pálfy, M., Reményi, A. & Korcsmáros, T. 2012, "Endosomal crosstalk: meeting points for signaling pathways", *Trends in cell biology*, vol. 22, no. 9, pp. 447-456.
- Ricci, V., Galmiche, A., Doye, A., Necchi, V., Solcia, E. & Boquet, P. 2000, "High cell sensitivity to *Helicobacter pylori* VacA toxin depends on a GPI-anchored protein and is not blocked by inhibition of the clathrin-mediated pathway of endocytosis", *Molecular biology of the cell*, vol. 11, no. 11, pp. 3897-3909.
- Riento, K., Frick, M., Schafer, I. & Nichols, B.J. 2009, "Endocytosis of flotillin-1 and flotillin-2 is regulated by Fyn kinase", *Journal of cell science*, vol. 122, no. Pt 7, pp. 912-918.
- Ring, A., Le Lay, S., Pohl, J., Verkade, P. & Stremmel, W. 2006, "Caveolin-1 is required for fatty acid translocase (FAT/CD36) localization and function at the plasma membrane of mouse embryonic fibroblasts", *Biochimica et biophysica acta*, vol. 1761, no. 4, pp. 416-423.
- Sabharanjak, S., Sharma, P., Parton, R.G. & Mayor, S. 2002, "GPI-anchored proteins are delivered to recycling endosomes via a distinct cdc42-regulated, clathrin-independent pinocytic pathway", *Developmental cell*, vol. 2, no. 4, pp. 411-423.
- Savdie, C., Ferguson, S.S., Vincent, J., Beaudet, A. & Stroh, T. 2006, "Cell-type-specific pathways of neurotensin endocytosis", *Cell and tissue research*, vol. 324, no. 1, pp. 69-85.
- Shamsul, H.M., Hasebe, A., Iyori, M., Ohtani, M., Kiura, K., Zhang, D., Totsuka, Y. & Shibata, K. 2010, "The Toll-like receptor 2 (TLR2) ligand FSL-1 is internalized via the clathrin-dependent endocytic pathway triggered by CD14 and CD36 but not by TLR2", *Immunology*, vol. 130, no. 2, pp. 262-272.
- Sharma, P., Varma, R., Sarasij, R.C., Ira, Gousset, K., Krishnamoorthy, G., Rao, M. & Mayor, S. 2004, "Nanoscale organization of multiple GPI-anchored proteins in living cell membranes", *Cell*, vol. 116, no. 4, pp. 577-589.
- Silverstein, R.L. & Febbraio, M. 2009, "CD36, a scavenger receptor involved in immunity, metabolism, angiogenesis, and behavior", *Science signaling*, vol. 2, no. 72, pp. re3.
- Skretting, G., Torgersen, M.L., van Deurs, B. & Sandvig, K. 1999, "Endocytic mechanisms responsible for uptake of GPI-linked diphtheria toxin receptor", *Journal of cell science*, vol. 112 (Pt 22), no. Pt 22, pp. 3899-3909.
- Surviladze, Z., Waller, A., Strouse, J.J., Bologna, C., Ursu, O., Salas, V., Parkinson, J.F., Phillips, G.K., Romero, E., Wandinger-Ness, A., Sklar, L.A., Schroeder, C., Simpson, D., Noth, J., Wang, J., Golden, J. & Aube, J. 2010, "A Potent and Selective Inhibitor of Cdc42 GTPase" in *Probe Reports from the NIH Molecular Libraries Program* Bethesda (MD).

Chapter 5- Endocytosis of CD36 in endothelial cells

- Tanifuji, S., Funakoshi-Tago, M., Ueda, F., Kasahara, T. & Mochida, S. 2013, "Dynamin isoforms decode action potential firing for synaptic vesicle recycling", *The Journal of biological chemistry*, vol. 288, no. 26, pp. 19050-19059.
- Tortorella, S. & Karagiannis, T.C. 2014, "Transferrin receptor-mediated endocytosis: a useful target for cancer therapy", *The Journal of membrane biology*, vol. 247, no. 4, pp. 291-307.
- Zeng, Y., Tao, N., Chung, K.N., Heuser, J.E. & Lublin, D.M. 2003, "Endocytosis of oxidized low density lipoprotein through scavenger receptor CD36 utilizes a lipid raft pathway that does not require caveolin-1", *The Journal of biological chemistry*, vol. 278, no. 46, pp. 45931-45936.

Chapter 6 - General discussion and conclusions

6.1 Discussion

Thrombospondin-based anti-angiogenic therapy can be key to cancer treatment and preventing its recurrence (Zhang, Lawler 2007). TSP-1 inhibits angiogenesis through its main receptor CD36 and subsequent Fyn activation which initiates a signaling cascade paramount to this anti-angiogenesis in ECs (Jimenez et al. 2000, Jimenez et al. 2001, Dawson et al. 1997). A deeper understanding of how TSP-1 binding to CD36 initiates this pathway could provide cues to designing more efficient TSP-1 mimicry. We have combined biochemical approaches, conventional and advanced microscopy techniques, as well as quantitative data analysis to shed light on how this pathway is initiated. We have also characterized the mechanism through which CD36 gets internalized.

In this study, we investigated the organization of CD36 on the plasma membrane of ECs in relation to the anti-angiogenic TSP-1-CD36-Fyn pathway. First to establish our experimental system, we revisited the dependency of TSP-1 binding and stimulatory capacity on CD36. Down regulation of CD36 by siRNA in primary HMVECs resulted in decreased binding of TSP-1 and a lack of activation of Fyn. Similarly, immortalized HMEC-1 cells that lost CD36 expression failed to bind TSP-1 and activate the kinase. Stable expression of CD36 or CD36 fusion proteins (mApple, PAmCherry, CD36-myc) restored both. This expression system provided us with the unique possibility to investigate more closely the relationship between the membrane receptor CD36 and its downstream effector Fyn.

Using super-resolution imaging approaches and spatial pattern analysis, we gained near molecular details of the reorganization of the receptor once engaged by its ligand. Using PALM, we were able to show that ~40% of surface CD36 exists in clusters at steady state. Upon TSP-1

Chapter 6- General discussion and conclusions

engagement, CD36 clusters grew in size (radius from ~70 nm to ~90 nm) while becoming denser. These rearrangements could only be possible if new individual CD36 receptors were recruited to site of TSP-1 induced cluster enhancement as the percent of CD36 molecules in clusters increased from ~40% to ~60%. Interestingly, decavalent anti-CD36 antibody SM ϕ , induced clustering and signaling similarly to TSP-1 while divalent anti-CD36 antibody FA6-152 could not. This implies, the binding of multivalent ligand to CD36 induces the consolidation of pre-existing cluster into larger and denser platform.

What are the consequences of this increase in CD36 clustering? One possibility is that enhanced clustering of receptors helps in the recruitment and activation of intracellular signaling molecules. This was evaluated by performing 2 channels PALM imaging of CD36 and Fyn. With this method, we were able to determine the fraction of Fyn molecules present in and out CD36 clusters. Our results revealed that at steady state, Fyn was enriched in the pre-existing CD36 clusters. Following activation by TSP-1, the larger number of Fyn molecules present in CD36 clusters was as a result of the increased cluster area, ruling out any active recruitment of new Fyn molecules within receptor clusters. However, the constitutive association of Fyn with CD36 clusters suggests that these platforms are ready to be engaged by their ligand and already primed to transduce the information to associated intracellular signaling molecules. Compaction of CD36 clusters by TSP-1 or SM ϕ can lead to 2 possible consequences: 1) bringing Fyn molecules closer together provides them with a higher opportunity to auto-phosphorylate themselves in trans on Y420 and activate each other (Boggon, Eck 2004, Cooper, MacAuley 1988); 2) The enhancement of these clusters causes an inclusion or exclusion of protein phosphatases or kinases in a manner that leads to dephosphorylation of the inhibitory Y531 and phosphorylation

Chapter 6- General discussion and conclusions

of activatory Y420 (Roskoski 2005). It is likely that both mechanism work hand in hand to activate Fyn. (Cooper, MacAuley 1988).

We have also uncovered two key regulators of this CD36 clustering, priming CD36-Fyn association for TSP-1 signaling in ECs: actin and lipid rafts. Our data suggests their contribution acts on five levels. 1) Actin and lipid rafts spatially organizes CD36-Fyn complexes along the cortical F-actin on ECs plasma membrane (Figure 4-3). Pharmacological perturbation of either actin or lipid rafts also disrupted this CD36-Fyn anisotropic spatial distribution (Figure 4-8). 2) The amount of TSP-1 binding to ECs also depends on actin and lipid rafts integrity, with either perturbations resulting in reduced binding (Figure 4-11). 3) Activation of Fyn by TSP-1 binding CD36 was localized along F-actin (Figure 4-9) and any disruption of F-actin or lipid rafts abrogated this activation (Figure 4-10). 4) CD36 cluster enhancement by TSP-1 was also significantly impaired under actin or lipid rafts perturbation. 5) Actin and lipid rafts also regulated CD36 mobility on the plasma membrane and their perturbations surprisingly immobilized most of CD36.

It is increasingly becoming evident that actin is actively involved in formation and dynamics of lipid rafts. While CD36-Fyn association seem to be primed in these lipid rafts signaling platforms, our data points to actin involvement in organizing these platforms, and possibly controlling exchange of molecules in and out of these domains, hence maintaining the basal CD36 clustering required at steady state. The binding of multivalent CD36 ligands results in active recruitment of CD36 molecules into these clusters, with the lipid rafts providing a compartmentalized signaling platforms. Whether CD36-Fyn complexes interact with actin directly or through an actin binding adaptor protein remains unclear. However, organizing these

Chapter 6- General discussion and conclusions

cluster along defined F-actin areas would increase the efficiency of new molecules recruitment to activate the pathway. This is in line with the aforementioned cytoskeletal controlled CD36 diffusion along cortical fibers troughs in macrophages, a feature that increased the probability of CD36 molecules interacting and clustering (Jaqaman et al. 2011).

The ‘picket and fence’ model postulates an actin cytoskeleton mesh that compartmentalizes plasma membrane proteins, proposing segregation of the receptors in the confinements resulting in an enhancement of clustering and signaling, say, upon ligand binding (Morone et al. 2006, Ritchie et al. 2003). Our observed directed mobility of CD36 along actin filaments (Figure 4-13), in line with earlier report (Jaqaman et al. 2011), suggests a possible actin directed trough compartments than confines CD36 diffusion. It is possible that these trough compartments extend throughout the actin filaments length, limiting the chances of CD36 ‘hop diffusing’ out of them. The confinement of CD36 was shown to be long-lived, approximately 10 seconds (Jaqaman et al. 2011), compared to Kusumi’s reported confinement of 1 millisecond timescale (Kusumi et al. 2005). This would indeed increase the chances of CD36 molecules coming together in these compartments as they diffuse along. The diffusion coefficient of membrane proteins in actin mesh compartments ranges between 5-10 $\mu\text{m}^2/\text{sec}$ (Ritchie et al. 2003, Fujiwara et al. 2002), 50 to 100 fold higher than that calculated for CD36 (Figure 4-14F). This is in line with earlier observations of membrane protein oligomerization induced trapping model which predicts reduced diffusivity with increasing membrane protein oligomerization (Ritchie et al. 2003, Iino, Koyama & Kusumi 2001). Of note, perturbing actin doubled CD36 immobile fraction (Figure 4-14E), in contrast to the ‘picket and fence’ model, which predicts that disruption of actin (the fence) allows faster unrestricted diffusion of membrane components (Morone et al. 2006). Removal of the barrier (such as actin mesh perturbation) should result in

Chapter 6- General discussion and conclusions

increased mobilization of receptors as expected in this model (Ritchie et al. 2003), this would be the case for receptors diffusing without any connection to actin. It is likely that CD36 diffusion is facilitated by its interaction with actin through some adaptor protein, hence, perturbing actin reduces CD36 mobility. Probing for CD36 connection to actin will shed more light into CD36-actin relationship in regards to its diffusion and compartmentalization.

Upon signaling initiation, TSP-1-CD36 get internalized 15 minutes post stimulation (Figure 3-9). Our data identified the CLIC/GEEC pathway as the endocytic pathway through which CD36 is endocytosed in ECs (Figure 5-1). This endocytosis was also dependent on actin and lipid raft component, cholesterol. Interestingly, even though steady state and TSP-1 stimulated CD36 partitions into CLIC/GEEC pathway marker areas (Figure 5-1), TSP-1 stimulation delayed part of CD36 endocytosis at 10 minutes (Figure 3-13D, Figure 5-2B). While the mechanism behind this delay is yet to be determined, there are two possible ways this is achieved. One, the recruitment of new CD36 molecules into larger, denser clusters by TSP-1 might act in a manner that brings along or activates proteins that would delay the endocytic machinery. For instance, PI(4,5)P₂ has been shown to be important in recruiting and interacting with dynamin (Vallis, Wigge et al. 1999, Antonescu, Aguet et al. 2011). The conversion of PI(4,5)P₂ to PI(3,4,5)P₃ in CD36 spots upon TSP-1 stimulation (Figure 4-15) would delay CD36 internalization as CD36 endocytosis is dynamin dependent (Figure 5-5). Two, the enlargement of CD36 clusters by multivalency ligands might form platforms beyond the maximum threshold size for CD36 endocytosis. Indeed the brightest surface CD36 spots corresponded with TSP-1 spots at 10 minutes stimulation timepoint (Figure 3-9). This would suggest that any internalized CD36 at this timepoint was not TSP-1 ligated and possibly not clustered enough to delay endocytosis. While steady state CD36 endocytosis features matched those of CLIC/GEEC

pathway, TSP-1-CD36 pair endocytic mechanism remains to be verified. Ligand ligation of its cognitive receptor can change the receptor endocytic mechanism as recently shown in the newly described endophilin mediated endocytosis (Du Toit 2015, Boucrot, Ferreira et al. 2015, Renard, Simunovic et al. 2015). This endophilin mediated endocytosis mechanism was only activated upon ligand stimulation and was dependent on dynamin, PI3K activity and formed tubule like invaginations just like CLIC/GEEC pathway (Du Toit 2015, Boucrot, Ferreira et al. 2015, Renard, Simunovic et al. 2015). Interestingly, just like in endophilin mediated endocytosis, TSP-1 induces PI3K activity, converting $PI(4,5)P_2$ to $PI(3,4,5)P_3$ (Figure 4-15). Formation of $PI(3,4,5)P_3$ followed by its subsequent dephosphorylation into $PI(3,4)P_3$ mediate the recruitment of endophilin in the endophilin mediated endocytosis (Boucrot, Ferreira et al. 2015). If it is verified that TSP-1-CD36 pair is endocytosis via a mechanism different from the CLIC/GEEC pathway, endophilin mediated endocytosis might be the possible alternate mechanism utilized given the above parallel features. Whether TSP-1-CD36 pair endocytosis results in downregulation of the activated Fyn or results in signaling endosomes was not tested. The internalization of CD36 through the CLIC/GEEC pathway also opens a new paradigm of cell type specific receptor internalization, as other endocytic mechanisms in different cell types have been characterized for CD36 endocytosis. Based on our findings, we propose a model for the TSP-1-CD36-Fyn pathway initiation and CD36 endocytosis below and consider some future work to further expound on these results.

6.2 Conclusions and future work

TSP-1-based anti-angiogenic therapy has been validated as a possible path that can be utilized in cancer treatment and to prevent its recurrence (Zhang, Lawler 2007). Clinical trials results for TSP-1 mimetics as anti-angiogenic cancer therapy have called for trial combinations

Chapter 6- General discussion and conclusions

with cytotoxic therapies and better understanding of the initial steps governing this anti-angiogenic pathway activation (Markovic et al. 2007, Hoekstra et al. 2006, Ebbinghaus et al. 2007). Super resolution imaging enabled us to resolve the initial step of TSP-1 effect on CD36 and Fyn at a near molecular level. Briefly, we outline the summarized model for the initiation of this pathway. At steady state in ECs, a fraction of CD36 pre-exist in clusters in lipid rafts nanodomains of about 70 nm in radius (Figure 6-1A). These clusters are spatially organized along regions rich in F-actin, in a manner dependent on actin and lipid raft platforms. Upon CD36 multivalent ligand binding (for example TSP-1 or SM ϕ), there is enrichment and compaction of these clusters with more CD36 molecules populating larger clusters of about 90 nm radius (Figure 6-1A). This growth and compaction is key in initiating Fyn activation, since disrupting the clusters with actin or lipid rafts perturbation abrogates Fyn activation. Our research also gave insights into CD36 endocytosis in ECs, a process that had not been previously studied in these cells. CD36 was endocytosed via CLIC/GEEC pathway through polymorphous tubules in a dynamin, actin, cholesterol and Cdc42 dependent manner (Figure 6-1B).

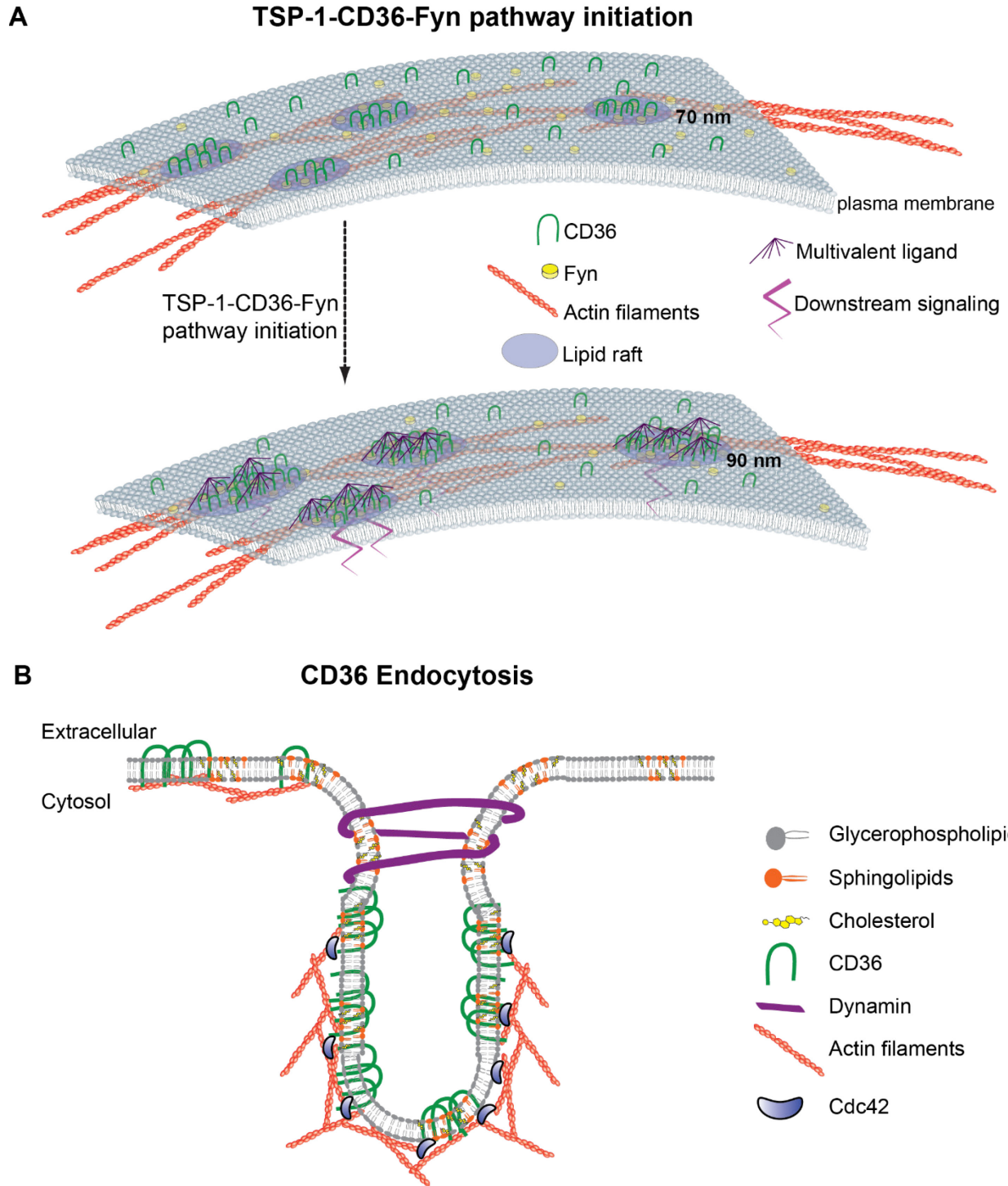


Figure 6-1: Proposed model for TSP-1-CD36-Fyn signaling initiation and CD36 endocytic mechanism

(A) Graphical representation of the proposed model for TSP-1-CD36-Fyn pathway

Chapter 6- General discussion and conclusions

initiation. Enlargement and compaction of CD36-Fyn association clusters by multivalent ligand, in an actin and lipid raft dependent manner, induces downstream signaling. **(B)** Graphical representation of the endocytic pathway CD36 takes through polymorphous tubules in a dynamin, actin, cholesterol and Cdc42 dependent manner.

The elucidation of CD36 cluster enhancement by TSP-1 or SM ϕ opens a new avenue in redesigning more effective and better-targeted TSP-1 based anti-angiogenic drugs. Our results indicate that clustering is necessary to trigger CD36 signal transduction, a feature that previous TSP-1 peptide mimics failed to take into account. CD36 internalization in the TSP-1-CD36-Fyn pathway will also need further investigation to clarify its role and how endocytosis might regulate further signaling. The findings also open new leads that future work could expound on understanding the world of receptor clustering and membrane domains. For instance, while the classic definition of lipid rafts involves cholesterol and sphingolipids being the main players, the dissolving of lipid rafts resident CD36 in 1% Triton at 4°C in actin perturbation condition, while still having cholesterol and sphingolipids on the membrane is intriguing (Figure 4-7). Indeed, it has been suggested that consolidating actin and lipid rafts cooperativity might help bridge the gap between believers and non-believers of the lipid rafts concept (Kraft 2013). Lipid rafts concept has been built around the notion of fluctuating nanoscale assemblies of sphingolipids and cholesterol enriched domains (Lingwood, Simons 2010, Simons, Gerl 2010). However, skepticism to this concept has partly emerged from observations of lipid raft proteins and sphingolipids clustering being more dependent on cortical actin than the lipid rafts ‘glue’, cholesterol (Goswami et al. 2008, Fujita, Cheng & Fujimoto 2009, Gowrishankar et al. 2012, Kraft 2013). In addition, while cholesterol-sphingolipids association favors ordered domains in model membranes, trapping of diffusing sphingolipids to form domains in live cell plasma

Chapter 6- General discussion and conclusions

membranes requires cortical actin and not just cholesterol-sphingolipid interactions (Mueller et al. 2011, Dinic, Ashrafzadeh & Parmryd 2013). More research is needed to fully decipher the precise role of actin in lipid rafts formation and existence.

In conclusion, our study proposes a modified model of CD36-Fyn organization and signaling, likely generalizable to many other signaling pathways. Instead of freely diffusing molecules where receptors must randomly encounter both ligand and downstream effector, our data demonstrate that CD36 and Fyn form a “receptor/transducer duo” that co-cluster at all times. This facilitates ligand binding, which then induces cluster reorganization, resulting in larger and more compact clusters that activate Fyn and robustly trigger downstream signaling. Ligand alone is not sufficient to induce cluster reorganization, rather this process depends on membrane integrity and the cytoskeleton. The overall cellular response, elicited by the ligand, is therefore not the result of the formation of novel complexes but is instead largely the result of local reorganization of receptors, effectors and accessory molecules supported by the membrane ultrastructure.

Further investigation will be needed to define the precise mechanisms and intermediates involved in the association of CD36 and Fyn and to explain how Fyn activation is specifically increased within the enhanced CD36 clusters. The possibility of other proteins linking CD36-Fyn complexes to cortical actin might unravel other regulators of this pathway besides actin and lipid nanodomains. Concerning CD36 endocytic pathway, since we have defined the molecular players implicated in TSP-1-CD36 pathway, we will be able to further investigate their role in long-term cell responses. One such experiment would be to monitor P-Y420 levels while inhibiting dynamin, hence blocking CD36 internalization. This would help to answer if TSP-1-

Chapter 6- General discussion and conclusions

CD36 endocytosis downregulates P-Y420 activation. Overall, insights provided by our research will be useful in re-designing TSP-1 based anti-angiogenic therapy and guiding future studies in the CD36 signaling and endocytosis pathways in ECs.

References

- Antonescu, C.N., Aguet, F., Danuser, G. & Schmid, S.L. 2011, "Phosphatidylinositol-(4,5)-bisphosphate regulates clathrin-coated pit initiation, stabilization, and size", *Molecular biology of the cell*, vol. 22, no. 14, pp. 2588-2600.
- Boggon, T.J. & Eck, M.J. 2004, "Structure and regulation of Src family kinases", *Oncogene*, vol. 23, no. 48, pp. 7918-7927.
- Boucrot, E., Ferreira, A.P., Almeida-Souza, L., Debard, S., Vallis, Y., Howard, G., Bertot, L., Sauvonnnet, N. & McMahon, H.T. 2015, "Endophilin marks and controls a clathrin-independent endocytic pathway", *Nature*, vol. 517, no. 7535, pp. 460-465.
- Cooper, J.A. & MacAuley, A. 1988, "Potential positive and negative autoregulation of p60c-src by intermolecular autophosphorylation", *Proceedings of the National Academy of Sciences of the United States of America*, vol. 85, no. 12, pp. 4232-4236.
- Dawson, D.W., Pearce, S.F., Zhong, R., Silverstein, R.L., Frazier, W.A. & Bouck, N.P. 1997, "CD36 mediates the In vitro inhibitory effects of thrombospondin-1 on endothelial cells.", *Journal of Cell Biology*, vol. 138, no. 3, pp. 707-717.
- Dinic, J., Ashrafzadeh, P. & Parmryd, I. 2013, "Actin filaments attachment at the plasma membrane in live cells cause the formation of ordered lipid domains", *Biochimica et biophysica acta*, vol. 1828, no. 3, pp. 1102-1111.
- Du Toit, A. 2015, "Endocytosis. A new gateway into cells", *Nature reviews.Molecular cell biology*, vol. 16, no. 2, pp. 68.
- Ebbinghaus, S., Hussain, M., Tannir, N., Gordon, M., Desai, A.A., Knight, R.A., Humerickhouse, R.A., Qian, J., Gordon, G.B. & Figlin, R. 2007, "Phase 2 study of ABT-510 in patients with previously untreated advanced renal cell carcinoma", *Clinical cancer research : an official journal of the American Association for Cancer Research*, vol. 13, no. 22 Pt 1, pp. 6689-6695.
- Fujita, A., Cheng, J. & Fujimoto, T. 2009, "Segregation of GM1 and GM3 clusters in the cell membrane depends on the intact actin cytoskeleton", *Biochimica et biophysica acta*, vol. 1791, no. 5, pp. 388-396.
- Fujiwara, T., Ritchie, K., Murakoshi, H., Jacobson, K. & Kusumi, A. 2002, "Phospholipids undergo hop diffusion in compartmentalized cell membrane.", *Journal of Cell Biology*, vol. 157, no. 6, pp. 1071-1081.
- Goswami, D., Gowrishankar, K., Bilgrami, S., Ghosh, S., Raghupathy, R., Chadda, R., Vishwakarma, R., Rao, M. & Mayor, S. 2008, "Nanoclusters of GPI-anchored proteins are formed by cortical actin-driven activity", *Cell*, vol. 135, no. 6, pp. 1085-1097.

Chapter 6- General discussion and conclusions

- Gowrishankar, K., Ghosh, S., Saha, S., C, R., Mayor, S. & Rao, M. 2012, "Active remodeling of cortical actin regulates spatiotemporal organization of cell surface molecules", *Cell*, vol. 149, no. 6, pp. 1353-1367.
- Hoekstra, R., de Vos, F.Y., Eskens, F.A., de Vries, E.G., Uges, D.R., Knight, R., Carr, R.A., Humerickhouse, R., Verweij, J. & Gietema, J.A. 2006, "Phase I study of the thrombospondin-1-mimetic angiogenesis inhibitor ABT-510 with 5-fluorouracil and leucovorin: a safe combination", *European journal of cancer (Oxford, England : 1990)*, vol. 42, no. 4, pp. 467-472.
- Iino, R., Koyama, I. & Kusumi, A. 2001, "Single molecule imaging of green fluorescent proteins in living cells: E-cadherin forms oligomers on the free cell surface", *Biophysical journal*, vol. 80, no. 6, pp. 2667-2677.
- Jaqaman, K., Kuwata, H., Touret, N., Collins, R., Trimble, W.S., Danuser, G. & Grinstein, S. 2011, "Cytoskeletal control of CD36 diffusion promotes its receptor and signaling function", *Cell*, vol. 146, no. 4, pp. 593-606.
- Jimenez, B., Volpert, O.V., Crawford, S.E., Febbraio, M., Silverstein, R.L. & Bouck, N. 2000, "Signals leading to apoptosis-dependent inhibition of neovascularization by thrombospondin-1", *Nature medicine*, vol. 6, no. 1, pp. 41-48.
- Jimenez, B., Volpert, O.V., Reiher, F., Chang, L., Munoz, A., Karin, M. & Bouck, N. 2001, "c-Jun N-terminal kinase activation is required for the inhibition of neovascularization by thrombospondin-1", *Oncogene*, vol. 20, no. 26, pp. 3443-3448.
- Kraft, M.L. 2013, "Plasma membrane organization and function: moving past lipid rafts", *Molecular biology of the cell*, vol. 24, no. 18, pp. 2765-2768.
- Kusumi, A., Ike, H., Nakada, C., Murase, K. & Fujiwara, T. 2005, "Single-molecule tracking of membrane molecules: plasma membrane compartmentalization and dynamic assembly of raft-philic signaling molecules", *Seminars in immunology*, vol. 17, no. 1, pp. 3-21.
- Lingwood, D. & Simons, K. 2010, "Lipid rafts as a membrane-organizing principle", *Science*, vol. 327, no. 5961, pp. 46-50.
- Markovic, S.N., Suman, V.J., Rao, R.A., Ingle, J.N., Kaur, J.S., Erickson, L.A., Pitot, H.C., Croghan, G.A., McWilliams, R.R., Merchan, J., Kottschade, L.A., Nevala, W.K., Uhl, C.B., Allred, J. & Creagan, E.T. 2007, "A phase II study of ABT-510 (thrombospondin-1 analog) for the treatment of metastatic melanoma", *American journal of clinical oncology*, vol. 30, no. 3, pp. 303-309.
- Morone, N., Fujiwara, T., Murase, K., Kasai, R.S., Ike, H., Yuasa, S., Usukura, J. & Kusumi, A. 2006, "Three-dimensional reconstruction of the membrane skeleton at the plasma membrane interface by electron tomography", *The Journal of cell biology*, vol. 174, no. 6, pp. 851-862.

Chapter 6- General discussion and conclusions

- Mueller, V., Ringemann, C., Honigmann, A., Schwarzmann, G., Medda, R., Leutenegger, M., Polyakova, S., Belov, V.N., Hell, S.W. & Eggeling, C. 2011, "STED nanoscopy reveals molecular details of cholesterol- and cytoskeleton-modulated lipid interactions in living cells", *Biophysical journal*, vol. 101, no. 7, pp. 1651-1660.
- Renard, H.F., Simunovic, M., Lemiere, J., Boucrot, E., Garcia-Castillo, M.D., Arumugam, S., Chambon, V., Lamaze, C., Wunder, C., Kenworthy, A.K., Schmidt, A.A., McMahon, H.T., Sykes, C., Bassereau, P. & Johannes, L. 2015, "Endophilin-A2 functions in membrane scission in clathrin-independent endocytosis", *Nature*, vol. 517, no. 7535, pp. 493-496.
- Ritchie, K., Iino, R., Fujiwara, T., Murase, K. & Kusumi, A. 2003, "The fence and picket structure of the plasma membrane of live cells as revealed by single molecule techniques (Review)", *Molecular membrane biology*, vol. 20, no. 1, pp. 13-18.
- Roskoski, R., Jr 2005, "Src kinase regulation by phosphorylation and dephosphorylation", *Biochemical and biophysical research communications*, vol. 331, no. 1, pp. 1-14.
- Simons, K. & Gerl, M.J. 2010, "Revitalizing membrane rafts: new tools and insights", *Nature Reviews Molecular Cell Biology*, vol. 11, no. 10, pp. 688-699.
- Vallis, Y., Wigge, P., Marks, B., Evans, P.R. & McMahon, H.T. 1999, "Importance of the pleckstrin homology domain of dynamin in clathrin-mediated endocytosis", *Current biology : CB*, vol. 9, no. 5, pp. 257-260.
- Zhang, X. & Lawler, J. 2007, "Thrombospondin-based antiangiogenic therapy", *Microvascular research*, vol. 74, no. 2-3, pp. 90-99.